

UNCLASSIFIED

AD NUMBER
ADB286348
NEW LIMITATION CHANGE
TO Approved for public release, distribution unlimited
FROM Distribution authorized to U.S. Gov't. agencies only; Proprietary Info.; Mar 2002. Other requests shall be referred to US Army Medical Research and Materiel Comd., 504 Scott St., Fort Detrick, MD 21702-5012.
AUTHORITY
USAMRMC ltr, dtd 28 July 2003

THIS PAGE IS UNCLASSIFIED

AD_____

Award Number: DAMD17-98-1-8590

TITLE: Signal Transduction Pathway in Maspin-induced Tumor
Suppression of Prostate Cancer

PRINCIPAL INVESTIGATOR: Karl X. Chai, Ph.D.

CONTRACTING ORGANIZATION: University of Central Florida
Orlando, Florida 32816

REPORT DATE: March 2002

TYPE OF REPORT: Final

PREPARED FOR: U.S. Army Medical Research and Materiel Command
Fort Detrick, Maryland 21702-5012

DISTRIBUTION STATEMENT: Distribution authorized to U.S. Government
agencies only (proprietary information, Mar 02). Other requests
for this document shall be referred to U.S. Army Medical Research
and Materiel Command, 504 Scott Street, Fort Detrick, Maryland
21702-5012.

The views, opinions and/or findings contained in this report are
those of the author(s) and should not be construed as an official
Department of the Army position, policy or decision unless so
designated by other documentation.

20030220 068

NOTICE

USING GOVERNMENT DRAWINGS, SPECIFICATIONS, OR OTHER DATA INCLUDED IN THIS DOCUMENT FOR ANY PURPOSE OTHER THAN GOVERNMENT PROCUREMENT DOES NOT IN ANY WAY OBLIGATE THE U.S. GOVERNMENT. THE FACT THAT THE GOVERNMENT FORMULATED OR SUPPLIED THE DRAWINGS, SPECIFICATIONS, OR OTHER DATA DOES NOT LICENSE THE HOLDER OR ANY OTHER PERSON OR CORPORATION; OR CONVEY ANY RIGHTS OR PERMISSION TO MANUFACTURE, USE, OR SELL ANY PATENTED INVENTION THAT MAY RELATE TO THEM.

LIMITED RIGHTS LEGEND

Award Number: DAMD17-98-1-8590
Organization: University of Central Florida

Those portions of the technical data contained in this report marked as limited rights data shall not, without the written permission of the above contractor, be (a) released or disclosed outside the government, (b) used by the Government for manufacture or, in the case of computer software documentation, for preparing the same or similar computer software, or (c) used by a party other than the Government, except that the Government may release or disclose technical data to persons outside the Government, or permit the use of technical data by such persons, if (i) such release, disclosure, or use is necessary for emergency repair or overhaul or (ii) is a release or disclosure of technical data (other than detailed manufacturing or process data) to, or use of such data by, a foreign government that is in the interest of the Government and is required for evaluational or informational purposes, provided in either case that such release, disclosure or use is made subject to a prohibition that the person to whom the data is released or disclosed may not further use, release or disclose such data, and the contractor or subcontractor or subcontractor asserting the restriction is notified of such release, disclosure or use. This legend, together with the indications of the portions of this data which are subject to such limitations, shall be included on any reproduction hereof which includes any part of the portions subject to such limitations.

THIS TECHNICAL REPORT HAS BEEN REVIEWED AND IS APPROVED FOR PUBLICATION.

Administrative Change
04/22/03

REPORT DOCUMENTATION PAGEForm Approved
OMB No. 074-0188

Public reporting burden for this collection of information is estimated to average 1 hour per response, including the time for reviewing instructions, searching existing data sources, gathering and maintaining the data needed, and completing and reviewing this collection of information. Send comments regarding this burden estimate or any other aspect of this collection of information, including suggestions for reducing this burden to Washington Headquarters Services, Directorate for Information Operations and Reports, 1215 Jefferson Davis Highway, Suite 1204, Arlington, VA 22202-4302, and to the Office of Management and Budget, Paperwork Reduction Project (0704-0188), Washington, DC 20503

1. AGENCY USE ONLY (Leave blank)		2. REPORT DATE March 2002	3. REPORT TYPE AND DATES COVERED Final (1 Sep 98 - 28 Feb 02)	
4. TITLE AND SUBTITLE Signal Transduction Pathway in Maspin-induced Tumor Suppression of Prostate Cancer			5. FUNDING NUMBERS DAMD17-98-1-8590	
6. AUTHOR(S) Karl X. Chai, Ph.D.				
7. PERFORMING ORGANIZATION NAME(S) AND ADDRESS(ES) University of Central Florida Orlando, Florida 32816 E-mail: kxchai@mail.ucf.edu			8. PERFORMING ORGANIZATION REPORT NUMBER	
9. SPONSORING / MONITORING AGENCY NAME(S) AND ADDRESS(ES) U.S. Army Medical Research and Materiel Command Fort Detrick, Maryland 21702-5012			10. SPONSORING / MONITORING AGENCY REPORT NUMBER	
11. SUPPLEMENTARY NOTES Original contains color plates: All DTIC reproductions will be in black and white.				
12a. DISTRIBUTION / AVAILABILITY STATEMENT Distribution authorized to U.S. Government agencies only (proprietary information, Mar 02). Other requests for this document shall be referred to U.S. Army Medical Research and Materiel Command, 504 Scott Street, Fort Detrick, Maryland 21702-5012.				12b. DISTRIBUTION CODE
13. Abstract (Maximum 200 Words) (abstract should contain no proprietary or confidential information) The original purpose was to identify a receptor for maspin, a serpin tumor suppressor of breast and prostate cancers. Proastasin and hepsin serine proteases were examined as candidates. Proastasin was found to be down-regulated in high-grade prostate cancers and absent in invasive prostate and breast cancer cells, in which proastasin promoter hypermethylation was found. Proastasin was shown to be an invasion suppressor, via its GPI-anchored membrane form. Proastasin is involved in epithelial sodium channel activation and is regulated by the serpin protease nexin-1 (PN-1). Other cellular protein changes elicited by proastasin expression were also observed. A new project has been initiated to investigate the mechanisms of proastasin's anti-invasion function. A second new project has been initiated to evaluate the potential of using proastasin as a metastasis suppressor of breast cancer. A new hypothesis is proposed for a potential indirect interaction between maspin and proastasin based on their individually confirmed roles in sodium transport regulation. We demonstrated an up-regulation of hepsin in prostate cancer, but no direct interaction was established between maspin and hepsin at the biochemical or cellular level. <i>Drosophila</i> genetics was and will continue to be employed to investigate hepsin's role in cancer.				
14. SUBJECT TERMS Prostate Cancer, maspin, receptor, proastasin, hepsin, <i>Drosophila</i> , mutation				15. NUMBER OF PAGES 156
				16. PRICE CODE
17. SECURITY CLASSIFICATION OF REPORT Unclassified	18. SECURITY CLASSIFICATION OF THIS PAGE Unclassified	19. SECURITY CLASSIFICATION OF ABSTRACT Unclassified	20. LIMITATION OF ABSTRACT Unlimited	

NSN 7540-01-280-5500

Standard Form 298 (Rev. 2-89)
Prescribed by ANSI Std. Z39-18
298-102

Table of Contents

Cover.....	
SF 298.....	2
Introduction.....	4
Body.....	4
Key Research Accomplishments.....	7
Reportable Outcomes.....	8
Conclusions.....	10
References.....	11
Appendices.....	Attached
Item 1: Chen <i>et al.</i> , 2001a	
Item 2: Chen <i>et al.</i> , 2001b	
Item 3: Narikiyo <i>et al.</i> , 2002	
Item 4: Chen and Chai, 2002a	
Item 5: Chen and Chai, 2002b (submitted manuscript)	
Item 6: Chen and Chai, 2002c (manuscript to be submitted)	
Item 7: Bayer <i>et al.</i> , 2002 (manuscript to be submitted)	

(4) INTRODUCTION:

Maspin is a serine protease inhibitor (serpin) capable of suppressing breast and prostate cancers. The investigation of maspin tumor suppression in breast and prostate cancer cells led to the speculation of maspin's interaction with a membrane-bound serine protease in these tissues or cancers. This interaction may be an initial signaling event to the tumor suppression pathways (manifested as inhibition of tumor cells' motility and invasiveness in *in vitro* and *in vivo* assays, as well as tumor suppression of nude mouse xenografts) (Sheng *et al.*, 1996). We had suggested in our original proposal that a human prostate-produced serine protease, prostasin, can serve the role of a maspin receptor/interactive protease based on our evaluation of prostasin's putative structure and its substrate preference (Yu *et al.*, 1994). We intended to investigate whether a direct interaction between maspin and prostasin can be established using conventional biochemistry and molecular biology methods. We also intended to identify the down-stream proteins in the maspin/prostasin signal transduction pathway taking advantage of *Drosophila* genetics methods. Further, an alternative candidate protease, human hepsin, will also be investigated for the same functions.

(5) BODY:

1). Prostasin serine protease is a novel invasion suppressor and may be a key molecule in epithelial function and signal transduction

In the execution of the work plan, we made the observation that prostasin serine protease is down-regulated in high-grade prostate cancers (Gleason 4/5) and absent in two invasive prostate cancer cell lines, DU-145 and PC-3. Maspin's anti-invasion properties in prostate cancer were observed in these two cell lines (Sheng *et al.*, 1996). The observation of an absence of prostasin in these cell lines effectively eliminated the prostasin serine protease as a direct receptor/interactive protein for maspin in its role of anti-invasion in prostate cancer. The experiments to investigate prostasin's expression in DU-145 and PC-3 cells were based on an excellent suggestion from the review comments to our original proposal. We have since modified the Statement of Work concerning the investigation on prostasin serine protease as our findings were potentially important toward the understanding of prostate cancer biology. In one published paper (Chen *et al.*, 2001a), we demonstrated that forced re-expression of recombinant human prostasin protein in DU-145 and PC-3 cells reduced the *in vitro* invasiveness by 68% and 42%, respectively, while showing no effect on cell proliferation. The results of this experiment suggest that the prostasin serine protease itself is a prostate cancer invasion suppressor. In this paper, we also established that prostasin's anti-invasion activity is associated with a membrane-bound form of the protease, but not with the secreted form (purified, and added back to the cells *via* the culture media). In a second published paper (Chen *et al.*, 2001b), we used a recombinant human prostasin serine protease (r-hPro) expressed in several human cell lines, including DU-145 and PC-3, to show that r-hPro is synthesized as a membrane-bound protein, while a free-form prostasin is secreted into the culture medium. Prostasin was also identified in nuclear and membrane fractions. The membrane-bound prostasin is anchored by a glycosylphosphatidylinositol (GPI)-linkage. Further, a novel prostasin-binding protein was identified exclusively in seminal vesicle fluid. Using an indirect enzymatic activity assay involving this prostasin-binding protein, we showed that prostasin is an active serine protease in its membrane-bound form. We had previously stated in an annual report (2001) that the identification of a specific prostasin-binding protein will facilitate the investigation of prostasin's potential natural substrates or interactive proteins, possibly including maspin, leading the project back to the originally proposed goals of prostasin-maspin interaction. On this front, we have now purified and characterized this prostasin-binding protein and submitted a manuscript to the Journal of Biological Chemistry for review (Chen and Chai, 2002b). The identity

of the prostasin-binding protein was established to be a serpin (serine protease inhibitor), previously identified as protease nexin-1 (PN-1), known to promote neurite outgrowth and inhibit thrombin serine protease (Scott *et al.*, 1985). Also on this front, many recent reports suggest that prostasin serine protease and its homologues in *Xenopus*, mice, and rats function as a proteolytic activator (CAP-1) of the epithelial sodium channel (ENaC), thus being implicated in kidney and airway diseases (Adachi *et al.*, 2001; Donaldson *et al.*, 2002; Vallet *et al.*, 2002; Vuagniaux *et al.*, 2000). We undertook a collaboration with one of the groups that reported such findings and together showed that prostasin is directly involved in ENaC activation and that prostasin expression in the kidney is regulated by aldosterone (Narikiyo *et al.*, 2002). Still on this front, there is recent evidence by others that both maspin and the homologue of prostasin (CAP-1) are involved in epithelial culture "dome formation", a phenomenon viewed as *in vitro* cell differentiation (Ichigi and Asashima, 2001; Zucchi *et al.*, 2001). Interestingly, the roles played by maspin and prostasin seemed to be on opposite ends, with prostasin/CAP-1 being the promoter for this cellular event (Ichigi and Asashima, 2001) while maspin being the inhibitor (Zucchi *et al.*, 2001). We have now formulated a new hypothesis that there may still be an interaction between prostasin serine protease and maspin, the serpin, at the cellular level, but it involves the membrane-bound prostasin and potentially other co-factors. Prostasin, maspin, and the putative co-factors regulate epithelial differentiation, potentially involving the ENaC. This new hypothesis will be further explored in our continued research endeavors as it represents a major under-explored area of research in prostate cancer: sodium transport. Our laboratory is in an advantageous position to pursue this line of research as we have gained the experience and re-tooled to work with membrane-bound proteases and their mechanisms.

As our new finding that prostasin itself is an invasion suppressor, we looked to investigate the cellular mechanisms and pathways involved in this process and observed major cellular protein changes resulting from prostasin re-expression in DU-145 and PC-3 cells. We have indicated in a previous annual report (2001), that in DU-145 and PC-3 cells expressing a recombinant human prostasin protein, a protein band migrating at approximately 120-130 kDa range in SDS-PAGE was found to be reduced in tyrosine phosphorylation, as compared to the vector-transfected control cells. We have proposed that the tyrosine phosphorylation-reduced 120-130-kDa protein could be focal adhesion kinase (FAK, 125 kDa) or p130Cas (130 kDa), both proteins have been implicated in promoting tumor invasion *via* increased cell motility when tyrosine-phosphorylated (Cary and Guan, 1999). Their tyrosine phosphorylation state in the prostate cancer cells expressing recombinant human prostasin is consistent with the fact that prostasin reduced invasiveness. A further observation was that protein kinase C alpha (PKC α) protein expression is reduced as a result of forced prostasin re-expression in the prostate cancer cells, also consistent with prostasin's anti-invasion role. Increased PKC α activity has been implicated in promoting cell motility, and in turn, tumor invasion (Timar *et al.*, 1996). These observations formed the basis of a new research grant proposal submitted to the DoD-PCRP01 and is now funded and active (Grant No. DAMD17-02-1-0032, "Prostasin's Role in Prostate Cancer"). In this project, the role of prostasin in prostate epithelial biology and signal transduction (normal *versus* pathological) will be examined.

We further investigated the molecular genetic mechanisms of prostasin gene inactivation in prostate cancer and observed prostasin promoter DNA hypermethylation at one location in DU-145 and PC-3 cells as compared to normal prostate epithelial cells and LNCaP (as indicated in Annual Report of 2001).

This study was expanded to human breast cancer cells with the purpose of establishing a more generalized molecular genetic gene inactivation mechanism for prostasin in cancer. We were able to show that prostasin is also down-regulated in highly invasive breast cancer cells as compared to normal breast epithelial cells and non-invasive breast cancer cells. Prostasin also reduced breast cancer cell invasiveness *in vitro* by 50%, and prostasin promoter DNA hypermethylation was observed at multiple locations in the highly invasive breast cancer cells. Demethylation coupled with histone deacetylase

inhibition re-activated prostatic mRNA expression in the invasive breast cancer cells, providing evidence to a causal relationship of the methylated state of prostatic promoter and the down-regulation of prostatic expression in cancer. These results have been published recently (Chen and Chai, 2002a). We then returned to the prostate cancer cells (LNCaP, DU-145, and PC-3) with the tools and methods developed in the breast cancer study. We demonstrated that prostatic promoter DNA hypermethylation, at multiple locations, is a causal mechanism of prostatic down-regulation in the invasive prostate cancer cell lines DU-145 and PC-3. These results have been summarized in a new manuscript to be submitted for publication (Chen and Chai, 2002c). Our results on prostatic expression and function in breast cancer cells formed the basis of an IDEA proposal to the DoD-BCRP01 and is now funded (Grant No. DAMD17-02-1-0338). In this project, we will examine the potential of using prostatic serine protease to limit human breast cancer invasion and metastasis in an animal model.

Overall, the original award that funded the research on the relationship between prostatic serine protease and the serpin tumor suppressor maspin has resulted in an unanticipated finding of a novel invasion suppressor (prostatic). Despite the evidence that there does not seem to be a direct molecular interaction between prostatic and maspin, recent progress by our own group and others points to the potential of an indirect interaction *via* the regulation of the epithelial sodium channel, implicating a role for both prostatic and maspin in epithelial differentiation. The present project, upon its completion, represents a major shift of focus in terms of the molecules under examination (from maspin and prostatic to prostatic), but maintains its original purpose of investigating signal transduction pathways in prostate cancer, that in the long term, will also address the maspin issue.

2). Maspin, hepsin, and prostatic transgenic flies for the elucidation of the tumor suppression signal pathway(s):

In the collaborating laboratory (led by Dr. von Kalm), transgenic *Drosophila* strains expressing human maspin, prostatic and hepsin genes were generated and was applied in *Drosophila* genetic manipulations to identify interactive genes/proteins. The maspin- or prostatic-expressing strains did not exhibit any observable phenotype, consistent with their tumor/invasion suppressor functions or roles in normal prostate tissue physiology. The hepsin-expressing strains all had malformed eyes, which were not corrected upon cross-breeding with the maspin-expressing strains, indicating that the *Drosophila* eye may not provide all necessary cellular pathways for the examination of a potential maspin-hepsin interaction. This observation does not rule out any potential interaction of maspin and hepsin.

We investigated hepsin expression in prostate cancer cell lines and in prostatectomy specimens to support the basis of a potential interaction between maspin and hepsin. In the LNCaP and PC-3 cells, RT-PCR analysis with hepsin-specific primers demonstrated its expression, and *in situ* histochemistry using an anti-sense hepsin RNA probe showed an up-regulation of hepsin in high-grade prostate cancer in 11 cases of radical prostatectomy (as indicated in Annual Report of 2000). The up-regulation of hepsin in prostate cancer was later corroborated by recent reports from other groups (Dhanasekaran *et al.*, 2001; Luo *et al.*, 2001; Magee *et al.*, 2001; Stamey *et al.*, 2001). A human hepsin antibody was obtained from Dr. Kurachi of University of Michigan for use in an investigation of direct maspin-hepsin interaction using the human cell lines, as planned in the original Statement of Work. This antibody reagent, however, does not recognize hepsin protein produced in the native form (such as that from the HepG2 cells, the source of the cloned hepsin cDNA), but only reacts with recombinant hepsin produced in *E. coli*. Our attempts of using recombinant hepsin for interaction studies with maspin were hampered by the high degree of difficulty in purifying recombinant hepsin. It is an active serine protease that tends to degrade itself upon purification, but adding protease

inhibitors is not applicable in our studies since we need to maintain the serine protease activity of hepsin to evaluate its interaction with maspin. Maspin was shown to be capable of inhibiting angiogenesis of human prostate cancer cells injected into animals by Dr. Ming Zhang's group in Baylor College of Medicine (Zhang *et al.*, 2000). Since hepsin is involved in angiogenesis (activating Factor VII) (Kazama *et al.*, 1995), we collaborated with Dr. Ming Zhang to perform a yeast two-hybrid assay on maspin and hepsin. Dr. Zhang's group was unable to establish a direct interaction between maspin and hepsin using the respective cDNA's in a yeast two-hybrid assay. This lack of proof from the yeast two-hybrid assay, however, still does not rule out an interaction between hepsin and maspin as in the yeast two-hybrid system the proteins may not be in the correct conformation, particularly for hepsin for being a transmembrane protein.

The transgenic *Drosophila* strains that express hepsin in the eyes were used to identify other potential interactive proteins for hepsin, a tumor-promoting serine protease (Torres-Rosado *et al.*, 1993) and a potential prostate cancer marker (Dhanasekaran *et al.*, 2001; Luo *et al.*, 2001; Magee *et al.*, 2001; Stamey *et al.*, 2001). Recent progress in Dr. von Kalm's laboratory has indicated that hepsin may be hyper-activating the epidermal growth factor receptor (EGFR) signaling pathway *via* proteolytically cleaving the *Drosophila* homologue of transforming growth factor alpha (TGF α). The preliminary results were obtained when the hepsin-expressing flies that manifest malformed eyes were bred with deletion mutants for phenotype rescue. It appeared that hepsin expression in the *Drosophila* eye causes the cells within the eye imaginal disc to adopt an inappropriate developmental fate. Specifically, of the two cell types that are present in the disc, photoreceptor cells and pigment cells, hepsin expression causes a conversion of photoreceptor cells to pigment cells. Since photoreceptor cell formation requires properly regulated EGFR signaling, it is consistent with the observation that a deletion mutant of the *Drosophila* homologue of TGF α can rescue the hepsin eye-malformation phenotype. These preliminary results will form the basis of a future joint research proposal between our two laboratories as EGFR signaling is highly relevant to prostate cancer (Kim *et al.*, 1999).

3). **Stubble, a membrane-bound serine protease in *Drosophila*, provides a model for studying signal pathway(s):**

Based on our new hypothesis, prostasin's anti-invasion mechanism may involve regulation of cell motility, in turn, the regulation of the structure and potential changes of structure of the cytoskeleton. In *Drosophila*, the stubble, a potentially membrane-bound serine protease, has been shown by genetic means to affect cytoskeleton organization, in that fly legs are malformed in stubble mutants (von Kalm *et al.*, 1995). Dr. von Kalm's laboratory has now further demonstrated that the stubble serine protease plays a role in RhoA signaling, which is involved in cell motility (Wittmann *et al.*, 2001). The data from Dr. von Kalm's group are summarized in a manuscript to be submitted for publication (Bayer *et al.*, 2002). Also, the stubble project is now potentially funded by the National Institutes of Health (Grant proposal No. 1R15GM65884-01; "Serine Protease Action in *Drosophila* Development"). The ultimate goal of this line of research is to help understand the roles played by membrane-bound serine proteases in cytoskeleton regulation, providing insights to prostate cancer relevant cytoskeleton and cell motility research.

(6) **KEY RESEARCH ACCOMPLISHMENTS:**

____ Prostasin expression is found to be down-regulated in high-grade (Gleason 4/5) prostate cancers.

____ Prostasin was shown to be a novel invasion suppressor of prostate and breast cancers.

____ Prostasin down-regulation in invasive prostate and breast cancer cells is the result of promoter DNA hypermethylation at multiple locations.

____ Prostasin's sub-cellular localization has been thoroughly investigated and prostasin's membrane anchorage was confirmed.

____ A prostasin-binding protein has been identified in mouse seminal vesicle. Using this serpin-like protein (in the context of the seminal vesicle extract mixture), we were able to show that the membrane-bound prostasin is an active serine protease.

____ The prostasin-binding protein has been purified and characterized. It is identified as a serpin type serine protease inhibitor, previously known as protease nexin-1 (PN-1).

____ Prostasin is involved in proteolytic activation of the epithelial sodium channel (ENaC), implicating a role for prostasin in epithelial differentiation, also implicating an interaction with maspin.

____ Prostasin re-expression in human prostate cancer cell lines DU-145 and PC-3 elicited cellular protein changes that potentially could implicate prostasin in regulating cell motility. These cellular protein changes are the reduction of tyrosine phosphorylation of a 120-130-kDa protein, suspected to be FAK or p130Cas; and the down-regulation of PKC α protein expression.

____ The speculated role of prostasin in regulating cell motility led to the undertaking of transgenic fly work to investigate membrane serine proteases' roles in cell signaling. *Drosophila* strains expressing human hepsin have been established and used to probe prostate cancer-relevant cell signaling events in flies.

(7) REPORTABLE OUTCOMES:

- manuscripts, abstracts, presentations;

The following papers have been published (reprints attached to report):

1. Chen LM, Hodge GB, Guarda LA, Welch JL, Greenberg NM, Chai KX. Down-regulation of prostasin serine protease: a potential invasion suppressor in prostate cancer. *Prostate*. 2001 Jul 1;48(2):93-103.
2. Chen LM, Skinner ML, Kauffman SW, Chao J, Chao L, Thaler CD, Chai KX. Prostasin is a glycosylphosphatidylinositol-anchored active serine protease. *J Biol Chem*. 2001 Jun 15;276(24):21434-42.
3. Chen LM, Chai KX. Prostasin serine protease inhibits breast cancer invasiveness and is transcriptionally regulated by promoter DNA methylation. *Int J Cancer*. 2002 Jan 20;97(3):323-9.
4. Narikiyo T, Kitamura K, Adachi M, Miyoshi T, Iwashita K, Shiraishi N, Nonoguchi H, Chen LM, Chai KX, Chao J, Tomita K. Regulation of prostasin by aldosterone in the kidney. *J Clin Invest*. 2002 Feb;109(3):401-8.

The following manuscript has been submitted for publication (attached to report):

1. Chen LM, Chai KX. Purification and characterization of the prostasin-binding protein. *J Biol Chem*. 2002, manuscript No. M2-02491

The following manuscripts will be submitted for publication (attached to report):

1. Chen LM, Chai KX. The prostatic gene promoter is hypermethylated in invasive human prostate cancer cells.
2. Bayer CA, Halsell SR, Kiehart DP, von Kalm LH. Genetic analysis of the *Drosophila melanogaster* *Stubble-stubblloid* locus during leg imaginal disc morphogenesis: a potential role for a type-II transmembrane serine protease in RhoA signaling.

The following presentations were made at the meeting indicated:

1. Dabirshahsahebi, S., Willey, J., Bayer, C., Leppert, A., Chai, K. X., and von Kalm, L. (1999) Genetic Analysis of Vertebrate Serine Proteases and Serpins by Mis-expression in the *Drosophila* Eye. Presented at the Southeast Regional *Drosophila* Meeting, Emory University, Atlanta, GA.
2. Chen, L-M., Suffoletto, M., Thaler, C. D., Hodge, G. B., Guarda, L. A., Welch, J. L., Greenberg, N. M., Chao, L., Chao, J., and Chai, K. X. (2000) Prostatic Serine Protease in Prostate Cancer and Identification of A Prostatic-binding Protein. The Society for Basic Urologic Research Fall Symposium at Sanibel Harbour Resort and Spa, Florida.

– patents and licenses applied for and/or issued;

1. A full utility patent application under the title of “A Method of Identifying and Treating Invasive Carcinomas” has been filed with the USPTO. Co-inventors: Karl X. Chai, Li-Mei Chen, Lee Chao, and Julie Chao.

– degrees obtained that are supported by this award;

1. James A. Murphy, Master of Science, 2000. Thesis “The Serine Proteinase Inhibitor, Maspin Does Not Interact with Prostatic in Controlling the Invasive Phenotype of Breast and Prostate Cancer Cells”, University of Central Florida
2. Shabnam Dabirshahsahebi, Master of Science, 2000. Thesis “Genetic Analysis of Human Serine proteases and Serpins by Expression in the *Drosophila* Eye”, University of Central Florida
3. Xiaoyan Zhang, M.D., Master of Science, 2001. Thesis “Prostatic-based Gene Therapy in Transgenic Adenocarcinomatous Mouse Prostate (TRAMP) Model”, University of Central Florida, partially supported by this award.

– funding applied for based on work supported by this award;

1. DoD-PCRP01, “Prostatic’s Role in Prostate Cancer”

Principal Investigator: Karl X. Chai, Ph.D.
 Co-investigator: Li-Mei Chen, M.D., Ph.D.
 Grant Number: DAMD17-02-1-0032
 Type: Idea Award
 Period: 11/19/2001 - 12/28/2004
 Total Direct Cost: \$353,167

2. National Institutes of Health, “The Role of Serine Protease Inhibitors in Fertility”,

Principal Investigator: Li-Mei Chen, M.D., Ph.D.
 Grant Number: HD40241

Period: 01/15/2002 – 01/14/2004
 Total Direct Cost: \$100,000

3. DoD-BCRP01, "Prostasin Serine Protease as A Breast Cancer Invasion Marker And A Metastasis Suppressor"

Principal Investigator: Karl X. Chai, Ph.D.
 Co-investigators: Li-Mei Chen, M.D., Ph.D.; Ying Zhang, Ph.D.
 Grant Number: DAMD17-02-1-0338
 Type: Idea Award
 Period: 07/01/2002 – 06/30/2005
 Total Direct Cost: \$232,776 (pending final negotiation)

The following proposal has been reviewed and is likely to be funded (Priority Score 151):

1. National Institutes of Health, "Serine Protease Action in *Drosophila* Development"

Principal Investigator: Laurence H. von Kalm, Ph.D.
 Proposal Number: 1R15GM65884-01
 Period: 07/01/02 – 06/30/05
 Total Direct Cost: \$100,000

- List of personnel receiving pay

Li-Mei Chen, M.D., Ph.D.
 Cynthia A. Bayer, Ph.D.

(8) CONCLUSIONS:

We have demonstrated that prostatic serine protease is a novel invasion suppressor of prostate and breast cancers and have discovered a molecular mechanism for its down-regulation in cancer, promoter DNA hypermethylation. We have investigated prostatic's cellular and biochemical properties and paved the way for an in-depth investigation of the mechanisms of prostatic's biological functions. We have also established a model system in the fruit fly for an in-depth investigation of hepsin signaling as hepsin is now recognized as a potential prostate cancer marker.

"So What Section" The currently completed research has the following implications toward the diagnosis or treatment of human prostate cancer:

- 1). An assay (test) may be established to determine the level of production of human prostatic in prostate cancer using an immunological reagent (antibody) for diagnosis or prognosis of the invasiveness of prostate cancer since we have demonstrated a correlation between prostatic's down-regulation and prostate cancer grade.
- 2). A molecular genetic assay (test) may also be established to determine the methylation state of the prostatic promoter in prostate cancer and the result may be applicable to prostate cancer diagnosis or prognosis.
- 3). Our demonstration of prostatic serine protease activity in the membrane-bound form may lead us to the identification of prostate cancer relevant molecules. The identification and investigation of these molecules will offer us better understanding of the progression of prostate cancer and may lead to the development of diagnostics and drugs.

REFERENCES:

- Adachi M, Kitamura K, Miyoshi T, Narikiyo T, Iwashita K, Shiraishi N, Nonoguchi H, Tomita K. Activation of epithelial sodium channels by prostasin in *Xenopus* oocytes. *J Am Soc Nephrol*. 2001 Jun;12(6):1114-21.
- Bayer CA, Halsell SR, Kiehart DP, von Kalm LH. Genetic analysis of the *Drosophila* melanogaster *Stubble-stubblloid* locus during leg imaginal disc morphogenesis: a potential role for a type-II transmembrane serine protease in RhoA signaling. 2002, to be submitted.
- Cary LA, Guan JL. Focal adhesion kinase in integrin-mediated signaling. *Front Biosci*. 1999 Jan 15;4:D102-13.
- (a) Chen LM, Hodge GB, Guarda LA, Welch JL, Greenberg NM, Chai KX. Down-regulation of prostasin serine protease: a potential invasion suppressor in prostate cancer. *Prostate*. 2001 Jul 1;48(2):93-103.
- (b) Chen LM, Skinner ML, Kauffman SW, Chao J, Chao L, Thaler CD, Chai KX. Prostasin is a glycosylphosphatidylinositol-anchored active serine protease. *J Biol Chem*. 2001 Jun 15;276(24):21434-42.
- (a) Chen LM, Chai KX. Prostasin serine protease inhibits breast cancer invasiveness and is transcriptionally regulated by promoter DNA methylation. *Int J Cancer*. 2002 Jan 20;97(3):323-9.
- (b) Chen LM, Chai KX. Purification and characterization of the prostasin-binding protein. *J Biol Chem*. 2002, manuscript No. M2-02491.
- (c) Chen LM, Chai KX. The prostasin gene promoter is hypermethylated in invasive human prostate cancer cells. 2002, to be submitted.
- Dhanasekaran SM, Barrette TR, Ghosh D, Shah R, Varambally S, Kurachi K, Pienta KJ, Rubin MA, Chinnaiyan AM. Delineation of prognostic biomarkers in prostate cancer. *Nature*. 2001 Aug 23;412(6849):822-6.
- Donaldson SH, Hirsh A, Li DC, Holloway G, Chao J, Boucher RC, Gabriel SE. Regulation of the epithelial sodium channel by serine proteases in human airways. *J Biol Chem*. 2002 Mar 8;277(10):8338-45.
- Ichigi J, Asashima M. Dome formation and tubule morphogenesis by *Xenopus* kidney A6 cell cultures exposed to microgravity simulated with a 3D-clinostat and to hypergravity. *In Vitro Cell Dev Biol Anim*. 2001 Jan;37(1):31-44.
- Kazama Y, Hamamoto T, Foster DC, Kisiel W. Hepsin, a putative membrane-associated serine protease, activates human factor VII and initiates a pathway of blood coagulation on the cell surface leading to thrombin formation. *J Biol Chem*. 1995 Jan 6;270(1):66-72.

- Kim HG, Kassis J, Souto JC, Turner T, Wells A. EGF receptor signaling in prostate morphogenesis and tumorigenesis. *Histol Histopathol*. 1999 Oct;14(4):1175-82.
- Luo J, Duggan DJ, Chen Y, Sauvageot J, Ewing CM, Bittner ML, Trent JM, Isaacs WB. Human prostate cancer and benign prostatic hyperplasia: molecular dissection by gene expression profiling. *Cancer Res*. 2001 Jun 15;61(12):4683-8.
- Magee JA, Araki T, Patil S, Ehrig T, True L, Humphrey PA, Catalona WJ, Watson MA, Milbrandt J. Expression profiling reveals hepsin overexpression in prostate cancer. *Cancer Res*. 2001 Aug 1;61(15):5692-6.
- Narikiyo T, Kitamura K, Adachi M, Miyoshi T, Iwashita K, Shiraishi N, Nonoguchi H, Chen LM, Chai KX, Chao J, Tomita K. Regulation of prostaticin by aldosterone in the kidney. *J Clin Invest*. 2002 Feb;109(3):401-8.
- Scott RW, Bergman BL, Bajpai A, Hersch RT, Rodriguez H, Jones BN, Barreda C, Watts S, Baker JB. Protease nexin. Properties and a modified purification procedure. *J Biol Chem*. 1985 Jun 10;260(11):7029-34.
- Sheng S, Carey J, Seftor EA, Dias L, Hendrix MJ, Sager R. Maspin acts at the cell membrane to inhibit invasion and motility of mammary and prostatic cancer cells. *Proc Natl Acad Sci U S A*. 1996 Oct 15;93(21):11669-74.
- Stamey TA, Warrington JA, Caldwell MC, Chen Z, Fan Z, Mahadevappa M, McNeal JE, Nolley R, Zhang Z. Molecular genetic profiling of Gleason grade 4/5 prostate cancers compared to benign prostatic hyperplasia. *J Urol*. 2001 Dec;166(6):2171-7.
- Timar J, Raso E, Fazakas ZS, Silletti S, Raz A, Honn KV. Multiple use of a signal transduction pathway in tumor cell invasion. *Anticancer Res*. 1996 Nov-Dec;16(6A):3299-306.
- Torres-Rosado A, O'Shea KS, Tsuji A, Chou SH, Kurachi K. Hepsin, a putative cell-surface serine protease, is required for mammalian cell growth. *Proc Natl Acad Sci U S A*. 1993 Aug 1;90(15):7181-5.
- Wittmann T, Waterman-Storer CM. Cell motility: can Rho GTPases and microtubules point the way? *J Cell Sci*. 2001 Nov;114(Pt 21):3795-803.
- von Kalm L, Fristrom D, Fristrom J. The making of a fly leg: a model for epithelial morphogenesis. *Bioessays*. 1995 Aug;17(8):693-702.
- Vallet V, Pfister C, Loffing J, Rossier BC. Cell-Surface Expression of the Channel Activating Protease xCAP-1 Is Required for Activation of ENaC in the *Xenopus* Oocyte. *J Am Soc Nephrol*. 2002 Mar;13(3):588-94.
- Vuagniaux G, Vallet V, Jaeger NF, Pfister C, Bens M, Farman N, Courtois-Coutry N, Vandewalle A, Rossier BC, Hummler E. Activation of the amiloride-sensitive epithelial sodium channel by the serine protease mCAP1 expressed in a mouse cortical collecting duct cell line. *J Am Soc Nephrol*. 2000 May;11(5):828-34.

Yu JX, Chao L, Chao J. Prostasin is a novel human serine proteinase from seminal fluid. Purification, tissue distribution, and localization in prostate gland. J Biol Chem. 1994 Jul 22;269(29):18843-8.

Zhang M, Volpert O, Shi YH, Bouck N. Maspin is an angiogenesis inhibitor. Nat Med. 2000 Feb;6(2):196-9.

Zucchi I, Bini L, Valaperta R, Ginestra A, Albani D, Susani L, Sanchez JC, Liberatori S, Magi B, Raggiaschi R, Hochstrasser DF, Pallini V, Vezzoni P, Dulbecco R. Proteomic dissection of dome formation in a mammary cell line: role of tropomyosin-5b and maspin. Proc Natl Acad Sci U S A. 2001 May 8;98(10):5608-13.

Down-Regulation of Prostasin Serine Protease: A Potential Invasion Suppressor in Prostate Cancer

Li-Mei Chen,¹ G. Byron Hodge,² Luis A. Guarda,³ James L. Welch,⁴
Norman M. Greenberg,⁵ and Karl X. Chai^{1*}

¹Department of Molecular Biology and Microbiology, University of Central Florida, Orlando, Florida

²Walt Disney Memorial Cancer Institute, Florida Hospital, Orlando, Florida

³Department of Pathology, Florida Hospital, Orlando, Florida

⁴Urologic Oncology, M.D. Anderson Cancer Center, Orlando, Florida

⁵Department of Cell Biology, Baylor College of Medicine, Houston, Texas

BACKGROUND. Prostasin is a serine protease predominantly expressed in normal prostate epithelial cells. The biological function of prostasin has not been determined.

METHODS. Western blot and RT-PCR analyses were used to examine the expression of prostasin in prostate cancer cell lines. Immunohistochemistry was used to evaluate prostasin protein expression in human prostate cancer. An in vitro Matrigel invasion assay was used to test the invasiveness of prostate cancer cell lines forced to express recombinant prostasin.

RESULTS. Both prostasin protein and mRNA were found to be expressed in normal human prostate epithelial cells and a non-invasive human prostate cancer cell line, the LNCaP, but neither was found in invasive human prostate cancer cell lines DU-145 and PC-3. Prostasin mRNA expression was absent in invasive prostate cancer cell lines of a transgenic mouse model. Immunohistochemistry analysis showed that prostasin protein expression is down-regulated in high-grade prostate cancer. Transfection of DU-145 and PC-3 cells with a full-length human prostasin cDNA restored prostasin expression and reduced the in vitro invasiveness by 68 and 42%, respectively.

CONCLUSIONS. Our data indicate that prostasin may be implicated in normal prostate biology and is able to suppress prostate cancer invasion in vitro. *Prostate* 48:93–103, 2001.

© 2001 Wiley-Liss, Inc.

KEY WORDS: cell line; gene expression; immunohistochemistry; prostatectomy; transfection

INTRODUCTION

For men in the US, prostate cancer is the most commonly diagnosed cancer, and the second leading cause of cancer-related death [1]. The primary goals of prostate cancer research are to find new markers or assays for early detection, and new methods to control invasion and metastasis. Our laboratory's research focus is on the roles played by serine proteases and serine protease inhibitors in the development or progression of cancer. In this report we describe the results on a serine protease, prostasin [2].

The conventional paradigm of protease involvement in the development and progression of cancer

has been the assignment of a usually negative role to the proteases, such as promoting tumor invasion [3]. In turn, the conventional paradigm of protease inhibitors in relation to cancer is usually a regard of

Grant sponsor: Department of Defense Prostate Cancer Research Program; Grant number: DAMD17-98-1-8590 (to K.X.C.); Grant sponsor: Florida Hospital Gala Endowed Program for Oncologic Research (to K.X.C.); Grant sponsor: National Cancer Institute Grant CA64851 (to N.M.G.).

*Correspondence to: Karl X. Chai, Department of Molecular Biology and Microbiology, University of Central Florida, 4000 Central Florida Boulevard, Orlando, FL 32816-2360.
E-mail: kxchai@mail.ucf.edu

Received 7 December 2000; Accepted 16 March 2001

a beneficial effect for the presence of these molecules [4]. Recently, however, the picture of a new paradigm is beginning to emerge for several serine proteases in breast, prostate, and testicular cancers. A "normal epithelial cell specific-1" (NES1) serine protease was found to be down-regulated in breast and prostate cancers, and it functions as a tumor suppressor [5]. A prostate-specific serine protease, prostase [6], was shown to be expressed in normal prostate but not in prostate cancer cell lines DU-145 and PC-3. The expression of a testis-specific serine protease, testisin, was shown to be lost in testicular cancer through either a loss of gene [7] or methylation in the promoter [8]. Further, transfection of human testicular cancer cells with a testisin cDNA reduced the tumor growth of xenografts of these cells in nude mice, suggesting a tumor suppressor function for testisin [8]. The testisin serine protease is potentially membrane-bound as suggested by its structure and confirmed by immunohistochemistry [7].

Prostasin serine protease is an acidic protein (pI 4.5–4.8) of approximately 40 kDa in molecular mass [2]. It is predominantly made in the prostate gland (~140 ng/mg protein), with lesser amounts (2–6 ng/mg protein) also found in the bronchi, colon, kidney, liver, lung, pancreas, and the salivary glands [2]. Prostasin is secreted in the prostatic fluid, and can be detected in the semen (~9 µg/ml). Prostasin expression is localized to the epithelial cells of human prostate gland by in situ hybridization histochemistry using an antibody or an anti-sense RNA probe [2,9]. Molecular cloning of a full-length human prostasin cDNA revealed that its predicted amino acid residue sequence contains a carboxyl-terminal hydrophobic region that can potentially anchor the protein on the membrane [9]. At the amino acid level, prostasin is similar to plasma kallikrein, coagulation factor XI, hepsin, plasminogen, acrosin, prostase, and, in particular, testisin (sharing 44% sequence identity) [6,7,9]. A membrane-bound, *Xenopus* kidney epithelial cell sodium channel-activating protease (CAP1) was shown to be highly homologous to human prostasin as well (sharing 53% sequence identity at the amino acid level) [10]. Prostasin is encoded by a single-copied gene, which is located on human chromosome 16p11.2 [11].

The secreted prostasin cleaves synthetic substrates in vitro preferentially at the carboxyl-terminal side of Arg residue, and is thus considered a trypsin-like serine protease [2]. The physiological function of prostasin, however, has remained unknown. In an effort to define the physiological function of prostasin, we examined the expression of this protease in primary human prostate epithelial cells or human prostate cancer cell lines. Our findings indicated a

potential down-regulation of prostasin in highly invasive prostate cancer cells. Three prostate cancer cell lines derived from the transgenic adenocarcinoma of the mouse prostate (TRAMP) model [12] were also shown to have null or reduced prostasin expression at the mRNA level. A down-regulation of prostasin protein expression was demonstrated in immunohistochemistry studies of prostate cancer tissue sections. These results implicate a function for prostasin serine protease in normal prostate, and its loss of expression may contribute to tumor progression. To test our hypothesis, we transfected invasive human prostate cancer cells with a full-length human prostasin cDNA, and showed that a restoration of prostasin expression reduces the invasiveness of the cancer cells in vitro.

MATERIALS AND METHODS

Cell Culture

All tissue culture media, sera, and supplements were purchased from LifeTechnologies (Gaithersburg, MD), except for those noted otherwise.

A normal human prostate epithelial cell primary culture (CC-2555) was obtained from Clonetics (San Diego, CA), and maintained in the supplied medium (prostate epithelial cell basal medium, containing bovine pituitary extract, hydrocortisone, human epidermal growth factor, epinephrine, transferrin, insulin, retinoic acid, tri-iodothyronine, gentamicin, and amphotericin). The culture was kept at 37°C with 5% CO₂ and used for experiments at the third passage.

Human prostate cancer cell lines LNCaP, DU-145, and PC-3 were obtained from the American Type Culture Collection (ATCC, Manassas, VA). The PC-3 cells were maintained in F-12K medium supplemented with 10% fetal bovine serum (FBS) while the LNCaP and the DU-145 cells were maintained in RPMI-1640 medium supplemented with 10% FBS and 1 mM sodium pyruvate, and all were kept at 37°C with 5% CO₂.

The TRAMP-C1, C2, and C3 cell lines derived from the TRAMP model were cultured as previously described [12], in D-MEM with high glucose and L-glutamine, but without sodium pyruvate; supplemented with 5% Nu-serum (Collaborative Biochemical, Bedford, MA), 5% FBS, 5 µg/ml insulin, and 10⁻⁸ M dihydrotestosterone (DHT, Sigma-Aldrich Co., St Louis, MO), at 37°C with 5% CO₂.

RNA Preparation and Analysis by RT-PCR–Southern Blot

Prostates of C57BL/6 mice (Harlan, Indianapolis, IN), or confluent cell cultures were used for total RNA

extraction using the RNeasy kit from QIAGEN (Valencia, CA). The use of animals was approved by the IACUC of the University of Central Florida.

The human prostasin-specific RT-PCR (reverse transcription-polymerase chain reaction)/Southern blot analysis was performed as described previously [9]. One microgram of total RNA was used in the RT-PCR with two human prostasin gene-specific oligonucleotide primers [9], a Southern blot of the resolved RT-PCR samples was probed with a third prostasin gene-specific oligonucleotide [9], detecting an amplified 232 bp fragment.

The mouse prostasin-specific RT-PCR was performed using the following oligonucleotide primers: upstream, 5'-ATC ACC GGT GGT GGC AGT GC-3', downstream, 5'-TGG CTG CAG GGA GGC AGA TG-3' which were derived from a mouse prostasin mRNA (cDNA) sequence (GenBank Accession Number: A1527990). This reported mouse prostasin cDNA sequence is 73% identical to the reported human prostasin cDNA sequence [9]. The sequence of the downstream RT-PCR primer is complementary to both the human and mouse prostasin mRNA, while the upstream PCR primer is unique to the mouse prostasin mRNA. The PCR fragment that was amplified with these two primers is 342 bp in length. We probed the amplified PCR product with a full-length human prostasin cDNA to confirm the identity of the amplified PCR fragment as the mouse prostasin homolog. One microgram of RNA was used in the RT (at 37°C for 1 h followed by 94°C for 5 min) and the PCR with the following program: 94°C/1 min-60°C/1 min-72°C/2 min for 30 cycles. One-fifth of the PCR product for each sample was resolved in a 0.8% agarose gel, Southern-transferred to an Immobilon-N membrane (Fisher Scientific, Pittsburgh, PA), and probed with a full-length human prostasin cDNA labeled by nick-translation using a reagent kit (Life Technologies). Following the hybridization, the membrane was washed to a final stringency of 1×SSPE/0.1% SDS (1×SSPE: 0.18 M NaCl, 10 mM NaH₂PO₄, 1 mM Na₂EDTA, pH 7.4), at 60°C before an exposure of 30 min at -80°C to an X-ray film without an intensifying screen.

In both the human and mouse prostasin-specific RT-PCR, the following primers were used to co-amplify the β -actin mRNA for control of RNA quality and quantity: upstream, 5'-GAA CCC TAA GGC CAA CCG TG-3', downstream, 5'-TGG CAT AGA GGT CTT TAC GG-3'.

Tissue Specimens and Immunohistochemistry

Human prostate tissues were obtained from radical prostatectomies performed at the Florida Hospital

South Orlando location, Orlando, FL, or the Orlando Regional Medical Center (ORMC), Orlando, FL. The procurement of human tissues was approved by the Institutional Review Boards (IRB) of Florida Hospital, ORMC, and the University of Central Florida. None of the subjects examined in our study underwent prior hormonal, radiation, or chemotherapy. Tissues were fixed in formalin, paraffin-embedded, and sectioned at 4 μ m thickness. The sections used in our study contained both benign and neoplastic tissues, as evaluated upon hematoxylin/eosin staining of the adjacent sections.

Immunohistochemistry was performed according to Yu et al. [2] with some modifications. Briefly, the human prostate sections were de-paraffinized in Hemo-De (Fisher Scientific) followed by rehydration in a decreasing series of alcohol. The prostate sections were subjected to a standard antigen retrieval procedure (BD PharMingen, San Diego, CA) in citrate buffer, pH 6.0, followed by treatment in 3% H₂O₂. After blocking the sections with 10% goat serum (Life Technologies) in TBS-T (10 mM Tris-HCl, pH 7.6, and 150 mM NaCl, containing 0.1% Triton X-100), a prostasin-specific antibody [2] (diluted at a ratio of 1:500 in the blocking solution) was added for an incubation of 2 h, followed by an incubation of 1 h with the secondary antibody, goat anti-rabbit IgG (Sigma-Aldrich Co., used at 20 μ g/ml). The sections were then incubated with the peroxidase: anti-peroxidase complex (Sigma-Aldrich Co., 1:200) for 1 h. Sections were washed in TBS/0.1% Tween-20 between steps. The color reaction was performed by incubating the sections with 3,3'-diaminobenzidine tetrahydrochloride (0.5 mg/ml, Life Technologies) and H₂O₂ (0.03%) for 15 min. The prostate sections were then counterstained with hematoxylin, dehydrated in an increasing series of alcohol, and mounted with Permount (Fisher Scientific). Control sections were treated with the same procedures as described above, except that a pre-immune rabbit serum was used in place of the prostasin-specific antiserum.

Evaluation of Immunohistochemical Staining

Sections from 39 radical prostatectomy specimens were subjected to prostasin immunostaining. For each section used in prostasin immunostaining, an adjacent section was stained with hematoxylin/eosin and evaluated by a pathologist (L.A.G.) to determine tumor Gleason grades [13]. Prostasin immunostaining in each tumor area with a distinct Gleason grade was recorded as a separate observation (n). For each case, we selected 1-4 sections to examine the different regions of the prostate from the patient. In total, 128 sections were evaluated. Prostasin immunostaining in

TABLE I. Summary of Prostatic Immunostaining in Human Prostate Sections

	Benign	Tumor Gleason grade		
		1-2	3	4-5
Total areas examined (n)	128	15	36	26
Positively stained areas (n)	114	14	16	4
Negatively stained areas (n)	14	1	20	22
Percentage of positive staining (%)	89.0	93.3	44.4	15.4
Mean staining score	2.024	1.933	0.889	0.308

Differences in prostatic staining intensity were examined by analysis of variance (ANOVA). The expression of prostatic was significantly decreased in high-grade prostate tumor as compared with benign prostate or lowgrade prostate tumor ($P < 0.0001$).

the prostate sections was evaluated by adopting, with modifications, the scoring system used for Hercep-Test™ (DAKO Corporation, Carpinteria, CA). A score of 0 is assigned to areas with no staining. A score of 1 (+) is assigned to areas with faint epithelial staining and/or staining in fewer than 10% of cells. Scores 0 and 1 are defined as negative for the data summarized in Table I. A score of 2 (++) is assigned to areas with moderate epithelial staining in more than 10% of cells, and a score of 3 (+++) is assigned to areas with strong staining in more than 10% of cells. Scores 2 and 3 are defined as positive for the data summarized in Table I. Areas selected for scoring were viewed under 100× magnifying power. The differences in prostatic-specific staining mean scores between tumor grades were examined by analysis of variance (ANOVA, defining $P < 0.05$ as being significant).

Transfection of Cell Lines with Plasmid DNA and Selection of Stable Transfectants

A pREP-8 (Invitrogen, Carlsbad, CA) plasmid carrying a full-length human prostatic cDNA [9] was provided by Dr. Julie Chao of the Medical University of South Carolina (Charleston, SC). This plasmid was used to transfect the DU-145 cells. For transfection of the PC-3 cells, we re-engineered the plasmid as follows. The histidinol-resistance element of this human prostatic cDNA plasmid was removed via a *Bgl* II digestion (a 3,475 bp fragment), and replaced with a neomycin (G418)-resistance element, via an *EcoR* V-*Dra* I fragment (3,439 bp) of the pcDNA3 vector (Invitrogen). The resulting plasmid contains a full-length human prostatic cDNA under the control of the RSV promoter, a G418-resistance element, and the EBNA-1 element for episomal expression in primate cells. A similar drug-resistance gene rearrangement was made for the pREP-8 plasmid without the

human prostatic cDNA, and the resulting plasmid was used as a vector control in our experiments. Drug-resistance genes were rearranged to make the new prostatic cDNA plasmid carry a G418-resistance element, because in our earlier experiments we found that the PC-3 cell line was not sensitive to the histidinol drug selection.

Transfection was carried out using a BTX-600 Electro-Cell-Manipulator (Gentronics, San Diego, CA) according to the recommended procedures. Briefly, 1,000,000 pelleted cells were re-suspended in 0.3 ml of the culture medium, and mixed with 50 µg of plasmid DNA dissolved in 0.1 ml of sterile distilled water. The cell/DNA mixture was then transferred to a 4 mm cuvette and pulsed at 200 V, 1600 µF, 72 Ω, and 500 V/C setting on the BTX-600. Following the pulse, cells remained in the cuvette at room temperature for 30 min before being transferred to a 25 cm² tissue culture flask containing the proper culture medium.

At 24 h post-electroporation, the culture medium was replaced with fresh medium containing either 5 mM histidinol (for DU-145 selection) or 800 µg/ml G418 (for PC-3 selection) and maintained in the presence of the drugs until colonies appeared (5–7 days). Colonies (100–200) were then dispersed via trypsinization, and maintained in the presence of drugs as a polyclonal culture without colony isolation. Cells transfected with the human prostatic cDNA plasmids were assayed in Western blot analysis for expression of the prostatic protein, using vector-transfected cells as negative control.

Western Blot Analysis

Cells grown to 80–100% confluence were washed three times in 1× PBS (phosphate-buffered saline, pH 7.4), and then lysed in TBS containing 1% Triton X-100 on ice for 30 min. The total lysates were

centrifuged at 14,000 rpm for 30 min at 4°C to remove the pellet. Protein concentration was determined using a DC (detergent compatible) protein assay kit (Bio-Rad, Hercules, CA). The samples were then subjected to SDS-PAGE followed by Western blot analysis using a prostasin-specific antibody [2]. Briefly, cell lysates were resolved in 10% gels under reducing conditions before electrotransfer to nitrocellulose (NC) membranes (Fisher Scientific). Upon complete protein transfer, the NC membranes were blocked in BLOTTO (5% non-fat milk made with TBS/0.1% Tween-20, pH 7.6), incubated with the prostasin-specific antibody diluted at a ratio of 1:2,000 in BLOTTO, followed by an incubation with the secondary antibody, goat anti-rabbit IgG conjugated to HRP (horse-radish peroxidase) (Sigma-Aldrich Co.; used at 1:10,000). The bound secondary antibody was detected using enhanced-chemiluminescence (ECL) reagents (Pierce, Rockford, IL) according to the supplier's recommendations. All procedures were performed at room temperature, and the membranes were washed between steps.

Matrigel Chemoinvasion Assay

An *in vitro* Matrigel chemoinvasion assay was performed as follows. Basement membrane Matrigel stock (10 mg/ml, Collaborative Biochemical, Bedford, MA) was thawed overnight on ice in a refrigerator (0–4°C). Transwell invasion chambers (Costar, Cambridge, MA) with 8 µm pore polycarbonate filters (growth area 0.33 cm²) were coated with a diluted Matrigel (50 µg/filter, a 1:3 dilution of the stock with chilled serum-free medium was used for coating). The gel was solidified by incubating the coated filters at 37°C for 60 min in a moist chamber. The lower chambers of the Transwell plates were filled with 0.6 ml serum-free medium, supplemented with 25 µg/ml fibronectin (Sigma-Aldrich Co.). Ten thousand cells in 0.1 ml serum-free OPTI-MEM I medium were placed onto each Matrigel-coated filter. The filter cartridge was then inserted into the lower chamber and the assembled plates were incubated at 37°C for 24 h. After removing the medium, the filters were washed three times in 1× PBS, fixed at room temperature for 20 min in 4% paraformaldehyde made with 0.1 M phosphate buffer (pH 7.4), and then washed three times with the phosphate buffer. The filters were then stained with 1% toluidine blue (LabChem, Inc., Pittsburgh, PA) for 2 min. The cells on the Matrigel surface were removed with a Q-tip, and all cells on the underside of each filter were counted under a light microscope after mounting the filter on a glass slide. The invasion assays were done in triplicates per cell type for three times.

RESULTS

Prostasin Expression Is Absent in Invasive Prostate Cancer Cell Lines

Normal human prostate epithelial cells and three human prostate cancer cell lines were subjected to Western blot analysis using a prostasin-specific antibody. As shown in Figure 1 (upper panel), prostasin is detected as a 40 kDa band in normal human prostate epithelial cells (CC-2555) and in the non-invasive prostate cancer cell line LNCaP. The prostasin protein was not detected in two highly invasive human prostate cancer cell lines, DU-145 and PC-3, when the same amount of total cellular protein was analyzed.

By means of RT-PCR/Southern blot analysis, we demonstrated a corresponding difference of prostasin mRNA expression in these cells as well. Prostasin mRNA is detected in the CC-2555 and LNCaP cells, but not in the DU-145 or PC-3 cells (Fig. 1, middle panel). A co-amplification of a house-keeping gene, β -actin, message (Fig. 1, lower panel) was used as a control for the quantity and quality of the RNA used.

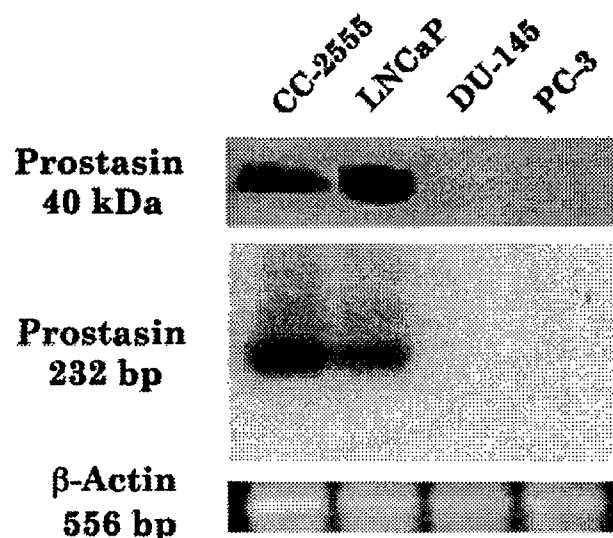


Fig. 1. Human prostasin expression in prostate epithelial cells. By means of Western blot analysis (upper panel), prostasin (as a 40 kDa band) was detected in normal human prostate epithelial cells (CC-2555) and the LNCaP cells, but not in the DU-145 or PC-3 cells. An equal amount of total protein (100 µg) was loaded for each sample. At the mRNA level, human prostasin mRNA (via a 232 bp amplified DNA band) was detected in normal prostate epithelial cells (CC-2555) and the LNCaP cells, but not in the DU145 or PC-3 cells as analyzed by RT-PCR/Southern blot hybridization (middle panel). Co-amplification of a 556 bp human β -actin message (as shown in the gel photograph in the lower panel) confirmed the quality and the quantity of the RNA applied in each RT-PCR.

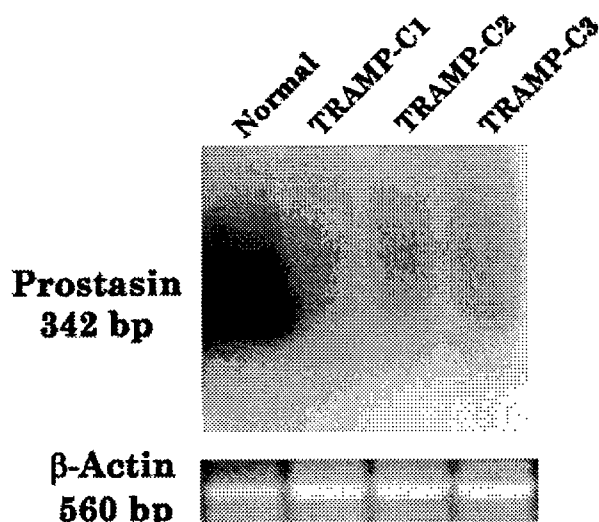


Fig. 2. Mouse prostatic mRNA expression. Total RNA (1 μ g) from a normal mouse prostate (whole), and the TRAMP-C cells were subjected to an RT-PCR using two mouse prostatic-specific oligonucleotide primers (see Materials and Methods). The amplified mouse prostatic message (a cDNA band of 342 bp) was then probed with a full-length human prostatic cDNA, as shown in the autoradiogram in the upper panel. Note the strong signal of mouse prostatic message in the normal prostate RNA sample but not in RNA samples of the TRAMP-C cells. Co-amplification of a 560 bp mouse β -actin message (as shown in the gel photograph in the lower panel) confirmed the quality and the quantity of the RNA applied in each RT-PCR.

The data indicate that prostatic expression is lost in highly invasive human prostate cancer cell lines.

Loss of prostatic expression was also seen in mouse prostate cancer cell lines. Since the human prostatic antibody does not cross-react with the mouse prostatic protein (data not shown), we examined mouse prostatic expression in the cell lines by RT-PCR/Southern blot hybridization with a human prostatic cDNA probe. Mouse prostatic mRNA was detected in normal mouse prostate, but was not detected in the TRAMP-C cell lines (Fig. 2, upper panel). Again, a co-amplification of a mouse house-keeping gene, β -actin, message was used as a control for RNA quantity and quality (Fig. 2, lower panel). A weak amplified mouse prostatic mRNA signal could be seen in the non-tumorigenic [12] TRAMP-C3 cells after a prolonged exposure, but not in the tumorigenic and invasive [12,14] TRAMP-C1 and TRAMP-C2 cells (data not shown).

Expression of Prostatic Protein Is Reduced in Human Prostate Cancer

Prostatectomy specimens from 39 patients (128 sections) were subjected to immunohistochemistry

using a prostatic-specific antibody. Overall, in non-tumor or benign prostate epithelia, 89.0% of the examined areas demonstrated positive staining for prostatic protein and 11.0% were considered negative (see MATERIALS AND METHODS for scoring criteria). In tumor specimens that were examined, prostatic was detected in 93.3% of the low Gleason grade areas (\leq grade 2), 44.4% of Gleason grade 3 areas, and 15.4% of Gleason grade 4–5 areas (data summarized in Table I). The mean prostatic immunostaining score was found significantly decreased in high-grade prostate tumors as compared to that of non-tumor or low-grade (1–2) areas (ANOVA, $P < 0.0001$).

Representative staining images of non-tumor (benign) areas and prostate tumor areas are shown in Figure 3. The prostatic protein was detected in the cytoplasm and on the plasma membrane (apical) of benign epithelial cells lining the secretory lumen as well as in the secretion inside the lumen (Fig. 3A and B, score 3, or +++), confirming the results of Yu et al. [2]. When a pre-immune rabbit serum was used in place of the prostatic antiserum, no staining was observed in either the non-tumor epithelia (Fig. 3C and D) or tumor epithelia (Fig. 3E). Tumor epithelia displayed various degrees of prostatic immunostaining as shown in Figure 3F–L. In Gleason grade 1–2 tumors, moderate prostatic staining was seen in the cytoplasm and on the plasma membrane of some epithelial cells, as well as in the secretion in the lumen (Fig. 3G and H, score 2, or ++). In Gleason grade 3 tumors, a lesser number of epithelial cells displayed the moderate level prostatic staining (Fig. 3I and J). In Gleason grade 4–5 tumors, most epithelial cells did not show any prostatic staining, while some prostatic staining can be seen in rare, sporadic tumor cells (Fig. 3K and L, as indicated by the arrow, score 0).

Re-Expression of Human Prostatic Protein in Invasive Human Prostate Cancer Cells Reduces Invasiveness In Vitro

Following the electroporation and drug selection, 100–200 colonies formed for each transfected cell type. All colonies for each transfected cell type were kept in a mixed culture as polyclonal transfectants for the ensuing experiments. Polyclonal DU-145 and PC-3 cells transfected with the human prostatic cDNA (designated DU-145/Pro, and PC-3/Pro, respectively) were confirmed to express the human prostatic protein, as shown in the Western blot analysis of the cell lysates (Fig. 4, upper panel). The vector-transfected cells, designated DU-145/Vector or PC-3/Vector, respectively, were used as negative control in

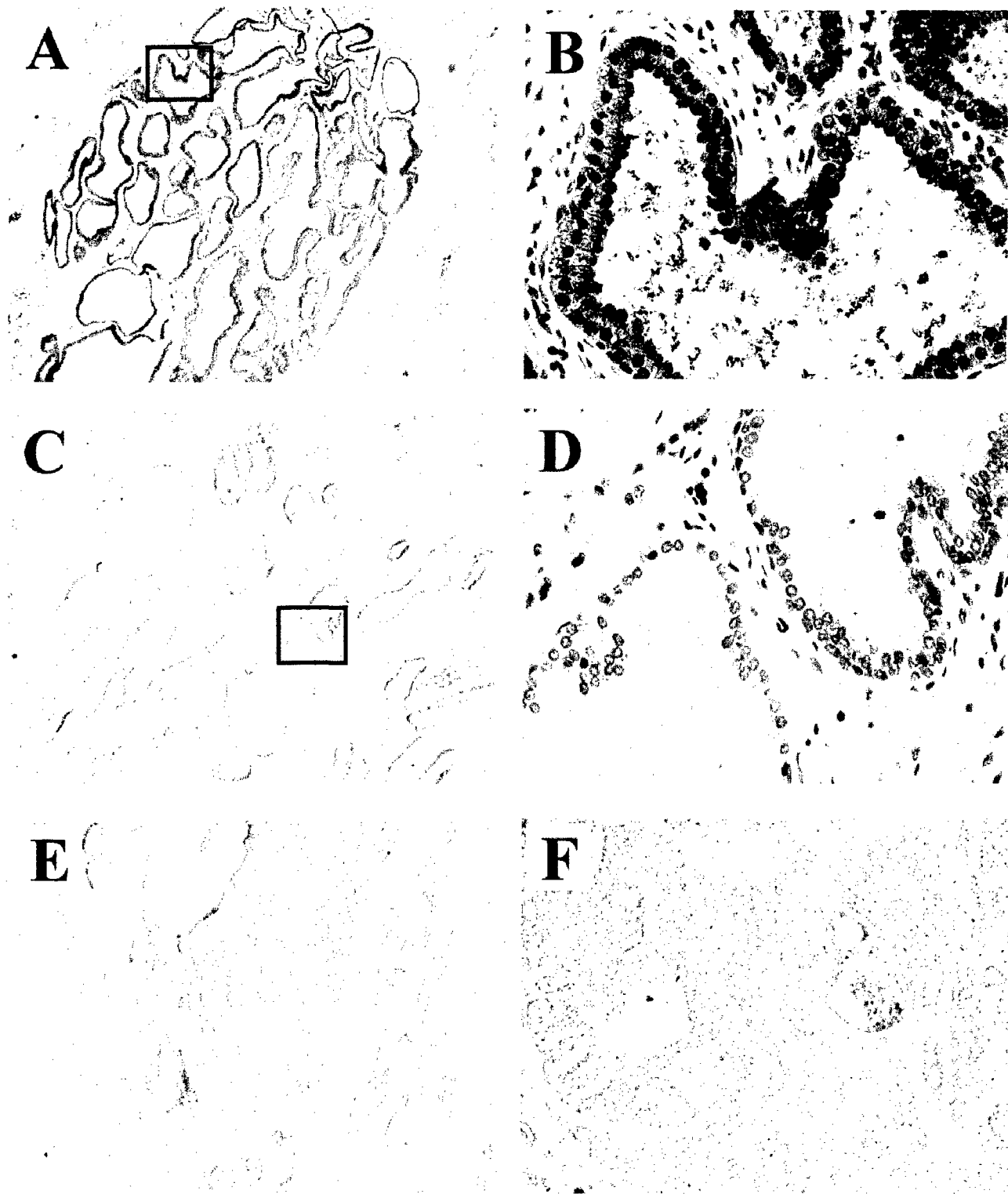


Fig. 3. Immunoperoxidase staining of prostaticin in human prostate. Paraffin-embedded human prostate sections were stained for prostaticin protein expression evaluation using a specific antibody [2] as described in MATERIALS AND METHODS. Prostaticin-positive staining (brown color) was detected in the cytoplasm and apical membrane in non-tumor or benign epithelial cells (image **A**, or **B**; the boxed area of **A**). When prostaticin antibody was omitted in the immunohistochemistry procedures, neither non-tumor (image **C**, or **D**; the boxed area of **C**), nor tumor epithelial cells (image **E**) displayed any staining. Tumor epithelial cells showed reduced prostaticin staining (image **F**) as compared to non-tumor epithelial cells in adjacent areas (image **F**). Representative areas in which prostaticin staining is reduced in tumor epithelial cells are shown in image **G**, or **H**: the boxed area of **G** (Gleason grade 2); image **I**, or **J**: the boxed area of **I** (Gleason grade 3), and image **K**, or **L**: the boxed area of **K** (Gleason grade 4). Magnification: **A**, **C**, **E**, **I**, and **K**: 25 \times ; **G**: 100 \times ; **B**, **D**, **F**, **H**, **J** and **L**: 200 \times .

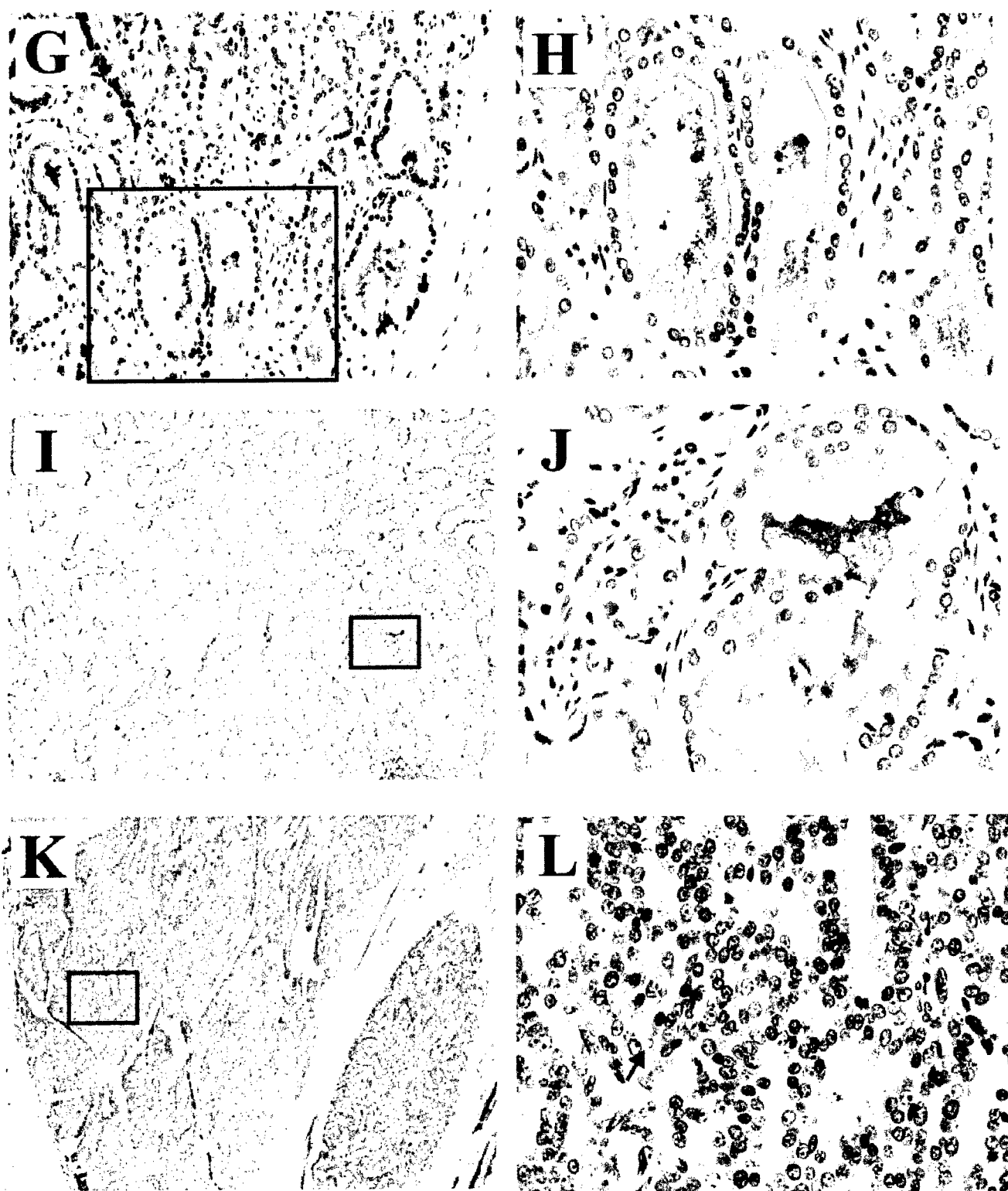


Fig. 3. (Continued)

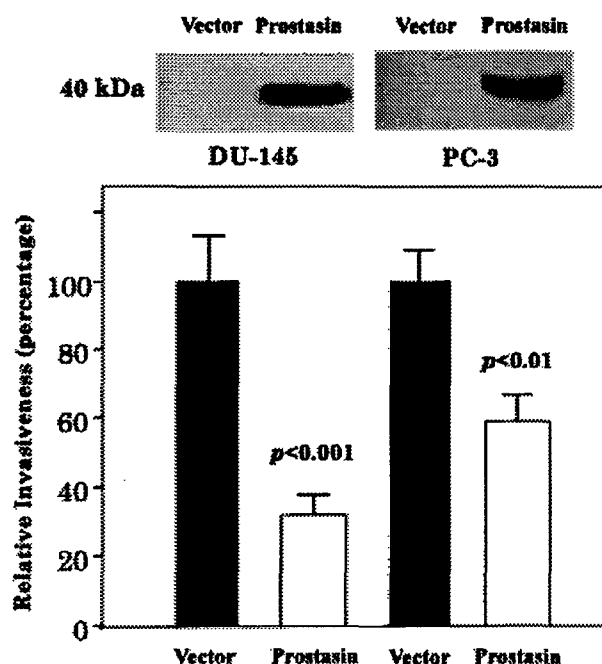


Fig. 4. Recombinant prostasin protein expression and in vitro invasive properties of the DU-145 and the PC-3 transfectants. DU-145 or PC-3 cells transfected with either a vector DNA (labeled as "vector") or a prostasin cDNA construct (labeled as "prostasin") were analyzed by a Western blot using a prostasin-specific antibody (upper panel) or subjected to an in vitro Matrigel chemoinvasion assay (lower panel) as described in MATERIALS AND METHODS. The expressed recombinant human prostasin protein (a 40 kDa band) was detected in the prostasin cDNA-transfected DU-145 or PC-3 cells, but not in the vector-transfected cells. In the Matrigel chemoinvasion assay, the vector-transfected cells are expressed as being 100% invasive (solid bars), the open bars represent the relative invasiveness of the human prostasin cDNA-transfected cells. The data were analyzed by a Student *t*-test using the StatView software (Abacus Concepts, Inc., Berkeley, CA).

the Western blot. We further examined the DU-145/Pro and the PC-3/Pro cells by immunocytochemistry, and confirmed that 100% of the cells expressed the prostasin protein (data not shown).

In the in vitro Matrigel chemoinvasion assays (Fig. 4, lower panel), the invasiveness of DU-145/Pro cells was determined to be at 32% of that of DU-145/Vector cells (or, the reduction of invasiveness was at 68%). The invasiveness of PC-3/Pro cells was determined to be at 58% of that of PC-3/Vector cells (or, the reduction of invasiveness was at 42%).

We performed in vitro cell proliferation assays on DU-145/Pro vs. DU-145/Vector cells, and on PC-3/Pro vs. PC-3/Vector cells, but did not observe any difference between the growth rates of the prostasin cDNA-transfected or the vector-transfected cells over an 8-day period (data not shown).

DISCUSSION

Human prostasin serine protease was discovered in 1994 but its function was not defined [2]. We present evidence in this report to demonstrate prostasin as a potential invasion suppressor of prostate cancer.

In the prostate, prostasin is synthesized by the epithelial cells and may assume a membrane-bound form in these cells [2,9]. The demonstration of prostasin protein and mRNA expression in normal human prostate epithelial cells (Fig. 1) suggested that prostasin may have a function in normal prostate biology. On the other hand, a loss of prostasin expression in prostate cancer may also suggest a role for prostasin in suppressing prostate cancer progression. In the present study, the following results support our hypothesis: (1) Two highly invasive human prostate cancer cell lines, the DU-145 and the PC-3 [15], do not express prostasin at either the protein level or the mRNA level, while a non-invasive human prostate cancer cell line, the LNCaP [15], expresses this serine protease at both the mRNA and the protein levels (Fig. 1). (2) A loss of mouse prostasin mRNA expression was demonstrated in the tumorigenic and invasive [12,14] prostate cancer cell lines TRAMP-C1 and -C2 (Fig. 2). (3) Immunohistochemistry analysis of human prostate cancer demonstrated a down-regulated pattern of prostasin protein expression in high-grade prostate tumors (Fig. 3, and Table I).

Genetically, prostate tumors are heterogeneous and multi-focal in nature, in that one patient's gross-anatomy tumor comes from multiple initial lesions which are caused by different initial transformation events and progress to different stages by different ensuing transformations [16]. The Gleason grading, when used as a percentage of each cancer occupied by Gleason grade 4-5 areas, is independently associated with prostate cancer progression [17]. We demonstrated a significant decrease of prostasin expression in the high-grade, i.e., the more progressively transformed tumors. In the case of mouse prostate adenocarcinomas in the TRAMP model, the tumors are induced by expression of the SV40 T-antigen as an initial transformation event [18]. The TRAMP-C cell lines were established from a primary prostate tumor of a TRAMP mouse at 32 weeks of age, and represent different stages of the prostate epithelial cell tumor transformation process [12]. In this mouse prostate cancer cell line model, the more progressively transformed cells (TRAMP-C1 and -C2) did not express the prostasin mRNA (Fig. 2). A weak level of mouse prostasin mRNA expression was detected only in TRAMP-C3 cells following a prolonged exposure of the Southern blot in Figure 2 (data not shown), the significance of such a weak level of expression

is presently unclear. In both the human prostate cancer cell lines and the primary tumors, as well as the mouse prostate cancer cell lines, however, the down-regulation of prostasin may be linked to the transformation stage and progression of prostate cancer.

An immediate step that could be taken to address prostasin's potential function in the prostate was to restore prostasin expression in the prostate cancer cell lines that lost expression. We used the human prostate cancer cell lines as a model to begin investigating prostasin's potential function. We forced the expression of prostasin in the DU-145 and PC-3 cells via transfection with a human prostasin cDNA. We found that a forced re-expression of the prostasin protein in DU-145 and PC-3 reduced the *in vitro* invasiveness of the cells by 68 and 42%, respectively (Fig. 4). We also tested our transfectants to determine if a forced re-expression of prostasin protein had any anti-proliferation effects on these cells grown in tissue culture. No significant difference was found between the growth rates of DU-145/Pro or PC-3/Pro cells and that of the vector-transfected cells, DU-145/Vector or PC-3/Vector (data not shown). This observation also validates the observed reduction of invasiveness in the invasion assay. We can attribute the reduced number of DU-145/Pro or PC-3/Pro cells invading through the Matrigel membrane to a change of their intrinsic invasive properties, not to a significantly slower growth rate over the assaying period. We further tested if the anti-invasion activity of prostasin may be attributed to the plasma membrane-bound, or to the secreted form of prostasin by adding purified recombinant human prostasin (the secreted form, at 0.5 μ M final concentration) in an invasion assay using the PC-3 cells. Our results indicated that the secreted prostasin did not reduce the invasiveness of PC-3 cells (data not shown).

CONCLUSIONS

The observation of down-regulation of prostasin expression in human and mouse prostate cancer suggests that prostasin serine protease may have a function in normal prostate, or play a role in suppressing prostate cancer progression. The *in vitro* anti-invasion activity of prostasin suggests that prostasin may be a potential invasion suppressor of prostate cancer.

ACKNOWLEDGMENTS

The authors thank Drs. Gary Pearl, Darian Kameh, and Diana Yin of the Department of Pathology at the Orlando Regional Medical Center; Drs. James Schoeck, Clark Kessel, Stan Sujka, and Marshall Melcer of

Orlando Urology Associates for their assistance in prostate specimen procurement; Mr. Scott Howe and the Florida Hospital Pathology/Histology Laboratory for providing tissue sectioning service. We acknowledge Dr. Ratna Chakrabarti for providing the PC-3 and the LNCaP cells, Dr. Julie Chao for providing the human prostasin antibody and the prostasin cDNA plasmid. We are especially grateful to Dr. Gary Meadows for his critique of the manuscript during its preparation.

REFERENCES

1. Greenlee RT, Murray T, Bolden S, Wingo PA. Cancer statistics, 1999. *CA Cancer J Clin* 2000;50:7-33.
2. Yu JX, Chao L, Chao J. Prostasin is a novel human serine proteinase from seminal fluid. Purification, tissue distribution, and localization in prostate gland. *J Biol Chem* 1994;269:18843-18848.
3. Mignatti P, Rifkin DB. Biology and biochemistry of proteinases in tumor invasion. *Physiol Rev* 1993;73:161-195.
4. Kennedy AR. Chemopreventive agents: protease inhibitors. *Pharmacol Ther* 1998;78:167-209.
5. Goyal J, Smith KM, Cowan JM, Wazer DE, Lee SW, Band V. The role for NES1 serine protease as a novel tumor suppressor. *Cancer Res* 1998;58:4782-4786.
6. Nelson PS, Gan L, Ferguson C, Moss P, Gelinis R, Hood L, Wang K. Molecular cloning and characterization of prostase, an androgen-regulated serine protease with prostate-restricted expression. *Proc Natl Acad Sci U S A* 1999;96:3114-3119.
7. Hooper JD, Nicol DL, Dickinson JL, Eyre HJ, Scarman AL, Normyle JF, Stuttgen MA, Douglas ML, Loveland KA, Sutherland GR, Antalis TM. Testisin, a new human serine proteinase expressed by premeiotic testicular germ cells and lost in testicular germ cell tumors. *Cancer Res* 1999;59:3199-3205.
8. Boucaut K, Douglas M, Clements J, Antalis T. The serine proteinase testisin may act as a tumor and/or growth suppressor in the testis and may be regulated by DNA methylation [abstract]. In *Cancer Genetics and Tumor Suppressor Genes Meeting Program*, August 16-20, 2000 Cold Spring Harbor Laboratory.
9. Yu JX, Chao L, Chao J. Molecular cloning, tissue-specific expression, and cellular localization of human prostasin mRNA. *J Biol Chem* 1995;270:13483-13489.
10. Vallet V, Chraïbi A, Gaeggeler HP, Horisberger JD, Rossier BC. An epithelial serine protease activates the amiloride-sensitive sodium channel. *Nature* 1997;389:607-610.
11. Yu JX, Chao L, Ward DC, Chao J. Structure and chromosomal localization of the human prostasin (PRSS8) gene. *Genomics* 1996;32:334-340.
12. Foster BA, Gingrich JR, Kwon ED, Madias C, Greenberg NM. Characterization of prostatic epithelial cell lines derived from transgenic adenocarcinoma of the mouse prostate (TRAMP) model. *Cancer Res* 1997;57:3325-3330.
13. Gleason DF. Classification of prostatic carcinomas. *Cancer Chemother Rep* 1966;50:125-128.
14. Kassis J, Moellinger J, Lo H, Greenberg NM, Kim H-G, Wells A. A role for phospholipase C- γ -mediated signaling in tumor cell invasion. *Clin Cancer Res* 1999;5:2251-2260.
15. Hoosein NM, Logothetis CJ, Chung LW. Differential effects of peptide hormones bombesin, vasoactive intestinal polypeptide,

- and somatostatin analog RC-160 on the invasive capacity of human prostatic carcinoma cells. *J Urol* 1993;149:1209-1213.
16. Isaacs WB, Bova GS. Prostate Cancer. In: Vogelstein B, Kinzler KW, editors. *The Genetic Basis of Human Cancer*. New York: McGraw-Hill Health Professions Division; 1998. pp 653-660.
17. Stamey TA, McNeal JE, Yemoto CM, Sigal BM, Johnstone IM. Biological determinants of cancer progression in men with prostate cancer. *JAMA* 1999;281:1395-1400.
18. Greenberg NM, DeMayo F, Finegold MJ, Medina D, Tilley WD, Aspinall JO, Cunha GR, Donjacour AA, Matusik RJ, Rosen JM. Prostate cancer in a transgenic mouse. *Proc Natl Acad Sci USA* 1995;92:3439-3443.

Prostasin Is a Glycosylphosphatidylinositol-anchored Active Serine Protease*

Received for publication, December 19, 2000, and in revised form, March 12, 2001
Published, JBC Papers in Press, March 26, 2001, DOI 10.1074/jbc.M011423200

Li-Mei Chen[‡], Melanie L. Skinner[‡], Steven W. Kauffmant[‡], Julie Chao[§], Lee Chao[§],
Catherine D. Thaler[‡], and Karl X. Chai[‡]

From the [‡]Department of Molecular Biology and Microbiology and the [¶]Department of Biology, University of Central Florida, Orlando, Florida 32816 and the [§]Department of Biochemistry and Molecular Biology, Medical University of South Carolina, Charleston, South Carolina 29425

A recombinant human prostasin serine protease was expressed in several human cell lines. Subcellular fractionation showed that this serine protease is synthesized as a membrane-bound protein while a free-form prostasin is secreted into the culture medium. Prostasin was identified in nuclear and membrane fractions. Membrane-bound prostasin can be released by phosphatidylinositol-specific phospholipase C treatment, or labeled by [³H]ethanolamine, indicating a glycosylphosphatidylinositol anchorage. A prostasin-binding protein was identified in mouse and human seminal vesicle fluid. Both the secreted and the membrane-bound prostasin were able to form a covalently linked 82-kDa complex when incubated with seminal vesicle fluid. The complex formation between prostasin and the prostasin-binding protein was inhibited by a prostasin antibody, heparin, and serine protease inhibitors. Prostasin's serine protease activity was inhibited when bound to the prostasin-binding protein in mouse seminal vesicle fluid. This study indicates that prostasin is an active serine protease in its membrane-bound form.

Prostasin is a serine protease discovered in ejaculated human semen in 1994 (1). The molecular mass of prostasin is 40 kDa when examined by SDS-polyacrylamide gel electrophoresis (PAGE)¹ under reducing conditions. Prostasin displays trypsin-like enzymatic activities by hydrolyzing peptidyl fluorogenic substrates such as D-Pro-Phe-Arg-AMC. This trypsin-like enzymatic activity can be inhibited by aprotinin, antipain, leupeptin, and benzamidin. Prostasin is present at high levels in normal human semen (8.61 ± 0.42 µg/ml) and in the prostate gland (143.7 ± 15.9 ng/mg). Lower amounts of prostasin can also be detected in other tissues. In the prostate gland, the prostasin protein is present in the epithelial cells as well as in the secretion inside the lumen. The full-length human prosta-

sin mRNA has been deduced (2). The predicted mature prostasin peptide sequence has a potential carboxyl-terminal hydrophobic membrane anchorage domain followed by a short cytoplasmic tail. The translated amino acid residue sequence of prostasin is similar to those of human prostatic testis, plasma kallikrein, coagulation factor XI, hepsin, plasminogen, and acrosin (2–4). A membrane-bound *Xenopus* kidney epithelial cell sodium channel-activating protease (CAP1) was found highly homologous to human prostasin, sharing 53% sequence identity at the amino acid level (5). Recently, the mouse counterpart of CAP1, mCAP1, has been cloned from a cortical collecting duct cell line (6). mCAP1 shares 77% amino acid sequence identity with human prostasin.

Serine proteases play important roles in a diverse range of the body's normal physiological processes, and they are implicated in various pathological processes such as cardiovascular disorders and cancers (7). The prostate produces a number of serine proteases such as prostate-specific antigen (8), human glandular kallikrein (9), and the most recently discovered prostatic (3). Some of these serine proteases are suspected to affect fertility or semen liquefaction (10), and others are implicated in normal prostate development or prostatic diseases (11–14). For example, both prostate-specific antigen and human glandular kallikrein have become important diagnostic and prognostic markers for prostate cancer. Serine proteases are usually regulated at the post-translational level in addition to the transcriptional regulation at their gene level. The body's own strategy of regulating the serine proteases is to bind the serine proteases with a protein inhibitor such as the inhibitors of the serpin class (15). These serpin-serine protease pairs are highly specific with regard to the two molecules involved; examples include α_1 -antitrypsin and elastase (15), kallistatin and kallikrein (16, 17), α_1 -antichymotrypsin and prostate-specific antigen (18). The mechanism of serpin inhibition of serine proteases involves the formation of a covalently linked complex at a 1:1 stoichiometry (19). Such a complex exhibits resistance to treatment with SDS or boiling (16, 17).

The physiological functions of prostasin are not fully understood. In a recent study (20) we showed that prostasin expression is significantly down-regulated in high grade prostate tumors and is lost in highly invasive human and mouse prostate cancer cell lines. Transfection of two human prostate cancer cell lines DU-145 and PC-3 with human prostasin cDNA reduced *in vitro* invasiveness of the cells, suggesting an invasion suppressor role for prostasin. This anti-invasion activity is apparently conferred by the cellular prostasin but not the secreted prostasin. In the present study, we determined that prostasin is a GPI-anchored membrane protein in addition to being a secreted protease. The subcellular localization of prostasin was investigated in cells expressing native or recombi-

* This work was supported by Department of Defense Prostate Cancer Research Program Grant DAMD17-98-1-8590. The costs of publication of this article were defrayed in part by the payment of page charges. This article must therefore be hereby marked "advertisement" in accordance with 18 U.S.C. Section 1734 solely to indicate this fact.

† To whom correspondence should be addressed: Dept. of Molecular Biology and Microbiology, University of Central Florida, 4000 Central Florida Blvd., Orlando, FL 32816-2360. Tel.: 407-823-6122; Fax: 407-823-3095; E-mail: kxchai@mail.ucf.edu.

¹ The abbreviations used are: PAGE, polyacrylamide gel electrophoresis; GPI, glycosylphosphatidylinositol; PBP, prostasin-binding protein; r-hPro, recombinant human prostasin; PBS, phosphate-buffered saline; MES, 4-morpholineethanesulfonic acid; PI-PLC, phosphatidylinositol-specific phospholipase C; ER, endoplasmic reticulum; mPBP, mouse prostasin-binding protein; AMC, 7-amino-4-methylcoumarin; AFC, 7-amino-4-trifluoromethylcoumarin.

nant prostatin. We have also identified a prostatin-binding protein (PBP), a potentially serpin class serine protease inhibitor specific for prostatin. We further demonstrated that the membrane-bound prostatin is an active serine protease. These results will provide structural and regulatory information for further investigation of the functions of prostatin in normal prostate development, prostatic diseases, as well as reproductive biology.

EXPERIMENTAL PROCEDURES

Cell Lines and Plasmid DNA Transfection—A human embryonic kidney epithelial cell line, 293-EBNA (Invitrogen, Carlsbad, CA), was maintained in Dulbecco's modified Eagle medium supplemented with 10% fetal bovine serum. Human prostate cancer cell lines LNCaP, DU-145, and PC-3 were obtained from the American Type Culture Collection (ATCC, Manassas, VA). The LNCaP and the DU-145 cells were maintained in RPMI 1640 medium supplemented with 10% fetal bovine serum and 1 mM sodium pyruvate; the PC-3 cells were maintained in F-12K medium supplemented with 10% fetal bovine serum. All cells were kept at 37 °C with 5% CO₂. All tissue culture media, sera, and supplements were purchased from Life Technologies, Inc.

A full-length human prostatin cDNA of 1,896 base pairs (including a 209-base pair 5'-untranslated region, 1,032 base pairs of the coding region, and a 655-base pair 3'-untranslated region) was generated by means of reverse transcription-polymerase chain reaction with the following two primers, 5'-AGA CAG TGC TGG TGA CTC GT-3' and 5'-TGT GCT CAA ACA TTT TAA TC-3', using the total RNA of LNCaP cells as template (2). The amplified cDNA was cloned into a mammalian expression vector, pREP-8 (Invitrogen), at its polylinker site. Transfection of the prostatin cDNA plasmid into 293-EBNA cells was carried out using electroporation. The electroporated cells were then subcultured for selection of transfectants (293/Pro) using 5 mM histidinol (Sigma) in the culture medium for 2 weeks. The pREP-8 vector plasmid was transfected into 293-EBNA cells and subjected to histidinol selection to establish the control cells (293/Vec).

The DU-145 and the PC-3 cells, which do not express prostatin (20), were also transfected using plasmids containing the full-length human prostatin cDNA. The methods for plasmid engineering and establishment of transfectants that express human prostatin have been described previously (20). The resulting cell lines that express human prostatin were designated DU-145/Pro and PC-3/Pro.

SDS-PAGE and Western Blot Analysis—These procedures were carried out for all experiments unless stated otherwise. Samples were suspended in 1 × SDS sample buffer (62.5 mM Tris-HCl at pH 6.8, 2% v/v glycerol, 2% w/v SDS, and 2% β-mercaptoethanol), boiled for 5 min, and resolved in a 10% polyacrylamide gel. The resolved proteins were then transferred to a nitrocellulose membrane. The membrane was stained with India ink for 15 min (1:1,000 in TBS-T: 20 mM Tris at pH 7.6 containing 0.137 M NaCl and 0.1% Tween 20), blocked in 5% non-fat milk for 1 h, and incubated with the primary antibody for 30 min in a tray or a Surf-blot apparatus (Idea Scientific, Inc., Minneapolis). After washing, the membrane was incubated with a secondary antibody conjugated with horseradish peroxidase (Sigma, used at a 1:10,000 dilution) for 30 min. Signals were detected using ECL (enhanced chemiluminescence) with WestPico reagents (Pierce) following the supplier's protocol. The membrane was then exposed to Kodak x-ray film. The primary antibodies used were as follows: polyclonal antibodies against prostatin (recombinant or native, used at 1:1,000), a monoclonal antibody against β₁-integrin (used at 1:1,000), and a monoclonal antibody against poly(ADP-ribose) polymerase (used at 1:500). Antibodies against β₁-integrin and poly(ADP-ribose) polymerase were from BD Transduction Laboratories (San Diego).

Purification of Recombinant Human Prostatin—The 293/Pro cells were grown to a confluent monolayer in Dulbecco's modified Eagle's medium and 10% fetal bovine serum containing 5 mM histidinol. Cells were then placed in Opti-MEM I serum-free medium (Life Technologies, Inc.) for 72 h before collection of the conditioned medium. The collected medium was tested for recombinant prostatin (r-hPro) by Western blot analysis using a prostatin-specific antibody (1). For purification of the secreted prostatin, the serum-free medium was centrifuged at 10,000 rpm for 20 min to remove dead cells or debris and then passed through an aprotinin-agarose column (1.5 × 20 cm, Sigma) equilibrated with 25 mM Tris-HCl at pH 7.6 at a flow rate of 25 ml/h. After extensive washing to remove any unbound proteins, the bound prostatin was eluted with 0.1 M glycine (pH 3.0) containing 0.1 M NaCl at a flow rate of 60 ml/h. The eluted prostatin was immediately neutralized with appropriate

amounts of 1 M Tris, combined, concentrated with Centricon-10 concentrators (Amicon Inc., Beverly, MA), and stored at -20 °C before use in other assays.

Preparation of a Polyclonal Antiserum against Recombinant Prostatin—250 μg of the purified r-hPro in 0.5 ml of phosphate-buffered saline (PBS, pH 7.4) was emulsified with an equal volume of complete Freund's adjuvant (Sigma) and was injected subcutaneously into a 1.5-kg female New Zealand White rabbit (Charles River Laboratories, Wilmington, MA). Booster injections with 100 μg of r-hPro (emulsified with incomplete Freund's adjuvant, Sigma) were performed three times at 3-week intervals. Preimmune rabbit serum was collected before the initial immunization.

Immunocytochemistry—The PC-3/Pro or LNCaP cells were seeded on glass coverslips (Fisher Scientific) at a density of 5 × 10⁴/coverslip and grown for 24–36 h prior to a double immunostaining. Briefly, cells were rinsed three times in 1 × PBS, fixed in 4% paraformaldehyde, and permeabilized with 0.18% Triton X-100 in PBS for 10 min. After blocking in 10% normal goat serum (Life Technologies, Inc.) in 1 × PBS, cells were incubated with the primary antibodies for 45 min, washed, incubated with the appropriate secondary antibodies at room temperature for 30 min, and then washed three times for 10 min each in 1 × PBS. A rabbit polyclonal antibody against prostatin was used at a dilution of 1:100. A monoclonal antibody against poly(ADP-ribose) polymerase was used as a nuclear specific marker at a dilution of 1:75. A goat anti-rabbit IgG conjugated with fluorescein (1:50, Life Technologies, Inc.) and a goat anti-mouse IgG conjugated with Cy3 (1:800, Jackson ImmunoResearch, West Grove, PA) were used as the secondary antibodies. The coverslips were mounted with Gel/Mount (Fisher Scientific) and analyzed on a Carl Zeiss LSM510 laser scanning microscope.

Subcellular Fractionation and Differential Extraction—Subcellular fractionation was performed as described in Krajewski *et al.* (21) and Pemberton *et al.* (22). Briefly, confluent cells in 4 × 150-cm² flasks (estimated 5–10 × 10⁷ cells/total) were washed three times with 1 × PBS and removed by mechanical force for the 293/Pro cells or trypsin treatment (0.25% with 1 mM EDTA) for the PC-3/Pro and LNCaP cells. The cells were resuspended in 7 ml of cold MES buffer (17 mM at pH 7.4, 2.5 mM EDTA, and 250 mM sucrose) containing protease inhibitors (1 mM phenylmethylsulfonyl fluoride, 2 μg/ml aprotinin, 2 μg/ml leupeptin, and 2 μg/ml antipain). The following steps were performed at 4 °C. Cell suspension was homogenized with a Dounce homogenizer for 60 strokes followed by centrifugation twice at 500 × g for 10 min, resulting in the crude nuclear fraction in the pellet. The supernatant was centrifuged twice at 10,000 × g for 15 min, resulting in the heavy membrane fraction in the pellet containing mitochondria, lysosomes, and peroxisomes. The supernatant from the 10,000 × g centrifugation was subjected to an ultracentrifugation at 100,000 × g for 60 min, resulting in a light membrane fraction in the pellet containing the plasma membrane, microsomes, and endoplasmic reticulum. The supernatant from the final centrifugation contains soluble or cytosolic proteins. The pellets from each centrifugation were washed with 2 × 10 ml of MES to eliminate carryovers.

Differential extraction of membrane fractions was carried out according to Pei *et al.* (23). Briefly, pellet/membrane fractions were divided equally into three portions and were extracted with 1% Triton X-114 in Tris buffer (10 mM Tris-HCl, pH 7.5) or high salt (350 mM NaCl in Tris buffer), or alkali (50 mM glycine/NaOH, pH 11.0) for 1 h on ice. The samples were centrifuged at 100,000 × g for 30 min. The resulting pellet was dissolved in 1 × SDS sample buffer for gel electrophoresis. The supernatant was subjected to a trichloroacetic acid precipitation to recover proteins for gel electrophoresis.

Detergent Phase Separation and Phosphatidylinositol-specific Phospholipase C (PI-PLC) Treatment—The procedure was adapted from those described by Bordier (24) and Rosenberg (25). Briefly, cells (5 × 10⁶) were lysed in 1 ml of ice-cold TBS (10 mM Tris-HCl at pH 7.5, 150 mM NaCl, 1 mM EDTA) containing 1% Triton X-114 (Sigma) and protease inhibitors for 2 h with gentle shaking at 4 °C. The lysate was then centrifuged at 14,000 rpm for 30 min. The supernatant (500 μl, or 700–800 μg of total protein) was overlaid onto a 300-μl sucrose cushion (6% w/v sucrose in TBS containing 0.06% Triton X-114). The solution was incubated at 37 °C for 3 min and centrifuged at 300 × g for 3 min at room temperature to separate the detergent phase (pellet) and the aqueous phase. The aqueous phase was removed and extracted further with 0.5% Triton X-114 and 2% Triton X-114. The aqueous phase after the final centrifugation contains the soluble proteins. The detergent phase (pellet) from the first centrifugation was resuspended in 500 μl of ice-cold TBS, incubated at 37 °C for 3 min, and centrifuged at 300 × g for 3 min at room temperature to ensure the purity of the detergent phase.

The detergent phase was resuspended in 100 μ l of ice-cold TBS. 10 μ l of the resuspended detergent phase was subjected to PI-PLC (Sigma) digestion at 37 °C for 1 h with gentle shaking in a total volume of 100 μ l of reaction buffer (10 mM Tris-HCl at pH 7.5, 144 mM NaCl). 100 μ l of ice-cold TBS containing 2% Triton X-114 was then added to the digestion mixture and subjected to phase separation as described above. At the final step, both the aqueous and detergent phases were precipitated with 6% w/v trichloroacetic acid and 0.013% sodium deoxycholate. The precipitates were resuspended in 30 μ l of 1 \times SDS sample buffer, neutralized with ammonium hydroxide (microliter amounts), boiled, and subjected to SDS-PAGE and Western blot analysis.

Human prostates removed by radical prostatectomy performed at Orlando Regional Medical Center (Orlando, FL) were sectioned with a cryostat at 20- μ m thickness. 80 sections were collected and rinsed with PBS twice to remove prostatic fluid. The washed prostate sections were lysed in 1 ml of TBS containing 1% Triton X-114 at 4 °C overnight with rocking. The lysed prostate tissues were centrifuged and subjected to the same phase separation and PI-PLC treatment procedures as described above. Several representative prostate sections (7 μ m) cut at intervals of the 80 20- μ m sections were subjected to standard hematoxylin and eosin staining for confirmation of benign prostate morphology. The use of human tissues was approved by the Institutional Review Boards of Orlando Regional Medical Center and the University of Central Florida.

[³H]Ethanolamine Labeling, Immunoprecipitation, and Fluorography—PC-3/Pro (3 \times 10⁶) or LNCaP (1 \times 10⁶) cells were seeded in a 35-mm dish in 1 ml of Opti-MEM I serum-free medium. The next day, [1-³H]ethanolamine hydrochloride (37 MBq, 1 mCi/ml, and 30.0 Ci/mmol, Amersham Pharmacia Biotech) was added to the culture medium at a concentration of 100 μ Ci/ml, and the cells were cultured for another 24 h. Cells were washed once with PBS and lysed in 0.5 ml of RIPA buffer (PBS at pH 7.4, 1% Nonidet P-40, 0.5% sodium deoxycholate, 0.1% SDS) containing protease inhibitors at 4 °C for 1 h. The lysate was centrifuged at 14,000 rpm for 30 min to remove insoluble material. The supernatant was subjected to immunoprecipitation with 2 μ g/ml anti-prostatin IgG (purified using Econo-Pac protein A cartridge, Bio-Rad) and protein A-Sepharose beads (Sigma) at 4 °C overnight. The beads were washed with RIPA buffer three times, resuspended in 2 \times SDS sample buffer with β -mercaptoethanol, boiled, and analyzed by SDS-PAGE. The gel was fixed in a solution of 2-propanol:water:acetic acid (12.5:32.5:5) for 30 min and soaked in Amplify fluorographic reagent (Amersham Pharmacia Biotech) for another 30 min. The gel was dried, and ³H-labeled molecules were detected by exposure to an x-ray film with an intensifying screen at -80 °C for 14 days.

Prostatin Binding Assay—Seminal vesicle fluid was expressed from one pair of mouse seminal vesicles (C57BL/6 mouse, Harlan, Indianapolis) and mixed with 1 ml of 25 mM Tris-HCl, pH 7.6, and centrifuged at 14,000 rpm at 4 °C for 30 min. 5 μ l of the supernatant (50 μ g of total protein) was incubated with either 0.5 μ g of the purified recombinant human prostatin or subcellular fractions of 293/Pro and PC-3/Pro cells (prepared in the absence of serine protease inhibitors) at 37 °C for 60 min, or for various time periods for a time course study. The binding reaction was stopped by the addition of SDS sample buffer and heating at 100 °C for 5 min. Mouse tissues were homogenized in PBS (1 g of tissue/5 ml) and centrifuged in a microcentrifuge at 14,000 rpm for 30 min at 4 °C. 40 μ g of total protein for each tissue extract was used in the binding assay. 1 μ l of human or mouse plasma was also subjected to prostatin binding assay. The use of animals was approved by the IACUC of the University of Central Florida. Human seminal vesicles were obtained from radical prostatectomy performed at Orlando Regional Medical Center. No seminal vesicle metastasis from prostate cancer was found according to the pathology report. Human seminal vesicle fluid was diluted with PBS at a ratio of 1:2, mixed by vortex, and spun. 10 μ l of the diluted fluid was incubated with 0.5 μ g of purified prostatin at 37 °C for 60 min.

Membrane Overlay Zymography—The membrane overlay zymography was carried out using the protocols of Enzyme System Product (Livermore, CA) and Beals *et al.* (26). Briefly, samples were first resolved in a 10% polyacrylamide gel without SDS or β -mercaptoethanol. After electrophoresis, the gel was equilibrated in a reaction buffer (50 mM Tris-HCl, pH 9.0) for 15 min. Pre-wet acetate-cellulose membrane impregnated with the prostatin substrate D-Pro-Phe-Arg-AFC (Enzyme System Product) was then carefully laid over the gel without entrapping air bubbles. The membrane-overlaid gel was placed in a moist chamber at 37 °C for 3–5 h. The reaction was monitored using an ultraviolet lamp and photographed.

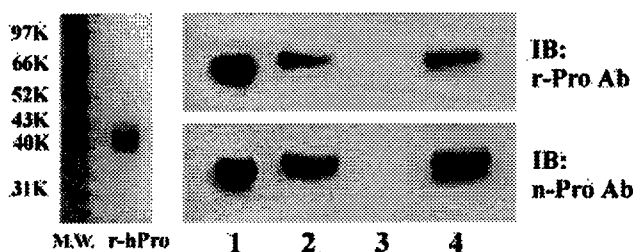


FIG. 1. SDS-PAGE and Western blot analysis. Recombinant human prostatin purified from serum-free conditioned medium of the 293/Pro cells was analyzed by 10% SDS-PAGE under reducing conditions. The purified recombinant prostatin (3 μ g) migrated at 40 kDa (left panel, *r-hPro*) and is recognized by an antibody made against the purified recombinant prostatin (*IB: r-Pro Ab*, lane 1) as well as a prostatin-specific antibody made against purified native prostatin (*IB: n-Pro Ab*, lane 1, Ref. 1). The quantity of purified prostatin in lanes 1 is 0.5 μ g. Samples from the 293/Pro cell lysate (lanes 2, 20 μ g), 293/Vec (lanes 3, 20 μ g) cell lysate, and human semen (lanes 4, 30 μ g) were immunoblotted with *r-Pro* antibody (upper right panel, 1:1,000 dilution) and *n-Pro* antibody (lower right panel, 1:1,000 dilution). Both antibodies recognize the recombinant prostatin as well as the native prostatin but do not have cross-reactivity with 293/Vec proteins.

RESULTS

Expression and Purification of Recombinant Human Prostatin—Serum-free conditioned medium from 293/Pro cell culture was prepared and passed through an aprotinin-agarose column for a one-step affinity-chromatographic purification of the recombinant prostatin as described under "Experimental Procedures" (see also Ref. 1). A Coomassie Blue staining of the purified recombinant prostatin is shown in Fig. 1, left panel (*r-hPro*). The *r-hPro* migrates at 40 kDa on an SDS-PAGE under reducing conditions. Because of glycosylation of the prostatin molecule (1, 2), it appeared as a rather diffused band on the gel. We prepared a polyclonal antibody (*r-Pro Ab*) using the purified *r-hPro* as an antigen. The *r-Pro* antibody recognized the purified recombinant prostatin (secreted form), the recombinant prostatin in 293/Pro total cell lysate (nonsecreted form), and the native prostatin in ejaculated human semen (obtained from healthy volunteers, Ref. 1) (Fig. 1, upper right panel, lanes 1, 2, and 4). The prostatin protein in the same set of samples was also recognized by a prostatin-specific antibody referenced previously (1) (Fig. 1, lower right panel). Neither antibody cross-reacts with any nonspecific protein in the control 293/Vec total cell lysate (Fig. 1, right panel, lanes 3). The results indicate that the polyclonal antibody against the recombinant prostatin is specific to prostatin and that the recombinant prostatin prepared using the amplified cDNA has an immunological reactivity similar to that of the native prostatin. The antibody against the recombinant prostatin was used in the ensuing assays conducted in this study.

Recombinant Prostatin Is a Membrane-bound Protein—A hydrophathy plot of the translated prostatin amino acid sequence indicated that the prostatin polypeptide has a potential membrane-anchorage domain at the carboxyl terminus (2). To confirm the presence of a potentially membrane-anchored form of the prostatin protein, the 293/Pro cells were subjected to subcellular fractionation by differential centrifugation. Fig. 2 shows that prostatin was present in the crude nuclear fraction (P1, 500-g pellet), heavy membranes (P2, 10,000-g pellet), and light membranes (P3, 100,000-g pellet), as determined by Western blot analysis. Prostatin was also detected in the cytosol (S). The purified *r-hPro* was used as positive control. Equal amounts of total protein (30 μ g) from each membrane fraction and the cytosol were applied in each lane.

To show that the membrane-anchored prostatin is not a peculiarity in the 293 cells, we performed similar subcellular

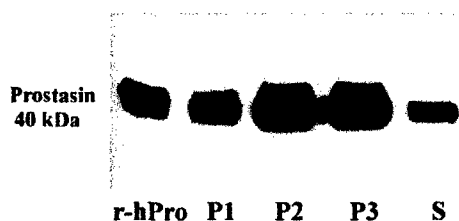


FIG. 2. Analysis of prostasin in 293/Pro cell fractions. The cells were fractionated through differential centrifugation. An equal amount of protein (30 μ g) from each centrifugation step was resolved by 10% SDS-PAGE followed by immunoblotting with a prostasin-specific polyclonal antibody (1:1,000 dilution). Prostasin (40 kDa) is detected in the nuclear fraction (P1), heavy membrane fraction (P2, including mitochondria, lysosomes, and peroxisomes), light membrane fraction (P3, including plasma membrane, microsomes, and endoplasmic reticula) as well as the cytosol (S) of 293/Pro. Purified r-hPro (0.5 μ g) was used as a positive control.

fractionation analysis on prostasin cDNA-transfected human prostate cancer cell line PC-3 (PC-3/Pro) and the human prostate cancer cell line LNCaP, which expresses endogenous prostasin (2, 20). As shown in Fig. 3A, prostasin is detected in P1, P2, and P3 fractions, but not in the cytosol (S) of PC-3/Pro. In the LNCaP cells, endogenously expressed prostasin is detected only in the P3 fraction. The membrane fractions from PC-3/Pro cells were then immunoblotted with a monoclonal antibody against a nuclear protein poly(ADP-ribose) polymerase or a monoclonal antibody against a plasma membrane-bound protein β 1-integrin to ensure the purity of each fraction. The results showed that the prostasin protein exists in a membrane-bound form in all cell lines tested. The cells transfected with the vector DNA alone (293/Vec and PC-3/Vec) were subjected to the same fractionation procedures followed by SDS-PAGE/Western blot analysis. No prostasin was detected (data not shown). We further subjected PC-3/Pro and LNCaP cells to a double immunostaining and analyzed the subcellular localization of prostasin using confocal microscopy. The confocal microscopic analysis of PC-3/Pro cells localized prostasin (green) to the ER-Golgi complex (Fig. 3B), consistent with the cell fractionation results shown in Fig. 3A. Because the nuclear membrane is practically a prominent component of the ER (27), it is not surprising that this portion of prostasin appeared in the P1 fraction. The LNCaP cells, however, did not show punctate or nuclear-ER-Golgi complex staining, again, consistent with the cell fractionation results shown in Fig. 3A.

To test if prostasin is truly a membrane-anchored protein rather than a membrane-associated protein, we subjected the P1, P2, and P3 fractions of the PC-3/Pro cells to treatment with a detergent, high salt, or alkali. As shown in Fig. 4, membrane-bound prostasin (pellet) was released into the supernatant only by the detergent treatment but not the high salt or alkali treatment. The detergent released prostasin and the membrane-bound prostasin had similar molecular weight. The results indicated that prostasin is a true membrane-anchored protein.

Membrane Prostasin Is GPI-anchored—A comparison of the potential carboxyl-terminal membrane-anchorage domain of prostasin (2) with GPI-anchored proteins (28) predicts a GPI linkage for prostasin as well (data not shown). Such a linkage may be susceptible to cleavage by PI-PLC, GPI-specific phospholipase D, or nitrous acid (25). In our studies, we first chose PI-PLC to test if prostasin is a GPI-anchored membrane protein. The 293/Pro cells were lysed in TBS containing 1% Triton X-114. After phase separation, the aqueous phase (Fig. 5, lane 1, 30 μ g of total protein) and the detergent phase (lane 2, 3 μ g of total protein) were analyzed by Western blot using the prostasin-specific antibody. The majority of the prostasin protein in

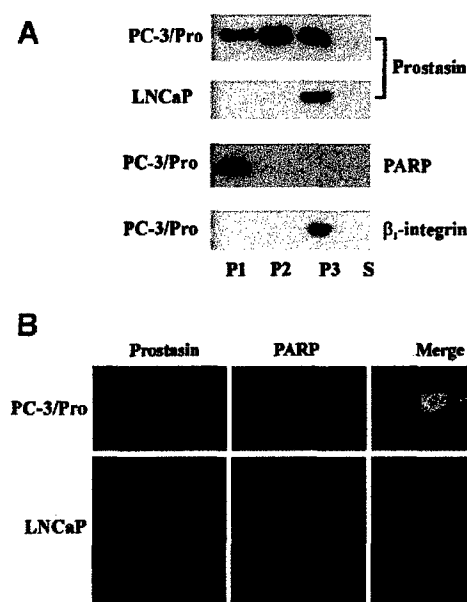


FIG. 3. Analysis of prostasin in prostate cancer cell lines. Panel A, Western blot analysis of membrane-bound prostasin in PC-3/Pro and LNCaP cells. The experimental procedures were the same as described in Fig. 2. Prostasin (40 kDa) is detected in the nuclear fraction (P1), heavy membrane fraction (P2), light membrane fraction (P3), but not in the cytosol (S) of PC-3/Pro. In LNCaP cell fractions, prostasin is detected only in P3. Antibodies against a nuclear protein, the poly(ADP-ribose) polymerase (PARP, 1:500, or 0.5 ng/ml), and a plasma membrane protein, β 1-integrin (1:1,000, or 0.25 ng/ml), were used as fractionation markers. Panel B, confocal microscopic localization of prostasin. The PC-3/Pro and LNCaP cells were fixed, permeabilized, and subjected to a double immunostaining. One focal plane for each cell type is presented to show prostasin signals (green). Prostasin is detected primarily at the nuclear-ER-Golgi complex as well as punctate regions in the PC-3/Pro cell. In the LNCaP cells, no punctate prostasin can be seen. The nuclear marker protein poly(ADP-ribose) polymerase (red) is seen in both cell types. A merge image for either cell type is presented to the right. The images were taken after subtracting background signal on a preimmune serum-stained control coverslip. Magnification, $\times 400$. The antibody dilution ratios are: anti-prostasin, 1:100; anti-poly(ADP-ribose) polymerase, 1:75 (or 3.3 ng/ml); goat anti-rabbit IgG conjugated with fluorescein isothiocyanate, 1:50; and goat anti-mouse IgG-Cy3, 1:800.

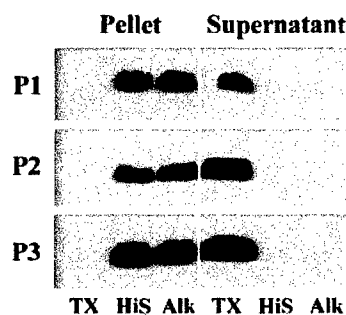


FIG. 4. Recombinant prostasin is a true membrane-bound protein. Approximately 80–100 μ g of total protein of each membrane fraction of PC-3/Pro cells (as described in legend to Fig. 3A) was subjected to detergent (TX), high salt (His), or alkali (Alk) treatment followed by centrifugation to separate the supernatant and the pellet for SDS-PAGE and Western blot analysis. Prostasin in all fractions can only be released from the membrane (pellet) to the supernatant (soluble protein) by the detergent treatment but not high salt or alkali treatment.

293/Pro cells is associated with the membrane, which was retained in the detergent phase. The size difference between the soluble and the membrane-bound prostasin may be attributed to the GPI moiety that is linked to prostasin (Fig. 5, lanes

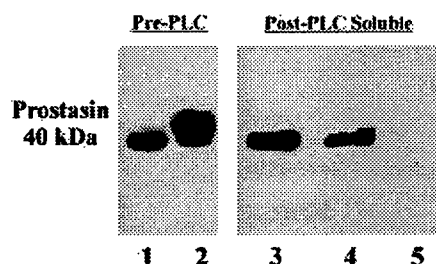


FIG. 5. Detergent phase separation of 293/Pro cells and phospholipase C treatment. The 293/Pro cells were lysed in TBS containing 1% Triton X-114 and subjected to phase separation (700–800 μ g of total protein as the starting quantity). The detergent phase containing membrane-associated proteins (equivalent to 1/10 of the total starting membrane-associated proteins) was further treated with PI-PLC followed by additional phase separation. The soluble proteins (lane 1, 30 μ g) and the detergent phase proteins (lane 2, 3 μ g) before PI-PLC treatment and the soluble proteins extracted from the detergent phase after PI-PLC treatment were subjected to SDS-PAGE and Western blot analysis using a prostatin-specific antibody. The membrane-bound prostatin is released from the membrane after PI-PLC digestion as it was detected in the post-PLC soluble phase. The amounts of PI-PLC used in the reactions are: lane 3, 0.25 unit; lane 4, 0.125 unit; and lane 5, 0 unit in a total reaction volume of 100 μ l. The results indicate that prostatin is anchored to membrane via GPI. The size difference between the membrane-bound prostatin and the soluble prostatin (lanes 1 and 2) may be attributed to the GPI moiety that is linked to prostatin.

1 and 2). The detergent phase was then subjected to PI-PLC digestion at various enzyme concentrations followed by a second phase separation. In Fig. 5, lanes 3–5 represent samples of the aqueous phases after PI-PLC digestion. The PI-PLC treatment released prostatin from the detergent phase in a dose-dependent manner (lane 3, 0.25 unit; lane 4, 0.125 unit, and lane 5, 0 units). The PI-PLC-released prostatin and the soluble prostatin are similar in molecular mass as shown in Fig. 5. The results support a GPI-anchoring mechanism for the membrane-bound prostatin.

One question that remained unclear was whether the native prostatin in the prostate tissue epithelial cells is membrane-bound by GPI anchorage as well. We selected a panel of prostate cancer cell lines and 293/Pro cells that express either recombinant or endogenous prostatin, and normal human prostate tissues in our next experiment. Cell lines that express recombinant prostatin were 293/Pro, PC-3/Pro, and DU-145/Pro. The human prostate cancer cell line LNCaP and normal human prostate tissues were used for testing native cellular prostatin. All samples (300 μ g of total protein as the starting quantity) were subjected to detergent phase separation before and after PI-PLC digestion as described under "Experimental Procedures." PC-3 transfected with a vector plasmid (PC-3/Vec) was used as negative control. The results are presented in Fig. 6A. Without PI-PLC treatment, both the recombinant and native prostatin are mainly membrane-anchored (found in the detergent phase). Soluble prostatin is detected in 293/Pro and prostate tissues. After PI-PLC treatment, the membrane-anchored prostatin is released into the soluble fraction from 293/Pro, PC-3/Pro, and prostate tissues, but not from DU-145/Pro and LNCaP. The results indicated that the native prostatin in normal human prostate tissue is also GPI-anchored. The membrane-bound prostatin in DU-145/Pro and LNCaP is resistant to PI-PLC digestion. We further tested if prostatin can be labeled biosynthetically with [3 H]ethanolamine, which is specifically incorporated in the GPI unit of GPI-anchored proteins (29). We chose the PC-3/Pro (expressing recombinant prostatin) and LNCaP (expressing native prostatin) cells for [3 H]ethanolamine biosynthetic labeling. As shown in Fig. 6B, [3 H]ethanolamine was incorporated into either recombinant or native prostatin, demonstrating that both are truly GPI-anchored.

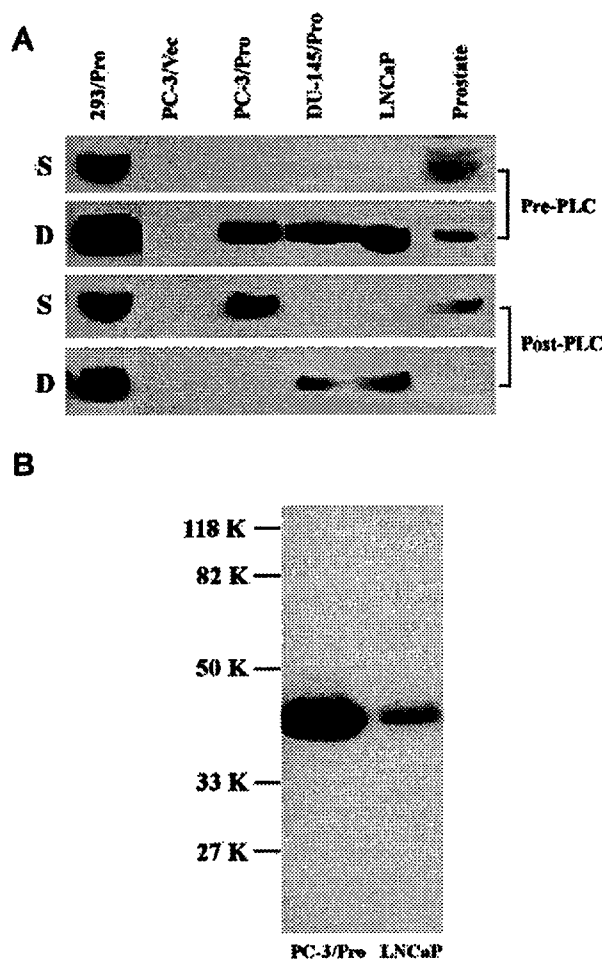


FIG. 6. Prostatin is a GPI-anchored membrane protein. Panel A, detergent phase separation and PI-PLC treatment. Human prostate tissues and cell lines that express either endogenous prostatin (LNCaP) or recombinant prostatin (293/Pro, PC-3/Pro, and DU-145/Pro) were subjected to detergent phase separation/PI-PLC digestion followed by prostatin immunoblotting (300 μ g of total protein was used for each sample as the starting quantity). Both the recombinant and native prostatin are mainly membrane-anchored (pre-PLC, detergent phase or D). Soluble prostatin is detected in 293/Pro and prostate tissues (pre-PLC, soluble phase or S). After PI-PLC treatment, the membrane-anchored prostatin is released into the soluble fraction from 293/Pro, PC-3/Pro, and prostate tissues (post-PLC, S) but not from DU-145/Pro and LNCaP (post-PLC, D). The PC-3/Vec cells showed negative results in all fractions tested. Because of a high level of prostatin expression in the 293/Pro cells, a portion of prostatin remained in the detergent phase after PI-PLC digestion. Panel B, incorporation of [3 H]ethanolamine into prostatin. PC-3/Pro or LNCaP cells were incubated with 100 μ Ci of [3 H]ethanolamine in 1 ml of Opti-MEM I serum-free medium for 24 h in 5% CO₂ at 37 °C. The cell lysates were subjected to immunoprecipitation using the prostatin antibody (purified IgG fraction, 2 μ g/ml) and protein A-Sepharose beads as described under "Experimental Procedures." After SDS-PAGE separation of the samples, the labeled protein was detected by fluorography using Amplify fluorographic reagent and exposure to an x-ray film at –80 °C with an intensifying screen for 14 days.

Identification of a Prostatin-binding Protein—An incubation of the purified r-hPro with mouse or human seminal vesicle fluid yielded a higher molecular weight form of prostatin-containing band as analyzed by SDS-PAGE and immunoblotting. The result presented in Fig. 7A indicated that the purified r-hPro formed an 82-kDa complex with a mouse seminal vesicle protein (named as the mouse prostatin-binding protein, or mPBP). The complex was apparently covalently linked and not via a disulfide bond because it was SDS- and heat-stable and

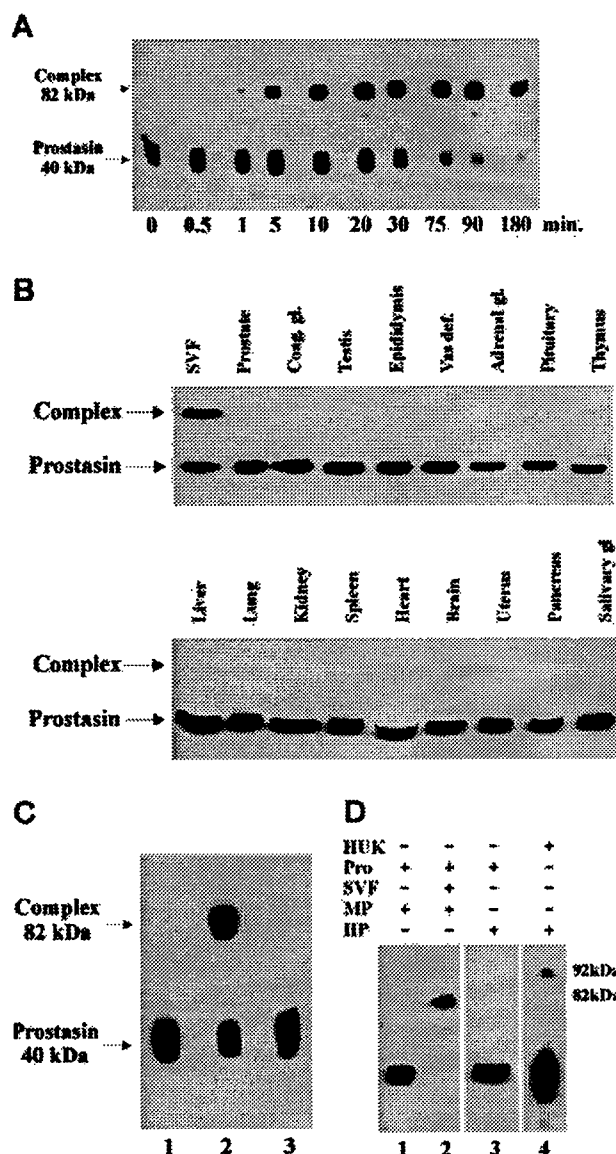


FIG. 7. Complex formation between prostasin and its binding protein. Panel A, 0.5 μ g of purified recombinant prostasin was incubated with mouse seminal vesicle fluid at 37 °C for various time periods as indicated. The samples were subjected to SDS-PAGE under reducing conditions followed by immunoblotting with a prostasin-specific antibody. Prostasin forms an 82-kDa complex (upper arrow) with mPBP in mouse seminal vesicle fluid. The complex formation can be detected as early as 1 min postincubation. Excess unbound prostasin is indicated by the lower arrow. Prostasin alone without incubation with mouse seminal vesicle fluid is labeled as 0 min. Panel B, various mouse tissue extracts were analyzed in a prostasin binding assay and prostasin immunoblotting as described. SVF, mouse seminal vesicle fluid; Coag. gl., coagulating gland; Vas def., vas deferens; Adrenal gl., adrenal gland; Salivary gl., salivary glands. Panel C, 0.5 μ g of purified recombinant prostasin was incubated with human seminal vesicle fluid at 37 °C for 60 min. Similarly, prostasin forms an 82-kDa complex with the hPBP in human seminal vesicle fluid (lane 2), and the complex formation was inhibited by 1 unit of heparin (lane 3). Purified recombinant prostasin alone was used as a control (lane 1). Panel D, human or mouse plasma was tested in a prostasin binding assay. HUK, human urinary (tissue) kallikrein (0.5 μ g); Pro, purified recombinant prostasin (0.5 μ g); SVF, mouse seminal vesicle fluid (5 μ l); MP, mouse plasma (1 μ l); HP, human plasma (1 μ l). Lanes 1–3, probed with prostasin antibody (1:1,000); lane 4, probed with a human kallikrein antibody (1:1,000).

resistant to β -mercaptoethanol. The complex formation was detected at as early as 1 min postincubation with a $t_{1/2}$ of ~5 min and reached a plateau at ~20 min. Densitometry meas-

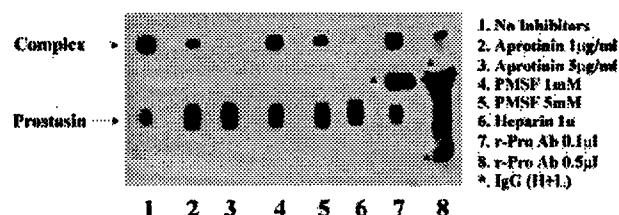


FIG. 8. Inhibition of complex formation between prostasin and mPBP. 0.5 μ g of Purified recombinant prostasin was incubated with 5 μ l of mouse seminal vesicle fluid in the presence of aprotinin (lanes 2 and 3), phenylmethylsulfonyl fluoride (PMSF; lanes 4 and 5), heparin (lane 6), prostasin antibody (lanes 7 and 8) at 37 °C for 1 h. All samples were subjected to SDS-PAGE under reducing conditions followed by immunoblotting with a prostasin-specific antibody. The complex formation (upper arrow) between prostasin and mPBP in mouse seminal vesicle fluid is inhibited by aprotinin, phenylmethylsulfonyl fluoride, heparin, and the antibody against prostasin. The asterisk (*) indicates the IgG heavy chain and light chain recognized by the goat anti-rabbit secondary antibody used in the Western blot analysis. Excess unbound prostasin is indicated by the lower arrow. Complex formation between r-hPro and mPBP in mouse seminal vesicle fluid without any other reagent was used as positive control (lane 1).

urements of the complex bands in different lanes were performed using the LabWork 3.0 software (Ultra-Violet Products, Upland, CA) (data not shown). Mouse plasma and various tissue extracts including the prostate, coagulating gland, testis, epididymis, vas deferens, adrenal gland, pituitary, thymus, liver, lung, kidney, spleen, heart, brain, uterus, pancreas, and salivary glands were subjected to the same prostasin-binding assay procedures. No SDS- and heat-stable complex was detected under the same experimental conditions (Fig. 7B). A PBP in human seminal vesicle fluid was also identified. As shown in Fig. 7C, lane 2, a higher molecular mass complex (82 kDa) was detected after an incubation of r-hPro with the human seminal vesicle fluid. The complex formation between prostasin and the human seminal vesicle PBP was inhibited by heparin (Fig. 7C, lane 3). Incubation of mouse or human plasma with r-hPro did not result in formation of any SDS- and heat-stable complex (Fig. 7D, lane 1, mouse plasma; lane 3, human plasma). In control assays, mouse plasma was incubated with prostasin for 30 min before seminal vesicle fluid was added for another 30 min of incubation to demonstrate the binding activity of the prostasin being tested in the presence of plasma (Fig. 7D, lane 2). Or, human plasma was incubated with purified human tissue kallikrein and subjected to a Western blot analysis using a human kallikrein-specific antibody (30) (Fig. 7D, lane 4). The control binding assay showed a 92-kDa kallikrein-kallistatin complex as described previously (16), demonstrating the quality of the human plasma being tested.

The complex formation between prostasin and mPBP was investigated further by incubating the purified r-hPro with serine protease inhibitors (Fig. 8, lanes 2–5) or the prostasin antibody (lanes 7 and 8) for 15 min at room temperature before an incubation with mouse seminal vesicle fluid for another 60 min at 37 °C. Or, mouse seminal vesicle fluid was first incubated with heparin before the addition of prostasin (Fig. 8, lane 6). The complex formation between prostasin and mPBP was inhibited by serine protease inhibitors such as aprotinin at dosages of 1 μ g/ml and 5 μ g/ml, phenylmethylsulfonyl fluoride at dosages of 1 mM and 5 mM, and prostasin antibody at 0.1 μ l and 0.5 μ l. The amount of the complex was either reduced or absent in the corresponding lanes of Fig. 8. Heparin (1 unit, lane 6) inhibited complex formation. Complex formation between prostasin and mPBP without additional reagents was used as the binding reaction control (Fig. 8, lane 1). The results suggested that mPBP interacts with prostasin at the serine

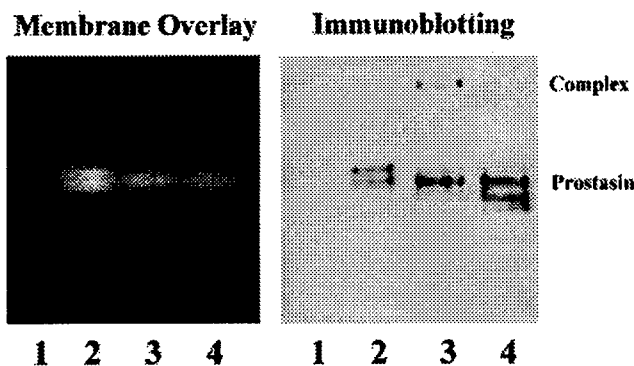


Fig. 9. Membrane overlay zymography. Samples from a prostatin binding assay were resolved on a 10% native acrylamide gel without SDS/boiling or β -mercaptoethanol. The gel was then either overlaid with a membrane impregnated with a prostatin substrate (D-Pro-Phe-Arg-AFC) (left panel) or transferred for prostatin immunoblotting (right panel). Lane 1, 5 μ l of mouse seminal vesicle fluid alone; lane 2, 0.5 μ g of purified r-hPro alone; lane 3, mixture of r-hPro and mouse seminal vesicle fluid; lane 4, same as lane 3 except r-hPro was preincubated with 5 μ g/ml aprotinin for 15 min before the addition of mouse seminal vesicle fluid. The fluorogenic substrate impregnated in the membrane was hydrolyzed by prostatin in the gel, and isoprostatin patterns in the membrane appear as fluorescent bands. The results suggest that mBPB not only binds to prostatin at the serine active site but also inhibits prostatin's serine protease activity *in vitro*.

active site and that heparin may alter mBPB binding property. The properties displayed by mBPB are shared by the serpin class serine protease inhibitors. We have observed similar properties for the serpin, kallistatin (16, 17). The predicated molecular mass of BPB (mouse or human) is estimated at ~47 kDa, given the 40-kDa apparent molecular mass of prostatin and considering the fact that serpin molecules lose a carboxyl-terminal fragment of ~5 kDa when complexed with a serine protease (31).

mBPB Inhibits the Serine Protease Activity of Prostatin—We performed a membrane overlay zymography analysis to test if mBPB inhibits prostatin activity *in vitro*. The prostatin binding assay was carried out by incubating the purified r-hPro with mouse seminal vesicle fluid in the absence of the serine protease inhibitor aprotinin (Fig. 9, lane 3) or in the presence of aprotinin (lane 4). Each sample was then divided into two equal portions and subjected to a native PAGE analysis (*i.e.*, SDS and β -mercaptoethanol were not included in the gel solution or the samples, and the samples were not heated before loading) followed by membrane overlay zymography (left panel) or Western blot analysis using the prostatin antibody (right panel). Mouse seminal vesicle fluid proteins alone (Fig. 9, lane 1) displayed no enzymatic activities toward the synthetic substrate D-Pro-Phe-Arg-AFC (left panel) nor cross-reactivity with the prostatin antibody (right panel). The purified r-hPro alone (lane 2) demonstrated enzymatic activity toward D-Pro-Phe-Arg-AFC (left panel) and was recognized by the prostatin antibody (right panel). When prostatin formed a complex with mBPB in the mouse seminal vesicle fluid, it no longer cleaves D-Pro-Phe-Arg-AFC because no fluorescence is present at the complex band location in lane 3 of the left panel, whereas the complex is identified by the prostatin antibody as the upper band in lane 3 of the right panel. The remaining unbound prostatin yielded, expectedly, lesser fluorescence (left panel, lower band in lane 3 compared with lane 2) and was recognized by the prostatin antibody (right panel, lane 3). When the purified r-hPro was preincubated with the serine protease inhibitor aprotinin before incubation with the mouse seminal vesicle fluid, no complex was detected (right panel, lane 4). A reduced level of fluorescence appeared at the prostatin band in lane 4 of

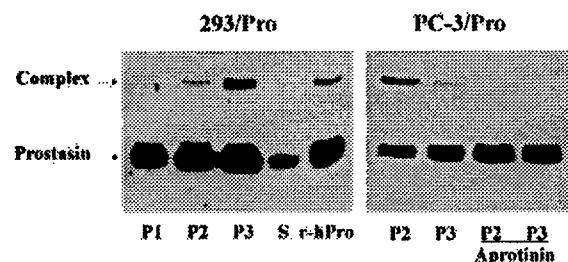


Fig. 10. Membrane-bound prostatin forms a complex with mBPB. Membrane fractions of 293/Pro and PC-3/Pro cells (30–40 μ g of total protein) were incubated with 5 μ l of mouse seminal vesicle fluid at 37 °C for 1 h. Right panel, samples where indicated, were preincubated with aprotinin before the addition of mouse seminal vesicle fluid. All sample mixtures were analyzed on an SDS-PAGE under reducing conditions followed by prostatin immunoblotting. P1, nucleus fraction; P2, heavy membranes; P3, light membranes; S, cytosolic proteins; and r-hPro, purified recombinant prostatin. The membrane-bound prostatin in heavy or light membrane fractions formed a complex (upper arrow) when incubated with mouse seminal vesicle fluid, whereas prostatin in P1 and cytosolic fractions showed no complex formation. r-hPro was used as a positive control in the *in vitro* binding assay. Excess unbound prostatin is indicated by the lower arrow. The addition of aprotinin at 5 μ g/ml inhibited complex formation as shown in the right panel.

the left panel because of the presence of aprotinin. Because the binding of aprotinin to prostatin was reversible while proteins were being resolved in the gel, the inhibition of prostatin activity seen in lane 4 was not complete. The results suggested that mBPB not only binds to prostatin at the serine active site but also inhibits the serine protease activity of prostatin *in vitro*. Two bands were observed in the prostatin alone sample in the immunoblot (Fig. 9, right panel, lane 2), the differential mobility may be caused by differential glycosylation (1). Aprotinin binding to prostatin changes the charge/mass ratio of the protein; therefore, migration of the aprotinin-bound prostatin in a native PAGE could change as well, potentially causing the multiple banding pattern seen in lane 4 of the immunoblot (Fig. 9, right panel).

Membrane Prostatin Binds to mBPB—To test if the membrane-bound prostatin has binding activity toward mBPB, the 293/Pro and PC-3/Pro cells were subjected to differential centrifugation as described under "Experimental Procedures" except that no protease inhibitors were added during membrane fractionation. Immediately after centrifugation, an aliquot of each membrane fraction (30–40 μ g of total protein) was incubated with an aliquot of mouse seminal vesicle fluid (5 μ l) at 37 °C for 1 h. The binding mixture was then analyzed by Western blot analysis using a prostatin-specific antibody. In Fig. 10, the left panel shows that the membrane-bound prostatin in 293/Pro cells (P2 and P3 fractions) formed an 82-kDa complex when incubated with mouse seminal vesicle fluid. The prostatin protein in the crude nuclear fraction (P1) and the cytosol (S) did not form any detectable complex. The purified r-hPro from the conditioned medium (*i.e.* the secreted prostatin) was used as positive control for the binding assay. In Fig. 10, right panel, we show that the membrane-bound prostatin in PC-3/Pro cells also formed a complex with mBPB, and this reaction was inhibited by the serine protease inhibitor aprotinin.

DISCUSSION

The prostatin serine protease is predominantly synthesized in the prostate in human (1). Recently our laboratory demonstrated that prostatin expression is significantly down-regulated in high grade prostate tumors and absent in invasive human and mouse prostate cancer cell lines. We have also shown, in an *in vitro* Matrigel invasion assay, that cellular prostatin may be an invasion suppressor of prostate cancer

(20). In the present study, we intended to investigate the intracellular distribution of prostaticin and to determine whether the cellular prostaticin is an active serine protease, to provide clues to the potential mechanisms of prostaticin's cellular function.

We first established a mammalian expression system to produce a recombinant human prostaticin. The purified secreted recombinant prostaticin displayed biochemical characteristics similar to those of the native prostaticin (purified from human semen, Ref. 1), such as the molecular mass on SDS-PAGE, immunological reactivity (Fig. 1), enzymatic activity toward the synthetic substrate D-Pro-Phe-Arg-AFC (Fig. 9), and responsiveness to serine protease inhibitors (Figs. 8 and 9). We then used a polyclonal antibody specific for human prostaticin to determine whether prostaticin can exist in a membrane-bound form because its predicted structure suggested this possibility (2). By means of sequential centrifugation of the 293/Pro and PC-3/Pro cell components (as shown in Figs. 2 and 3A), we were able to identify prostaticin in various subcellular compartments such as the crude nuclei, heavy membranes (including mitochondria, lysosomes, and peroxisomes), and light membranes (including plasma membrane, microsomes, and endoplasmic reticula). A confocal microscopy analysis of the PC-3/Pro cells (Fig. 3B) revealed prostaticin's subcellular localization to be primarily at the nuclear-ER-Golgi complex (27). The immunofluorescently localized prostaticin at the nuclear-ER-Golgi complex is believed to be that identified in the Western blot analysis of the nuclear fraction P1. The endogenously expressed prostaticin in the LNCaP cells, however, was only detected in the light membrane fraction P3 (Fig. 3A) not at the nuclear-ER-Golgi complex (Fig. 3B). The different subcellular localization of prostaticin between the recombinant expression system and the endogenous expression system may be caused by expression level differences. Cells expressing recombinant prostaticin produced high amounts of prostaticin with the 293/Pro being the highest followed by PC-3/Pro and DU-145/Pro. The prostaticin expression level in the LNCaP cells was considerably lower than that in these transfected cell lines. The expression levels were determined by a semiquantitative Western blot analysis (data not shown). Alternatively, different cell lines may have different protein sorting mechanisms, leading to different subcellular localization patterns (32). On the other hand, GPI-anchored prostaticin might be associated with sterols and therefore can be found in many compartments of the cell including the plasma membrane, the Golgi apparatus, ER, nucleus, lysosomes and mitochondria, and in lipid particles (33). Prostaticin in the nuclear fraction (P1) did not show binding activity to PBP (Fig. 10). It is presently unclear why prostaticin in this fraction was unable to form a complex with mPBP. The functional significance of prostaticin in the nuclear-ER-Golgi complex is also unclear at present and will be investigated in the future.

Despite the apparently different subcellular localization of prostaticin in overexpressing cells *versus* endogenously expressing cells, prostaticin is found in an membrane-bound form in all cell lines tested as well as in normal human prostate tissues (Fig. 6A). The membrane-bound prostaticin was released when extracted with a detergent but remained membrane-bound when treated with high salt or alkali (Fig. 4), ruling out the possibility that prostaticin is associated with another membrane-bound protein via noncovalent linkages. We also demonstrated that the membrane-bound and the detergent-released prostaticin have similar molecular mass (Fig. 4), ruling out the possibility that prostaticin is covalently linked to another membrane-bound protein.

The native prostaticin in normal prostate tissue and the re-

combinant prostaticin in 293/Pro and PC-3/Pro cells were easily released from the membrane with PI-PLC treatment (Figs. 5 and 6A), suggesting that prostaticin is bound to the membrane via a GPI anchor rather than through a true transmembrane domain. The membrane-bound prostaticin in LNCaP cells (native) or DU-145/Pro cells (recombinant), however, was resistant to PI-PLC treatment (Fig. 6A). As reported in Englund (34) and Hiroshi *et al.* (35), not all GPI-anchored proteins are susceptible to PI-PLC digestion. The membrane-anchored prostaticin in LNCaP and DU-145/Pro could potentially be susceptible to other phospholipases such as GPI-phospholipase D (34, 35). Our results from the [3 H]ethanolamine biosynthetic labeling experiment with PC-3/Pro and LNCaP cells, however, provided direct evidence that in the prostate epithelial cells recombinant or native prostaticin is GPI-anchored, regardless of its sensitivity to PI-PLC treatment (Fig. 6B).

Among all four human cell lines that express either recombinant or native prostaticin, as well as normal human prostate tissue, prostaticin exists mainly as a membrane-bound protein (Fig. 6A). A small portion of prostaticin in the 293/Pro cells is in the cytosolic fraction. This cytosolic prostaticin could be a misprocessed or misfolded form that was exported from the ER before GPI anchor attachment, a mechanism documented previously (36). The presumably misfolded prostaticin in the cytosol had no binding activities when it was incubated with mouse seminal vesicle fluid, possibly because of the misfolding. The secreted recombinant prostaticin, when purified from the 293/Pro culture medium, however, is enzymatically active and able to form a complex with mPBP (Figs. 9 and 10), indicating that the cytosolic prostaticin is not the source of secreted prostaticin. The soluble fraction of prostaticin seen in the human prostate tissues (Fig. 6A) before PI-PLC treatment may also be a misfolded form by the same mechanism described above or may be attributed to residual prostatic fluid caused by possible incomplete washing before tissue lysis.

We identified a PBP in mouse and human seminal vesicles (Fig. 7). Prostaticin forms an 82-kDa, SDS- and heat-stable complex when incubated with seminal vesicle fluid as determined by SDS-PAGE under reducing conditions followed by prostaticin immunoblotting. This complex is apparently covalently formed between prostaticin and PBP and not via a disulfide linkage. We have chosen to use mouse seminal vesicles for an in-depth analysis of PBP because of easier availability. Complex formation between prostaticin and mPBP was inhibited by the polyclonal prostaticin antibody, heparin, and serine protease inhibitors. In a membrane overlay zymography analysis (Fig. 9), the prostaticin-mPBP complex showed no activities to a synthetic substrate D-Pro-Phe-Arg-AFC, whereas unbound prostaticin was active. These results suggest that mPBP may be a serpin class serine protease inhibitor. The true nature of the mechanism of prostaticin inhibition by mPBP will be investigated upon purification and sequence analysis of this protein. An incubation of mouse or human plasma with r-hPro did not result in formation of any covalently-bound complex. This result would rule out the possibility of mPBP being one of the known members of the serpin family present normally in the blood, such as α_1 -antitrypsin, α_1 -antichymotrypsin, kallistatin, plasminogen activator inhibitor, and protein C inhibitor. At present, the functional significance of PBP with respect to prostate biology is unclear. Future studies will be aimed at determining the prostaticin binding site in PBP, which could potentially reveal clues on prostaticin's natural protein substrate.

One of our goals for the present study was to determine whether the membrane-anchored prostaticin is an active serine protease. To accomplish this, we needed a prostaticin-specific

enzymatic activity assay that is applicable for membrane-bound prostatic because this form of prostatic exists in a complex mixture. The membrane overlay zymography assay was not applicable for the membrane-anchored prostatic because lipid-associated proteins cannot be well resolved in non-denaturing native gel electrophoresis. The identification of mPBP offered us an indirect but prostatic-specific assay to address this question. As presented in Fig. 10, the membrane-bound human prostatic also displayed binding activity to mPBP, and the binding is inhibited by a serine protease inhibitor (aprotinin) that competes for the serine active site, suggesting that the membrane-bound prostatic is likely an active serine protease. Demonstration of membrane-bound prostatic being an active serine protease will provide clues for investigating the signal transduction pathway(s) involved in the anti-invasion activity of prostatic because this anti-invasion activity is conferred by the cellular prostatic but not the secreted prostatic (20).

Prostatic is made in the prostate and secreted as an active serine protease (1), whereas PBP is made in the seminal vesicles. The fact that prostatic forms a complex with PBP suggests that the two proteins interact with each other when semen is ejaculated, thereby implicating a role for both proteins in semen coagulation and liquefaction. Prostatic and PBP in male reproductive tracts may serve together in a partnership to affect fertility. Investigating the prostatic-PBP partnership could also lead to a better understanding of the various factors affecting fertility or, causing infertility. Overall, prostatic, as a GPI-anchored or a secreted active serine protease, may have multiple physiological functions, depending on the localization of the prostatic protein, whether it is membrane-bound or secreted.

REFERENCES

1. Yu, J. X., Chao, L., and Chao, J. (1994) *J. Biol. Chem.* **269**, 18843-18848
2. Yu, J. X., Chao, L., and Chao, J. (1995) *J. Biol. Chem.* **270**, 13483-13489
3. Nelson, P. S., Gan, L., Ferguson, C., Moss, P., Gelin, R., Hood, L., and Wang, K. (1999) *Proc. Natl. Acad. Sci. U. S. A.* **96**, 3114-3119
4. Hooper, J. D., Nicol, D. L., Dickinson, J. L., Eyre, H. J., Scarman, A. L., Normyle, J. F., Stutgen, M. A., Douglas, M. L., Loveland, K. A., Sutherland, G. R., and Antalis, T. M. (1999) *Cancer Res.* **59**, 3199-3205
5. Vallet, V., Chraïbi, A., Gaeggele, H. P., Horisberger, J. D., and Rossier, B. C. (1997) *Nature* **388**, 607-610
6. Vuagniaux, G., Vallet, V., Jaeger, N. F., Pfister, C., Bens, M., Farman, N., Courtis-Couty, N., Vandewalle, A., Rossier, B. C., and Hummler, E. (2000) *J. Am. Soc. Nephrol.* **11**, 828-834
7. Rawlings, N. D., and Barrett, A. J. (1994) *Methods Enzymol.* **244**, 19-61
8. Wang, M. C., Papisidero, L. D., Kuriyama, M., Valenzuela, L. A., Murphy, G. P., and Chu, T. M. (1981) *Prostate* **2**, 89-96
9. Frenette, G., Deperthes, D., Tremblay, R. R., Lazure, C., and Dube, J. Y. (1997) *Biochim. Biophys. Acta* **1334**, 109-115
10. Lilja, H., Oldbring, J., Rannev, G., and Laurell, C. B. (1987) *J. Clin. Invest.* **80**, 281-285
11. Guinan, P., Bhatti, R., and Ray, P. (1987) *J. Urol.* **137**, 686-689
12. Stamey, T. A., Kabalin, J. N., McNeal, J. E., Johnstone, I. M., Freiha, F., Redwine, E. A., and Yang, N. (1989) *J. Urol.* **141**, 1076-1083
13. Recker, F., Kwiatkowski, M. K., Piironen, Y., Pettersson, K., Lummen, G., Wernli, M., Wiefelsputz, J., Graber, S. F., Goepel, M., Huber, A., and Tscholl, R. (1998) *Cancer* **83**, 2540-2547
14. Stenman, U. H. (1999) *Clin. Chem.* **45**, 753-754
15. Carrell, R. W., Pemberton, P. A., and Boswell, D. R. (1987) *Cold Spring Harbor Symp. Quant. Biol.* **52**, 527-535
16. Chen, L.-M., Chao, L., Mayfield, R. K., and Chao, J. (1990) *Biochem. J.* **267**, 79-84
17. Zhou, G. X., Chao, L., and Chao, J. (1992) *J. Biol. Chem.* **267**, 25873-25880
18. Christensson, A., Laurell, C. B., and Lilja, H. (1990) *Eur. J. Biochem.* **194**, 755-763
19. Wright, H. T., and Scarsdale, J. N. (1995) *Proteins Struct. Funct. Genet.* **22**, 210-225
20. Chen, L.-M., Hodge, G. B., Guarda, L. A., Welch, J. L., and Chai, K. X. (2001) *Prostate*, **48**, in press
21. Krajewski, S., Tanaka, S., Takayama, S., Schibler, M. J., Fenton, W., and Reed, J. C. (1993) *Cancer Res.* **53**, 4701-4714
22. Pemberton, P. A., Tipton, A. R., Pavloff, N., Smith, J., Erickson, J. R., Mouchaback, Z. M., and Kiefer, M. C. (1997) *J. Histochem. Cytochem.* **45**, 1697-1706
23. Pei, D., Kang, T., and Qi, H. (2000) *J. Biol. Chem.* **275**, 33988-33997
24. Bordier, C. (1981) *J. Biol. Chem.* **256**, 1604-1607
25. Rosenberg, I. M. (1996) *Protein Analysis and Purification*, p. 254, Birkhauser, Boston
26. Beals, D. F., Stedman, E., and Kouns, D. M. (1969) *Clin. Chem.* **15**, 1210-1217
27. Rolls, M. M., Stein, P. A., Taylor, S. S., Ha, E., McKeon, F., and Rapoport, T. A. (1999) *J. Cell Biol.* **146**, 29-44
28. Itoh, Y., Kajita, M., Kinoh, H., Mori, H., Okada, A., and Seiki, M. (1999) *J. Biol. Chem.* **274**, 34260-34266
29. Hirose, S., Knez, J. J., and Medof, M. E. (1995) *Methods Enzymol.* **250**, 582-614
30. Shimamoto, K., Chao, J., and Margolius, H. S. (1980) *J. Clin. Endocrinol. Metab.* **51**, 840-848
31. Niemann, M. A., Narkates, A. J., and Miller, E. J. (1992) *Matrix* **12**, 233-241
32. Soole, K. L., Jepson, M. A., Hazlewood, G. P., Gilbert, H. J., and Hirst, B. H. (1995) *J. Cell Sci.* **108**, 369-377
33. Muniz, M., and Riezman, H. (2000) *EMBO J.* **19**, 10-15
34. Englund, P. T. (1993) *Annu. Rev. Biochem.* **62**, 121-138
35. Hiroshi, T., Yoshio, M., Noboru, T., and Yukio, I. (1998) *Biochem. Biophys. Res. Commun.* **251**, 737-743
36. Ali, B. R. S., Tjernberg, A., Chait, B. T., and Field, M. C. (2000) *J. Biol. Chem.* **275**, 33222-33230



PROSTASIN SERINE PROTEASE INHIBITS BREAST CANCER INVASIVENESS AND IS TRANSCRIPTIONALLY REGULATED BY PROMOTER DNA METHYLATION

Li-Mei CHEN and Karl X. CHAI*

Department of Molecular Biology and Microbiology, University of Central Florida, Orlando, FL, USA

We have shown that prostatic serine protease is down-regulated in high-grade prostate tumors and inhibits invasiveness of prostate cancer cell lines upon enforced reexpression. In our study, prostatic mRNA and protein were shown to be expressed in normal human mammary epithelial cells (NHMEC), the poorly invasive breast carcinoma cell line MCF-7 and the nonmetastatic breast carcinoma cell line MDA-MB-453, but absent in highly invasive and metastatic breast carcinoma cell lines MDA-MB-231 and MDA-MB-435s. Enforced reexpression of prostatic in MDA-MB-231 and MDA-MB-435s reduced the *in vitro* invasiveness of either cell line by 50%. Examination of the prostatic gene promoter and first exon revealed a GC-enriched region that contains transcription regulatory elements. The promoter and exon 1 region of the prostatic gene was investigated for DNA methylation in NHMEC and the carcinoma cell lines. The results revealed a methylation pattern that correlates with prostatic expression in these cells. Demethylation coupled with histone deacetylase inhibition resulted in reactivated expression of the prostatic mRNA in MDA-MB-231 and MDA-MB-435s cells. These results suggest that prostatic expression in breast cancer cells may be regulated by DNA methylation and that an absence of prostatic expression may contribute to breast cancer invasiveness and metastatic potential.

© 2002 Wiley-Liss, Inc.

Key words: prostatic; serine protease; invasion suppressor; breast cancer; transcription regulation; DNA methylation

Prostatic, a prostate-abundant serine protease originally discovered in human seminal fluid,¹ has recently been shown to be downregulated in high-grade (Gleason 4/5) prostate cancers and to have the ability of inhibiting invasion *in vitro* upon enforced reexpression in highly invasive human prostate cancer cells DU-145 and PC-3.² Prostatic is a glycosylphosphatidylinositol (GPI)-anchored active serine protease expressed in normal prostate epithelial cells and can also be secreted into the prostatic fluid.³ The membrane-anchored but not the secreted prostatic confers the invasion suppression of prostate cancer cells.² Enforced reexpression of prostatic in DU-145 and PC-3 cells did not have any effect on cell proliferation.² Together with normal epithelial specific 1 (NES1),⁴ prostatic⁵ and testisin,⁶ these 4 and potentially more serine proteases form the foundation of a new paradigm of serine proteases and cancer.² First, these serine proteases are expressed in either normal prostate epithelia or cells (prostatic, NES1 and prostatic),^{2,4,5} normal breast epithelial cells (NES1)⁴ or the pachytene spermatocytes in normal testis (testisin).⁶ But they are absent or expression level-reduced in tumors or tumor cell lines of these tissues.^{2,4–6} Second, NES1 and testisin have been shown to be tumor suppressors^{4,7} and prostatic may be a potential invasion suppressor.² These new roles of serine proteases in cancer are in sharp contrast to the view held of serine proteases' role in cancer by the conventional paradigm, that they are usually upregulated in cancer and promote cancer invasion and metastasis.⁸ A classical example of the conventional paradigm of serine proteases' role in prostate and breast cancers is given with the urokinase-type plasminogen activator (uPA). uPA is upregulated in prostate and breast cancers and promotes tumor invasion.^{9,10} In breast cancer cell lines, uPA expression was observed in the highly invasive, hormone-insensitive MDA-MB-231, but not in the poorly invasive, hormone-sensitive MCF-7, T-47D or normal human mammary epithelial cells (NHMEC).¹¹ uPA expression in breast cancer cells is regulated by promoter DNA methylation.¹¹

Prostatic's expression was mainly found in the prostate while a lesser amount was found in various tissues.^{1,12} Prostatic expression in the breast, however, has not been examined. Several prostate-abundant serine proteases, for example, prostate-specific antigen (PSA) and human glandular kallikrein 2 (hK2), have been shown to be expressed in human breast cancer cell lines.¹³ In our study, we have examined prostatic expression in NHMEC and a panel of human breast carcinoma cell lines, including the poorly invasive MCF-7, the nonmetastatic MDA-MB-453 and the highly invasive and metastatic MDA-MB-231 and MDA-MB-435s. Enforced reexpression of a recombinant human prostatic protein in the invasive cell lines was performed and the effect of prostatic reexpression on *in vitro* invasiveness was examined. Prostatic gene promoter in these cell lines was examined for DNA methylation, and the effect of demethylation coupled with histone deacetylase inhibition on prostatic expression in the MDA-MB-231 and MDA-MB-435s cells was investigated.

MATERIAL AND METHODS

Cell culture maintenance

All cell culture media, sera and supplements were purchased from Life Technologies (Gaithersburg, MD), except for those noted otherwise.

A normal human mammary epithelial cell primary culture (catalog number CC-2551) was obtained from Clonetics (San Diego, CA) and maintained in the mammary epithelial basal medium (supplemented with bovine pituitary extract, recombinant human epidermal growth factor, bovine insulin and hydrocortisone) according to the supplier's protocols. The culture was kept at 37°C with 5% CO₂ and used for experiments at the 9th overall passage.

Human breast carcinoma cell lines MCF-7, MDA-MB-453, MDA-MB-231 and MDA-MB-435s were obtained from the American Type Culture Collection (ATCC, Manassas, VA). The MCF-7 cells were maintained in DMEM supplemented with 10% FBS and kept at 37°C with 5% CO₂. The MDA-MB-231 and MDA-MB-453 cells were maintained in Lebovitz-15 (L-15) medium supplemented with 10% FBS and kept at 37°C without CO₂. The MDA-MB-435s cells were maintained in L-15 medium supplemented with 15% FBS and 10 µg/ml bovine insulin and kept at 37°C without CO₂.

Transfection of cell lines with plasmid DNA and selection of stable transfectants

Construction of a plasmid containing a full-length human prostatic cDNA under the control of a Rous sarcoma virus (RSV)

Grant sponsor: Department of Defense Prostate Cancer Research Program; Grant number: DAMD17-98-1-8590.

*Correspondence to: Department of Molecular Biology and Microbiology, University of Central Florida, 4000 Central Florida Boulevard, Orlando, FL 32816-2360, USA. Fax: +407-823-3095.
 E-mail: kxchai@mail.ucf.edu

Received 23 April 2001; Revised 27 July 2001; Accepted 6 August 2001

; DOI 10.1002/ijc.1601

promoter and transfection of cells were carried out as described previously.² Briefly, 1,000,000 MDA-MB-231 or MDA-MB-435s cells were resuspended in 0.3 ml of the culture medium and mixed with 50 µg of plasmid DNA dissolved in 0.1 ml of sterile distilled water. The cell/DNA mixture was then transferred to a 4 mm cuvette and pulsed at 200 volts, 1,600 µF, 72 ohms and 500 V/Capacitance setting on a BTX-600 Electro-cell-manipulator (Genetronics, San Diego, CA). Selection of transfectants was carried out in the presence of 800 µg/ml G418 (final concentration) until colonies appeared (5–7 days). Colonies (~200 in number) were then dispersed via trypsinization and maintained in G418-containing culture medium without colony-isolation. Cells transfected with the human prostatic cDNA construct were assayed in Western blot analysis for expression of the prostatic protein, using vector-transfected cells as controls.

RNA preparation and analysis by RT-PCR/Southern blot

Cells grown to 80–100% confluence (in 60 mm tissue culture dish) were lysed directly with 1 ml of the Trizol Reagent (Life Technologies) and RNA was isolated according to the manufacturer's protocol. The human prostatic-specific RT-PCR/Southern blot analysis was performed as described previously.¹² One microgram of total RNA was used in the RT-PCR with 2 human prostatic gene-specific oligonucleotide primers, and a Southern blot of the resolved RT-PCR samples was probed with a third prostatic gene-specific oligonucleotide, detecting an amplified 232 bp fragment.¹² A co-amplification of the β-actin mRNA for control of RNA quality and quantity was performed as described previously.²

Western blot analysis

Cells grown to 80–100% confluence were washed 3 times in 1 × PBS (pH 7.4) and then lysed in RIPA buffer (1 × PBS, pH 7.4, 1% NP-40, 0.5% sodium deoxycholate, 0.1% SDS). The total lysate were centrifuged at 14,000 rpm for 30 min at 4°C to remove the pellet. Protein concentration was determined using a DC (detergent-compatible) protein assay kit (Bio-Rad, Hercules, CA). The samples were then subjected to SDS-PAGE followed by Western blot analysis using a prostatic-specific antibody.³ Briefly, cell lysate were resolved in 10% gels under reducing conditions before electrotransfer to nitrocellulose (NC) membranes (Fisher Scientific, Pittsburgh, PA). Upon complete protein transfer, the NC membranes were blocked in BLOTTO (5% nonfat milk made with Tris-buffered saline/0.1% Tween-20, pH 7.6), incubated with the prostatic-specific antibody diluted at a ratio of 1:2,000 in BLOTTO, followed by an incubation with the secondary antibody, goat antirabbit IgG conjugated to HRP (horseradish peroxidase; used at 1:10,000) (Sigma-Aldrich, St. Louis, MO). The bound secondary antibody was detected using enhanced-chemiluminescence (ECL) reagents (Pierce, Rockford, IL) according to the supplier's recommendations. All procedures were performed at room temperature, and the membranes were washed between steps.

Matrigel chemoinvasion assay

The Matrigel chemoinvasion assay was carried out essentially as described previously.² Basement membrane Matrigel stock (10 mg/ml; Collaborative Biochemical, Bedford, MA) was thawed overnight on ice in a refrigerator (0–4°C). Transwell invasion chambers (Costar, Cambridge, MA) with 8 µm pore polycarbonate filters (growth area 0.33 cm²) were coated with Matrigel (50 µg/filter, a 1:3 dilution of the stock with chilled serum-free medium was used for coating). The gels were solidified by incubating the coated filters at 37°C for 60 min in a moist chamber before use. The lower chambers of the Transwell plates were filled with 0.6 ml serum-free medium (L-15), supplemented with 25 µg/ml fibronectin (Sigma-Aldrich). Fifty thousand cells in 0.1 ml serum-free OPTI-MEM I medium were placed onto each Matrigel-coated filter. The filter cartridge was then inserted into the lower chamber and the assays were performed at 37°C for 24 hr (MDA-MB-435s transfectants) or 72 hr (MDA-MB-231 transfectants). After removing the medium, the filters were washed 3 times in 1 × PBS, fixed

at room temperature for 20 min in 4% paraformaldehyde made with 0.1 M sodium phosphate buffer (pH 7.4) and then washed 3 times with the sodium phosphate buffer. The filters were then stained with 1% toluidine blue (LabChem, Pittsburgh, PA) for 2 min. The cells on the Matrigel surface were removed with a Q-tip and all cells on the underside of the filters were counted under a light microscope after mounting the filter on a glass slide. All invasion assays were done in triplicate for at least 3 times.

Genomic Southern blot analysis of prostatic promoter methylation

High molecular weight genomic DNA was isolated from various cell lines as described previously.¹⁴ Genomic DNA from each cell line was digested with the following restriction enzyme combinations: Xho I/BamH I (X/B), Xho I/BamH I/Hha I (X/B/Hh), Xho I/BamH I/Aci I (X/B/A), Xho I/BamH I/BsaA I (X/B/Bs), Xho I/BamH I/Msp I (X/B/M) or Xho I/BamH I/Hpa II (X/B/H) using 10 µg of DNA per digestion combination. The X/B cutting sites flank the CpG sites to be investigated for differential methylation by the methylation-sensitive restriction endonucleases. The digests were resolved in a 0.8% agarose gel and analyzed by Southern blot hybridization as described previously.¹⁴ A nick-translated prostatic promoter probe (bases 703–1,649 of the prostatic gene sequence, GenBank accession number U33446) was used for the hybridization. The base numbering of the prostatic gene sequence was described in Yu *et al.*¹⁵

Demethylation of prostatic gene promoter and reactivation of prostatic expression

For demethylation of prostatic gene promoter, MDA-MB-231 and MDA-MB-435s cells were seeded in 100 mm dishes at an initial density of 50% confluence and cultured in the presence of 500 nM 5-aza-2'-deoxycytidine (5-aza-2'-dC; Sigma-Aldrich) for 8 days, with renewal of medium and 5-aza-2'-dC performed at 2-day intervals. Genomic DNA was then isolated for Southern blot analysis as described. For reactivation of prostatic expression, MDA-MB-231 and MDA-MB-435s cells were seeded in 60 mm dishes at 80% confluence and cultured in the presence of 500 nM 5-aza-2'-dC for 24 hr, and were then treated for an additional 24 hr with either 1 µM trichostatin A (TSA; Sigma-Aldrich) or an equal volume of 95% ethanol used to dissolve TSA. For measuring time-dependence of prostatic gene reactivation, cells were treated as described above but were harvested at 6 or 12 hr after the addition of TSA. RNA was isolated for prostatic-specific RT-PCR/Southern blot analysis as described. The MCF-7 and the MDA-MB-453 cell lines were subjected to the same 5-aza-2'-dC/TSA treatment and prostatic RT-PCR/Southern blot analysis procedures.

RESULTS

Prostatic expression in breast cancer cell lines

Expression of prostatic protein and mRNA in NHMEC and human breast carcinoma cell lines was examined by Western blot analysis using a prostatic-specific antibody³ or RT-PCR/Southern blot analysis as described.² For our study, we chose 4 human breast carcinoma cell lines based on their differences in invasiveness and metastatic potential. The MCF-7 cell line is poorly invasive to noninvasive,^{16,17} tumorigenic but nonmetastatic.¹⁸ The MDA-MB-453 cells are poorly tumorigenic and nonmetastatic.¹⁹ The MDA-MB-231 and MDA-MB-435s cells are both highly invasive¹⁶ and highly metastatic.^{20,21}

As shown in Figure 1 (top panel), a 40 kDa prostatic protein band was detected in the total cell lysate of NHMEC, the poorly invasive breast carcinoma cell line MCF-7 and the nonmetastatic breast carcinoma cell line MDA-MB-453. No prostatic protein was detected in the cell lysate of highly invasive and metastatic breast carcinoma cell lines MDA-MB-231 and MDA-MB-435s. The 2 breast cancer cell lines that express the prostatic protein (MCF-7 and MDA-MB-453) appeared to show a greater level of expression than the NHMEC. It is presently unclear what factors

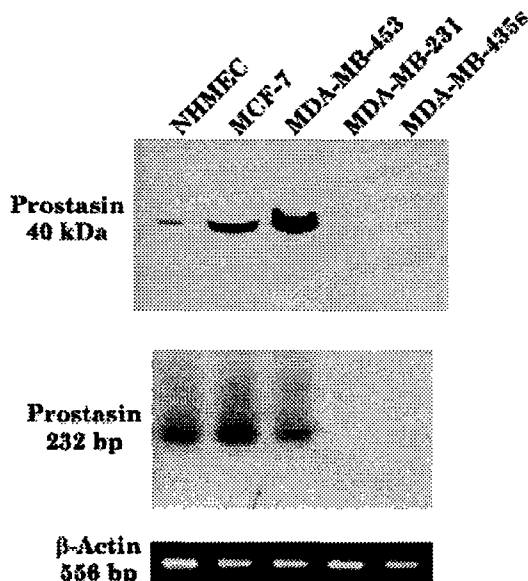


FIGURE 1—Human prostatic expression in mammary epithelial cells. By means of Western blot analysis (top panel), prostatic (as a 40 kDa band) was detected in NHMEC and breast cancer cell lines MCF-7 and MDA-MB-453, but not in breast cancer cell lines MDA-MB-231 or MDA-MB-435s. An equal amount of total protein (100 μ g) was loaded for each sample. At the mRNA level, human prostatic mRNA (via a 232 bp amplified DNA band) was detected in NHMEC, MCF-7 and MDA-MB-453, but not in MDA-MB-231 or MDA-MB-435s as analyzed by RT-PCR/Southern blot hybridization (middle panel). Co-amplification of a 556 bp human β -actin message (as shown in the gel photograph in the bottom panel) confirmed the quality and the quantity of the RNA applied in each RT-PCR.

may have contributed to this apparent difference of prostatic protein expression levels in these cells. Expression of prostatic mRNA in these cells corresponds with the presence of prostatic protein expression. As shown in Figure 1 (middle panel), a 232 bp amplified prostatic message was detected in total RNA of NHMEC, MCF-7 and MDA-MB-453, but not MDA-MB-231 or MDA-MB-435s. A co-amplification of β -actin message is shown in the bottom panel of Figure 1 to demonstrate the quality and quantity of total RNA used in each RT-PCR. In addition to the expected 232 bp prostatic amplification product, a faint band of retarded mobility was also detected in the Southern blot analysis. This retarded band does not represent a new prostatic message, but rather is a single-stranded form of the expected prostatic PCR product.²² In a separate experiment, we were able to remove this single-stranded form by treating the PCR products with S1 nuclease prior to electrophoresis (data not shown).

Reexpression of recombinant human prostatic in invasive breast cancer cells reduced *in vitro* invasiveness

Following the electroporation and drug selection, ~200 colonies formed for each transfected cell type. All colonies for each transfected cell type were kept in a mixed culture as polyclonal transfectants for the ensuing experiments. Polyclonal MDA-MB-231 and MDA-MB-435s cells transfected with the human prostatic cDNA were confirmed to express the recombinant human prostatic protein, as shown by Western blot analysis of the cell lysate (Fig. 2, top panel). The vector-transfected cells were used as negative control in the Western blot analysis.

In the *in vitro* Matrigel chemoinvasion assays (Fig. 2, bottom panel), transfected MDA-MB-231 or MDA-MB-435s cells expressing the recombinant human prostatic protein showed a significantly reduced level of invasiveness, at 50% of that of their vector-transfected controls, respectively.

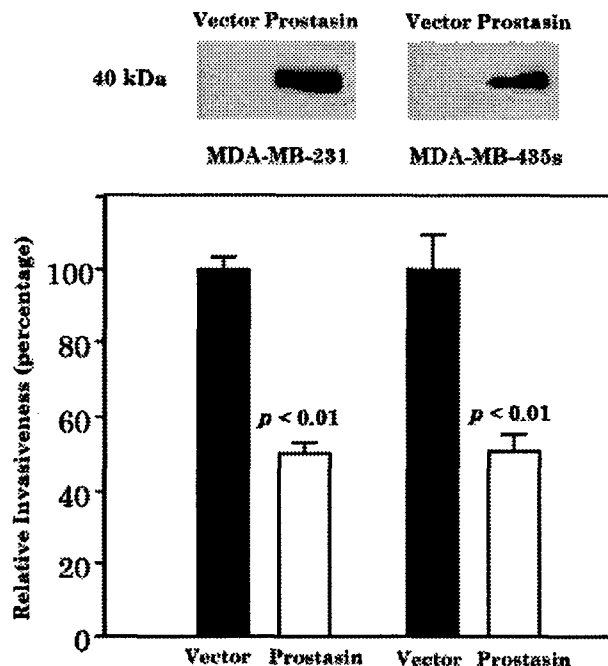


FIGURE 2—Recombinant prostatic protein expression and *in vitro* invasive properties of the MDA-MB-231 or MDA-MB-435s transfectants. MDA-MB-231 or MDA-MB-435s cells transfected with either a vector DNA (labeled as "vector") or a prostatic cDNA construct (labeled as "prostatic") were subjected to a Western blot analysis using a prostatic-specific antibody (top panel) or subjected to an *in vitro* Matrigel chemoinvasion assay (bottom panel) as described in Material and Methods. The expressed recombinant human prostatic protein (a 40 kDa band) was detected in the prostatic cDNA-transfected MDA-MB-231 or MDA-MB-435s cells, but not in the vector-transfected cells. In the Matrigel chemoinvasion assay, the vector-transfected cells are expressed as being 100% invasive (solid bars). The open bars represent the relative invasiveness of the human prostatic cDNA-transfected cells. The data were analyzed by Student's *t*-test using the StatView software (Abacus Concepts, Berkeley, CA).

Prostatic gene promoter is hypermethylated in invasive breast cancer cell lines

Examination of the prostatic gene locus by genomic Southern blot-RFLP (restriction fragment length polymorphism) analysis did not reveal any evidence of gene loss or gross rearrangement in the cell lines that did not show prostatic expression, namely, MDA-MB-231 and MDA-MB-435s (data not shown). We then considered the possibility of prostatic gene-silencing by epigenetic mechanisms. Postsynthetic methylation of cytosine residues in the 5'-CpG islands is often involved in long-term silencing of certain genes during mammalian development and in the progression of cancers.²³ An examination of the prostatic promoter and exon 1 region sequence (GenBank accession number U33446) identified 28 CpG dinucleotides in a segment defined by an Xho I site (base number 374 of U33446, or -1,048 relative to the transcription initiation site) and a BamH I site (base number 1,649 of U33446, or +228 relative to the transcription initiation site) (Fig. 3a). A GC-enriched domain containing 2 consensus G/C boxes with the sequence GGGCGG²⁴ is identified encompassing the transcription initiation site. This GC-enriched domain extends from base number 1,101 to the BamH I site (1,649), at a length of 549 bp and has a GC content of 58.6%. The 549 bp GC-enriched domain contains 19 CpG dinucleotides, but failed to qualify as a true CpG island by the standards of Gardiner-Garden and Frommer.²⁴

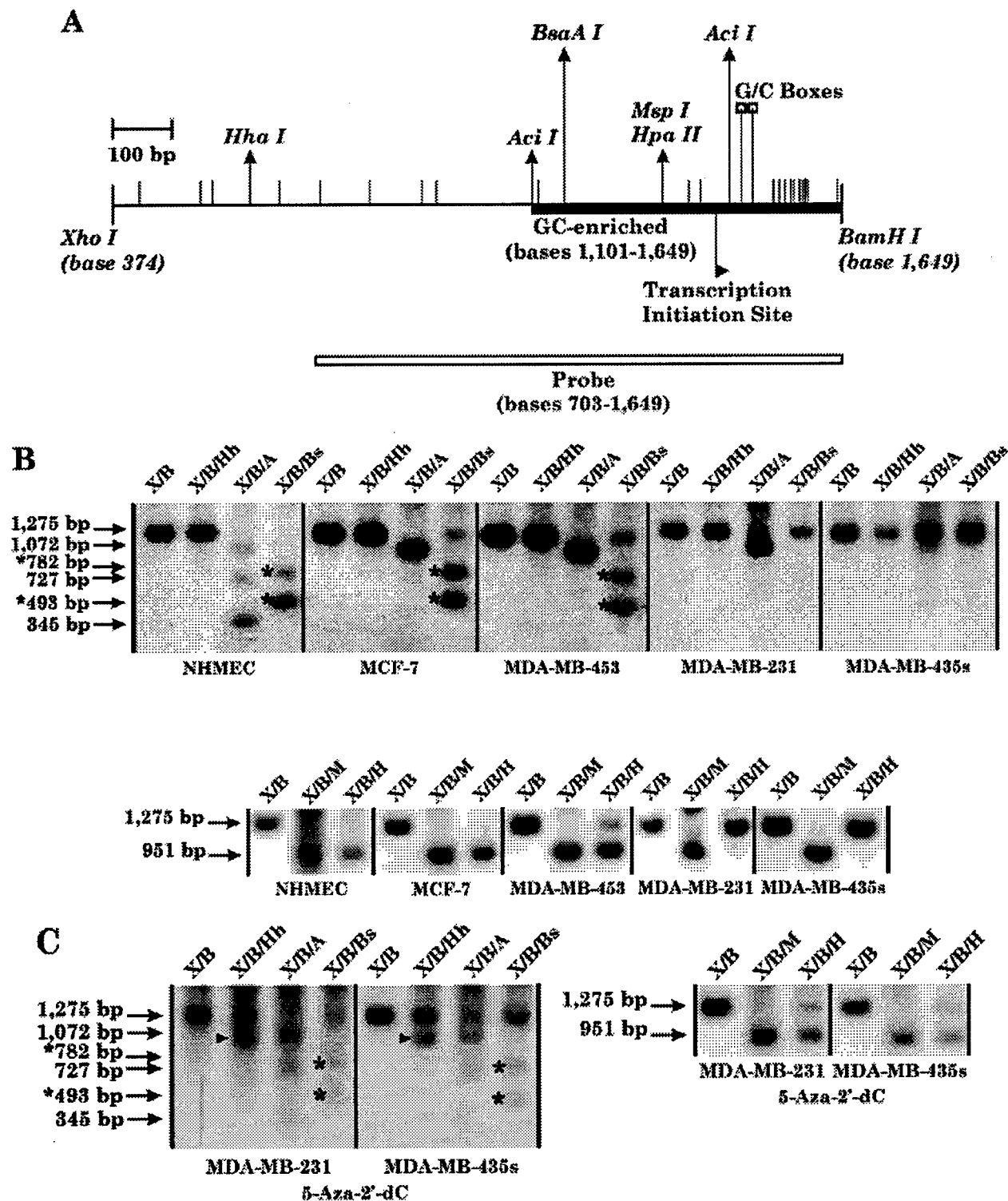


FIGURE 3.

Genomic DNA methylation state of this Xho I-BamH I segment in the prostatic promoter-exon 1 region was investigated by Southern blot analysis using methylation-sensitive restriction endonucleases, which cut at unmethylated sites that contain CpG dinucleotide. The sites being investigated were an Hha I site at base number 615 (of

U33446, same below)/-807 (relative to the transcription initiation site, same below), an AcI I site at 1,102/-320, a BsaA I site at 1,156/-266, an Hpa II site at 1,326/-96 and an AcI I site at 1,445/+24 (Fig. 3a). The results of the genomic Southern blot analysis are presented in Figure 3b and summarized in Table I.

TABLE I—SUMMARY OF CPG METHYLATION STATES IN THE PROSTASIN GENE PROMOTER-EXON 1 REGION IN HUMAN BREAST CELLS

Cell type	Prostasin expression	Hha I (−807)	Aci I (−320)	BsaA I (−266)	Msp I/Hpa II (−96)	Aci I (+24)
NHMEC	Yes	Methyl	Hetero-methyl	Un-methyl	Un-methyl	Un-methyl
MCF-7	Yes	Methyl	Methyl	Hetero-methyl	Un-methyl	Un-methyl
MDA-MB-453	Yes	Methyl	Methyl	Hetero-methyl	Hetero-methyl	Un-methyl
MDA-MB-231	No	Methyl	Methyl	Methyl	Methyl	Un-methyl
MDA-MB-435s	No	Methyl	Methyl	Methyl	Methyl	Methyl
MDA-MB-231/Aza	Yes ¹	Hetero-methyl	Hetero-methyl	Hetero-methyl	Hetero-methyl	Un-methyl
MDA-MB-435s/Aza	Yes ¹	Hetero-methyl	Hetero-methyl	Hetero-methyl	Hetero-methyl	Hetero-methyl

Methyl, homogeneously methylated; Hetero-methyl, heterogeneously methylated; Un-methyl, homogeneously unmethylated.—¹Prostasin mRNA expression was detected when these cell lines were further treated with TSA (Fig. 4a).

In all 4 breast cancer cell lines and the NHMEC, Xho I/BamH I/Hha I digestion yielded a 1,275 bp prostasin promoter band seen in the Xho I/BamH I digestion (Fig. 3b, upper panel), indicating that the −807 Hha I site-CpG is homogeneously methylated.

In the NHMEC, digestion with Xho I/BamH I/Aci I yielded a 1,072 bp, a 727 bp and a 345 bp band, but no 1,275 bp band, indicating that the −320 Aci I site-CpG is heterogeneously methylated, but the +24 Aci I site-CpG is homogeneously unmethylated. In MCF-7, MDA-MB-453 and MDA-MB-231, digestion with Xho I/BamH I/Aci I yielded only the 1,072 bp band, indicating that the −320 Aci I site-CpG is homogeneously methylated, but the +24 Aci I site-CpG is homogeneously unmethylated. In MDA-MB-435s, digestion with Xho I/BamH I/Aci I yielded only the 1,275 bp band, indicating that both the −320 and the +24 Aci I site-CpG's are homogeneously methylated.

In the NHMEC, digestion with Xho I/BamH I/BsaA I yielded a 782 bp and a 493 bp band, indicating that the −266 BsaA I site-CpG is homogeneously unmethylated. In MCF-7 and MDA-MB-453, digestion with Xho I/BamH I/BsaA I yielded the 782 bp and the 493 bp bands, but also the 1,275 bp band, indicating that the −266 BsaA I site-CpG is heterogeneously methylated. In MDA-MB-231 and MDA-MB-435s, digestion with Xho I/BamH I/BsaA I yielded only the 1,275 bp band, indicating that the −266 BsaA I site-CpG is homogeneously methylated.

In the NHMEC and MCF-7 cells, the 1,275 bp Xho I-BamH I band can be digested by the methylation-insensitive Msp I as well as by the methylation-sensitive Hpa II, yielding an 951 bp band, indicating that the CpG at the −96 M/H restriction site is homogeneously unmethylated. In MDA-MB-453, the 1,275 bp band can be fully digested by Msp I, but only partially by Hpa II, indicating heterogeneous methylation of the −96 M/H site-CpG. In MDA-MB-231 and MDA-MB-435s, the 1,275 bp band was undigested

by Hpa II while having been completely digested by Msp I, indicating that the −96 M/H site-CpG is homogeneously methylated.

Overall, in the prostasin-expressing cells, the NHMEC is the least methylated in this region and the methylation is restricted to beyond −266, relative to the transcription initiation site. The prostasin gene promoter-exon 1 region in MCF-7 and MDA-MB-453 cells is methylated to a higher extent than that in the NHMEC. In the MCF-7, methylation is restricted to beyond −96, while in the MDA-MB-453, methylation is observed at the −96 position and beyond. In the cells that do not express prostasin, the promoter-exon 1 region is the most heavily methylated. While in MDA-MB-231 the methylation is still restricted to the 5'-flanking region, all CpG sites examined, including 1 of exon 1 (+24 Aci I site-CpG) were found to be homogeneously methylated in the MDA-MB-435s cells. Our results showed that the prostasin gene promoter-exon 1 region CpG methylation patterns correlate with the absence of prostasin expression in the human breast cells examined in our study.

Prostasin expression was reactivated by demethylation and histone deacetylase inhibition in the invasive and metastatic breast cancer cell lines

Methylated promoter DNA may contribute to repression of gene expression by interfering with the binding of transcription factors,²⁵ or by interacting with various methyl-CpG binding proteins, such as the MeCP1 complex, MeCP2 and the MBD's,^{26–29} depending on cell type, sequence of the methylated regulatory region and binding of other transcription factors.³⁰ Histone deacetylases are recruited by the methyl-CpG binding proteins to co-repress gene expression via chromatin restructuring.^{31–35} Histone deacetylases act synergistically with DNA methylation in the co-repres-

FIGURE 3—(a) Schematic illustration of the promoter-exon 1 region of the prostasin gene. The solid horizontal line represents the promoter-exon 1 region of the human prostasin gene (GenBank U33446).¹⁵ The Xho I site is located at base number 374, and the BamH I site is located at base number 1,649 of the U33446 sequence, respectively. The methylation-sensitive restriction sites used for differential methylation analysis, Hha I (615/−807), Aci I (1,102/−320 and 1,445/+24), BsaA I (1,156/−266) and Msp I/Hpa II (1,326/−96) are indicated by arrows. Four additional Aci I sites and a second Msp I/Hpa II site are present between the +24 Aci I site and the BamH I site, but not shown in the figure since they do not affect the results of the genomic DNA Southern blot analysis. The transcription initiation site¹⁵ is indicated by the triangle on an extended vertical bar. Thin vertical bars map the location of the 28 CpG dinucleotides identified in this region. A 549 bp GC-enriched domain is indicated by the filled rectangular box. The extended vertical bars with open square boxes indicate the locations of the consensus G/C boxes. The location of the probe used in the genomic DNA Southern blot analysis is shown by the open rectangular box. **(b)** Genomic Southern blot analysis of DNA from NHMEC and human breast cancer cell lines. Panels of genomic DNA Southern blot analysis results are as indicated for each cell type. Restriction endonucleases used in each digestion mixture are identified as follows: X, Xho I; B, BamH I; Hh, Hha I; A, Aci I; Bs, BsaA I; M, Msp I; H, Hpa II. Hha I, Aci I, BsaA I and Hpa II only cut unmethylated DNA, while Msp I, an isoschizomer of Hpa II, cuts unmethylated or methylated DNA. Genomic DNA (10 µg) from each cell type was cut with X/B or with X/B/M to serve as controls for the detection of differential methylation. In the upper panel, prostasin promoter DNA will yield a 1,275 bp X/B fragment. When Hha I was added to the X/B digestion mixture, a fragment of 1,037 bp was expected if the −807 Hha I site-CpG was not methylated. When Aci I was added to the X/B digestion mixture, 3 smaller bands might be expected depending on CpG methylation states at −320 and +24 Aci I sites. They are 1,072 bp (from Xho I to +24 Aci I), 727 bp (from Xho I to −320 Aci I) and 345 bp (from −320 Aci I to +24 Aci I) in length, respectively. When BsaA I was added to the X/B digestion mixture, 2 smaller bands might be expected depending on CpG methylation state at the −266 BsaA I. They are 782 bp (from Xho I to BsaA I) and 493 bp (from BsaA I to BamH I) in length, respectively (indicated by asterisks in the figure). In the lower panel, the upper arrow points to the X/B fragment, while the lower arrow points to the fragment that is generated by Msp I, regardless of DNA methylation, or by Hpa II, only when DNA is unmethylated. **(c)** Genomic Southern blot analysis of MDA-MB-231 and MDA-MB-435s cells following demethylation. Cells treated with 5-aza-2'-dC for 8 days were harvested for genomic DNA isolation and Southern blot analysis as described. The arrowhead indicates the 1,037 bp Hha I-BamH I fragment when the −807 Hha I site was cut by the enzyme following DNA demethylation.

sion, with DNA methylation being the dominant force for stable maintenance of gene silencing in cancer.³⁶ Treatment of cancer cells with the demethylation agent 5-aza-2'-deoxycytidine (5-aza-2'-dC) may restore a minimal expression for genes silenced by promoter methylation, and the combined treatment of 5-aza-2'-dC with the histone deacetylase inhibitor, trichostatin A (TSA), may further stimulate the restored expression.³⁶ We next investigated if demethylation and/or histone deacetylase inhibition could reactivate prostatic gene expression in the MDA-MB-231 and MDA-MB-435s cells.

After 8 days of treatment with the DNA methyltransferase inhibitor 5-aza-2'-dC, a significant level of demethylation was observed in the prostatic promoter-exon 1 region in the MDA-MB-231 and MDA-MB-435s cells, as genomic DNA of this region in these cells was partially digested by Hha I at -807, Aci I at -320, BsaA I at -266 and Hpa II at -96 (Fig. 3c). The +24 Aci I was also partially digested in MDA-MB-435s following demethylation (Fig. 3c). Examination of total RNA of these cells by RT-PCR/Southern blot analysis following the 8-day 5-aza-2'-dC treatment, however, failed to detect prostatic mRNA expression (data not shown).

We then further investigated the combined effect of treating the cells with 5-aza-2'-dC and TSA, an inhibitor of histone deacetylase.³⁶ As shown in Figure 4a (upper panel), by RT-PCR/Southern blot analysis, a time-dependent reactivated expression of prostatic mRNA was observed in both the MDA-MB-231 and the MDA-MB-435s cells after a treatment with 5-aza-2'-dC for 24 hr followed by a treatment with TSA for 6, 12 or 24 hr. Treatment of the cells with 5-aza-2'-dC alone, TSA alone or 5-aza-2'-dC followed by 95% ethanol (solvent for TSA) did not result in prostatic mRNA reexpression. A co-amplification of the β -actin message confirmed the quality and quantity of the total RNA used in each

RT-PCR (Fig. 4a, lower panel). When MCF-7 and MDA-MB-453 cells were subjected to the same 5-aza-2'-dC/TSA treatment and prostatic RT-PCR/Southern blot analysis procedures, no increase of prostatic mRNA expression was observed for either cell line (Fig. 4b).

DISCUSSION

Prostatic serine protease has recently been shown to be an *in vitro* invasion suppressor of prostate cancer and to be downregulated in high-grade (Gleason 4/5) prostate tumors.² Carcinomas of the prostate and of the breast drew close comparisons of each other as both originate from secretory epithelial cells and respond to changes of sex hormone levels in the body.³⁷ On a molecular basis, carcinomas of these 2 sites have been shown to have common upregulated proteins that promote tumor progression and invasiveness and also common downregulated proteins that have been shown to be suppressors of tumorigenesis and/or invasiveness. For example, uPA, a serine protease that promotes tumor invasion, is upregulated in both of these cancers.⁹ The mechanism of uPA's tumor invasion-promoting activity is believed to be 2-fold, since it is capable of degrading the extracellular matrix (ECM) and also increasing cell motility.³⁸ NES1, a serine protease and a tumor suppressor, is downregulated in both of these cancers.⁴ Further, a tumor/invasion suppressor serine protease inhibitor, maspin, is effective in inhibiting *in vitro* tumor invasion in both of these cancers by inhibiting cell motility.³⁹ These findings suggest that in addition to the anatomical and physiological similarities between prostate and breast carcinomas, the cellular pathways that regulate tumor cell behaviors, such as invasiveness, may also be similar in these cancers. We have demonstrated that prostatic is a GPI-anchored active serine protease, prompting the reasoning that it may serve as a cell signaling molecule, as the importance of signaling via GPI-anchored proteins is increasingly appreciated in nonhematopoietic cells.⁴⁰ For example, the cell motility-promoting action elicited by uPA is signaled via its cell surface receptor, uPAR.³⁸ uPAR is a GPI-anchored protein and interacts with integrin during cell motility signal transduction.⁴¹ In our study, we demonstrated for the first time prostatic protein expression in normal human mammary epithelial cells and the loss of prostatic protein and mRNA expression in invasive and metastatic human breast cancer cell lines. This observation led to our transfection experiments of 2 invasive and metastatic breast cancer cell lines, MDA-MB-231 and MDA-MB-435s, to establish cell lines that reexpress the prostatic protein. We further demonstrated that enforced prostatic reexpression in these highly invasive human breast cancer cell lines resulted in significant (50%) inhibition of *in vitro* invasiveness. Our findings suggest that prostatic serine protease may be a breast cancer invasion suppressor and its expression in breast tumors should be investigated in future studies.

A 549 bp GC-enriched domain containing 19 CpG dinucleotides and 2 consensus G/C boxes was identified in the 5'-promoter-exon 1 region of the prostatic gene (Fig. 3a). Despite the fact that this region does not qualify as a true CpG island, we have shown CpG methylation patterns that indicate an epigenetic regulation mechanism for prostatic gene expression in breast cancer cell lines. Our results showed that the -320 Aci I-site CpG is homogeneously methylated in the cells that express prostatic (MCF-7 and MDA-MB-453) (Fig. 3b, Table I), therefore, the potential regulatory sequences for prostatic gene expression may lie within the region of -266 and the transcription initiation site. To demonstrate that methylation at the -266 BsaA I-site CpG and the -96 M/H site-CpG is relevant to prostatic gene silencing in breast cancer, we treated the MDA-MB-231 and MDA-MB-435s cells with the DNA methyltransferase inhibitor 5-aza-2'-deoxycytidine (5-aza-2'-dC) and the histone deacetylase inhibitor TSA, each alone or in sequence (TSA following 5-aza-2'-dC). Treatment of cells with 5-aza-2'-dC for 8 days resulted in a significant level of DNA demethylation at the -266 BsaA I site-CpG and the -96 M/H site-CpG (Fig. 3c), but no expression of prostatic mRNA was observed (data not shown). However, a time-dependent prostatic

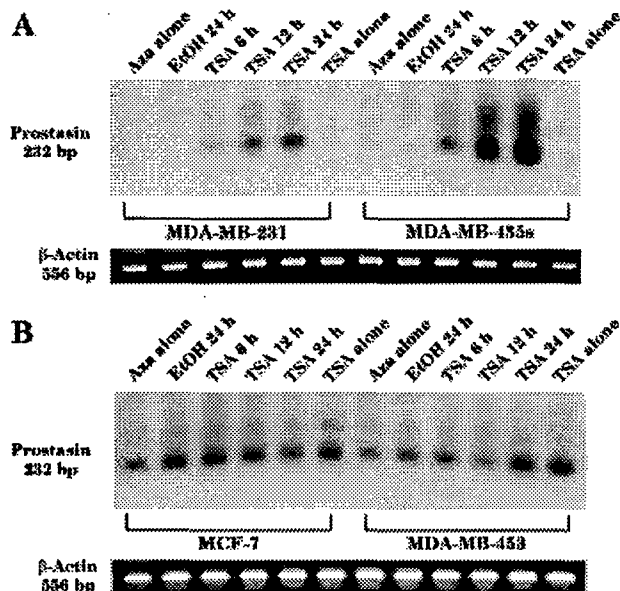


FIGURE 4—(a) Reactivation of prostatic expression in MDA-MB-231 and MDA-MB-435s cells. Cells treated with 5-aza-2'-dC (500 nM) for 24 hr were treated with TSA (1 μ M) for an additional 6, 12 or 24 hr before being harvested for total RNA isolation and RT-PCR/Southern blot analysis as described. Cells treated with 5-aza-2'-dC alone (shown as Aza), with TSA alone and treated with 5-aza-2'-dC followed by 95% ethanol (shown as EtOH) were used as controls. Sample loading order is as indicated for each cell type in the figure (upper panel). Co-amplification of a 556 bp human β -actin message (as shown in the gel photograph in the lower panel) confirmed the quality and the quantity of the RNA applied in each RT-PCR. **(b)** Prostatic mRNA expression in MCF-7 and MDA-MB-453 cells was unaffected by treatment with 5-aza-2'-dC and TSA as described above.

mRNA expression reactivation was observed when MDA-MB-231 and MDA-MB-435s cells were treated with TSA following a treatment with 5-aza-2'-dC for only 24 hr, while TSA treatment alone did not reactivate prostatic mRNA expression (Fig. 4a). The same 5-aza-2'-dC/TSA treatment procedures did not result in a prostatic mRNA expression increase when applied to the MCF-7 and MDA-MB-453 cells, confirming that the reactivation of prostatic mRNA expression in the MDA-MB-231 and MDA-MB-435s cells was the result of these inhibitors working on the silent prostatic promoter. These observations suggest that DNA methylation in the prostatic gene promoter defined by the region of -266 to -96 may be relevant to prostatic gene silencing in the invasive breast cancer cell lines MDA-MB-231 and MDA-MB-435s. Examination of MDA-MB-231 and MDA-MB-435s cells

treated with 5-aza-2'-dC for 8 days followed by TSA treatment for 24 hr in a Western blot analysis or following an immunoprecipitation using a prostatic-specific antibody³ did not reveal any expression of the prostatic protein (data not shown). It is possible that expression of prostatic in the breast is regulated by transcription factors that are lost in these highly invasive breast cancer cells and the reactivated prostatic mRNA expression detected by RT-PCR/Southern blot analysis represents the basal expression.

The finding that prostatic gene may be silenced by promoter DNA methylation in invasive breast cancer cells provides the molecular basis of a potential method of differentially diagnosing invasive breast cancer. Further, the prostatic gene may also provide the molecular basis for a gene-reactivation approach to treating invasive breast cancer.

REFERENCES

1. Yu JX, Chao L, Chao J. Prostatic is a novel human serine proteinase from seminal fluid. Purification, tissue distribution, and localization in prostate gland. *J Biol Chem* 1994;269:18843-8.
2. Chen L-M, Hodge GB, Guarda LA, et al. Down-regulation of prostatic serine protease, a potential invasion suppressor in prostate cancer. *Prostate* 2001;48:93-103.
3. Chen L-M, Skinner ML, Kauffman SW, et al. Prostatic is a glycosylphosphatidylinositol-anchored active serine protease. *J Biol Chem* 2001;276:21434-42.
4. Goyal J, Smith KM, Cowan JM, et al. The role for NES1 serine protease as a novel tumor suppressor. *Cancer Res* 1998;58:4782-6.
5. Nelson PS, Gan L, Ferguson C, et al. Molecular cloning and characterization of prostatic, an androgen-regulated serine protease with prostate-restricted expression. *Proc Natl Acad Sci USA* 1999;96:3114-9.
6. Hooper JD, Nicol DL, Dickinson JL, et al. Testisin, a new human serine proteinase expressed by premeiotic testicular germ cells and lost in testicular germ cell tumors. *Cancer Res* 1999;59:3199-205.
7. Boucalt K, Douglas M, Clements J, et al. The serine proteinase testisin may act as a tumor and/or growth suppressor in the testis and may be regulated by DNA methylation [abstract]. In: *Cancer genetics and tumor suppressor genes meeting program*. Cold Spring Harbor, NY: Cold Spring Harbor Laboratory, 2000 Aug 16-20.
8. Mignatti P, Rifkin DB. Biology and biochemistry of proteinases in tumor invasion. *Physiol Rev* 1993;73:161-95.
9. Rabbani SA, Xing RH. Role of urokinase (uPA) and its receptor (uPAR) in invasion and metastasis of hormone-dependent malignancies. *Int J Oncol* 1998;12:911-20.
10. Duffy MJ, Maguire TM, McDermott EW, et al. Urokinase plasminogen activator: a prognostic marker in multiple types of cancer. *J Surg Oncol* 1999;71:130-5.
11. Xing RH, Rabbani SA. Transcriptional regulation of urokinase (uPA) gene expression in breast cancer cells: role of DNA methylation. *Int J Cancer* 1999;81:443-50.
12. Yu JX, Chao L, Chao J. Molecular cloning, tissue-specific expression, and cellular localization of human prostatic mRNA. *J Biol Chem* 1995;270:13483-9.
13. Magklara A, Grass L, Diamandis EP. Differential steroid hormone regulation of human glandular kallikrein (hK2) and prostate-specific antigen (PSA) in breast cancer cell lines. *Breast Cancer Res Treat* 2000;59:263-70.
14. Chai KX, Ward DC, Chao J, et al. Molecular cloning, sequence analysis, and chromosomal localization of the human protease inhibitor 4 (kallistatin) gene (PI4). *Genomics* 1994;23:370-8.
15. Yu JX, Chao L, Ward DC, Chao J. Structure and chromosomal localization of the human prostatic (PRSS8) gene. *Genomics* 1996;32:334-40.
16. Liu Z, Brattain MG, Appert H. Differential display of reticulocalbin in the highly invasive cell line, MDA-MB-435, versus the poorly invasive cell line, MCF-7. *Biochem Biophys Res Comm* 1997;231:283-9.
17. Sliva D, Mason R, Xiao H, English D. Enhancement of the migration of metastatic human breast cancer cells by phosphatidic acid. *Biochem Biophys Res Comm* 2000;268:471-9.
18. Mukhopadhyay R, Theriault RL, Price JE. Increased levels of alpha6 integrins are associated with the metastatic phenotype of human breast cancer cells. *Clin Exp Met* 1999;17:325-32.
19. Clinchy B, Gazdar A, Rabinovsky R, et al. The growth and metastasis of human, HER-2/neu-overexpressing tumor cell lines in nude SCID mice. *Breast Cancer Res Treat* 2000;61:217-28.
20. Price JE, Polyzos A, Zhang RD, et al. Tumorigenicity and metastasis of human breast carcinoma cell lines in nude mice. *Cancer Res* 1990;50:717-21.
21. Chernicky CL, Yi L, Tan H, et al. Treatment of human breast cancer cells with antisense RNA to the type I insulin-like growth factor receptor inhibits cell growth, suppresses tumorigenesis, alters the metastatic potential, and prolongs survival *in vivo*. *Cancer Gene Ther* 2000;7:384-95.
22. Valentine JE, Boyle MJ, Sewell WA, et al. Presence of single-stranded DNA in PCR products of slow electrophoretic mobility. *Biotechniques* 1992;13:222-4.
23. El-Osta A, Wolffe AP. DNA methylation and histone deacetylation in the control of gene expression: basic biochemistry to human development and disease. *Gene Exp* 2000;9:63-75.
24. Gardiner-Garden M, Frommer M. CpG islands in vertebrate genomes. *J Mol Biol* 1987;196:261-82.
25. Tate PH, Bird AP. Effects of DNA methylation on DNA-binding proteins and gene expression. *Curr Opin Genet Dev* 1993;3:226-31.
26. Meehan RR, Lewis JD, McKay S, et al. Identification of a mammalian protein that binds specifically to DNA containing methylated CpGs. *Cell* 1989;58:499-507.
27. Lewis JD, Meehan RR, Henzel WJ, et al. Purification, sequence, and cellular localization of a novel chromosomal protein that binds to methylated DNA. *Cell* 1992;69:905-14.
28. Nan X, Campoy FJ, Bird A. MeCP2 is a transcriptional repressor with abundant binding sites in genomic chromatin. *Cell* 1997;88:471-81.
29. Hendrich B, Bird A. Identification and characterization of a family of mammalian methyl-CpG binding proteins. *Mol Cell Biol* 1998;18:6538-47.
30. Magdinier F, Wolffe AP. Selective association of the methyl-CpG binding protein MBD2 with the silent p14/p16 locus in human neoplasia. *Proc Natl Acad Sci USA* 2001;98:4990-5.
31. Jones PL, Veenstra GJ, Wade PA, et al. Methylated DNA and MeCP2 recruit histone deacetylase to repress transcription. *Nat Genet* 1998;19:187-91.
32. Nan X, Ng HH, Johnson CA, et al. Transcriptional repression by the methyl-CpG-binding protein MeCP2 involves a histone deacetylase complex. *Nature* 1998;393:386-9.
33. Wade PA, Geggion A, Jones PL, et al. Mi-2 complex couples DNA methylation to chromatin remodelling and histone deacetylation. *Nat Genet* 1999;23:62-6.
34. Ng HH, Zhang Y, Hendrich B, et al. MBD2 is a transcriptional repressor belonging to the MeCP1 histone deacetylase complex. *Nat Genet* 1999;23:58-61.
35. Zhang Y, Ng HH, Erdjument-Bromage H, et al. Analysis of the NuRD subunits reveals a histone deacetylase core complex and a connection with DNA methylation. *Genes Dev* 1999;13:1924-35.
36. Cameron EE, Bachman KE, Myohanen S, et al. Synergy of demethylation and histone deacetylase inhibition in the re-expression of genes silenced in cancer. *Nat Genet* 1999;21:103-7.
37. Adlercreutz H. Western diet and Western diseases: some hormonal and biochemical mechanisms and associations. *Scand J Clin Lab Invest Suppl* 1990;201:3-23.
38. Wang Y. The role and regulation of urokinase-type plasminogen activator receptor gene expression in cancer invasion and metastasis. *Med Res Rev* 2001;21:146-170.
39. Sheng S, Carey J, Sefter EA, et al. Maspin acts at the cell membrane to inhibit invasion and motility of mammary and prostatic cancer cells. *Proc Natl Acad Sci USA* 1996;93:11669-74.
40. Brown DA, London E. Functions of lipid rafts in biological membranes. *Annu Rev Cell Dev Biol* 1998;14:111-36.
41. Yebra M, Goretzki L, Pfeifer M, et al. Urokinase-type plasminogen activator binding to its receptor stimulates tumor cell migration by enhancing integrin-mediated signal transduction. *Exp Cell Res* 1999;250:231-40.

Regulation of prostasin by aldosterone in the kidney

Takefumi Narikiyo,¹ Kenichiro Kitamura,¹ Masataka Adachi,¹ Taku Miyoshi,¹
Kozo Iwashita,¹ Naoki Shiraishi,¹ Hiroshi Nonoguchi,¹ Li-Mei Chen,² Karl X. Chai,²
Julie Chao,³ and Kimio Tomita¹

¹Third Department of Internal Medicine, Kumamoto University School of Medicine, Kumamoto, Japan

²Department of Molecular Biology and Microbiology, University of Central Florida, Orlando, Florida, USA

³Department of Biochemistry and Molecular Biology, Medical University of South Carolina, Charleston, South Carolina, USA

Address correspondence to: Kenichiro Kitamura, Third Department of Internal Medicine,
Kumamoto University School of Medicine, 1-1-1 Honjo, Kumamoto, Kumamoto 860-8556, Japan.

Phone: 81-96-373-5164; Fax: 81-96-366-8458; E-mail: ken@gpo.kumamoto-u.ac.jp.

Received for publication May 10, 2001, and accepted in revised form December 27, 2001.

Prostasin is a serine protease present in mammalian urine that increases the activity of the epithelial sodium channel (ENaC) when the two are coexpressed in *Xenopus* oocytes. To determine if aldosterone, one of the principal regulators of urinary Na reabsorption by the distal nephron, affects prostasin expression, we examined prostasin mRNA and protein in a cultured mouse cortical collecting duct cell line (M-1), whole rats, and patients with primary aldosteronism. Aldosterone treatment of M-1 cells substantially increased prostasin expression and stimulated ²²Na uptake. Urinary excretion of prostasin in rats that were infused with aldosterone likewise increased by ~4-fold when compared with the vehicle-infused rats. Finally, urinary excretion of prostasin in patients with primary aldosteronism was substantially increased when compared with normal patients. Adrenalectomy reduced urinary prostasin excretion to control levels, whereas urinary prostasin levels were not altered in patients undergoing surgery for other reasons. In patients with primary aldosteronism, reduction in the urinary excretion of prostasin correlated with the increase in the urinary Na/K ratio. These findings, together with our previous report that prostasin activates the amiloride-sensitive Na currents through ENaC, demonstrate that prostasin regulates Na balance in vivo by virtue of its heightened expression in the presence of aldosterone.

J. Clin. Invest. 109:401–408 (2002). DOI:10.1172/JCI200213229.

Introduction

Aldosterone is the primary hormone that regulates Na balance, extracellular fluid volume, and blood pressure (1–3). Aldosterone increases the rate of Na reabsorption across epithelia at the distal nephron, the distal colon, and the ducts of exocrine glands by increasing Na transport through the epithelial Na channel (ENaC), one of the principal physiologic targets of aldosterone (4, 5). Regulation of ENaC by aldosterone has been extensively studied in the A6 renal cell line (6). In A6 cells, the effect of aldosterone on ENaC is characterized by a three-phase response: (a) a latent period, lasting 45 minutes; (b) an early response, lasting about 3 hours, in which Na transport increases and the transepithelial electrical resistance falls; and (c) a late response, lasting 12 to 24 hours, during which Na transport further increases while transepithelial resistance does not change significantly. The early and late effects of aldosterone appear to be mediated by transcriptional mechanisms because actinomycin D fully inhibits both actions (7). In addition to transcriptional regulation, May et al. reported that aldosterone increases the rate of de novo synthesis of ENaC α subunit 60 minutes after treatment, raising the possibility that aldosterone may exert its early phase action on ENaC through translational mechanisms (6). Further-

more, Weisz et al. reported the importance of aldosterone-induced trafficking and turnover of individual ENaC subunits in A6 cells (8). They demonstrated that long-term treatment with aldosterone stimulated Na influx by the selective insertion of β ENaC at the apical membrane of A6 cells.

In 1997, a novel mechanism by which serine proteases regulate ENaC activity was identified. Vallet et al. cloned a new serine protease, xCAP-1, from A6 cells (9, 10). They showed that coexpression of xCAP-1 and ENaC in *Xenopus* oocytes increased the amiloride-sensitive Na current (I_{Na}) by two- to threefold. Chraïbi et al. also reported that low concentrations of trypsin (2 μ g/ml) increased I_{Na} by two- to fivefold in oocytes expressing ENaC (11). The precise molecular mechanisms of activation of ENaC by serine proteases are not fully understood. Vuagniaux et al. isolated a cDNA clone of mCAP-1 from a mouse cortical collecting duct (CCD) cell line and suggested that CAP-1 is an orthologous gene for prostasin (12). They also demonstrated that mCAP-1/prostasin activates ENaC when expressed in oocytes. Recently, we isolated a cDNA clone of rat prostasin, a serine protease that is expressed in the same epithelial tissues as ENaC, from the rat kidney (13). We demonstrated that prostasin is expressed in rat kidney collecting ducts and that coexpression of rat prostasin with rat ENaC increased I_{Na}

two- to threefold in *Xenopus* oocytes. We proposed that prostasin might play an important role in Na handling in the kidney by activating ENaC. However, regulation of prostasin mRNA, protein, or activity by physiologic stimuli, or under pathophysiologic conditions, is not yet established. Therefore, we investigated the regulation of prostasin expression by aldosterone because aldosterone is one of the principal regulators of Na reabsorption in the distal nephron.

We found that treatment of a mouse CCD cell line with aldosterone increased the secretion of prostasin protein into culture media and that aldosterone stimulated ^{22}Na uptake by increasing prostasin expression. We also found that increased aldosterone levels in rats markedly increased the urinary excretion of prostasin. Furthermore, we demonstrated that the urinary excretion of prostasin was substantially increased in patients with primary aldosteronism and that adrenalectomy significantly reduced urinary prostasin excretion. These results indicate that prostasin is an important physiologic regulator of Na handling in the kidney.

Methods

Cloning of mouse prostasin cDNA. A partial cDNA fragment of mouse prostasin was obtained by PCR with two degenerate primers that correspond to amino acid sequences of human prostasin as described previously (13–15). A first-strand cDNA was synthesized from mouse kidney total RNA by the oligo (dT) primer method and amplified by these primers. The amplified DNA fragment was subcloned into pGEM-T Easy vector (Promega Corp., Madison, Wisconsin, USA) and sequenced. The 5' and 3' ends of mouse prostasin cDNA was cloned by the 5' and 3' rapid amplification of cDNA ends (RACE) system (Life Technologies Inc., Rockville, Maryland, USA), following the manufacturer's protocol. Briefly, mouse kidney total RNA was reverse-transcribed with antisense primer 5A-m1 (5'-CCCAACTCA-CATGCCTGCCAA-3') for the 5'-RACE reaction. The cDNA that was generated was amplified by nested antisense primers, 5A-m2 (5'-ACCCTGGCAGGCATCCTTGC-3') and 5A-m3 (5'-CGGCTGATGAGTGGTACCTC-3'), sequentially with the abridged anchor primer and the abridged universal amplification primer (AUAP). For the 3' RACE reaction, total RNA was reverse-transcribed and amplified by nested PCR with two sense primers, 3S-m1 (5'-GAGGTACCACTCATCAGCCG-3') and 3S-m2 (5'-GGCCCACTCTCTGTCCCAT-3'), and the AUAP primer. Both 5' and 3' RACE products were subcloned into pGEM-T Easy vector and sequenced. A full-length mouse prostasin cDNA was obtained by ligating the 5' cDNA end, the partial cDNA fragment, and the 3' cDNA end. The nucleotide sequence (mouse prostasin cDNA) reported in this paper has been submitted to the Genbank/EMBL/DBJ Data Bank with accession number AB038244.

Cell culture. M-1 cells, an SV40-transformed mouse CCD cell line, were obtained from the American Type Culture Collection (Rockville, Maryland, USA). Cells

were maintained in DMEM/Ham's F-12 (1:1) mixture (Life Technologies Inc.) supplemented with 5% FBS and 100 nM dexamethasone in a humidified incubator at 37°C and 5% CO_2 . Experiments were performed when cells were confluent. Serum and dexamethasone were removed 48 hours before experiments. All studies described in this paper were performed on cells between the 5th and 20th passages.

Northern blot analysis. Total RNA from M-1 cells grown in 10-cm plastic dishes under experimental conditions was isolated by using an RNeasy kit (QIAGEN GmbH, Hilden, Germany). Total RNA (20 µg) of each sample was resolved on agarose-formaldehyde gels and transferred onto nylon membranes. A full-length cDNA of mouse prostasin and rat β -actin was individually labeled with [α - ^{32}P] dCTP, and probes were hybridized with the membranes as described previously (13).

Preparation of proteins and TCA precipitation. After incubation under experimental conditions, culture medium (10 ml/10-cm dish) was collected and centrifuged at 1,200 g to pellet cell debris. Total protein in the culture media was precipitated by trichloroacetic acid (TCA) (final concentration: 15%). The samples were centrifuged at 12,000 g, and the pellets were washed three times with ice-cold 80% acetone. The precipitated proteins were dried and solubilized at 100°C for 5 minutes in 1× TCA buffer (200 mM unbuffered Tris, 1% SDS, 10% glycerol, 1% β -mercaptoethanol). For preparation of membrane and cytosolic fractions of M-1 cells, confluent M-1 cells were washed twice in PBS, scraped into lysis buffer (25 mM Tris-HCl, pH 7.5, 4 µg/ml aprotinin, 4 µg/ml leupeptin, 1 mM PMSF, and 4 µg/ml pepstatin A), and lysed in a glass Dounce homogenizer. The homogenate was centrifuged at 800 g to remove nuclei, and the supernatant was centrifuged at 12,000 g to separate the membrane and cytosolic fractions. The membrane fraction was then dissolved in RIPA buffer (50 mM Tris-HCl, pH 7.5, 150 mM NaCl, 0.1% SDS, 0.5% deoxycholate, 1% vol/vol Triton-X 100, 2 mM EDTA, 4 µg/ml aprotinin, 4 µg/ml leupeptin, 1 mM PMSF, and 4 µg/ml pepstatin A). All these procedures were performed at 4°C.

Immunoblotting. Samples were resolved on 12% SDS-PAGE and transferred onto nitrocellulose filters. After blocking with 5 g/dl nonfat dry milk, the blots were probed with a polyclonal Ab against prostasin (15) in Tris-buffered saline with 0.05% Tween-20 for 1 hour, followed by a secondary Ab (goat anti-rabbit IgG conjugated with horseradish peroxidase) for 1 hour at room temperature. Bands were visualized using chemiluminescence substrate (ECL; Amersham Pharmacia Biotech, Amersham, United Kingdom) followed by exposure to x-ray film. The band densities were quantitated by densitometry (Densitograph 4.0; ATTO Co., Tokyo, Japan).

^{22}Na influx studies. The activities of ENaC in M-1 cells were determined by measurement of amiloride-sensitive ^{22}Na uptake (16). Preliminary experiments determined that amiloride-sensitive uptake of ^{22}Na was linear for up to 15 minutes. After incubation under experimental con-

ditions, cells on six-well dishes were rinsed twice and preincubated for 15 minutes at 37°C in a Na-free solution composed of 137 mM *N*-methylglucamine (NMDG), 5.4 mM KCl, 1.2 mM MgSO₄, 2.8 mM CaCl₂, and 15 mM HEPES (pH 7.4). At the end of the preincubation, the Na-free solution was replaced by the uptake solution composed of 14 mM NaCl, 35 mM KCl, 96 mM NMDG, and 20 mM HEPES (pH 7.4) containing 1 mM ouabain and 1.5 µCi/ml of ²²NaCl (specific activity: 748 µCi/mg Na; New England Nuclear, Boston, Massachusetts, USA) in the presence or absence of 1 mM amiloride. After a 5-minute incubation, uptake was stopped by washing the cells four times with 1 ml/well of an ice-cold solution containing 120 mM NMDG and 20 mM HEPES (pH 7.4). The cells were then solubilized in 0.5% Triton X-100. Tracer activities were measured in a gamma scintillation counter. The amount of protein per well was measured using the BCA kit (Pierce Chemical Co., Rockford, Illinois, USA). All assays were performed in duplicate. ENaC activity was determined as the difference between ²²Na uptake in the presence or absence of amiloride. The results were normalized for protein concentration and expressed as percentage of control.

Aldosterone infusion studies. Experiments were conducted in male Sprague-Dawley rats (160–170 g) from Charles River Laboratories (Wilmington, Massachusetts, USA). Rats were anesthetized with pentobarbital sodium (Nembutal; Abbot Laboratories, North Chicago, Illinois, USA) before subcutaneous implantation of osmotic minipumps (model 2001; Alza Corp., Palo Alto, California, USA) that delivered 100 µg/100 g body weight aldosterone per day (17). Aldosterone (Sigma Chemical Co., St. Louis, Missouri, USA) was dissolved in DMSO and diluted with isotonic saline. Control rats received vehicle alone. All rats were kept in metabolic cages, and 24-hour urine collections were made. Urine samples, corrected for creatinine excretion, were concentrated by TCA precipitation, and the amount of prostasin was determined by immunoblotting as described above. Blood samples were obtained at the end of the experiments to measure plasma aldosterone, serum potassium, and serum bicarbonate concentrations. All animal procedures were approved by the institutional ethics committee.

Patients with primary aldosteronism. Three patients with primary aldosteronism and three patients undergoing surgery for other reasons with general anesthesia were enrolled in the study. Institutional approval was received from the Kumamoto University Human Subject Review Board, and written informed consent was obtained from each patient prior to the studies. All patients with primary aldosteronism were treated with adrenalectomy, and 24-hour urine collections were obtained before and after surgery. The prostasin excretion level in urine samples was determined by the same method as described above.

Results

Cloning of full-length mouse prostasin cDNA. To evaluate the level of prostasin mRNA expression in the M-1 cell

line by Northern blotting, we isolated a full-length prostasin cDNA from mouse kidney using RT-PCR, 5' and 3' RACE methods. The prostasin cDNA encodes a 339-amino acid polypeptide, including a 29-amino acid signal peptide, a 15-amino acid light chain, and a 295-amino acid heavy chain. The catalytic triad that is highly conserved among the serine proteases is also found in mouse prostasin (His⁸⁵, Asp¹³⁴, and Ser²³⁸). Vuagniaux et al. proposed that mCAP-1, xCAP-1, and human prostasin are orthologous genes (12). Our cloning of mouse prostasin cDNA also revealed that mouse prostasin is identical to the mCAP-1 at the amino acid level.

Effect of aldosterone on prostasin expression in M-1 cells. Previously, we demonstrated that expression of prostasin stimulates ENaC in *Xenopus* oocytes (13). May et al. also reported that aldosterone increases ENaC activity as well as ENaC protein translation in A6 cells (6). These findings motivated us to study the effect of aldosterone on the expression of prostasin. We used M-1 cells to study the regulation of prostasin by aldosterone because both prostasin and ENaC are expressed in the CCD segment (12, 13, 18) and aldosterone modulates Na transport in M-1 cells (19). We measured prostasin mRNA abundance in M-1 cells following aldosterone treatment. Figure 1 shows the time course of prostasin mRNA induction by aldosterone. Prostasin transcripts were readily detected under basal conditions. Aldosterone induced an increase in prostasin mRNA after 6 hours of stimulation. Maximum induction occurred at 24 hours (1.9-fold ± 0.2-fold), and elevated mRNA levels were still present for up to 48 hours.

We then determined the distribution of prostasin protein between M-1 cell membranes and cytosol. Based on its predicted secondary structure, prostasin is presumed to be a secreted and/or a glycosylphosphatidylinositol-anchored protein, so we also determined if it was present in cell culture medium. Proteins in the membrane and cytosolic fractions of M-1 cells and culture media were precipitated by TCA and subjected to immunoblotting. As shown in Figure 2a, the antiprostasin Ab detected a single band of 40 kDa only in the culture media under reducing conditions. The band was barely detectable in either the membrane or cytosolic fractions (left panel). The 40-kDa band was completely blocked by the incubation of Ab with the synthetic prostasin peptide used for immunization, demonstrating the specificity of the immunodetection (Figure 2a, right panel). We could not detect prostasin protein in the membrane or cytosolic fractions even when we immunoblotted 80 µg of protein. While prostasin protein was shown to be secreted when synthesized in the prostate (15), recent findings also indicated that it can assume a membrane-anchored form via glycosylphosphatidylinositol in prostate epithelial cells that naturally express prostasin (20). In the M-1 cells, it is possible that the distribution of the membrane-anchored versus the secreted prostasin protein for the total pool of prostasin protein synthesized is

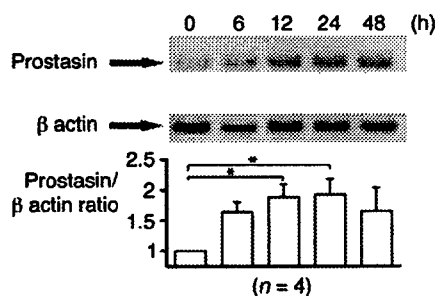


Figure 1

Effect of aldosterone on the expression of prostasin mRNA in M-1 cells. M-1 cells, which were serum deprived for 48 hours, were treated with 1 μ M aldosterone and harvested at various time points (0, 6, 12, 24, and 48 hours) for isolation of total RNA. Each lane contains 20 μ g of total RNA. The abundance of prostasin mRNA was normalized for β -actin (bottom). Aldosterone induced an increase in prostasin mRNA after 6 hours of stimulation. Maximum induction occurred at 24 hours (1.9-fold \pm 0.2-fold increase), and this effect was observed for up to 48 hours. This blot is representative of four separate experiments. Values are mean \pm SEM (n = 4). *P < 0.02.

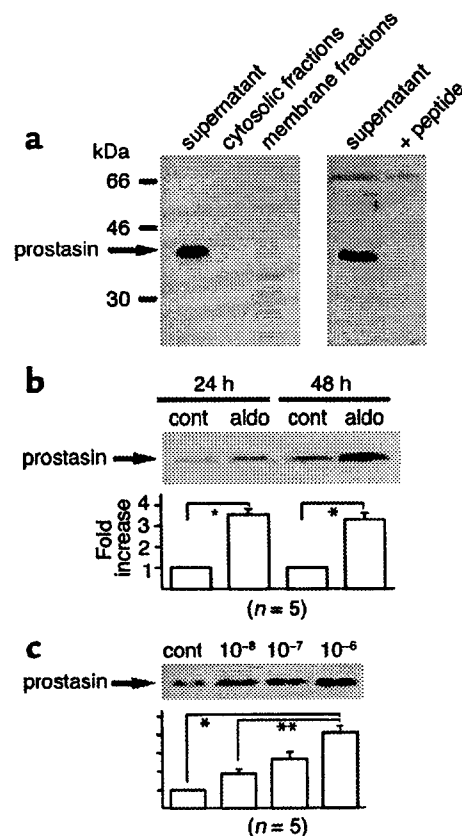
different from that in the prostate cells. We speculate that prostasin is synthesized as a membrane protein that is quickly cleaved by some mechanism and released into the extracellular medium. Consequently, in subsequent studies, we analyzed expression of prostasin protein in the culture media of M-1 cells. Figure 2b shows that treatment with aldosterone increased the expression of prostasin protein by 3.5-fold \pm 0.6-fold and 3.3-fold \pm 0.3-fold when compared with the controls during 24-hour and 48-hour incubations. This stimulatory effect of aldosterone on prostasin protein expression was dose dependent over the range 0–10⁻⁶ M (Figure 3c). Even after treatment with aldosterone, we could not detect prostasin protein in either membrane or cytosolic fractions (data not shown). These findings demonstrate that aldosterone stimulates expression of prostasin at the levels of mRNA as well as protein in M-1 cells.

Effect of aprotinin on aldosterone-induced ²²Na uptake in M-1 cells. To determine if the aldosterone-induced increase in prostasin protein abundance in M-1 cells indeed has a role in activating ENaC, we measured amiloride-sensitive ²²Na uptake. M-1 cells were treated for 24 hours with 1 μ M aldosterone or vehicle in the

presence or absence of 28 μ g/ml aprotinin, a potent prostasin inhibitor (IC₅₀ of aprotinin for prostasin is 11.7 ng/ml) (15), and then amiloride-sensitive ²²Na uptake was measured. As shown in Figure 3a, treatment with aprotinin decreased the amiloride-sensitive ²²Na uptake by 25% \pm 9% under basal conditions. Nakhoul et al. reported that aprotinin reduced the *I*_{sc} in M-1 cells by 49% \pm 9% (19). The difference in the magnitude of the aprotinin-sensitive component in the basal Na current in M-1 cells could have resulted from the differences of the methods used. Aldosterone increased the ²²Na uptake by 189% \pm 25%, and aprotinin significantly reduced the Na influx in aldosterone-treated cells. Interestingly, aprotinin-sensitive Na uptake was markedly increased by twofold in aldosterone-treated cells when compared with the control. Also, aldosterone increased the aprotinin-insensitive component. To address the question if sufficient

Figure 2

Effect of aldosterone on the expression of prostasin protein in M-1 cells. (a) Cellular distribution of prostasin protein in M-1 cells. Forty micrograms of membrane and cytosolic proteins as well as 3 ml of TCA-precipitated culture medium from M-1 cells were subjected to SDS-PAGE. Blots were probed with the antiprostasin Ab and with Ab preadsorbed with the immunizing peptide. Prostasin was detected as a 40-kDa band in the culture medium only. (b) Effect of aldosterone on the expression of prostasin protein in M-1 cells. M-1 cells were treated with 1 μ M aldosterone or vehicle for 24 and 48 hours. Proteins in the culture medium were TCA precipitated and subjected to SDS-PAGE. Treatment with 1 μ M aldosterone increased prostasin protein expression by 3.5-fold \pm 0.6-fold (for 24 hours) and 3.3-fold \pm 0.3-fold (for 48 hours) when compared with the corresponding controls. This blot is representative of five separate experiments. Aldo, aldosterone; cont, control. Values are mean \pm SEM (n = 5). (c) Dose dependence of aldosterone effect on prostasin. M-1 cells were treated with increasing concentrations of aldosterone (0, 10⁻⁸, 10⁻⁷, and 10⁻⁶ M) for 24 hours. The expression level of prostasin in the culture media was determined by immunoblotting. The stimulatory effect of aldosterone on prostasin protein expression was dose dependent over the range of 0–10⁻⁶ M. This blot is representative of five separate experiments. Values are mean \pm SEM (n = 5). *P < 0.001, **P < 0.02.



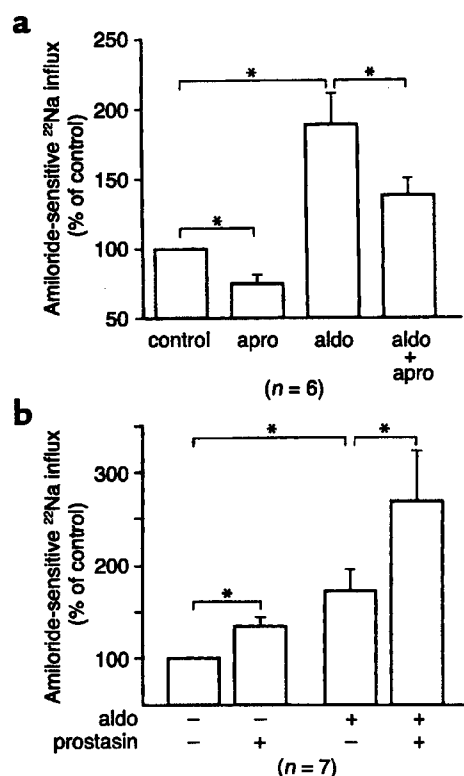


Figure 3 Role of prostasin in the aldosterone-induced increase in ^{22}Na uptake in M-1 cells. (a) Effect of aprotinin on aldosterone-induced ^{22}Na uptake in M-1 cells. M-1 cells were treated with 1 μM aldosterone or vehicle for 24 hours in the presence or absence of 28 $\mu\text{g}/\text{ml}$ aprotinin. Amiloride-sensitive ^{22}Na uptake was determined in the presence of 1 mM amiloride and 1 mM ouabain. Treatment with aprotinin partially inhibited the basal Na influx as well as the aldosterone-induced Na influx. Aldosterone significantly increased the aprotinin-sensitive Na uptake twofold. Apro, aprotinin. Values are mean \pm SEM (n = 6). (b) Effect of recombinant prostasin on aldosterone-induced ^{22}Na uptake in M-1 cells. M-1 cells were treated with 1 μM aldosterone or vehicle for 24 hours, then cells were treated with 2 $\mu\text{g}/\text{ml}$ of recombinant prostasin. Amiloride-sensitive ^{22}Na uptake was determined as described above. Treatment with recombinant prostasin further increased the basal Na influx as well as the aldosterone-induced Na influx (1.35-fold and 1.56-fold, respectively). Values are mean \pm SEM (n = 7). * $P < 0.05$.

prostasin might be present in the culture media under basal conditions to activate ENaC, and if an aldosterone-mediated increase in prostasin secretion into culture media might have a minimal effect on further enhancing ENaC activity, we treated M-1 cells with purified recombinant prostasin (20) in the presence or absence of aldosterone and measured the amiloride-sensitive ^{22}Na uptake. Figure 3b shows that the addition of recombinant prostasin further increased the ^{22}Na uptake by 1.35-fold in control cells and by 1.56-fold in aldosterone-treated cells, suggesting that ENaC expressed on the apical membrane of M-1 cells are not fully activated by prostasin under basal conditions and that an aldosterone-induced increase in the prostasin abundance in the culture media has a definite role in the activation of ENaC. These results, taken together

with the findings that aldosterone increases prostasin protein expression in M-1 cells, demonstrate that M-1 cells have aprotinin-sensitive Na uptake under basal conditions that is probably due to prostasin expression and that aldosterone substantially increases the prostasin-dependent Na uptake by increasing prostasin protein abundance. Furthermore, these findings strongly support our hypothesis that aldosterone-induced increase in prostasin protein has a key role in the aldosterone-induced activation of ENaC.

Effect of amiloride on aldosterone-induced prostasin expression in M-1 cells. Aldosterone activates Na transport in M-1 cells (19) and distal tubules of other species (2) through activation of ENaC. Prostasin expression could be increased by mechanisms that are a consequence of activation of ENaC, such as an increase in the intracellular Na concentration. To determine whether an increase in prostasin expression is secondary to an event following the activation of ENaC by aldosterone, we studied the effect of amiloride, a potent ENaC inhibitor, on the aldosterone-induced increase in prostasin expression in the cell culture media. M-1 cells were preincubated with 5 μM amiloride for 30 minutes, and then aldosterone (final 1 μM) was added to the media in the presence of amiloride. Twenty-four hours after incubation, medium was collected and subjected to immunoblotting. As shown in Figure 4, amiloride treatment had no effect on either basal or aldosterone-induced prostasin protein expression. These results suggest that the induction of prostasin by aldosterone is not mediated by an amiloride-sensitive mechanism that is secondary to ENaC activation. We then studied the effect of prostasin on the amiloride sensitivity of ENaC. The K_{amil} of ENaC in the absence of prostasin (0.10 ± 0.006 μM ; n = 12) did not significantly differ from the K_{amil} in the presence of prostasin (0.094 ± 0.005 μM ; n = 14).

Aldosterone-infusion studies. To study the stimulatory effect of aldosterone on prostasin expression in vivo, we infused rats with aldosterone through subcuta-

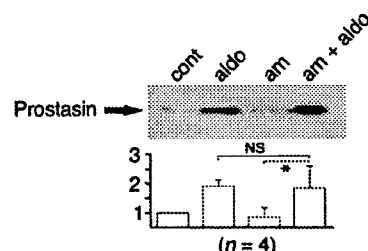


Figure 4 Effect of amiloride on aldosterone-induced expression of prostasin protein in M-1 cells. M-1 cells were treated with 1 μM aldosterone or vehicle in the presence or absence of 5 μM amiloride for 24 hours. Prostasin protein abundance was determined by immunoblotting. Treatment of M-1 cells with amiloride had no effect on the secretion of prostasin in the culture media (aldosterone: 1.9-fold \pm 0.2-fold, aldosterone + amiloride: 1.8-fold \pm 0.7-fold, not significant). This figure is representative of four separate experiments. Am, amiloride. Values are mean \pm SEM (n = 4). NS, not significant; * $P < 0.02$.

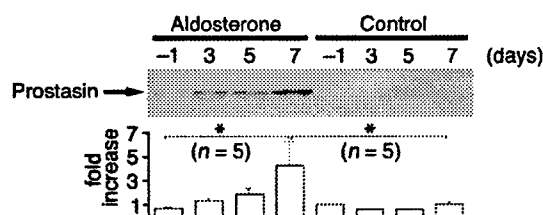


Figure 5

Effect of aldosterone infusion on prostasin excretion in the urine. Immunoblot showing the effect of aldosterone infusion (100 µg/100 g body weight/day) for 7 days on the abundance of prostasin excreted into rat urine. Urine samples that are equivalent to 80 µg creatinine excretion were TCA precipitated, and urinary prostasin excretion was determined by immunoblotting. Aldosterone infusion resulted in a substantial increase in prostasin excretion into the urine. The effect of aldosterone was time dependent, and maximum induction was observed at day 7 (4.3-fold ± 2.0-fold increase over control). This figure is representative of five separate experiments. Values are mean ± SEM (n = 5). *P < 0.004.

neously implanted osmotic minipumps for 7 days. Plasma aldosterone levels were significantly increased in aldosterone-infused rats (control: 134 ± 23 pg/ml, n = 5, and aldosterone: 3,425 ± 354 pg/ml, n = 5, P < 0.05). The aldosterone-treated rats also exhibited hypertension (control: 111 ± 5 mmHg, n = 5, and aldosterone: 127 ± 2 mmHg, n = 5, P < 0.05), hypokalemia (control: 5.0 ± 0.2 mEq/l, n = 5, and aldosterone: 3.3 ± 0.8 mEq/l, n = 5, P < 0.05), and metabolic alkalosis (control: 27.0 HCO₃ ± 1.9 mEq/l, n = 5, and aldosterone: HCO₃ 41.3 ± 1.7 mEq/l, n = 5, P < 0.05) 7 days after pump implantation. There was not any significant difference in the body weight between control rats and aldosterone-treated rats (control: 220 ± 6 g, n = 5, and aldosterone: 215 ± 5 g, n = 5, P = not significant). We could not detect prostasin expression by immunoblotting membrane or cytosolic fractions of rat kidney cortex and medulla with or without aldosterone infusion (data not shown). However, we easily detected prostasin in rat urine under basal conditions. These data suggest that prostasin is released from the apical membrane of kidney tubules by some mechanisms in rats as well as in the mouse CCD cell line. As shown in Figure 5,

aldosterone infusion resulted in a substantial increase in prostasin excretion into the urine. The effect of aldosterone was time dependent, and the maximum induction was observed at day 7 (4.3-fold ± 2.0-fold increase over control). These findings indicate that aldosterone induces prostasin expression in the kidney in whole animals as well as in cultured cells and that it may play an important role in the impaired Na handling in patients with hyperaldosteronism.

Urinary prostasin levels in patients with primary aldosteronism. To determine whether aldosterone increases prostasin protein expression in humans, we measured urinary prostasin protein expression in patients with primary aldosteronism before and after adrenalectomy. The diagnosis of an aldosterone-secreting adrenal adenoma was made on the basis of measurement of plasma renin activity and plasma aldosterone levels and by radiologic examinations, including computed tomography and magnetic resonance imaging scans. Patient profiles, plasma renin activities, plasma aldosterone concentration (PAC), and serum potassium levels of the patients are shown in Table 1. To study urinary prostasin excretion, 24-hour urine collections were obtained before and 7 days after adrenalectomy. Figure 6a shows the results of Western blot analysis of urinary prostasin excretion before and after adrenalectomy from patient number 1. Adrenalectomy resulted in a marked decrease in urinary prostasin protein abundance. PAC was also reduced to the normal range after the operation (Table 1). Interestingly, the urinary Na/K ratio correlated with the expression level of prostasin, suggesting that aldosterone-induced prostasin plays a role in activation of ENaC (Figure 6a). Patients with high PAC level (numbers 1–3) had substantially higher urinary prostasin excretion when compared with normal PAC level patients (numbers 4–6) (Figure 6b). In all three patients with primary aldosteronism, adrenalectomy resulted in a significant decrease in the urinary prostasin excretion, while no change in urinary prostasin excretion was observed in the three patients with normal PAC levels (Figure 6b). These results indicate that prostasin is regulated by aldosterone in humans as well as in rats.

Table 1

Clinical profiles of the patients with primary aldosteronism and other diseases

Patients	Sex	Age (years old)	Height (cm)	BW (kg)	PRA (ng/ml/h) before/after	PAC (pg/ml) before/after	p-K (mEq/l)	Diseases
1	Male	22	175	69.6	<0.1/0.1	330/50	2.8	PA
2	Female	51	155	51.1	<0.1/0.2	189/51	3.2	PA
3	Female	43	160	57.6	<0.1/0.1	778/34	2.0	PA
4	Male	26	171	89.0	0.6/0.5	80/58	4.2	Achalasia
5	Female	51	151	45.0	0.5/0.2	91/49	3.9	PHP
6	Male	37	178	92.5	1.8/1.3	94/110	4.2	Cholelithiasis

Values are mean ± SEM. Plasma renin activities PRA and PAC were measured before and 7 days after the operation in each patient. BW, body weight; p-K, serum potassium; PA, primary aldosteronism; PHP, primary hyperparathyroidism, PRA, plasma renin activities.

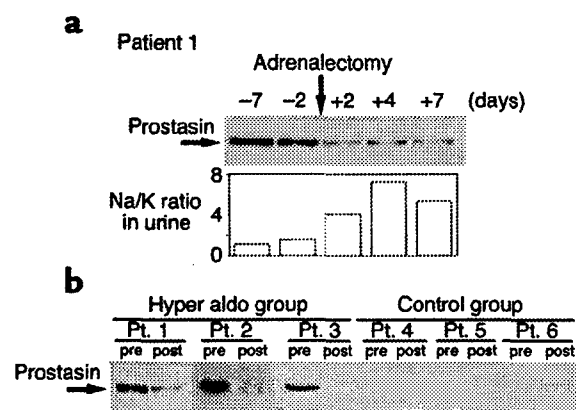


Figure 6 Urinary prostasin levels in patients with primary aldosteronism and control patients. (a) Time course of urinary prostasin expression in patients with primary aldosteronism (patient 1) before and after the adrenalectomy. Sample volumes were adjusted to be equivalent to 750 μ g creatinine excretion, and urinary excretion of prostasin was determined by the immunoblotting. Urinary Na/K ratio is shown at the bottom. (b) Urinary prostasin excretion in two other independent patients with primary aldosteronism (patients 2 and 3) and in three other independent patients with normal PAC level who had the surgery for other reasons (patients 4, 5, and 6). Twenty-four-hour urine collections were made before and 7 days after surgery. The urinary excretion of prostasin was determined by immunoblotting as described above. Pt, patient.

Discussion

Serine proteases such as CAP-1, trypsin, and chymotrypsin have been shown to stimulate I_{Na} in *Xenopus* oocytes expressing ENaC, although the precise mechanisms of activation are not known (10–12). We cloned a rat prostasin cDNA and demonstrated that expression of rat prostasin increased the Na current through ENaC (13). Proastasin is expressed in epithelial tissues that are known to be the sites of amiloride-sensitive transepithelial Na transport. Therefore, we hypothesized that prostasin may play an important role in Na handling by the kidney through the activation of ENaC. In the present studies, we addressed the question of whether aldosterone, a major natriuretic hormone that increases Na uptake in the distal nephron by activation of ENaC, could regulate the expression of prostasin in mammals. We showed that aldosterone stimulates Na uptake by increasing the expression of prostasin mRNA and protein in cultured mouse CCD cells. We also showed that urinary excretion of prostasin is increased in aldosterone-infused rats and in patients with primary aldosteronism.

Regulation of prostasin by aldosterone. In the study presented here, we showed that aldosterone induces a twofold increase in prostasin mRNA in M-1 cells. Because we have not yet measured the rate of transcription of this gene, we do not know whether the increased abundance of mRNA is mediated by a direct transcriptional effect and/or by an effect on mRNA turnover. The stimulatory effect of aldosterone on the

accumulation of prostasin protein in the culture media or urine was proportional to the effect on mRNA abundance. Aldosterone significantly induced prostasin excretion in rat and human urine by approximately twofold. In the current study we have not addressed the question of whether aldosterone could regulate the assembly of prostasin in the endoplasmic reticulum, its transport to the plasma membrane, its release from the plasma membrane, and the stability of the released protein in the culture media or urine; each step could be separate sites of hormonal regulation.

Possible involvement of prostasin in aldosterone-induced Na absorption. Here we demonstrated that treatment of M-1 cells increases aprotinin-sensitive, further, prostasin-sensitive, Na uptake by increasing the prostasin protein abundance. Until this report, there was no direct evidence showing that serine proteases are involved in Na reabsorption in the distal nephron. However, data in several papers support the concept that serine proteases may play a key role in Na uptake in the kidney (9–13). Nakhoul et al. demonstrated that aprotinin added to the luminal side of M-1 cells induces a 50% decrease in the I_{sc} , suggesting that serine proteases such as prostasin could stimulate ENaC activity since aprotinin is a potent inhibitor of prostasin activity (19). More recently, Masilamani et al. reported that aldosterone infusion in rats resulted in a molecular weight shift of γ ENaC from 85 kDa to 70 kDa (21). They speculated that proteolytic cleavage of the γ ENaC by serine proteases such as CAP-1 might be responsible for this phenomenon. Since prostasin is expressed in the collecting ducts and is excreted into urine, it may participate in the molecular weight shift of γ ENaC and subsequent activation of ENaC in mammals. Nafamostat mesilate (NM), a synthetic serine protease inhibitor, inhibits various serine proteases including trypsin, thrombin, activated factor X, and activated complement. Although NM has been shown to be effective in the treatment of pancreatitis and disseminated intravascular coagulation, it is associated with hyponatremia and hyperkalemia in some cases (22). Muto et al. reported that perfusion of rabbit CCD with NM inhibited I_{Na} , resulting in inhibition of potassium secretion (23, 24). They suggested that hyponatremia and/or hyperkalemia associated with NM treatment could be caused in part by inhibition of amiloride-sensitive Na conductance. This finding also implies physiologic involvement of serine proteases such as prostasin in Na handling in renal tubules.

Aldosterone stimulates Na reabsorption by multiple actions on multiple proteins involved in Na transport or its regulation. Aldosterone stimulates the transcription of ENaC in the kidney and increases the channel number at the apical membrane of the collecting duct, leading to an enhanced Na reabsorption in the distal nephron segment. Sgk, a serine/threonine kinase that activates electrogenic Na transport by increasing the number of Na channels (ENaC) at the cell surface, is also an aldosterone-induced protein and may play a key role in the aldosterone-mediated

regulation of Na absorption (25). Our current study suggests an additional mechanism by which aldosterone could stimulate Na transport through ENaC by way of increasing the expression of prostasin in the kidney. Our results provide a new insight into the regulation of distal nephron Na transport and pathogenesis of hypertension and provide the rationale for development of new therapeutic agents for hypertension and Na-retaining states.

Acknowledgments

We thank Shizuka Iida (Kurume University School of Medicine) and Junnosuke Inoue (Jikei Hospital) for sharing the urine samples of the primary aldosteronism patients. This work was supported by the Grants-in-Aid for Scientific Research from the Ministry of Education, Science and Culture in Japan (11770599 and 13770602 to K. Kitamura and 10671000, 11470219, and 11877177 to K. Tomita), The Salt Science Research Foundation (to K. Tomita), and Department of Defense Prostate Cancer Research Program Grants (DAMD 17-98-1-8590 and DAMD 17-02-1-0032 to K.X. Chai).

1. Barbry, P., and Lazdunski, M. 1996. Structure and regulation of the amiloride-sensitive epithelial sodium channel. *Ion Channels*. 4:115-167.
2. Garty, H., and Palmer, L.G. 1997. Epithelial sodium channels: function, structure, and regulation. *Physiol. Rev.* 77:359-396.
3. Funder, J.W. 1993. Aldosterone action. *Annu. Rev. Physiol.* 55:115-130.
4. Rossier, B.C. 1997. 1996 Homer Smith Award Lecture. Cum grano salis: the epithelial sodium channel and the control of blood pressure. *J. Am. Soc. Nephrol.* 8:980-992.
5. Verrey, F. 1999. Early aldosterone action: toward filling the gap between transcription and transport. *Am. J. Physiol.* 277:F319-F327.
6. May, A., Puoti, A., Gaeggeler, H.P., Horisberger, J.D., and Rossier, B.C. 1997. Early effect of aldosterone on the rate of synthesis of the epithelial sodium channel α subunit in A6 renal cells. *J. Am. Soc. Nephrol.* 8:1813-1822.
7. Verry, F., and Beron, J. 1996. Activation and supply of channels and pumps by aldosterone. *News Physiol. Sci.* 11:126-133.
8. Weisz, O.A., Wang, J.M., Edinger, R.S., and Johnson, J.P. 2000. Non-coordinate regulation of endogenous epithelial sodium channel (ENaC) subunit expression at the apical membrane of A6 cells in response to various transporting conditions. *J. Biol. Chem.* 275:39886-39893.
9. Valler, V., Horisberger, J.D., and Rossier, B.C. 1998. Epithelial sodium channel regulatory proteins identified by functional expression cloning. *Kidney Int. Suppl.* 67:S109-S114.
10. Valler, V., Chraïbi, A., Gaeggeler, H.P., Horisberger, J.D., and Rossier, B.C. 1997. An epithelial serine protease activates the amiloride-sensitive sodium channel. *Nature*. 389:607-610.
11. Chraïbi, A., Valler, V., Firsov, D., Hess, S.K., and Horisberger, J.D. 1998. Protease modulation of the activity of the epithelial sodium channel expressed in *Xenopus* oocytes. *J. Gen. Physiol.* 111:127-138.
12. Vuagniaux, G., et al. 2000. Activation of the amiloride-sensitive epithelial sodium channel by the serine protease mCAP1 expressed in a mouse cortical collecting duct cell line. *J. Am. Soc. Nephrol.* 11:828-834.
13. Adachi, M., et al. 2001. Activation of epithelial sodium channels by prostasin in *Xenopus* oocytes. *J. Am. Soc. Nephrol.* 12:1114-1121.
14. Yu, J.X., Chao, L., and Chao, J. 1995. Molecular cloning, tissue-specific expression, and cellular localization of human prostasin mRNA. *J. Biol. Chem.* 270:13483-13489.
15. Yu, J.X., Chao, L., and Chao, J. 1994. Prostasin is a novel human serine proteinase from seminal fluid. Purification, tissue distribution, and localization in prostate gland. *J. Biol. Chem.* 269:18843-18848.
16. Folkesson, H.G., et al. 1998. Upregulation of alveolar epithelial fluid transport after subacute lung injury in rats from bleomycin. *Am. J. Physiol.* 275:L478-L490.
17. Kim, G.H., et al. 1998. The thiazide-sensitive Na-Cl cotransporter is an aldosterone-induced protein. *Proc. Natl. Acad. Sci. USA*. 95:14552-14557.
18. Duc, C., Farman, N., Canessa, C.M., Bonvalet, J.P., and Rossier, B.C. 1994. Cell-specific expression of epithelial sodium channel α , β , and γ subunits in aldosterone-responsive epithelia from the rat: localization by *in situ* hybridization and immunocytochemistry. *J. Cell Biol.* 127:1907-1921.
19. Nakhoul, N.L., Hering-Smith, K.S., Gambala, C.T., and Hamm, L.L. 1998. Regulation of sodium transport in M-1 cells. *Am. J. Physiol.* 275:F998-F1007.
20. Chen, L.M., et al. 2001. Prostasin is a glycosylphosphatidylinositol-anchored active serine protease. *J. Biol. Chem.* 276:21434-21442.
21. Masilamani, S., Kim, G.H., Mitchell, C., Wade, J.B., and Knepper, M.A. 1999. Aldosterone-mediated regulation of ENaC α , β , and γ subunit proteins in rat kidney. *J. Clin. Invest.* 104:R19-R23.
22. Kitagawa, H., Chang, H., and Fujita, T. 1995. Hyperkalemia due to Nafamostat mesilate. *New Engl. J. Med.* 332:687.
23. Muto, S., Imai, M., and Asano, Y. 1993. Effect of nafamostat mesilate on Na⁺ and K⁺ transport properties in the rabbit cortical collecting duct. *Br. J. Pharmacol.* 109:673-678.
24. Muto, S., Imai, M., and Asano, Y. 1994. Mechanisms of the hyperkalemia caused by nafamostat mesilate: effects of its two metabolites on Na⁺ and K⁺ transport properties in the rabbit cortical collecting duct. *Br. J. Pharmacol.* 111:173-178.
25. Chen, S.Y., et al. 1999. Epithelial sodium channel regulated by aldosterone-induced protein sgk. *Proc. Natl. Acad. Sci. USA*. 96:2514-2519.

Purification and Characterization of the Prostasin-binding Protein

Li-Mei Chen and Karl X. Chai[§]

Department of Molecular Biology and Microbiology, University of Central Florida,
Orlando, FL 32816

Running title: prostasin-binding protein

This work was supported by Department of Defense Prostate Cancer Research Program grants No. DAMD17-98-1-8590 and DAMD17-02-1-0032 to KXC, and by National Institutes of Health grant No. HD 40241 to LMC.

[§]To whom request for reprints should be addressed at:

Dr. Karl X. Chai

Department of Molecular Biology and Microbiology

University of Central Florida

4000 Central Florida Boulevard, Orlando, FL 32816-2360

Phone: (407) 823-6122, Fax: (407) 823-3095, e-mail: kxchai@mail.ucf.edu

Summary

Prostasin serine protease is synthesized as a glycosylphosphatidylinositol (GPI)-anchored membrane protein, and can be secreted via an unknown mechanism. Prostasin has been implicated for a function in the regulation of epithelial sodium channel activity and in cancer biology. A prostasin-binding protein was identified in mouse and human seminal vesicles. In this study, we have purified the prostasin-binding protein from mouse seminal vesicle (mPBP). The purified mPBP formed a covalent complex with purified recombinant human prostasin in a time-dependent and pH-dependent manner. The complex formation was detected after 30 seconds, with the optimum pH at 9.0. A polyclonal antibody against mPBP was generated. The antibody recognized a free-form mPBP and the complex of mPBP-prostasin. The purified mPBP inhibits prostasin's activity toward a synthetic substrate. A trypsin-digested fragment of mPBP was sequenced, the amino acid sequence matched a region in the serpin protease nexin-1 (PN-1) sequence. Recombinant mouse or human PN-1 was shown to form a covalent complex with prostasin. Together, these data indicate that the prostasin-binding protein is PN-1. The identification of an interaction between prostasin and PN-1 suggests new functions and mechanisms where these molecules are present.

Introduction

Serine proteases play important roles in a diverse range of essential physiological processes and are implicated in various pathological processes such as cardiovascular disorders, inflammation, and cancers; hence, methods to inhibit these proteases have been explored for potential therapeutic applications (1). A subgroup of serine proteases with trypsin-like activities has attracted great attention because of their potential or confirmed membrane-anchorage. Examples are prostasin, testisin, and gamma-trypases (2-5). These membrane-anchored serine proteases may potentially act in very different ways than the classical secreted serine proteases such as trypsin. In our laboratory, we are interested in defining the physiological functions of prostasin, and identifying its regulators. Human prostasin was discovered in 1994 (2). The function of prostasin was unknown until Vallet *et al.* (6) identified a sodium channel activator in a *Xenopus* kidney epithelial cell line (A6), *Xenopus* CAP-1 (xCAP-1), which shared 53% sequence homology at the amino acid level with human prostasin. The CAP-1 is regarded as the homologue of prostasin. Later, Vuagniaux *et al.* (7) isolated mouse CAP-1 (mCAP-1) from a mouse cortical collecting duct (CCD) cell line. The mCAP-1 shares >80% sequence homology at the nucleic acid level with human prostasin. They further demonstrated that mCAP-1 activates the epithelial sodium channel (ENaC). A rat prostasin cDNA was also cloned (8). Co-expression of rat prostasin with rat ENaC increased the sodium current by two- to three-fold in *Xenopus* oocytes. In human airways, prostasin has now been suggested to be a regulator of the ENaC (9). Its role in airway ENaC activation is thought to be dependent on its serine protease activity as the serine protease inhibitor aprotinin had an opposing effect. In a

recent study (10), Narikiyo *et al.* demonstrated that aldosterone increased the secretion of prostasin protein into the culture medium of mouse CCD cell line, and also in urinary excretion in rats treated with aldosterone. Patients with primary aldosteronism showed increased prostasin level in the urine, and adrenalectomy significantly reduced the urinary prostasin excretion. The role of prostasin in sodium balance regulation in the kidney is also associated with its serine protease activity as the sodium current changes in response to aldosterone were inhibited by aprotinin (10). Most recently, Vallet *et al.* (11) further demonstrated that the glycosylphosphatidylinositol (GPI)-anchorage of xCAP/prostasin is required for its sodium channel activating function. A catalytic mutant of xCAP-1/prostasin decreased the ENaC activation by 90% but did not fully abolish it, suggesting that alternative mechanisms may also be involved (11). These results indicate that prostasin, most likely through its serine protease activity, is an important physiologic regulator of sodium balance.

We have shown that prostasin is a glycosylphosphatidylinositol (GPI)-anchored active serine protease expressed in normal prostate epithelial cells, and that prostasin can also be secreted into the prostatic fluid or culture media (12). Prostasin expression is down-regulated in high-grade (Gleason 4/5) prostate cancers, and in highly invasive human prostate and breast cancer cell lines (13-14). Enforced re-expression of prostasin in prostate and breast cancer cells reduced the invasiveness of these cells *in vitro* (13-14). The down-regulation of prostasin in the invasive human breast cancer cell lines is due to promoter DNA methylation (14). At present it remains to be determined whether the anti-invasion function of prostasin is dependent on its serine protease activity.

Serine protease inhibitors, or the serpins, are natural specific inhibitors of serine proteases. The serpins bind to the serine proteases to form a covalent complex at the serine active site, thereby inhibiting the protease (15). The process of serpins binding to their target proteases is usually rapid. Some serpins, however, are not good inhibitors alone, but become quite excellent inhibitors when they are complexed with cofactors, such as heparin. Examples of this type of serpins are antithrombin III, heparin cofactor II, protease nexin-1 (PN-1), and protein C inhibitor (16-19). Heparin is believed to cause a conformational change in the serpin molecule, in turn, facilitating the interaction of the protease and the serpin. While prostasin's physiological functions are not fully characterized at present, the knowledge of its potential inhibitors is also lacking. In a previous study, we identified a prostasin-binding protein in mouse and human seminal vesicles. In the present study, we have purified and characterized this prostasin-binding protein, and provided evidence to show that the prostasin-binding protein is a serpin, previously identified as protease nexin-1 (PN-1) (20).

Experimental Procedures

Purification of Prostasin-binding Protein

Sample preparation – The procedure was carried out as described previously (12) with modifications. Briefly, mouse seminal vesicle fluid was expressed in buffer A (20 mM sodium phosphate, pH 6.8) at a ratio of one pair of seminal vesicles per 1.0 ml of buffer. The sample was then centrifuged at 10,000 x g for 30 min at 4°C to remove insoluble material.

The following chromatography steps were performed at room temperature.

Anion-exchange chromatography – Two milliliters of the mouse seminal vesicle supernatant were applied onto an anion-exchange Econ-Cartridge (Q, 1 ml; Bio-Rad, Hercules, CA) equilibrated with buffer A, at a flow rate of 1 ml/min. After washing with 10 ml buffer A, the cartridge was eluted with 10 ml of 1 M NaCl/buffer A. Prostasin-binding activity was monitored by means of a prostasin-binding assay as described (12).

Hydroxylapatite chromatography – Fractions containing the prostasin-binding activity from the Q cartridge were applied onto a hydroxylapatite Econ-Cartridge (HTP, 1 ml; Bio-Rad) equilibrated with buffer A. The cartridge was washed with buffer A (10 ml), and eluted with 0.2 M sodium phosphate buffer (pH 6.8, 10 ml), followed by 0.5 M sodium phosphate buffer (pH 6.8, 10 ml).

Cation-exchange chromatography – Fractions containing the prostasin-binding activity from the HTP cartridge were diluted with buffer A and applied onto a cation-exchange Econ-Cartridge (CM, 1 ml; Bio-Rad) equilibrated with buffer A. After washing with buffer A, the cartridge was eluted with a 0 – 0.75 M linear NaCl gradient in buffer A

(20 ml). Fractions containing prostasin-binding activity were collected and concentrated through a Centricon-10 concentrator (Millipore, Bedford, MA) with several changes of PBS (phosphate-buffered saline, pH 7.4, LifeTechnologies, Gaithersburg, MD), and then stored at -20°C before further characterization.

Scaled-up purification was performed as described above, except that the first anion-exchange chromatography was performed using the DEAE CL-6B agarose (2.5 x 20 cm, Amersham Pharmacia Biotech, Piscataway, NJ). The subsequent purification steps were carried out by using 5-ml cartridges (Bio-Rad).

Preparation of A Polyclonal Antiserum

An antiserum against mPBP was prepared according to the procedure described in Chen *et al.* (12). Briefly, 0.5 ml of the purified mPBP (250 μg) was emulsified with an equal volume of complete Freund's adjuvant (Sigma-Aldrich, St. Louis, MO), and injected subcutaneously into a 1.5-kg New Zealand White female rabbit (Charles River Laboratories, Wilmington, MA). Booster injections were made with 100 μg of mPBP (emulsified with incomplete Freund's adjuvant, Sigma-Aldrich) for 3 times at 3-week intervals. Pre-immune rabbit serum was collected before the initial immunization.

Prostasin-binding Assay and Western Blot Analysis

The procedures were performed according to Chen *et al.* (12). Briefly, purified recombinant prostasin (12) was incubated with samples from each purification step or the final purified mPBP at 37°C for 1 hour or for various times as indicated. The binding

reaction was stopped by the addition of SDS-sample buffer [1xSDS sample buffer=62.5 mM Tris-HCl at pH 6.8, 2% (v/v) glycerol, 2% SDS (w/v), and 2% β -mercaptoethanol]. The reaction mixtures were then boiled for 5 min, and resolved in 10% SDS-polyacrylamide gels. The resolved proteins were then transferred to nitrocellulose membranes, and analyzed with either a prostasin antibody (12) or the mPBP antibody. Signals were detected using an ECL detection procedure with the WestPico reagents (Pierce, Rockford, IL) following the manufacturer's protocol. The membrane was then exposed to X-ray film (Midwest Scientific, St. Louis, MO). The prostasin antibody was used at 1:2,000 dilution, the mPBP antibody was used at 1:10,000 dilution, and the secondary antibody (goat anti-rabbit IgG, Sigma-Aldrich) was used at 1:10,000 dilution. All antibodies were diluted in 5% non-fat milk in TBS-T (TBS-T = 20 mM Tris-HCl at pH 7.6, 0.14 M NaCl, and 0.1% Tween-20).

Amino Acid Sequence Analysis

The purified mPBP (6 μ g) was incubated with various amounts of trypsin (LifeTechnologies) at 37°C for 1 hour. Samples were then mixed with SDS-sample buffer containing β -mercaptoethanol, incubated at 37°C for 30 min, and subjected to Tricine/SDS-PAGE (21) followed by transferring to the Immobilon-P membrane (Fisher, Pittsburgh, PA). One membrane was subjected to immunodetection with the mPBP antibody, an identical membrane was stained with 0.02% Coomassie blue R-250 in 40% methanol and 5% acetic acid for 30 seconds. The membrane was then destained in 40% methanol and 5% acetic acid for 1 min, rinsed in distilled water for 3 x 5 min to remove the destaining solution, and air dried. A stained band at ~10 kDa, which was

recognized by the mPBP antibody, was sent for amino acid sequence analysis at the Protein Core Facility of the University of Florida (Gainesville, FL).

Enzymatic Assay

Recombinant human prostasin was purified as described previously (12). A synthetic substrate, N-t-Boc-Gln-Ala-Arg-7-amido-4-methyl coumarin (QAR-AMC) was purchased from Sigma-Aldrich. The purified mPBP (concentration range 0–0.4 μM) was incubated with prostasin (0.8 μM) for 30 min at 37°C. The binding reaction mixture (20 μl) was then added to 80 μl of 50 mM Tris-HCl (pH 8.0)/0.1% bovine serum albumin containing the QAR-AMC substrate (final concentration: 100 μM) in 96-well microtiter plates (Costar 3903, Costar, Cambridge, MA). The velocity of substrate hydrolysis was measured using a Wallac 1420 Victor² multilabel counter at λ_{ex} 355 nm and λ_{em} 460 nm. The residual activity of prostasin (velocity of the inhibited enzyme reaction/velocity of the uninhibited enzyme reaction) was plotted versus the mPBP concentration.

Molecular Cloning, Expression and Purification of Recombinant Mouse and Human Protease Nexin-1 (PN-1, Spi-4)

A cDNA encoding the mature peptide of mouse protease nexin-1 (PN-1, or Spi-4) was cloned from mouse seminal vesicle mRNA by reverse-transcription-polymerase chain reaction (RT-PCR). Total RNA of mouse seminal vesicle was isolated using a procedure described previously (22), an Oligotex mRNA Mini Kit from QIAGEN (Valencia, CA) was used to isolate the mRNA. The following oligonucleotide primers

were used in the RT-PCR to generate the mouse PN-1 cDNA: upstream: 5'-GGAATTC TCC CAG TTC AAC TCT CTG TC -3'; and downstream: 5'- CCGCCTCGAG TCA GGG CTT GTT CAC CTG GC -3'. The underlined sequences are adapters for restriction enzyme sites. The mouse PN-1 specific sequences were derived from the GenBankTM mouse PN-1 sequence of X70296. The upstream primer sequence corresponds to base numbers 206-225 of X70296, the first codon (206-208) is that of Ser, the amino-terminal residue of the mature mouse PN-1 peptide (20). The downstream primer sequence corresponds to base numbers 1,323-1,342, including the termination codon (1,340-1,342). The RT-PCR was performed as described previously (13), using 3 µg of mouse seminal vesicle mRNA as the template. A single cDNA band was amplified. The Taq DNA polymerase was removed by phenol/chloroform extraction, and the cDNA was treated with *EcoR* I and *Xho* I under proper buffer conditions. The restriction-modified cDNA was then inserted into the pGEX-6P-1 vector (Amersham Pharmacia Biotech) at the corresponding sites, resulting in a fusion gene construct that encodes GST-mPN-1 (GST: glutathione-S-transferase). The amplified PN-1 portion of the fusion gene was completely sequenced, no error in the PN-1 sequence was found. A human PN-1 cDNA encoding the mature peptide was cloned from the total RNA of the human breast carcinoma cell line MDA-MB-435s (American Type Culture Collection, Manassas, VA) essentially as described above, resulting in the GST-hPN-1 construct. The primers used for the cloning were: upstream: 5'-GGAATTC TCC CAC TTC AAT CCT CTG TC -3'; downstream: 5'-GGAATTC TCA GGG TTT GTT TAT CTG CC-3'. The underlined sequences are adapters for restriction enzyme sites. The human PN-1 specific sequences were derived from the GenBankTM human PN-1 sequence of A03911. The

upstream primer sequence corresponds to base numbers 82-101 of A03911, the first codon (82-84) is that of Ser, the amino-terminal residue of the mature human PN-1 peptide (23). The downstream primer sequence corresponds to base numbers 1,199-1,218, including the termination codon (1,216-1,218). The GST-mPN-1 and the GST-hPN-1 constructs were then transformed into the TOPP-10 strain of *E. coli* cells (Stratagene, La Jolla, CA). For production of the recombinant fusion proteins, cells harboring the constructs were grown to an optical density of 0.8 (at 600-nm wavelength), and recombinant protein expression was induced with 0.2 mM of IPTG (isopropylthio- β -galactoside) at 37°C with shaking at 250 rpm for 1 h. Cells were collected by centrifugation at 4,000 rpm for 20 minutes at 4°C, washed in 1 x PBS (pH 7.4) and re-centrifuged with the same settings. GST-mPN-1 or GST-hPN-1 was then purified by glutathione-agarose affinity chromatography using protocols recommended by the manufacturer (Amersham Pharmacia Biotech).

Results

Purification of Prostasin-binding Protein from Mouse Seminal Vesicle

The presence of mouse prostasin-binding protein (mPBP) in each purification step was monitored using a prostasin-binding assay as described in "Experimental Procedures". Figure 1A shows the representative purification profiles for each step. Two milliliters of mouse seminal vesicle fluid were applied onto the Q cartridge and eluted with 1 M NaCl/buffer A. Fractions were subjected to the prostasin-binding assay followed by western blotting using a prostasin antibody (12). The mPBP was present in the flow-through fractions (peak a, indicated by the horizontal solid bar), but not the 1 M NaCl eluent (peak b). The mPBP-containing fractions were pooled and applied onto the HTP cartridge. After washing with buffer A, the cartridge was first eluted with 0.2 M sodium phosphate buffer at pH 6.8 (to result in peak d), and then eluted with 0.5 M sodium phosphate buffer at pH 6.8 (to result in peak e). Neither peak c (the flow-through) nor peak d contained any detectable amount of mPBP. The mPBP was detected in peak e (indicated by the horizontal solid bar). Fractions corresponding to peak e were pooled and further separated by using a CM cartridge. The CM cartridge was eluted with a linear NaCl gradient from 0 to 0.75 M in buffer A. The mPBP was eluted at 0.25-0.55 M NaCl/buffer A (peak g, as indicated by the horizontal solid bar). The flow-through fractions (peak f) did not contain mPBP. The purified mPBP was used to generate a polyclonal antibody using rabbit as the host. Proteins from each purification step were subjected to SDS-PAGE/Coomassie blue staining (Figure 1B); or western blot analysis using the mPBP antibody (Figure 1C). As shown in Figure 1B, the purified mPBP (lane 4, 5 μ g) migrated at ~45 kDa in an SDS-PAGE under reducing

conditions. As shown in Figure 1C, lanes 1-4, the mPBP antibody recognized a 45-kDa protein in mouse seminal vesicle fluid, as well as the purified mPBP itself.

Characterization of Mouse Prostasin-binding Protein

The purified mPBP was tested for its biochemical activities using the prostasin-binding assay (12). Complex formation between mPBP and purified prostasin was analyzed by western blotting using the mPBP antibody and a prostasin antibody (12). Both antibodies recognized the complex of prostasin-mPBP at 82 kDa (Figure 2A, lanes 2 & 5). The prostasin antibody also recognized the purified prostasin (Figure 2A, lane 1), unbound prostasin (Figure 2A, lane 2), as expected, but not the purified mPBP (Figure 2A, lane 3). The mPBP antibody recognized the purified mPBP (Figure 2, lane 6), unbound mPBP (Figure 2, lane 5), as expected, but not the purified prostasin (Figure 2, lane 4). Figure 2B shows the time-course of complex formation between prostasin and mPBP. The complex was detected after 30 seconds of incubation and progressed during the incubation time course (60 minutes). As shown in Figure 2C, the complex formation was inhibited in the presence of the serine protease inhibitor aprotinin (lane 3), or PMSF¹ (lane 4), or heparin (lane 5), or the mPBP antibody (lane 1). The complex formation of prostasin and mPBP was used as a control (Figure 2C, lane 2).

To reveal the identity of mPBP, the purified mPBP was subjected to a trypsin digestion and the digested mixture was separated using Tricine/SDS-PAGE. After transferring the resolved samples to the Immobilon-P membrane, one set of the samples was immunodetected with the mPBP antibody. In the sample without trypsin

digestion (Figure 3, lane 1), the mPBP antibody recognized a single band at 45 kDa. With increasing amounts of trypsin added in the digestion mixture, several mPBP immunoreactive bands were detected (Figure 3, lanes 2-5). In particular, a 10-kDa band (indicated by an arrow) was separated furthest in the gel from other bands. The corresponding band in a set of the exact samples transferred to an Immobilon-P membrane, stained with Coomassie blue, was sent for amino acid sequence analysis. The amino-terminal sequence of this fragment was determined to be SLEELGSNTGIQ, which is identical to the sequences between position 26 and position 37 of the GenBankTM mouse protease nexin-1 (PN-1) translated sequence (accession number: X70296). This result suggests that PBP may be identical to PN-1, a serine protease inhibitor (serpin) (20).

It has been known that PN-1 can form complexes with various serine proteases, including thrombin (24). We then tested if our purified mPBP can form a complex with thrombin. Figure 4A shows the complex formation between prostasin-mPBP, and that between thrombin-mPBP. We also tested if the complex formation is pH dependent because prostasin's optimum pH is 9.0 (2). The results showed that the purified mPBP formed a complex with prostasin as well as with thrombin. The complex formation of mPBP and prostasin is increased with higher pH in the binding conditions, while the complex formation of mPBP and thrombin is somewhat decreased with increasing pH. We further tested if heparin may have a different effect on the complex formation between prostasin-mPBP, versus on that between thrombin-mPBP. In Figure 4B we show that heparin, at 0.25 unit/reaction, completely abolished the complex formation

¹ PMSF = phenylmethylsulfonyl fluoride

between prostasin-mPBP; but not between thrombin-mPBP.

Prostasin-binding Protein Inhibits Prostasin's Activity

As described previously, the prostasin-binding protein that was identified in the seminal vesicle inhibits prostasin's activity as determined by membrane-overlay zymography (12). Here, we used QAR-AMC as a substrate for prostasin to test the inhibitory activity of the purified mPBP. Prostasin (0.8 μ M) was incubated with 0, 0.05, 0.1, 0.2 or 0.4 μ M mPBP at 37°C for 30 min. The reaction mixture was then added to the assay buffer containing a final concentration of 100 μ M QAR-AMC substrate (see "Experimental Procedures" for details). As shown in Figure 5, when incubated with mPBP at different concentrations, prostasin's activity was inhibited in a dose dependent manner.

Prostasin Forms A Complex with Recombinant Protease Nexin-1

To establish if mPBP is indeed protease nexin-1, mouse and human protease nexin-1 (PN-1) cDNA were cloned into the pGEX-6P-1 expression vector. The recombinant protein products have the schistosomal glutathione-S-transferase (GST) fused to the N-terminus of the PN-1. The GST fusion proteins were affinity-purified using glutathione-conjugated agarose-beads. For each type of recombinant protein, cleared supernatant of cell lysate from one liter of culture was incubated with 1 ml of 50% glutathione-beads. The beads were eluted with 1 ml of fresh 10 mM glutathione in 50 mM Tris-HCl, pH 8.0. Twenty microliters of the eluent were incubated with 0.5 μ g of

recombinant prostasin at 37°C for 60 min in the absence or presence of aprotinin. Both the GST-mPN-1 (Figure 6, lane 1, alone at 64 kDa) and the GST-hPN-1 (Figure 6, lane 4, alone at 64 kDa) formed a 100-kDa complex when incubated with prostasin (Figure 6, lanes 2 & 5). The complex formation was inhibited by the serine protease inhibitor aprotinin (Figure 6, lanes 3 & 6). These results further indicate that the mPBP that we had purified is the serpin protease nexin-1. For this immunoblot, both the prostasin antibody and the mPBP antibody were used as the primary antibody, and a goat anti-rabbit IgG conjugated with HRP was used as a secondary antibody. An immunoreactive band at 30 kDa, and two other minor immunoreactive bands at 42 kDa and 60 kDa were likely the products of non-specific degradation of the recombinant PN-1, since no protease inhibitors were added in the cell lysate during purification.

Discussion

In the present study, we have characterized a previously identified prostasin-binding protein following purification from mouse seminal vesicle. The prostasin-binding protein was further confirmed to be a serpin, previously identified as protease nexin-1 (PN-1). The purified mouse prostasin-binding protein was shown to inhibit prostasin's serine protease activity.

A prostasin-binding protein (PBP) was first identified when extracts of a number of mouse tissues were subjected to a prostasin-binding assay (12). The results indicated that a high level of a functional PBP appeared to be present only in the seminal vesicle. To reveal the identity of PBP, we used mouse seminal vesicle as the source for purification. By means of liquid chromatography, mPBP was purified to homogeneity as determined by SDS-PAGE (Figure 1). The purified mPBP migrated at 45 kDa and formed a covalent complex with prostasin as analyzed by SDS-PAGE under reducing conditions. The complex formation was fast, detected after 30 seconds of incubation, and was inhibited by the serine protease inhibitor aprotinin or PMSA, and by heparin (Figure 2). We also tested if mPBP binds to heparin by applying mouse seminal vesicle fluid to heparin-agarose. Prostasin-binding activity was found in the proteins eluted from heparin-agarose in the 0.3 – 0.6 M NaCl range, indicating that mPBP binds to heparin directly (data not shown). We have generated a polyclonal antibody against mPBP, developed an enzyme-linked immunosorbent assay to detect mPBP in tissues. Again, seminal vesicle was shown to contain the highest amount of mPBP (~5 μ g mPBP/mg total protein), confirming our previous findings (12). The level of mPBP in other tissues was at nanograms per milligram total protein (data not shown). The tissue

distribution of mPBP is consistent with that of mouse PN-1 mRNA reported previously (20). The results of the amino acid sequence analysis of a trypsin-digested fragment of mPBP, and of binding assays using the mouse or human recombinant PN-1 with prostasin had indicated that the PBP is identical to PN-1 (Figures 3 & 6).

PN-1 is a serpin with a broad spectrum of target serine proteases, such as thrombin, trypsin, plasmin, and urokinase-type plasminogen activator (uPA) (23). We provided evidence herein that PN-1 also inhibits prostasin. Several synthetic substrates were used by Yu *et al.* (2) for testing prostasin's activity in an *in vitro* enzymatic assay, such as D-Pro-Phe-Arg-AMC, D-Phe-Phe-Arg-AMC, D-Val-Leu-Arg-AMC, and Z-Gly-Pro-Arg-AFC². We also tested other substrates, including N-t-Boc-Gln-Ala-Arg-AMC (QAR-AMC), MeOSuc-Ile-Gly-Arg-AFC, N-Benzoyl-Val-Gly-Arg-PNA³, and MeOSuc-Ala-Ala-Ala-Arg-PNA. None of these substrates seems to be the best substrate for prostasin, as the *K_m* was high for all of these substrates (data not shown, also see ref. 2). We chose QAR-AMC for our study to test mPBP's inhibitory activity on prostasin. Since the QAR-AMC or any other substrate listed above is not the best substrate for prostasin, resulting in a low, and slowly-progressing velocity of prostasin-catalyzed hydrolysis, we were not able to determine the *K_{ass}* of mPBP with prostasin. As a control, we used QAR-AMC, an excellent trypsin substrate (25), to test the inhibitory activity of mPBP/PN-1 toward trypsin, the *K_{ass}* of mPBP/PN-1 to trypsin was at a range of 10^5 to 10^6 M⁻¹S⁻¹, similar to the previously published results for protease nexin-1 (23). Using the QAR-AMC substrate, we did, however, observe the inhibition of prostasin by mPBP in a dose-dependent manner (Figure 5), demonstrating that mPBP/PN-1 is an

² AFC = 7-amido-4-trifluoromethyl coumarin

inhibitor of prostasin serine protease.

A heparin-binding site has been mapped in PN-1 (26). In the presence of heparin, the inhibitory activity of PN-1 to several serine proteases, such as thrombin and factor Xa, is enhanced (26). In the presence of heparin, however, the binding between prostasin and PN-1 is abolished (Figure 4B). Also, in an enzymatic assay using the QAR-AMC substrate, pre-incubation of mPBP and heparin was able to prevent prostasin inhibition by mPBP (data not shown). This is a novel finding of PN-1's serine protease inhibition mechanism, having potentially profound implications, especially in cancer biology. PN-1 can bind to heparin-like molecules, or heparan sulfate proteoglycans (HSPG), on the cell surface and this binding apparently accelerates thrombin inhibition by PN-1 (27). The HSPG, as a component of the extracellular matrix (ECM), is suggested to play a major role in cell-matrix signaling (28). As we described previously, prostasin is a GPI-anchored membrane protease (12) which has an anti-invasion activity *in vitro* (13-14). It is likely that prostasin's anti-invasion activity is regulated by PN-1 and the ECM in the tissue microenvironment. Both the membrane-bound and the secreted prostasin can bind to and be inhibited by mPBP (12). The membrane-bound prostasin may be a proteolytic regulator of cell surface events, but may also serve as a receptor or a ligand in ECM signaling or tissue remodeling under physiological or pathological conditions. The complex formation between PN-1 with two of its target enzymes, prostasin and thrombin, is affected by pH (Figure 4). Changes in intracellular pH have been shown to be a mechanism of cell signaling (29), our finding may have significant implications to the control of the active prostasin serine protease

³ PNA = p-nitroanilide

inside the cell (12). On the other hand, extracellular pH change may also affect the signaling mechanisms for the plasma membrane-bound active prostasin.

There has been a large body of literature addressing the various functions of the serpin PN-1, especially for its roles in promoting the growth of neurites (30). The investigation of prostasin's functions, though still at its beginning, has indicated a number of possibilities, these include anti-invasion and epithelial sodium channel (ENaC) activation (6-14). Identifying an interaction between prostasin and PN-1 will undoubtedly facilitate further understanding of the biological functions of both prostasin and PN-1. Expression of serpin molecules has been linked to protection against tumor invasion (31-32), but non-protease-inhibition mechanisms are also suggested for serpin's roles in tumor invasion and metastasis (33). We now have identified a serpin that inhibits a serine protease that reduces *in vitro* invasiveness of prostate and breast cancer cells. In our continued research, we will investigate the tissue and cell-type specific expression of this serpin in relation to the expression of prostasin. Another important aspect of this present finding is that the reactive site sequence of the serpin PN-1, in particular, its P1-P4 residues Leu-Ile-Ala-Arg, may very well reveal sequence or structure information about the natural substrates of the prostasin serine protease. It has been shown with the serpin kallistatin (34), that its reactive site sequence was also the best for a substrate (35). Identification of prostasin's natural substrates will further the understanding of this protease's role in normal physiology and pathological conditions.

In the kidney, both prostasin and PN-1 are expressed (2, 36). While prostasin seems to activate ENaC, and the activation seems dependent on prostasin's serine

protease activity (10-11); PN-1 then, can serve the role of regulating this proteolytic activation process. In this role, PN-1 may be a potential therapeutic agent for diseases that involve activated ENaC as part of the mechanism. This idea is also potentially applicable to diseases of the respiratory system since there is recent evidence that prostasin may be involved in ENaC activation in the airway (9); and PN-1 is also expressed in the lung (37). Investigation of the spatial and temporal control of the coordinated expression of these two counteracting molecules will be of great importance for interests in renal and respiratory diseases. Alternatively, for potential therapeutic applications, inhibition of prostasin serine protease may also be accomplished by using synthetic inhibitors containing the sequences derived from the PN-1 reactive center.

PN-1 deficient mice display significant defects in fertility, evident through altered semen protein composition, inadequate semen coagulation, and deficient vaginal plug formation (38). Previously, the expression of prostasin and of PN-1 in the semen has been noted separately (2, 20). The findings of the present study suggest that prostasin and PN-1 may play an interactive role in the functions of male fertility.

Yet another tissue site for a potential prostasin/PN-1 interaction to have a profound effect to the body is the liver. Prostasin expression is noted in the liver (2). PN-1, though apparently not expressed in the liver (37), but has been shown to covalently bind factor Xa on the surface of hepatoma cells (39). As active factor Xa activates thrombin (40), while the latter can be inhibited by PN-1, the introduction of prostasin into this complex multi-player system must change or add to the views on how these players are regulated in a concerted way. The role of heparin in this complex

multi-player system will also need to be investigated as we have shown that heparin inhibits the interaction between prostasin and PN-1, but it enhances the interaction between thrombin and PN-1 (27).

References

1. Walker, B., and Lynas, J. F. (2001) *Cell. Mol. Life Sci.* **58**, 596-624
2. Yu, J. X., Chao, L., and Chao, J. (1994) *J. Biol. Chem.* **269**, 18843-18848
3. Yu, J. X., Chao, L., and Chao, J. (1995) *J. Biol. Chem.* **270**, 13483-13489
4. Hooper, J. D., Nicol, D. L., Dickinson, J. L., Eyre, H. J., Scarman, A. L., Normyle, J. F., Stuttgen, M. A., Douglas, M. L., Loveland, K. A., Sutherland, G. R., and Antalis, T. M. (1999) *Cancer Res.* **59**, 3199-3205
5. Caughey, G. H., Raymond, W. W., Blount, J. L., Hau, L. W., Pallaoro, M., Wolters, P. J., and Verghese, G. M. (2000) *J. Immunol.* **164**, 6566-6575
6. Vallet, V., Chraïbi, A., Gaeggeler, H. P., Horisberger, J. D., and Rossier, B. C. (1997) *Nature* **389**, 607-610
7. Vuagniaux, G., Vallet, V., Jaeger, N. F., Pfister, C., Bens, M., Farman, N., Courtois-Coutry, N., Vandewalle, A., Rossier, B. C., and Hummler E. (2000) *J. Am. Soc. Nephrol.* **11**, 828-834
8. Adachi, M., Kitamura, K., Miyoshi, T., Narikiyo, T., Iwashita, K., Shiraishi, N., Nonoguchi, H., and Tomita, K. (2001) *J. Am. Soc. Nephrol.* **12**, 1114-1121
9. Donaldson, S. H., Hirsh, A., Li, D. C., Holloway, G., Chao, J., Boucher, R. C., and Gabriel, S. E. (2002) *J. Biol. Chem.* **277**, 8338-8345
10. Narikiyo, T., Kitamura, K., Adachi, M., Miyoshi, T., Iwashita, K., Shiraishi, N., Nonoguchi, H., Chen, L. M., Chai, K. X., Chao, J., and Tomita, K. (2002) *J. Clin. Invest.* **109**, 401-408

11. Vallet, V., Pfister, C., Loffing, J., and Rossier, B. C. (2002) *J. Am. Soc. Nephrol.* **13**, 588-594
12. Chen, L. M., Skinner, M. L., Kauffman, S. W., Chao, J., Chao, L., Thaler, C. D., and Chai, K. X. (2001) *J. Biol. Chem.* **276**, 21434-21442
13. Chen, L. M., Hodge, G. B., Guarda, L. A., Welch, J. L., Greenberg, N. M., and Chai, K. X. (2001) *Prostate* **48**, 93-103
14. Chen, L. M., and Chai, K. X. (2002) *Int. J. Cancer* **97**, 323-329
15. Silverman, G. A., Bird, P. I., Carrell, R. W., Church, F. C., Coughlin, P. B., Gettins, P. G., Irving, J. A., Lomas, D. A., Luke, C. J., Moyer, R. W., Pemberton, P. A., Remold-O'Donnell, E., Salvesen, G. S., Travis, J., and Whisstock, J. C. (2001) *J. Biol. Chem.* **276**, 33293-33296
16. Jordan, R. E., Kilpatrick, J., and Nelson, R. M. (1987) *Science* **237**, 777-779
17. Tollefsen, D. M., Majerus, D. W., and Blank, M. K. (1982) *J. Biol. Chem.* **257**, 2162-2169
18. Wallace, A., Rovelli, G., Hofsteenge, J., and Stone, S. R. (1989) *Biochem. J.* **257**, 191-196
19. Pratt, C. W., Macik, B. G., and Church, F. C. (1989) *Thromb. Res. Suppl.* **53**, 595-602
20. Vassalli, J. D., Huarte, J., Bosco, D., Sappino, A. P., Sappino, N., Velardi, A., Wohlwend, A., Erno, H., Monard, D., and Belin, D. (1993) *EMBO J.* **12**, 1871-1878
21. Schagger, H., and von Jagow, G. (1987) *Anal. Biochem.* **166**, 368-379

22. Chirgwin, J. M., Przybyla, A. E., MacDonald, R. J., and Rutter, W. J. (1979) *Biochemistry* **18**, 5294-5299
23. Scott, R. W., Bergman, B. L., Bajpai, A., Hersh, R. T., Rodriguez, H., Jones, B. N., Barreda, C., Watts, S., and Baker, J. B. (1985) *J. Biol. Chem.* **260**, 7029-7034
24. Evans, D. L., McGrogan, M., Scott, R. W., and Carrell, R. W. (1991) *J. Biol. Chem.* **266**, 22307-22312
25. Kawabata, S., Miura, T., Morita, T., Kato, H., Fujikawa, K., Iwanaga, S., Takada, K., Kimura, T., and Sakakibara, S. (1988) *Eur. J. Biochem.* **172**, 17-25
26. Stone, S. R., Brown-Luedi, M. L., Rovelli, G., Guidolin, A., McGlynn, E., and Monard, D. (1994) *Biochemistry* **33**, 7731-7735
27. Farrell, D. H., and Cunningham, D. D. (1986) *Proc. Natl. Acad. Sci. U. S. A.* **83**, 6858-6862
28. Lin, X., and Perrimon, N. (2000) *Matrix Biol.* **19**, 303-307
29. Lyall, V., and Biber, T. U. (1994) *Am. J. Physiol.* **266**, F685-F696
30. Cunningham, D. D., and Gurwitz, D. (1989) *J. Cell. Biochem.* **39**, 55-64
31. Sheng, S., Carey, J., Seftor, E. A., Dias, L., Hendrix, M. J., and Sager, R. (1996) *Proc. Natl. Acad. Sci. U. S. A.* **93**, 11669-11674
32. Sternlicht, M. D., Kedeshian, P., Shao, Z. M., Safarians, S., and Barsky, S. H. (1997) *Clin. Cancer Res.* **3**, 1949-1958
33. Andreassen, P. A., Kjoller, L., Christensen, L., and Duffy, M. J. (1997) *Int. J. Cancer* **72**, 1-22

34. Chai, K. X., Chen, L. M., Chao, J., and Chao, L. (1993) *J. Biol. Chem.* **268**, 24498-24505
35. Pimenta, D. C., Juliano, M. A., and Juliano, L. (1997) *Biochem. J.* **327**, 27-30
36. Moll, S., Schaeren-Wiemers, N., Wohlwend, A., Pastore, Y., Fulpius, T., Monard, D., Sappino, A. P., Schifferli, J. A., Vassalli, J. D., and Izui, S. (1996) *Kidney Int.* **50**, 1936-1945
37. Mansuy, I. M., van der Putten, H., Schmid, P., Meins, M., Botteri, F. M., and Monard, D. (1993) *Development* **119**, 1119-1134
38. Murer, V., Spetz, J. F., Hengst, U., Altrogge, L. M., de Agostini, A., and Monard, D. (2001) *Proc. Natl. Acad. Sci. U. S. A.* **98**, 3029-3033
39. Kazama, Y., Komiyama, Y., and Kisiel, W. (1993) *Blood* **81**, 676-682
40. Davie, E. W., Fujikawa, K., and Kisiel, W. (1991) *Biochemistry* **30**, 10363-10370

Figure Legends:

Figure 1. Purification of mouse prostasin-binding protein (mPBP). Two milliliters of mouse seminal vesicle fluid were fractionated in sequence on a Q-Cartridge (anion exchange), an HTP (hydroxylapatite), and a CM cartridge (cation exchange). A: a representative purification profile. Protein contents in fractions were monitored at 280 nm with different AUFS (Absorbance Units Full Scale) as indicated. Fractions containing prostasin-binding activity were determined with the prostasin-binding assay (Experimental Procedures), and indicated by the horizontal solid bars. B: Coomassie blue staining of proteins of crude mouse seminal vesicle fluid (lane 1, 50 μ g), flow-through fractions of Q-Cartridge (lane 2, 50 μ g), 0.5 M sodium phosphate eluent of HTP-Cartridge (lane 3, 25 μ g), and the purified mPBP from the CM-Cartridge (lane 4, 5 μ g). C: Western blot analysis of samples from B using the polyclonal antibody against mPBP.

Figure 2. Complex formation between prostasin and mouse prostasin-binding protein. Purified recombinant human prostasin (0.5 μ g) (12) was incubated with purified mPBP (0.5 μ g) at 37°C for 60 min. The binding mixtures were resolved in 10% SDS-PAGE under reducing conditions and were examined by western blot analysis using either a prostasin antibody (12) or the mPBP antibody. A: Lanes 1 & 4: prostasin alone; lanes 2 & 5: the binding mixtures; and lanes 3 & 6: purified mPBP alone. The blot shown in the left panel was detected with the prostasin antibody (IB: Prostasin) and that in the right panel was detected with the mPBP antibody (IB: mPBP). B: Prostasin was

incubated with mPBP at 37°C for various time periods as indicated. The samples were examined on a western blot with the prostasin antibody. The complex can be observed at as early as 30 sec after incubation. C: Prostasin was incubated with mPBP in the presence of aprotinin (lane 3, 1 μ g), PMSF (lane 4, 5 mM), heparin (lane 5, 5 units), and the mPBP antibody (lane 1, 0.5 μ l). The samples were examined on a western blot with the prostasin antibody. The 50-kDa band indicated by the asterisk in lane 1 is the mPBP antibody (IgG) recognized by the secondary antibody. The complex formation of prostasin-mPBP was inhibited by serine protease inhibitors, heparin, and the mPBP antibody.

Figure 3. Trypsin digestion of mPBP. Purified mPBP (6 μ g) was incubated with various amounts of trypsin (lane 1, zero μ g; lane 2, 2.5 μ g; lane 3, 5.0 μ g; lane 4, 10 μ g; and lane 5, 20 μ g) at 37°C for 60 min. The digested mixtures were analyzed in 16.5% Tricine-SDS/PAGE and immunoblotted with the mPBP antibody. The band at ~ 10 kDa (indicated by the arrow) was cut from a stained duplicate membrane and sent for amino-terminal sequencing.

Figure 4. Effects of pH and heparin on complex formation. Prostasin (0.3 μ g) or thrombin (0.2 μ g) was incubated with mPBP (0.5 μ g) at different pH as indicated (A), or in the presence of various amounts of heparin (B) at 37°C for 1 hour. The binding mixtures (20 μ l) were analyzed in 10% SDS-PAGE followed by immunoblotting. Prostasin-binding assay was analyzed with a prostasin antibody (12) and labeled as IB:

Prostasin, while thrombin-binding assay was analyzed with the mPBP antibody and labeled as IB: mPBP. The amount of heparin in each reaction is as follows: lanes 1 & 5, zero unit; lanes 2 & 6, 0.25 unit; lanes 3 & 7, 0.5 unit; and lanes 4 & 8, 1.0 unit. The complex formation of prostasin-mPBP is increased with increasing pH, and that of thrombin-mPBP is somewhat decreased. Heparin abolished complex formation between prostasin-mPBP, but not between thrombin-mPBP.

Figure 5. mPBP/PN-1 inhibits prostasin's activity. Prostasin's serine protease activity was measured using a synthetic substrate, QAR-AMC as described in "Experimental Procedures". When prostasin (0.8 μ M) was first incubated with mPBP (0, 0.05, 0.10, 0.20, and 0.40 μ M) for 30 min at 37°C, then added to the QAR-AMC (100 μ M) solution, prostasin's activity was inhibited in a dose-dependent manner. The residual prostasin activity was determined by the fraction of velocity of the inhibited prostasin reaction versus velocity of the uninhibited prostasin reaction. The experiment was repeated for 3 times.

Figure 6. Recombinant mouse or human PN-1 forms a complex with prostasin. GST-mPN-1 and GST-hPN-1 were cloned, expressed, and purified as described in "Experimental Procedures". The purified GST-fusion PN-1 proteins were incubated with prostasin at 37°C for 60 min without (lanes 2 & 5) or with aprotinin (lanes 3 & 6, 1 μ g); or examined alone without incubation with prostasin (lanes 1 & 4). The binding mixtures were analyzed in 10% SDS-PAGE followed by immunoblotting with both prostasin and

Prostasin-binding Protein

mPBP antibodies. The complex of prostasin-GST-mPN-1 or prostasin-GST-hPN-1 migrated at 100 kDa (labeled as "Complex"). Unbound prostasin is labeled as "Prostasin".

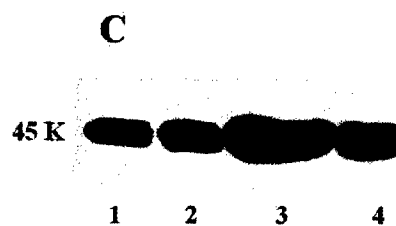
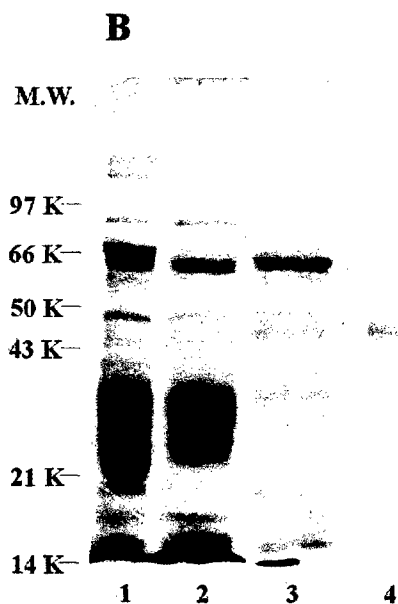
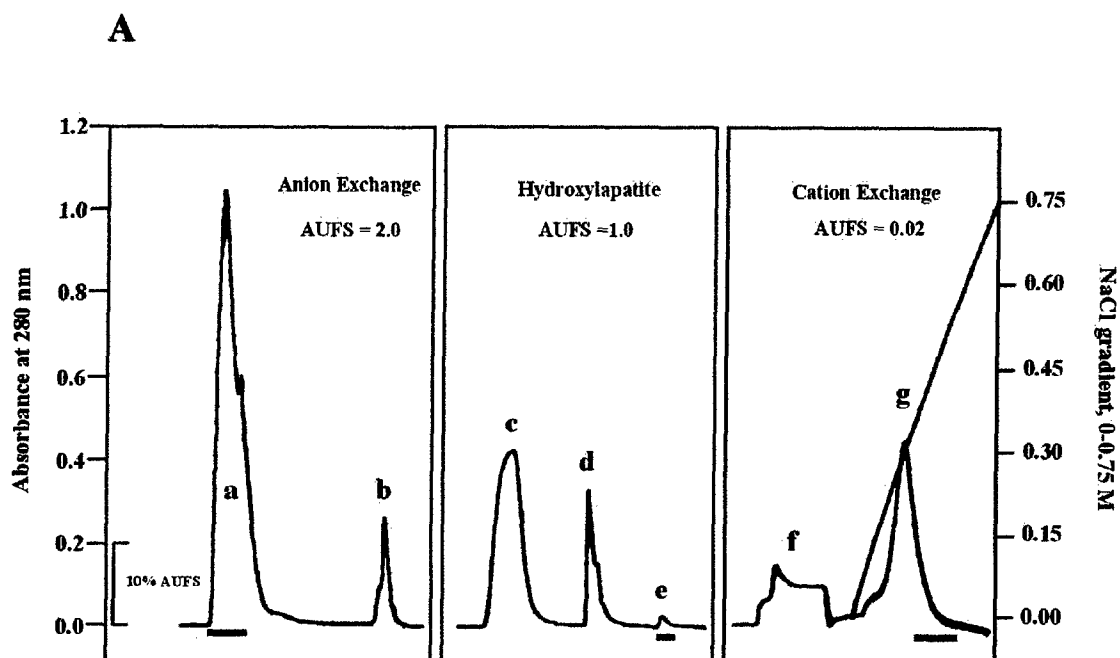


Figure 1

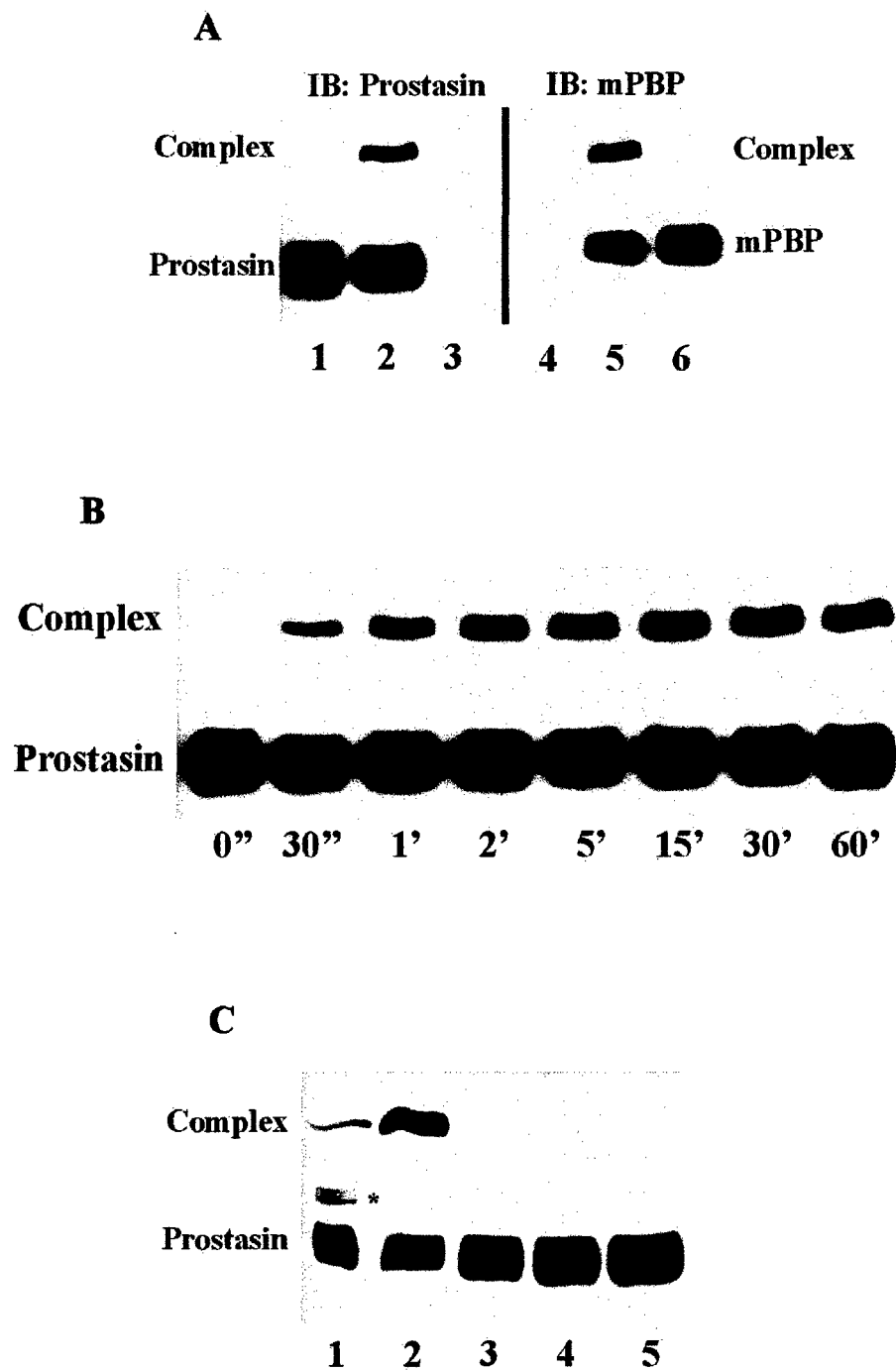


Figure 2

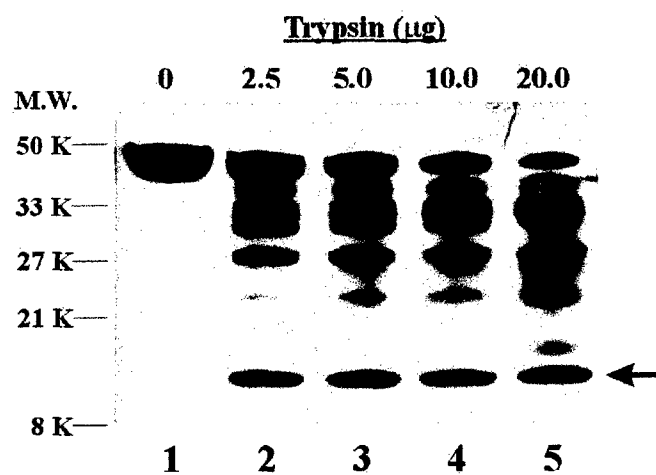


Figure 3

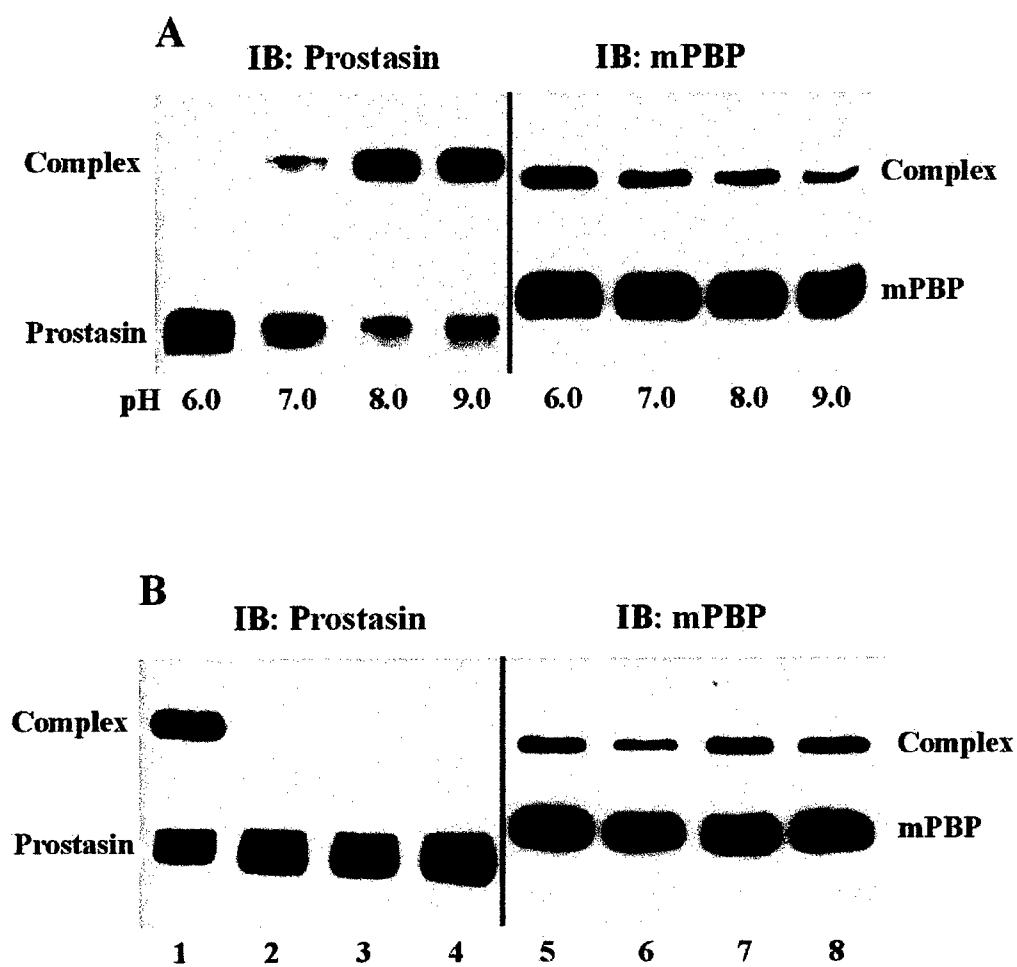


Figure 4

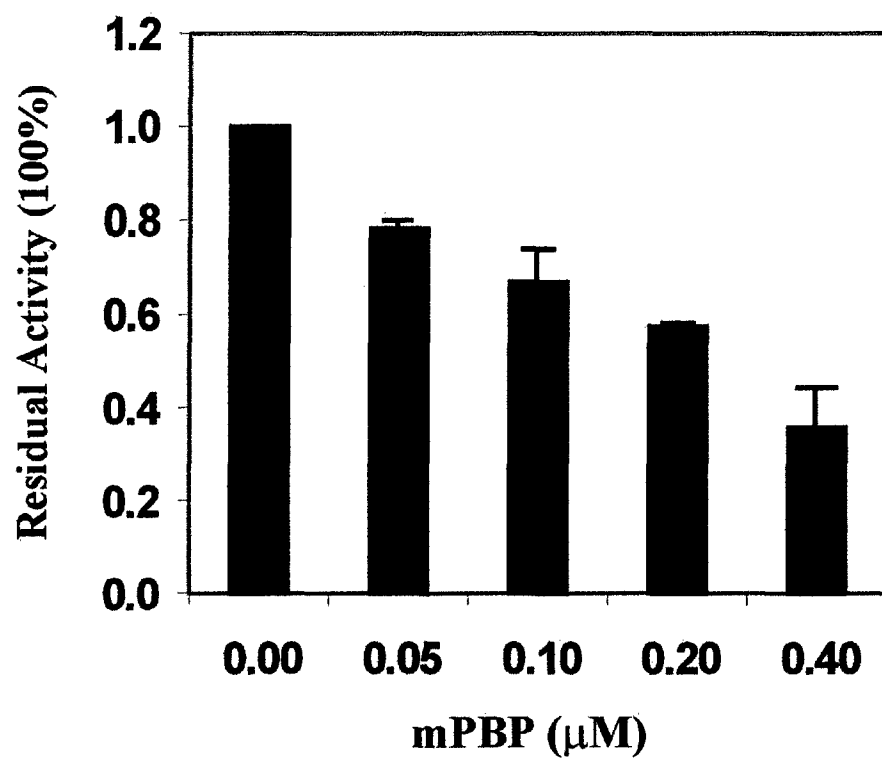


Figure 5

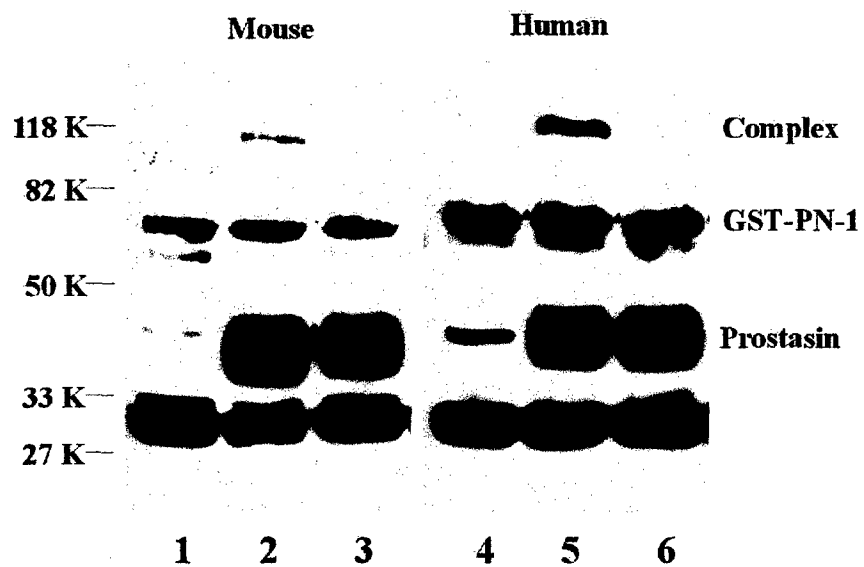


Figure 6

**The Prostaticin Gene Promoter Is Hypermethylated
in Invasive Human Prostate Cancer Cells**

Li-Mei Chen and Karl X. Chai*

Department of Molecular Biology and Microbiology, University of Central Florida

Orlando, Florida 32816

Short Title: Prostaticin Methylation in Prostate Cancer

*Correspondence to: Department of Molecular Biology and Microbiology, University of Central Florida, 4000 Central Florida Boulevard, Orlando, Florida 32816-2360, Phone: (407) 823-6122; Fax: (407) 823-3095; E-mail: kxchai@mail.ucf.edu

ABSTRACT

We have shown recently that prostatic serine protease is down-regulated in high-grade prostate cancers, and inhibits invasiveness of prostate and breast cancer cell lines upon enforced re-expression. Further, prostatic expression in breast cancer cells is regulated by DNA methylation in the prostatic gene promoter-exon 1 region. In the present study, normal human prostate epithelial cells, and human prostate cancer cell lines (LNCaP, DU-145, and PC-3) were investigated for prostatic gene promoter methylation. The methylation pattern of the prostatic gene promoter correlates with prostatic expression in these cells. Demethylation coupled with histone deacetylase inhibition resulted in reactivated expression of the prostatic mRNA in DU-145 and PC-3 cells. Prostatic gene promoter methylation may be explored as a marker for invasiveness of prostate cancer.

Keywords: Prostatic, Serine Protease, Invasion Suppressor, Prostate Cancer, DNA Methylation

INTRODUCTION

Prostasin serine protease has recently been suggested as an invasion suppressor for human prostate and breast cancers (1-2). Its expression is down-regulated in high-grade (Gleason 4/5) prostate cancers (1) and also absent in highly invasive human prostate (1) and breast cancer cells (2). Prostasin is a glycosylphosphatidylinositol (GPI)-anchored active serine protease and can also be secreted (3). In the kidney and the airway epithelia, prostasin has been shown to be a sodium channel (ENaC) activator (4-5), most likely through its serine protease activity (6). The ENaC activation function of prostasin requires its GPI-anchorage (6). The invasion suppression by prostasin is also dependent on its membrane-anchorage (1), but it remains to be determined whether invasion suppression requires prostasin's serine protease activity.

The prostasin gene promoter-exon 1 regulatory region was shown to be methylated in the highly invasive human breast cancer cell lines MDA-MB-231 and MDA-MB-435s (2). This methylated state is causal to prostasin's absence in these cell lines, suggesting that prostasin promoter methylation may be explored as a marker for invasiveness (2). We have also shown that two highly invasive human prostate cancer cell lines DU-145 and PC-3 do not express prostasin protein or mRNA, while normal human prostate epithelial cells and a non-invasive human prostate cancer cell line LNCaP express both the prostasin mRNA and protein (1). In the present study, we examined the methylation state of the prostasin gene promoter-exon 1 regulatory region in normal human prostate epithelial cells, and LNCaP, DU-145, and PC-3 cell lines.

MATERIALS AND METHODS

Cell culture maintenance

A normal human prostate epithelial cell (PrEC) primary culture (Catalog Number CC-2555) was obtained from Clonetics (San Diego, CA), and maintained as described previously (1). Human prostate cancer cell lines LNCaP, DU-145, and PC-3 were obtained from the American Type Culture Collection (ATCC, Manassas, VA), and maintained as described previously (1).

RNA preparation and analysis by RT-PCR/Southern blot

Cells grown to 80% confluence (in 60-mm tissue culture dish) were used for RNA isolation as described previously (2). The human prostatic-specific RT-PCR (reverse transcription-polymerase chain reaction)/Southern blot analysis was performed as described previously (1-2).

Genomic Southern blot analysis of prostatic promoter methylation

High molecular weight genomic DNA was isolated from the cell lines as described previously (7). Genomic DNA from each cell line was digested with restriction enzymes (methylation sensitive and non-sensitive) for Southern blot analysis as described previously (2).

Demethylation of prostatic gene promoter and reactivation of prostatic expression

DU-145 and PC-3 cells were seeded in 60-mm dishes at 80% confluence and cultured in the presence of 500 nM 5-aza-2'-dC for 24 hr, and were then treated for an additional 24 hr with either 1 μ M trichostatin A (TSA, Sigma-Aldrich Co.) or an equal volume of 95% ethanol used to dissolve TSA. RNA was isolated for prostatic-specific RT-PCR/Southern blot analysis as described.

RESULTS AND DISCUSSION

Prostasin gene promoter is hypermethylated in invasive prostate cancer cell lines

In this study, we examined, in the human prostate epithelial cells and prostate cancer cell lines, the prostasin promoter and exon 1 region which was shown to be hypermethylated in invasive human breast cancer cell lines (2). This region is defined by an Xho I-BamH I fragment and contains multiple CpG dinucleotides. The sites being investigated were identical to those examined for the breast cancer cell lines previously. These are, an Hha I site at base number 615/-807 (relative to the transcription initiation site, same below), an Aci I site at 1,102/-320, a BsaA I site at 1,156/-266, an Hpa II site at 1,326/-96, and an Aci I site at 1,445/+24. The results of the genomic Southern blot analysis are presented in Figure 1 and summarized in Table 1.

In all three prostate cancer cell lines and the PrEC, Xho I/BamH I/Hha I digestion yielded a 1,275-bp prostasin promoter band seen in the Xho I/BamH I digestion (Figure 1, upper panel), indicating that the -807 Hha I site-CpG is homogeneously methylated.

In the PrEC, digestion with Xho I/BamH I/Aci I yielded a 1,072-bp, a 727-bp, and a 345-bp band, but no 1,275-bp band, indicating that the -320 Aci I site-CpG is heterogeneously methylated, but the +24 Aci I site-CpG is homogeneously unmethylated. In LNCaP and DU-145, digestion with Xho I/BamH I/Aci I yielded only the 1,072-bp band, indicating that the -320 Aci I site-CpG is homogeneously methylated, but the +24 Aci I site-CpG is homogeneously unmethylated. In PC-3, digestion with Xho I/BamH I/Aci I yielded the 1,072-bp band, and to a lesser extent the 1,275-bp band, indicating that the -320 Aci I site-CpG is homogeneously methylated, while the +24 Aci I site-CpG is heterogeneously methylated.

In the PrEC and LNCaP, digestion with Xho I/BamH I/BsaA I yielded a 782-bp and a 493-bp band, indicating that the -266 BsaA I site-CpG is homogeneously unmethylated. In DU-145, digestion with Xho I/BamH I/BsaA I yielded the 782-bp and the 493-bp bands, but also the

1,275-bp band, indicating that the -266 BsaA I site-CpG is heterogeneously methylated. In PC-3, digestion with Xho I/BamH I/BsaA I yielded only the 1,275-bp band, indicating that the -266 BsaA I site-CpG is homogeneously methylated.

In the PrEC and LNCaP cells, the 1,275-bp Xho I-BamH I band can be digested by the methylation-insensitive Msp I as well as by the methylation-sensitive Hpa II, yielding a 951-bp band (Figure 1, lower panel), indicating that the CpG at the -96 M/H restriction site is homogeneously unmethylated. In DU-145 and PC-3, the 1,275-bp band can be fully digested by Msp I, but only partially by Hpa II (Figure 1, lower panel), indicating heterogeneous methylation of the -96 M/H site-CpG.

The PrEC express both the prostatic mRNA and protein (1), and is the least methylated in the prostatic promoter-exon 1 region (methylation is only observed at beyond -266, relative to the transcription initiation site). The prostatic gene promoter-exon 1 region in LNCaP cells is methylated to a higher extent than that in the PrEC. In LNCaP, which also express both the prostatic mRNA and protein (1), methylation is only observed at beyond -96. In DU-145, which does not express either the prostatic protein or mRNA (1), methylation is observed at the -96 position and beyond. In PC-3, which also does not express either the prostatic protein or mRNA (1), the promoter-exon 1 region is the most heavily methylated. While in DU-145 the methylation is limited to the 5'-flanking region, all CpG sites examined, including one of exon 1 (+24 Aci I site-CpG) show heterogeneous to homogeneous methylation in the PC-3 cells. The prostatic gene promoter-exon 1 region CpG methylation patterns correlate with the absence of prostatic expression in the human prostate cells.

The methylation state of the prostatic promoter region may be examined for a potential diagnostic application to indicate prostate cancer invasiveness. The prostatic gene promoter methylation state at the -96 M/H CpG site, for example, is seen methylated only in invasive cell types (Figure 1, lower panel, and Table 1).

Prostasin expression was reactivated by demethylation and histone deacetylase inhibition in DU-145 and PC-3 cell lines

We next investigated if DNA methylation in the promoter is causal to the lack of prostasin gene expression in the prostate cancer cell lines DU-145 and PC-3. Treatment of these cell lines for 8 days with the DNA methyltransferase inhibitor 5-aza-2'-dC resulted in significant level of demethylation, but no prostasin mRNA expression was detected in an RT-PCR/Southern blot analysis of the DNA-demethylated cells (data not shown). Treatment of the cells with the combination of 5-aza-2'-dC and trichostatin A (TSA), an inhibitor of histone deacetylase (8), however, restored prostasin mRNA expression in DU-145 and PC-3 (Figure 2). We further examined whether the prostasin protein was expressed in the 5-aza-2'-dC/TSA-treated cells by western blot analysis, the result was negative (data not show). It appears that, although promoter DNA methylation is causal to absence of prostasin expression in the invasive prostate cancer cells, the reactivated expression represents only the basal expression, similar to what we have observed previously in breast cancer cells (2).

ACKNOWLEDGEMENTS

This work was supported by Department of Defense Prostate Cancer Research Program Grant No. DAMD17-98-1-8590.

REFERENCES

1. Chen, L. M., Hodge, G. B., Guarda, L. A., Welch, J. L., Greenberg, N. M., and Chai, K. X. (2001) Down-regulation of prostasin serine protease: a potential invasion suppressor in prostate cancer. *Prostate* **48**, 93-103.
2. Chen, L. M., and Chai, K. X. (2002) Proastin serine protease inhibits breast cancer invasiveness and is transcriptionally regulated by promoter DNA methylation. *Int. J. Cancer*. **97**, 323-329.
3. Chen, L. M., Skinner, M. L., Kauffman, S. W., Chao, J., Chao, L., Thaler, C. D., and Chai, K. X. (2001) Proastin is a glycosylphosphatidylinositol-anchored active serine protease. *J. Biol. Chem.* **276**, 21434-21442.
4. Narikiyo, T., Kitamura, K., Adachi, M., Miyoshi, T., Iwashita, K., Shiraishi, N., Nonoguchi, H., Chen, L. M., Chai, K. X., Chao, J., and Tomita, K. (2002) Regulation of prostasin by aldosterone in the kidney. *J. Clin. Invest.* **109**, 401-408.
5. Donaldson, S. H., Hirsh, A., Li, D. C., Holloway, G., Chao, J., Boucher, R. C., Gabriel, S. E. (2002) Regulation of the epithelial sodium channel by serine proteases in human airways. *J. Biol. Chem.* **277**, 8338-8345.
6. Vallet, V., Pfister, C., Loffing, J., and Rossier, B. C. (2002) Cell-surface expression of the channel activating protease xCAP-1 is required for activation of ENaC in the *Xenopus* oocyte. *J. Am. Soc. Nephrol.* **13**, 588-594.
7. Chai, K. X., Ward, D. C., Chao, J., and Chao, L. (1994) Molecular cloning, sequence analysis, and chromosomal localization of the human protease inhibitor 4 (kallistatin) gene (PI4). *Genomics* **23**, 370-378.

8. Cameron, E. E., Bachman, K. E., Myohanen, S., Herman, J. G., and Baylin, S. B. (1999) Synergy of demethylation and histone deacetylase inhibition in the re-expression of genes silenced in cancer. *Nat. Genet.* **21**, 103-107.

FIGURE LEGENDS

Figure 1. Genomic Southern blot analysis of DNA from PrEC and human prostate cancer cell lines. Panels of genomic DNA Southern blot analysis results are as indicated for each cell type. Restriction endonucleases used in each digestion mixture are identified as follows: X = Xho I, B = BamH I, Hh = Hha I, A = Aci I, Bs = BsaA I, M = Msp I, and H = Hpa II. Hha I, Aci I, BsaA I, and Hpa II only cut unmethylated DNA while Msp I, an isoschizomer of Hpa II, cuts unmethylated or methylated DNA. Genomic DNA (10 μ g) from each cell type was cut with X/B, or with X/B/M to serve as controls for the detection of differential methylation. In the upper panel, prostaticin promoter DNA will yield a 1,275-bp X/B fragment. When Hha I was added to the X/B digestion mixture, a fragment of 1,037 bp was expected if the -807 Hha I site-CpG was not methylated. When Aci I was added to the X/B digestion mixture, three smaller bands might be expected depending on CpG methylation states at -320 and +24 Aci I sites. They are 1,072 bp (from Xho I to +24 Aci I), 727 bp (from Xho I to -320 Aci I), and 345 bp (from -320 Aci I to +24 Aci I) in length, respectively. When BsaA I was added to the X/B digestion mixture, two smaller bands might be expected depending on CpG methylation state at the -266 BsaA I. They are 782 bp (from Xho I to BsaA I) and 493 bp (from BsaA I to BamH I) in length, respectively (indicated by asterisks in the figure). In the lower panel, the upper arrow points to the X/B fragment, while the lower arrow points to the fragment that is generated by Msp I, regardless of DNA methylation; or by Hpa II, only when DNA is unmethylated.

Figure 2. Reactivation of prostaticin expression in DU-145 and PC-3 cells. Cells treated with 5-aza-2'-dC (500 nM) for 24 hr were treated with TSA (1 μ M) for an additional 24 hr, before being harvested for total RNA isolation and RT-PCR/Southern blot analysis as described. Cells treated with 5-aza-2'-dC and 95% ethanol (indicated as EtOH) were used as controls.

Table 1. CpG methylation in the prostaticin gene promoter-exon 1 region in human prostate cells.

Cell Type	Prostaticin Expression	Hha I (-807)	Aci I (-320)	BsaA I (-266)	Msp II/Hpa II (-96)	Aci I (+24)
PrEC	Yes	Methyl	Hetero-Methyl	Un-Methyl	Un-Methyl	Un-Methyl
LNCaP	Yes	Methyl	Methyl	Un-Methyl	Un-Methyl	Un-Methyl
DU-145	No	Methyl	Methyl	Hetero-Methyl	Hetero-Methyl	Un-Methyl
PC-3	No	Methyl	Methyl	Methyl	Hetero-Methyl	Hetero-Methyl

Table Legend:

Methyl = homogeneously methylated.

Hetero-methyl = heterogeneously methylated.

Un-methyl = homogeneously unmethylated.

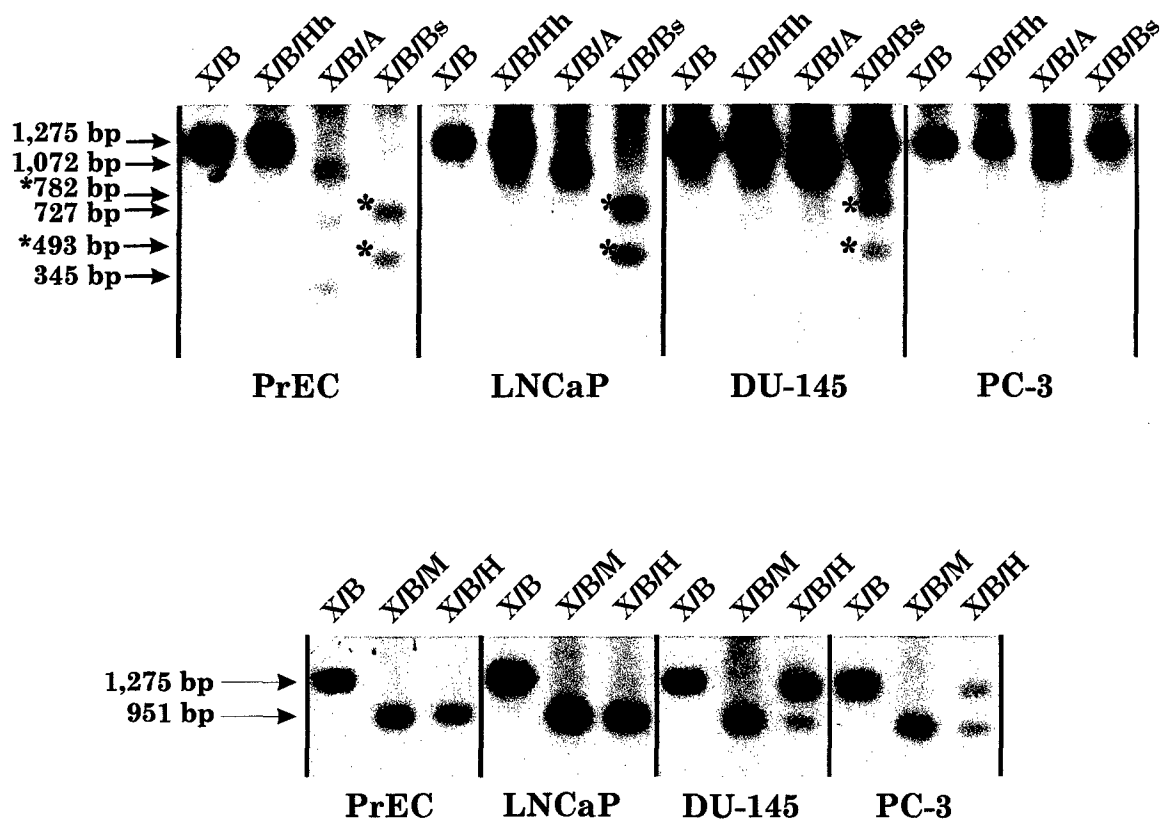


Figure 1

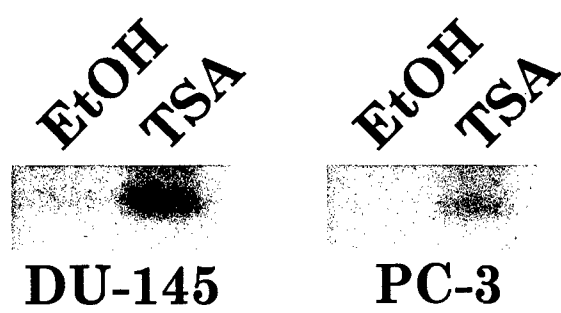


Figure 2

Appendix 7

Genetic Analysis of the *Drosophila melanogaster* *Stubble-stubblويد* locus During Leg Imaginal Disc Morphogenesis: A Potential Role for a Type II Transmembrane Serine Protease in RhoA Signaling.

Cynthia A. Bayer *, Susan R. Halsell ^{†,‡}, Daniel P. Kiehart [‡] and Laurence von Kalm*

* Department of Biology, University of Central Florida, Orlando, FL 32816-2368

† Department of Biology, Department of Biology, James Madison University, Harrisonburg, VA 22807

‡ DCMB Group, Department of Biology, Duke University, Durham, NC 27708-1000

Running Head: Serine Protease Action and RhoA Signaling

Key Words: actin, myosin, zipper, Rho kinase, cell shape changes

Corresponding Author: Laurence von Kalm
Department of Biology
4000 Central Florida Blvd.
Orlando, FL 32816-2368
Phone: (407) 823-6684
FAX: (407) 823-5769
email: lvonkalm@mail.ucf.edu

ABSTRACT

The *Drosophila Stubble-stubblويد* (*Sb-sbd*) locus encodes a member of the type II transmembrane serine protease family. *Sb-sbd* function is required for cell shape changes that control leg elongation in prepupal imaginal discs. Here we demonstrate that *Sb-sbd* mutants act as genetic enhancers of mutant leg defects associated with mutations in *RhoA* and several members of the RhoA signaling pathway. Over-expression of *Sb-sbd* in prepupal leg discs results in a malformation phenotype that is suppressed by reducing the gene dosage of *RhoA* suggesting that *RhoA* acts downstream of *Sb-sbd* as leg disc cells change their shape. We propose that induction of *Sb-sbd* by ecdysone in leg discs triggers *RhoA* signaling leading directly to cell shape change. To identify additional components of a hypothetical *Sb-sbd*-*RhoA* signaling pathway in leg discs we have characterized six mutations identified as enhancers of *zipper* (myosin II heavy chain) mutant leg defects. The enhancer of *zipper* mutants show significant interactions with *Sb-sbd* and *RhoA* mutants. Three of these genes encode known members of the *RhoA* signaling pathway suggesting that the remaining genes also encode gene products with functions related to *Sb-sbd*-*RhoA* signaling to the actin cytoskeleton. Our results provide evidence that the type II transmembrane serine proteases, a class of proteins strongly associated with human developmental abnormalities and pathology, can regulate an intracellular signaling pathway required for normal development.

INTRODUCTION

METAMORPHOSIS in *Drosophila* is a remarkable developmental process mediated by the steroid hormone 20-OH ecdysone (hereafter referred to as ecdysone; ANDRES and THUMMEL 1992; RIDDIFORD 1993; FRISTROM and FRISTROM 1993). Ecdysone regulates two distinct developmental programs during metamorphosis. In one program, most larval tissues such as the salivary glands, fat body, and gut undergo programmed cell death and histolysis. Concurrently in the second program, the precursors of adult structures -- the imaginal discs, imaginal rings, imaginal islands, and histoblast nests -- undergo dramatic morphogenetic changes. The imaginal discs, which form the adult eyes, antennae, legs, and wings, as well as the adult epidermis, develop from small clusters of epithelial cells set aside in the embryo (FRISTROM and FRISTROM 1993; COHEN 1993). During the larval period imaginal disc development is characterized by rapid cellular proliferation to form a highly-folded sac attached via a stalk to the larval epithelium. The rapid increase in ecdysone titer associated with the onset of metamorphosis triggers unfolding of the imaginal disc epithelium and dramatic changes in tissue shape. Within a few hours structures resembling the adult appendages are formed and evert to the outside of the animal. Subsequent fusion of the disc epithelia gives rise to the adult head and thoracic epidermis.

Leg imaginal discs are a particularly useful system for the study of epithelial tissue shaping and morphogenesis. Leg imaginal disc morphogenesis has been extensively characterized at a cell biological level, providing a solid foundation for further genetic and molecular analyses (CONDIC *et al.* 1991; FRISTROM and FRISTROM 1993). Distal portions of the leg, including all tarsal segments and the distal portion of the tibia, form during the 12-

hour prepupal period. Final morphogenesis of the proximal portion of the tibia and the femur occurs later during the pupal period. Prepupal leg development is characterized by elongation of the presumptive leg as the disc epithelium unfolds, and concurrent eversion to the outside of the animal, a morphogenetic process collectively referred to as evagination. The prepupal elongation of leg discs to form presumptive leg segments is of particular interest because it is primarily driven by apical cell shape changes (CONDIC *et al.* 1991). Before elongation, leg disc cells are highly anisometric. They are wide in the presumptive circumferential axis and short in the proximal-distal axis. In fully elongated legs, these cells become isometric, having decreased in width and increased in length. The number of cells encircling each segment remains unchanged. Thus, the change in cell shape from anisometric to isometric results in the elongation and narrowing of the leg segments and is a major morphogenetic force in the shaping of the adult leg.

The current model describing the mechanical forces driving cell shape changes and elongation in leg discs is based on studies in vertebrate and invertebrate epithelia (reviewed in FRISTROM and FRISTROM 1993). Cells within the epithelium of leg imaginal discs are linked via sub-apically localized adherens junctions. The cytoplasmic side of each adherens junction is connected to an actin-myosin contractile ring. In response to the rise in ecdysone titer at the onset of metamorphosis the heavy chain of non-muscle myosin II becomes activated. The head domains of activated myosin dimers bind to and slide actin filaments past each other within the contractile ring. The result is a "purse string" effect whereby contraction of the actin-myosin ring causes the apical surface of the disc cell to adopt an isometric shape. The contractile force in one cell is transmitted to neighboring cells via adherens junctions, causing all of the cells of the epithelial sheet to change shape in a concerted manner and coordinating elongation of the presumptive leg (ODELL *et al.* 1981; FRISTROM 1988).

Mutations affecting prepupal leg disc elongation have been identified in a number of genes including *Stubble-stubblloid* (*Sb-sbd*), the *Broad-Complex* (*BR-C*), *zipper* (*zip*), *RhoA*, *DRhoGEF2*, *spaghetti squash* (*sqh*), *blistered*, *dachsous*, *E74*, *crooked legs*, *vulcan* and *bancal* (see Table 1). These mutants have a characteristic malformed leg phenotype in which some or all leg segments are thicker and shorter than normal, and often twisted or kinked (Figure 1). Confocal microscopic analysis of the leg imaginal disc cells of *Sb-sbd* and *BR-C* mutants shows that these cells fail to undergo proper cell shape changes at the beginning of metamorphosis, suggesting that inability to control cell shape changes underlies the malformed leg phenotype (CONDIC *et al.* 1991; VON KALM *et al.* 1995). Thus the malformed leg phenotype has proven to be a valuable tool to genetically identify regulators of cell shape changes during leg elongation.

Genetic regulators of cell shape changes during leg elongation can be divided into two classes based on their response to ecdysone. The *Sb-sbd*, *BR-C*, *E74*, *crooked legs*, *vulcan*, and *bancal* loci are all transcriptionally induced in response to ecdysone at the onset of metamorphosis (ANDRES *et al.* 1993; APPEL *et al.* 1993; BAYER *et al.* 1996; BURTIS *et al.* 1990; D'AVINO and THUMMEL 1998; GATES and THUMMEL 2000), whereas the *zip*, *sqh*, *RhoA*, and *DRhoGEF2* loci are not induced in response to ecdysone (WARD and THUMMEL 2002; A. HAMMONDS and J. FRISTROM, pers. comm.). Thus, control of cell shape changes during prepupal leg imaginal disc elongation requires the coordinated activities of both ecdysone inducible and non-inducible proteins. Because leg morphogenesis is triggered by ecdysone, it is likely that the activities of ecdysone insensitive proteins are directed by one or more ecdysone inducible gene products at the onset of morphogenesis.

The *Sb-sbd* locus is of particular interest for understanding how leg morphogenesis is controlled because it is transcriptionally induced by ecdysone at the onset of metamorphosis. In addition, *Sb-sbd* mutations interact genetically with mutant alleles of genes known to have important roles in prepupal leg morphogenesis. These genes include the *Broad-Complex*, which encodes a family of transcriptional regulators, and *zipper*, which encodes the heavy chain of non-muscle myosin II (hereafter referred to as myosin; DIBELLO *et al.* 1991; GOTWALS and FRISTROM 1991; YOUNG *et al.* 1993). Upon induction by ecdysone, the *Sb-sbd* protein is localized to the apical surface of leg disc epithelial cells (VON KALM *et al.* 1995). The *Sb-sbd* locus encodes a typical member of an unusual family of membrane-associated serine proteases, the type II transmembrane serine proteases (TTSPs; APPEL *et al.* 1993). All TTSP family members have an intracellular N-terminus and an extracellular C-terminus that ends in a trypsin-like serine protease domain (HOOPER *et al.* 2001). To date nine members of the TTSP class of serine proteases have been described. A striking feature of these proteases is their association with changes in cellular morphology, differentiation, and physiology, as well as pathologies including viral infection, and cancer, heart, and respiratory disease. Although the TTSPs have obvious developmental and clinical significance little is known about their cellular mode of action.

Sb-sbd mutants are commonly known for their effects on bristle morphogenesis. Bristles form as apical extensions of specialized imaginal disc cells. As the bristle cell develops, actin microfilament bundles appear around the cortex of the cell in a regular arrangement of 15-18 actin bundles associated with the plasma membrane (OVERTON 1967; APPEL *et al.* 1993). The bristle grows at its tip by continuous polymerization of short actin bundles that are joined end to end with the distal tips of previously synthesized bundles (LEES and PICKEN 1944 ; TILNEY

et al. 1996). The Sb-sbd protease is essential for bristle extension. Both recessive loss-of-function (*sbd*) and dominant (*Sb*) mutations have been identified at the locus on the basis of their shortened bristle phenotype and genetic and gene structure analyses indicate that many *Sb-sbd* mutants lack protease activity (LINDSLEY and ZIMM 1992; APPEL *et al.* 1993). Interestingly, defects in the organization of the actin cytoskeleton appear to underlie the shortened bristle phenotype associated with both *Sb* and *sbd* mutations. In homozygous recessive *sbd* mutants microfilament organization in bristles is initially normal. However, the actin bundles become frayed and disorganized at their tips as the bristle develops (APPEL *et al.* 1993). In dominant *Sb* mutants the number of actin bundles is increased to 25-30 per bristle, and their arrangement is irregular with some bundles located in the core of the bristle. In either type of mutant (*Sb* or *sbd*), extension of the actin microfilaments ceases prematurely. Thus, the Sb-sbd protease appears to regulate the organization of the actin cytoskeleton during bristle extension.

The role of the Sb-sbd serine protease in leg disc morphogenesis is less well understood. Interestingly, both *Sb* and *sbd* mutations behave as recessive alleles in the context of leg morphogenesis, suggesting a fundamental difference in the function of the Sb-sbd protease in bristle versus leg development. The observation that exogenous application of trypsin to *Sb-sbd* mutant leg discs in *in vitro* culture leads to rapid elongation of the discs initially suggested that the Sb-sbd protease might function in leg disc elongation by cleaving apical extracellular matrix proteins to facilitate cell shape changes (APPEL *et al.* 1993). However, the discovery that *Sb-sbd* mutants act as genetic enhancers of leg morphogenesis defects associated with *zipper* mutations (GOTWALS and FRISTROM 1991) raises the possibility that Sb-sbd regulates actin cytoskeletal dynamics in elongating legs via by inducing contraction of the apical actin-myosin belt.

Recent evidence has shown that mutations in *Drosophila RhoA* and *DRhoGEF2* also act as genetic enhancers of *zipper* with respect to leg malformation (HALSELL *et al.* 2000). The Rho family of small GTPases regulate actin cytoskeletal dynamics in a variety of vertebrate and invertebrate systems via activation of myosin (reviewed in TAPON and HALL 1997; VAN AELST and D'SOUZA-SCHOREY 1997; HALL 1998). The observation that *Sb-sbd* is also a genetic enhancer of *zipper* leg malformation defects (GOTWALS and FRISTROM 1991) lead us to investigate the possibility that the Sb-sbd protease is involved in RhoA signaling in leg imaginal discs. We find that significant genetic interactions occur between *Sb-sbd* mutations and *RhoA* mutations and between *Sb-sbd* mutations and mutations in other RhoA signaling pathway members. We also find that a reduction in the dosage of *RhoA* suppresses the penetrance of the leg malformation phenotype associated with over-expression of the Sb-sbd protease. Our data are consistent with the possibility that the Sb-sbd protease regulates myosin activation and actin cytoskeletal dynamics via RhoA signaling during leg imaginal disc morphogenesis, perhaps acting as an ecdysone inducible trigger to control the timing of RhoA pathway activation.

In order to identify additional genes encoding products that participate in a hypothetical Sb-sbd/RhoA signaling pathway required to regulate cell shape changes in elongating leg imaginal discs, we analyzed mutations in six genes on the second chromosome that enhance *zipper* mutant leg defects. We find that mutations in these *enhancer of zipper* genes -- *en(zip)* -- show significant interactions with *Sb-sbd* and *RhoA* mutants. Three of the *en(zip)* mutations have been identified as new alleles of the *RhoA*, *DRhoGEF2*, and *zipper* loci. This strongly suggests that the remaining 3 uncharacterized genes identified in our screen encode products with roles in Sb-sbd-RhoA regulation of actin cytoskeletal dynamics during leg imaginal disc morphogenesis.

MATERIALS AND METHODS

Stocks: The genotypes of all stocks tested and the molecular nature of mutant lesions (where known) are described in Table 2.

Genetic complementation analysis: To ensure that the viability of emerging progeny classes was not distorted by environmental factors (*e.g.* overcrowding) the following crossing regimen was established empirically in preliminary experiments. In each cross 4 virgin females (1-7 days old) were mated to 3-5 males. All crosses were set up in triplicate on standard cornmeal medium. Cultures were incubated for 3 days at 25°C followed by transfer of adults to fresh medium. Subsequent cultures were incubated for 2 days at 25°C generating a total of nine cultures for each cross. The legs of all emerging F1 progeny classes were scored for malformation. F1 progeny were scored for 19 days from the date parental adults were first placed in each vial.

Second-site non-complementation (SSNC) assays were conducted by mating animals heterozygous for the mutant genes of interest. Leg malformation was scored in the doubly heterozygous F1 progeny class. Genotypes needed to test for dominant interactions were obtained by first mating animals carrying the mutant of interest, *e.g.* **/CyO*, to *CyO*, *P{sevRas1.V12}FK1/Sco*; *red sbd²⁰¹ e/TM6B*, *Tb Hu e* animals. F1 male progeny heterozygous for both mutations, *e.g.* **/CyO*, *P{sevRas1.V12}FK1*; *red sbd²⁰¹ e/+*, were mated to virgin female *sbd¹ ro e ca* homozygotes. Leg malformation was scored in the F2 progeny class heterozygous for the mutation of interest and transheterozygous for the *sbd¹/sbd²⁰¹* mutations (*i.e.* **/+; sbd¹/sbd²⁰¹*). For both SSNC and dominant interaction tests, sibling progeny classes were also scored, *e.g.* *+/+; sbd¹/sbd²⁰¹*, and the highest percentage of leg malformation observed in

any sibling class was subtracted from the percent malformation observed in progeny classes being tested for interaction.

Heat-induced induction of *hs-Stubble* transgene: 30 *Rho*⁷²⁰/*CyO* females were crossed to 20 *w*¹¹¹⁸; *hs-Stubble* males in bottles at 25°C, and turned into fresh bottles every 3 days. The progeny were picked as 0h white prepupae and transferred to food vials. They were either immediately subjected to a 1 hour heat shock by immersion in a 37°C water bath (= HS 0h AP), or allowed to develop for 3 hours at 25°C before being heat shocked (= HS 3h AP). Treated animals were allowed to continue development at 25°C. Eclosed animals were sorted into 2 progeny classes, *CyO*/+; *hs-Stubble*/+ or *Rho*⁷²⁰/+; *hs-Stubble*/+, and scored for leg malformation. The induction of *hs-Stubble* at either of these times in development affects 2nd and 3rd leg pairs differently, so the 2nd and 3rd pairs of legs of each animal were scored separately. An animal was scored as malformed if either the left or right leg of a pair was malformed.

Enhancer of zipper mutations: Mutations in six second chromosome genes that behave as enhancers of *zipper* mutant leg defects were previously identified by Dr. Jim Fristrom (U.C. Berkeley). Prior to testing these mutations for interactions with *Sb-sbd* and *RhoA* mutants they were outcrossed to Canton S flies for 3 generations to remove recessive lethal mutations linked to but independent of the *enhancers of zipper*. Outcrossed chromosomes were recovered and balanced over *SM5*, *CyO* or *CyO*, *P{sevRas1.V12}FK1*.

Mounting of adult legs: Adult flies were transferred to 80% glycerol for at least 24 hours. Legs were dissected from the preserved animals and mounted in a drop of glycerol under of coverslip sealed with nail polish. The legs were observed by brightfield microscopy using a 4x Acroplan objective on a Zeiss Axiophot MC80 microscope. Images were acquired into Adobe Photoshop 6.0 software to crop and montage using a Kodak DC290 Zoom digital camera.

Molecular lesions associated with *RhoA* and *Sb-sbd* mutant alleles used in this study:

All of the *RhoA* mutations used in these studies have been characterized at a molecular level (Table 2). *RhoA*^{E3.10} is a CAAX box missense mutation (C to Y), while *RhoA*^{J3.8} is a deletion of the 13 C-terminal amino acids, including the CAAX box (HALSELL *et al.* 2000). These mutations are likely to be loss-of-function alleles since the CAAX box motif is required for RhoA association with the plasma membrane (ZHANG and CASEY 1996; SEABRA 1998). The *RhoA*^{72F} and *RhoA*^{72O} mutations are P-element excision mutants and are also likely null mutations (STRUTT *et al.* 1997). *Df(2R)Jp8* is a small deficiency that uncovers *RhoA* but does not uncover the nearby *myosin light chain kinase* gene (HALSELL *et al.* 2000). Five of the *Sb* and *sbd* mutant alleles used in this study have also been characterized to varying degrees at a molecular level. The *Sb*^{63b} mutation is associated with a transpositional *blood element* insertion close to the junction of the extracellular stem region and the proteolytic domain (APPEL *et al.* 1993; A. HAMMONDS and J. FRISTROM, pers.comm). Sequence analysis indicates that translation would be terminated a few nucleotides into the *blood element* insertion effectively truncating the proteolytic domain from the Sb-sbd protein. The *Sb*¹ and *Sb*⁷⁰ mutations are also associated with transpositional insertions (APPEL *et al.* 1993), although the precise molecular locations of these insertions have not been determined. The *sbd*²⁰¹ mutation is associated with a histidine to arginine substitution of residue 572 in the proteolytic domain (A. HAMMONDS and J. FRISTROM, pers.comm). The affected residue is adjacent to a conserved cysteine in the substrate binding pocket. The resulting protease is likely to have defective substrate binding capabilities and/or reduced proteolytic activity. The *sbd*¹⁰⁵ mutation is associated with a large deficiency that removes the entire *Sb-sbd* locus and flanking genomic DNA (APPEL *et al.* 1993).

Finally, the *sbd*² mutation is not associated with coding region defects and is presumed to be regulatory in nature (A. HAMMONDS and J. FRISTROM, pers. comm.).

RESULTS

***RhoA* mutations show significant second-site non-complementation and dominant genetic interactions with *Sb-sbd* alleles:** Mutations in *Drosophila RhoA* exhibit second-site non-complementation (SSNC) with mutations in the heavy chain of non-muscle myosin (*zipper*), with 100% of heterozygous double mutant animals (*i.e. RhoA +/+ zip*) exhibiting a leg malformation phenotype (HALSELL *et al.* 2000). The observation that *Sb-sbd* is also a genetic enhancer of *zipper* with respect to leg malformation (GOTWALS and FRISTROM 1991) lead us to investigate the possibility that *Sb-sbd* mutations interact genetically with *RhoA* mutations in elongating leg imaginal discs. In Table 3 and subsequent tables we define interactions as strong when greater than 40% of animals have at least one malformed leg, moderate when 20-40% of animals are malformed, and weak when 5-19% malformation is observed. In almost all cases, “background” leg malformation in animals heterozygous for only one mutant allele (*e.g. Sb/+*) ranged from 0-2 %. Thus, a moderate interaction indicates that animals have malformation frequencies 10-20 times background, while a strong interaction indicates that the frequency is greater than 20-fold above background. Molecular lesions associated with *RhoA* and *Sb-sbd* mutants used in this study are described in the Materials and Methods.

Leg malformation genetic interaction data for *Sb-sbd* and *RhoA* mutant alleles are shown in Table 3. The *Sb*^{63b} and *Sb*⁷⁰ alleles interact very strongly with *RhoA* mutant alleles and the *RhoA* deficiency *Df(2R)Jp8* in SSNC assays, with the frequency of animals with leg malformation ranging from 59% to 96% (see also Figure 1). The interactions with the *RhoA*^{J3.8} and *RhoA*^{E3.10} mutations are particularly strong. In our experiments we find these particular *RhoA* alleles to be the most genetically sensitive in leg malformation assays with *Sb-sbd* mutants. Many of the *RhoA*^{+/+}; *Sb-sbd*^{+/+} double mutant animals exhibit malformation of both second and

third legs, a phenotype associated with severe malformation. In the cases where *RhoA*^{J3.8}, *RhoA*^{E3.10}, and *Df(2R)Jp8* were tested for interactions with *Sb*^{63b} and *Sb*⁷⁰ almost all animals exhibited severe malformation. In contrast, only weak SSNC interactions are observed between the *Sb*^l and *Sb*^{spike} and *RhoA* alleles. The *Sb*^l and *Sb*^{spike} alleles have also been previously reported to interact weakly in SSNC assays with the historically interactive *zipper* allele *zip*^{Ebr}, and *Broad-Complex* allele *br*^l (BEATON *et al.* 1988; GOTWALS and FRISTROM 1991).

The *sbd*^{l05} mutation exhibits moderate levels of SSNC interaction with the *RhoA*^{J3.8} and *RhoA*^{E3.10} alleles (Table 3). No interactions were observed with the *sbd*²⁰¹ allele. The *sbd*^{l05} and *sbd*²⁰¹ alleles have previously shown only weak to moderate interactions with *Broad-Complex* and *zipper* mutants in SSNC assays (BEATON *et al.*, 1988; GOTWALS and FRISTROM, 1991). Therefore we asked if *RhoA* mutants interact dominantly with *sbd* alleles. Because *sbd*^{l05} homozygotes are inviable and *sbd*²⁰¹ homozygotes have reduced viability and exhibit 100% malformation, we tested the transheterozygotes *sbd*²⁰¹/*sbd*^l and *sbd*²⁰¹/*sbd*² which exhibit malformation rates of 10% and 1% respectively. The *RhoA*^{E3.10}, *RhoA*^{J3.8}, and *Df(2R)Jp8* alleles all show very strong dominant interactions with *sbd*²⁰¹/*sbd*^l transheterozygotes. In contrast, weak to moderate interactions are observed between *sbd*²⁰¹/*sbd*² transheterozygotes and the *RhoA*^{E3.10}, *RhoA*^{J3.8}, and *Df(2R)Jp8* alleles. Therefore, in subsequent tests for dominant interactions with *sbd* alleles we used the *sbd*²⁰¹/*sbd*^l combination. Collectively, our data show that *Sb-sbd* mutations interact strongly with mutations in *RhoA* and raise the possibility that *Sb-sbd* proteolytic activity plays a role in the *RhoA* signaling pathway during leg morphogenesis.

***Sb-sbd* mutants interact with *RhoA* signaling pathway mutants.** We extended our analysis by asking if *Sb-sbd* mutations interact with mutations in other known components of the *RhoA* signaling pathway. Mutations in the gene encoding the guanine nucleotide exchange factor

DRhoGEF2 have been previously reported to affect RhoA-mediated cell shape changes during *Drosophila* gastrulation (BARRETT *et al.* 1997). These *DRhoGEF2* mutants show weak to moderate interactions in leg discs with *zip*^{Ebr} in SSNC genetic assays (HALSELL *et al.* 2000), and moderate to strong interactions with *RhoA* mutations (C. BAYER and L. VON KALM, data not shown). Three *DRhoGEF2* alleles, *DRhoGEF2*^{1.1}, *DRhoGEF2*^{4.1}, and the P-element insertion mutant *DRhoGEF2*⁰⁺²⁹¹, show mostly weak interactions with *Sb-sbd* alleles in SSNC and dominant interaction assays (Table 4). These findings initially suggested that *DRhoGEF2* might not be involved in a hypothetical *Sb-sbd*-RhoA signaling pathway in leg imaginal discs. However, we have identified a new allele of *DRhoGEF2* (see below). This new allele, *DRhoGEF2*¹¹⁻³, was tested with *Sb-sbd* alleles in SSNC and dominant interaction assays (Table 4). *DRhoGEF2*¹¹⁻³ interacts strongly with *Sb*^{63b} and *Sb*⁷⁰, and moderately in a dominant interaction assay with *sbd*²⁰¹/*sbd*¹ transheterozygotes. The apparent allele-specific nature of genetic interactions involving *DRhoGEF2* in our leg malformation assays is consistent with other reports (*e.g.* BEATON *et al.* 1988; GOTWALS and FRISTROM 1991; HALSELL and KIEHART 1998). A striking example of an allele-specific interaction is the observation that null alleles of *zipper* fail to enhance *BR-C* or *Sb-sbd* mutant leg defects in SSNC assays, whereas high percentages of animals are malformed when the *zip*^{Ebr} allele is tested in similar assays with *BR-C* or *Sb-sbd* mutants. The *zip*^{Ebr} mutation is associated with a missense alteration in the myosin ATP-binding pocket and may encode a weakly dominant negative allele of myosin with the potential to form unproductive dimers with wild-type myosin molecules (HALSELL *et al.* 2000). Consistent with the possibility of dominant negative activity we observe up to 4% leg malformation in *zip*^{Ebr}/+ animals, suggesting that *zip*^{Ebr} heterozygotes are highly sensitized to further genetic perturbations affecting the actin cytoskeleton. In contrast, the complete loss of

one copy of the *zipper* locus apparently does not reduce myosin levels sufficiently to interfere with actin cytoskeletal dynamics during leg morphogenesis. Thus, by analogy, even though although only one of the *DRhoGEF2* mutants tested interacts significantly with *Sb-sbd* alleles in our assays, the strength of the interactions between *Sb-sbd* mutants and *DRhoGEF2*¹¹⁻³ clearly implicates DRhoGEF2 function in leg imaginal disc morphogenesis.

Previous reports have indicated that the downstream RhoA effector kinase, Rho kinase, plays an important role in actin cytoskeletal dynamics in vertebrates via phosphorylation of the myosin regulatory light chain (AMANO *et al.*, 1996; BURRIDGE and CHRZANOWSKA-WODNICKA 1996; RIDLEY 1996). A recent report demonstrates that the *Drosophila* homolog of Rho kinase (Drok) is also a RhoA effector kinase in wing imaginal discs (WINTER *et al.*, 2001). In this study Drok was shown to be involved in the control of planar cell polarity in a Frizzled-mediated signaling pathway to the actin cytoskeleton via phosphorylation of the *Drosophila* myosin regulatory light chain protein, Spaghetti Squash. We therefore tested two alleles of *drok* for interactions with *Sb-sbd* mutations (Table 4). *drok*¹ and *drok*² show strong interactions with *Sb*⁷⁰, and weak to moderate interactions with *Sb*^{63b}. In contrast, both *drok* mutants show weak dominant interactions with *sbd* alleles. None-the-less, the strength of the SSNC interaction of both *drok* alleles tested with the *Sb*⁷⁰ mutation strongly indicates that Rho kinase acts as a downstream effector of RhoA in the control of cell shape changes in leg imaginal discs.

The second chromosome deficiency *Df(2R)Jp1* uncovers the cytogenetic interval 51C3-52F8/9 and therefore should delete the *myosin light chain kinase* gene located at 52D11/E1 (CHAMPAGNE *et al.* 2000; KOJIMA *et al.* 1996; TOHTONG *et al.* 1997; www.Flybase.org). In vertebrate systems the myosin light chain kinase functions in conjunction with other effector kinases such as Rho kinase to activate myosin via phosphorylation of the myosin regulatory light

chain (reviewed in TAN *et al.* 1992). We find that *Df(2R)Jp1* shows strong and moderate interactions respectively with *Sb*^{63b} and *Sb*⁷⁰ in SSNC assays, and interacts very strongly in a dominant genetic interaction test with *sbd*²⁰¹/*sbd*^l transheterozygotes (Table 4). *Df(2R)Jp1* has been previously reported to interact genetically in leg malformation assays with the *RhoA* alleles used in this study (HALSELL *et al.* 2000). If the published right breakpoint for *Df(2R)Jp1* is correct this deficiency might also uncover the *RhoA* locus recently placed in cytogenetic region 52F8-9 by deficiency mapping analysis (HALSELL *et al.* 2000). However, although lethal recessive *RhoA* mutations show SSNC interactions with *Df(2R)Jp1*, they are viable over this Deficiency in doubly heterozygous combinations. In contrast, the same *RhoA* alleles are inviable over *Df(2R)Jp8* which does uncover *RhoA*, indicating that *Df(2R)Jp1* does not uncover *RhoA*. Further evidence that *Df(2R)Jp1* uncovers a *RhoA* signaling pathway member distinct from *RhoA* comes from our observation that SSNC genetic interactions between *Sb-sbd* mutants and *Df(2R)Jp4*, a deficiency predicted to uncover both *RhoA* and *MLCK*, are stronger than those observed for *Sb-sbd* and *Df(2R)Jp1* or *Sb-sbd* and *Df(2R)Jp8* (data not shown). Thus, our observation of strong genetic interactions between *Sb-sbd* mutants and *Df(2R)Jp1* are consistent with the possibility that *Sb-sbd* mutants interact genetically with loss-of-function *MLCK* alleles and provide additional evidence that the *Sb-sbd* protease participates in *RhoA* signaling to myosin to control cell shape changes in prepupal leg imaginal discs.

We also tested mutant alleles of the myosin regulatory light chain gene, *spaghetti squash* and *Drosophila Pkn* for interactions with *Sb-sbd* alleles. We observe no interaction between *Sb-sbd* alleles and the strongly hypomorphic *sqh*^l or amorphic *sqh*² (data not shown; KARESS *et al.* 1991; EDWARDS and KEIHART 1996). However, *sqh* null alleles also fail to interact with *zipper* mutations including *zip*^{Ebr} in SSNC assays even though biochemical evidence clearly demonstrates a direct physical interaction between these proteins. Here, one dose of the wild-

type myosin regulatory light chain gene in *sqh/+; zip/+* animals produces sufficient protein to drive cell shape changes in elongating leg imaginal discs. Thus we are not surprised by the failure of strong loss-of-function *sqh* mutations to interact with *Sb-sbd* mutants. *Drosophila* Pkn binds specifically to GTP-activated RhoA and is required for epidermal cell shape changes during dorsal closure in the embryo (LU and SETTLEMAN 1999). We therefore asked if *Pkn* mutants interact with *Sb-sbd* alleles. We find that *Pkn*³ and the P-element insertion mutant *Pkn*⁰⁶⁷³⁶ fail to interact with *Sb*^{63b} or *Sb*⁷⁰ in SSNC assays and exhibit weak dominant enhancement of leg malformation with *sbd*²⁰¹/*sbd*¹ transheterozygotes (data not shown). Thus we conclude that our data do not support a major role for Pkn in *Sb-sbd-RhoA* mediated cell shape changes during leg morphogenesis.

Leg malformation associated with over-expression of *Sb-sbd* is suppressed by reducing *RhoA* gene dosage. In experiments aimed at characterizing and rescuing *Sb-sbd* mutations we generated transgenic flies carrying a full length *Sb-sbd* cDNA placed under the control of a heat-inducible promoter in the transposon pCaSpeR-hs (Thummel and Pirrotta, 1992). We have used this *hs-Sb-sbd* transgene (*hs-Stubble*) to rescue leg defects associated with homozygous *sbd*²⁰¹ mutations by inducing the transgene with a 1 hour 37° heat shock in staged 0hr or 3hr prepupae. In the course of these experiments we discovered that induction of *hs-Stubble* in wild-type 0hr or 3hr prepupae results in a high percentage of severe leg malformation in adults involving second as well as third legs. In contrast, we find that over-expression of *Sb-sbd* either 12hr before or 10hr after pupariation does not effect leg morphogenesis. Thus, the leg malformation associated with over-expression of *Sb-sbd* is highly specific to a critical period of leg development.

We took advantage of the leg defect associated with *Sb-sbd* over-expression at the beginning of the prepupal period to test the hypothesis that RhoA acts downstream of *Sb-sbd* in elongating leg discs. We asked if reducing the gene dosage of *RhoA* to one copy could suppress the leg phenotype associated with over-expression of *Sb-sbd*. We find that in *RhoA*⁷²⁰/+; *hs-Stubble*/+ animals heat-shocked as 3hr prepupae, second leg malformation is reduced 2.7-fold, from 69% to 25% (Table 5). When *RhoA*⁷²⁰/+; *hs-Stubble*/+ animals are heat-shocked as 0hr prepupae, 2nd leg malformation is reduced 2-fold, from 17% to 8%. A similar degree of suppression is also seen for third leg malformation (Table 5). Similar results to those shown in Table 5 were obtained in experiments using the *RhoA*^{E3.10} allele (data not shown). The observation that *hs-Stubble* induced leg malformation can be suppressed by reducing *RhoA* gene dosage strongly suggests that RhoA functions downstream of *Stubble* in a signaling pathway regulating myosin as cells change their shape during leg elongation.

Enhancer of zipper mutations interact genetically with *Sb-sbd* and *RhoA* mutations during leg elongation. In order to identify additional genes encoding products that participate in a hypothetical *Sb-sbd*/*RhoA* signaling pathway required to regulate cell shape changes in elongating leg imaginal discs, we analyzed mutations in six genes on the second chromosome that enhance *zipper* mutant leg defects. These mutations were originally identified by Dr. Jim Fristrom in an EMS based genetic screen (unpublished data). These mutations, referred to as *enhancers of zipper*, *en(zip)*, were outcrossed to Canton S flies for three generations to remove recessive lethal mutations linked to but independent of the enhancers. We tested the *en(zip)* mutations for interaction with *Sb-sbd* and *RhoA* mutants. Five of the six *en(zip)* mutations are homozygous lethal. The one exception is *31-6* which is semi-lethal with approximately one quarter of viable animals exhibiting leg malformation. Of the six mutants, three are alleles of

known genes. One mutant, *11-3* (described in Table 4), fails to complement *DRhoGEF2^{1.1}*, *DRhoGEF2^{4.1}*, and *DRhoGEF2⁰⁴²⁹¹*, indicating that *11-3* is a new allele of *DRhoGEF2*. Another mutant, *12-6*, fails to complement *RhoA^{J3.8}* and *RhoA^{E3.10}* mutants and *Df(2R)Jp8* which uncovers *RhoA*. Thus we conclude that *12-6* is likely to be a new *RhoA* allele. A third mutant, *33-1*, fails to complement *zipper* null mutations and *Df(2R)ES1* which uncovers *zipper*, and is therefore likely to be a new allele of *zipper*. *zip³³⁻¹* is semi-viable over *zip^{Ebr}* and these animals have severe leg malformation (see Table 6). It is possible that one or more of the non-complementation results we have observed are due to lethal SSNC interactions rather than non-complementation between two alleles of the same gene. We are therefore currently initiating rescue experiments with full length cDNAs or cosmid clones carrying genomic clones for each of the genes involved to confirm our genetic complementation data.

With the exception of the moderately interacting *31-6* mutant, the *en(zip)* alleles all show strong interactions with *zip^{Ebr}* (Table 6). The strongest interactions are seen with the *DRhoGEF2¹¹⁻³*, *RhoA¹²⁻⁶*, and *zip³³⁻¹* alleles. We find that *RhoA¹²⁻⁶* interacts very strongly with *zip^{Ebr}* with reduced viability. Similar results were reported by HALSELL *et al.* (2000) for interactions between *RhoA^{J3.8}* or *RhoA^{E3.10}* and *zip^{Ebr}*. In contrast, our *DRhoGEF2¹¹⁻³* allele is considerably more interactive with *zip^{Ebr}* than the previously reported *DRhoGEF2⁰⁴²⁹¹*, *DRhoGEF2^{1.1}*, and *DRhoGEF2^{4.1}* alleles (HALSELL *et al.* 2000). The combination *zip³³⁻¹/zip^{Ebr}* exhibits 97% malformation with greatly reduced viability. As stated above, *zip³³⁻¹* fails to complement *zip* null alleles and a deficiency that uncovers *zipper*. The six *en(zip)* alleles also interact to varying degrees with *Sb-sbd* mutants (Table 6). *DRhoGEF2¹¹⁻³* and *RhoA¹²⁻⁶* exhibit strong SSNC with *Sb^{63b}* and *Sb⁷⁰*, while the remaining *en(zip)* alleles interact moderately with at least one of these *Sb* alleles. All of the *en(zip)* alleles show moderate to strong dominant interactions with *sbd²⁰¹/sbd^l* transheterozygotes.

The *en(zip)* mutations exhibit universally strong SSNC interactions with *RhoA* alleles and *Df(2R)Jp8* (Table 6). As stated above, *RhoA*¹²⁻⁶ fails to complement the two *RhoA* alleles and deficiency tested. The strongest interactions are seen between *RhoA* mutants and *DRhoGEF2*¹¹⁻³ and *zip*³³⁻¹ which exhibit 93-100% malformation and in the case of *DRhoGEF2*¹¹⁻³ greatly reduced viability in combination with all *RhoA* alleles tested. The uncharacterized *en(zip)* alleles, 12-5, 18-5, and 31-6, also interact strongly with *RhoA* mutants. The viability of animals doubly heterozygous for 12-5 and *RhoA*^{J3.8} or *RhoA*^{E3.10} is reduced. Somewhat surprisingly the *en(zip)* mutants fail to interact with *DRhoGEF2*⁰⁴²⁹¹, *DRhoGEF2*^{1.1}, *DRhoGEF2*^{4.1}, *drok*¹, *drok*², or *Df(2R)Jp1*. There are two exceptions to these observations. First, *RhoA*¹²⁻⁶ exhibits 20% malformation with the *drok*¹ and *drok*² alleles, and 13% malformation with *Df(2R)Jp1* (data not shown). Second, *DRhoGEF2*¹¹⁻³ is lethal with all *DRhoGEF2* alleles tested, and exhibits 17% malformation with *Df(2R)Jp1* (data not shown). As positive controls we tested all *DRhoGEF2* and *drok* alleles for interaction with *RhoA* and *zipper* alleles. The *DRhoGEF2*⁰⁴²⁹¹, *DRhoGEF2*^{1.1}, and *DRhoGEF2*^{4.1} alleles exhibit moderate to strong interactions ranging from 21-64% malformation with *RhoA*^{J3.8}, *RhoA*^{E3.10}, and *zip*^{Ebr} in SSNC assays (data not shown and HALSELL et al. 2000). The *drok* mutants also exhibit moderate to strong interactions with *RhoA*^{J3.8}, *RhoA*^{E3.10}, and *zip*^{Ebr} in SSNC assays (48-68% malformation for *drok*¹ and 19-38% malformation for *drok*²).

We have tested the three uncharacterized *en(zip)* mutants (12-5, 18-5, and 31-6) for non-complementation with mutations in second chromosome genes thought to have a role in RhoA signaling, and with genes reported to exhibit the malformed leg phenotype in the mutant condition. Genes tested include *Drosophila Pkn* (LU and SETTLEMAN, 1999), *blistered* (GOTWALS and FRISTROM, 1991), *vulcan* and *bancal* (GATES and THUMMEL, 2000), and *crol* (D'AVINO and THUMMEL, 1998). Other mutants tested include *Df(2R)Jp1* which

putatively uncovers the myosin light chain kinase gene, *concertina* which has been proposed to act as an upstream regulator of RhoA signaling leading to cell shape changes during *Drosophila* gastrulation (BARRETT *et al.* 1997), and the protein 4.1 family members *coracle*, *inscuteable*, and *expanded* (FEHON *et al.* 1994; BOEDIGHEIMER and LAUGHON 1993; KRAUT and CAMPOS-ORTEGA, 1996). The 12-5, 18-5, and 31-6 alleles are fully viable over all of these mutations and exhibit wild-type leg morphology.

The *en(zip)* mutants interact with each other but not with the *br^l* allele of the *Broad-Complex*: We also asked if the *en(zip)* alleles interact with each other in SSNC assays. As seen in Table 7 there are significant genetic interactions between *en(zip)* alleles in these assays. Of particular interest are the uncharacterized 12-5, 18-5, and 31-6 mutants. The 12-5 mutant exhibits moderate to strong interactions with all *en(zip)* mutants tested. A very strong interaction is observed with 18-5. In addition to severe malformation, 12-5 *+/+* 18-5 animals have reduced viability. A significant interaction (35% malformation) is also observed between the 18-5 and 31-6 mutants. With the exception of *DRhoGEF2¹¹⁻³*, the semi-viable 31-6 mutant interacts at moderate to strong levels with all *en(zip)* mutants tested. In addition, approximately one quarter of 31-6 homozygotes have malformed legs, an observation fully consistent with a role for the 31-6 gene product in leg morphogenesis.

Finally we asked if the *br^l* allele of the *Broad-Complex* (*BR-C*) interacts with RhoA pathway members and the *en(zip)* mutants. The *br^l* mutant is highly interactive in leg malformation assays and has previously been shown to interact strongly with *Sb-sbd* and *zipper* mutations (BEATON *et al.* 1988; GOTWALS and FRISTROM 1991). The *br^l* allele also exhibits temperature sensitivity with typically greater penetrance of leg malformation observed at 18° as compared to 25° (BEATON *et al.* 1988). The *br* genetic function of the *BR-C* is

essential for prepupal leg development. Animals carrying amorphic mutations that affect this *BR-C* function completely fail to elongate and evert their leg imaginal discs (KISS et al. 1988; BAYER et al. 1996). At a molecular level the *br* genetic function is strongly associated with the Z2 zinc-finger transcription factor product of the *BR-C* (DIBELLO et al. 1991; BAYER et al. 1997). To date little is understood of the role played by this critical regulator of imaginal disc morphogenesis. We find that *RhoA* mutants interact dominantly with *br^l* mutants at both 18° and 25° with stronger interactions observed at 18° (Table 8). Weak to moderate interactions are also observed between *br^l* and *Df(2R)Jp1*. However, the *br^l* allele fails to show significant interactions with *DRhoGEF2*, *drok*, *Df(2R)Jp1*, or the *en(zip)* mutants, including *zip³³⁻¹*.

DISCUSSION

The *Drosophila Sb-sbd* locus is required for normal cell shape changes in prepupal elongating leg imaginal discs (CONDIC *et al.* 1991; VON KALM *et al.* 1995). Genetic interactions between *Sb-sbd* and the *Drosophila* gene encoding non-muscle myosin II (*zipper*) suggest a role for the *Sb-sbd* protease in regulating contractility of the apical actin-myosin belt found in imaginal disc epithelia (GOTWALS and FRISTROM 1991). *Zipper* mutations also interact genetically with mutations in the small GTPase *RhoA* indicating that phosphorylation of the myosin regulatory light chain (*Sqh*) is a necessary pre-requisite to myosin activation in developing leg imaginal discs (HALSELL *et al.* 2000). In order to learn more about the relationships between the molecules encoded by the *Sb-sbd*, *zipper* and *RhoA* loci we asked if *Sb-sbd* and *RhoA* mutations interact genetically during prepupal leg development. We observe very strong SSNC and dominant interactions between mutant alleles of these genes. In addition, we find that *Sb-sbd* alleles show significant interactions with members of the *RhoA* signaling pathway including a new allele of *DRhoGEF2*, *Rho kinase*, and a deficiency, *Df(2R)Jp1*, that uncovers the gene encoding the myosin light chain kinase. In addition, we have shown that leg malformation associated with over-expression of *Sb-sbd* during leg elongation is suppressed by reducing the gene dosage of *RhoA*. Taken as a whole these data strongly implicate *Sb-sbd* in *RhoA* signaling and suggest that *Sb-sbd* acts upstream of *RhoA* to regulate cell shape changes in elongating leg discs.

Previous studies have clearly established a connection between signaling by the small GTPase *RhoA* and regulation of actin cytoskeletal dynamics (reviewed in HALL 1998). Evidence from both vertebrate and invertebrate systems indicate that *RhoA* signaling serves to activate non-muscle myosin and thereby control the assembly and contractility of actomyosin-

based structures (NUSRAT et al. 1995; BROCK et al. 1996; BARRETT et al. 1997; KOZMA et al. 1997; HALL 1998; HALSELL et al. 2000; WINTER et al. 2001). Although several of the molecules that act downstream of RhoA as it signals to myosin have been characterized, little is known of membrane associated events leading to activation of the RhoA signaling pathway. Our studies with the membrane associated *Sb-sbd* protease raise the possibility that proteolytic events on the apical membrane are required to trigger RhoA signaling in elongating prepupal leg imaginal discs.

Based on the strength of the SSNC interactions we have observed between *Sb-sbd* and *RhoA* mutants, and *Sb-sbd* and *RhoA* pathway members we favor a linear signaling pathway from *Sb-sbd* to RhoA as a likely explanation of our data. We propose a model in which ecdysone-mediated induction of the *Sb-sbd* locus is required to activate the RhoA signaling pathway in late larval leg discs (Figure 2). Following induction by ecdysone the *Sb-sbd* zymogen is secreted to the apical surface of leg disc cells. At the cell surface *Sb-sbd* is activated, possibly by auto-proteolytic cleavage (APPEL *et al.* 1993), and signals to DRhoGEF2 via an unknown mechanism. Signaling to DRhoGEF2 could involve cleavage of another extracellular protein (pathway 1 in Figure 2), or signaling via the Stubble cytoplasmic domain (pathway 2 in Figure 2). RhoA is then cycled into the active GTP-bound form via interaction with DRhoGEF2 leading to downstream effector kinase signaling, myosin assembly, and changes in actin dynamics. Genetic interactions between *Sb-sbd* and members of the *RhoA* pathway can be interpreted in ways other than a linear signaling pathway. For example, *Sb-sbd* and RhoA might act in parallel pathways. These pathways might converge to activate myosin, or regulate different components of the contractile apparatus. Alternatively, the *Sb-sbd* protease may facilitate cell shape changes via cleavage of apical extracellular matrix while RhoA signals to activate myosin. We have also

considered the possibility that *Sb-sbd* could be a transcriptional target of RhoA signaling in leg imaginal discs. This latter possibility seems unlikely in view of the fact that *Sb-sbd* is rapidly induced in response to ecdysone (APPEL et al. 1993), and to date no ecdysone responsive member of the RhoA signaling pathway has been identified (WARD AND THUMMEL 2002; see below.). Ultimately, molecular genetic and biochemical approaches will be required to resolve the mechanism underlying the genetic interactions between Sb-Sbd and the RhoA signaling pathway.

Our initial experiments to investigate the mechanism underlying the genetic interactions between Sb-Sbd and the RhoA signaling pathway do not support a role for the Sb-sbd 58 amino acid cytoplasmic domain in signaling. We have constructed transgenic animals expressing the cytoplasmic domain with or without its associated transmembrane region under heat-inducible control. We hypothesized that over-expression of the cytoplasmic domain might result in a dominant negative effect on leg development by sequestration of a gene product critical for RhoA signaling if the cytoplasmic domain is required for intracellular signaling events. However, over-expression of cytoplasmic domain with or without the transmembrane region in white prepupae and 3 hour prepupae has no discernable effect on leg development and these animals are fully viable. Thus, if a linear signaling model is correct, Sb-sbd proteolytic activity on the apical surface of elongating leg disc cells is a more likely mechanism to trigger RhoA signaling.

In addition to *Sb-sbd* the ecdysone-inducible *Broad-Complex* (*BR-C*) and *E74* genes are good candidates to regulate RhoA signaling in leg imaginal discs. The *BR-C* and *E74* are both active in leg imaginal discs during early prepupal development. Amorphic mutations in the *br* genetic function of the *BR-C* completely block leg development (KISS et al. 1988). The *br*

genetic function encodes the Z2 zinc-finger transcription factor product of the *BR-C* and Z2 is essential for normal leg development (DIBELLO *et al.* 1991; BAYER *et al.* 1997). *In vitro* and *in vivo* analyses show that Z2 RNA and protein are strongly induced by ecdysone in imaginal discs at the onset of metamorphosis (EMERY *et al.* 1994; BAYER *et al.* 1996). A small percentage of animals carrying mutations specific to the E74A and E74B isoforms develop far enough into pupal development to permit assessment of leg morphology (FLETCHER *et al.* 1995). Those animals that do reach the later stages of the pupal period exhibit malformed legs. However, the *BR-C* and *E74* loci both encode families of transcription factors (BURTIS *et al.* 1990; DIBELLO *et al.* 1991). Thus, if *BR-C* or *E74* gene products are required to initiate RhoA signaling it is very likely that one or more components of the RhoA signaling pathway will be transcriptionally induced by *BR-C* or *E74* gene products. The RhoA pathway genes targeted by *BR-C* or *E74* transcription factors should therefore behave as ecdysone responsive genes. However, to date none of the genes encoding RhoA signaling pathway members have been shown to be ecdysone responsive at a transcriptional level. Genes tested for ecdysone responsiveness include *RhoA*, *DRhoGEF2*, *drok*, *RhoGAPs*, *guanine nucleotide dissociation inhibitors (GDIs)*, and *zipper* (WARD AND THUMMEL 2002; C. BAYER and J. FRISTROM, unpublished data). Until a *BR-C* or *E74*-dependent ecdysone inducible gene is identified, other ecdysone responsive genes, such as *Sb-sbd*, that do not encode transcription factors are more probable candidates to initiate RhoA signaling.

We have identified three potentially novel genes likely to have important roles in a hypothetical *Sb-sbd*-RhoA signaling pathway. These genes, *12-5*, *18-5*, and *31-6*, were originally identified as EMS mutations on the second chromosome that behaved genetically as enhancers of *zipper* mutant leg defects (J. FRISTROM, pers. comm.). All three mutant genes also show

significant interactions with *Sb-sbd* and *RhoA* mutations. However, the *12-5*, *18-5*, and *31-6*, mutants fail to interact with several *DRhoGEF2* alleles tested, *drok*¹, *drok*², or *Df(2R)Jp1*. In addition *31-6* does not interact with the new *DRhoGEF*¹¹⁻³ allele described in this study (*12-5* and *18-5* show moderate and weak interactions respectively with *DRhoGEF*¹¹⁻³; Table 7). Because we have only one allele of each of the uncharacterized *en(zip)* mutations the lack of interactions with members of the RhoA signaling pathway may be attributable to the specific nature of the mutations in each of these genes. The fact that known components of the RhoA signaling pathway (*RhoGEF2*¹¹⁻³; *RhoA*¹²⁻⁶, and *zip*³³⁻¹) were also isolated in the original enhancer of zipper screen gives us confidence that molecular characterization of the protein products encoded by the *12-5*, *18-5*, and *31-6* genes will provide new insights into *Sb-sbd*-RhoA signaling in leg imaginal discs..

The role of the *BR-C* in prepupal leg development remains unclear. *BR-C* mutants interact genetically with both *Sb-sbd* and *zipper* mutations during leg development (BEATON *et al.* 1988; GOTWALS AND FRISTROM, 1991). In addition, the *br*¹ allele of the *BR-C* interacts with mutations in *RhoA* and *Df(2R)Jp1* (Table 8; see also WARD AND THUMMEL 2002). However, the *br*¹ allele does not interact with *DRhoGEF2*, *drok*, or *en(zip)* mutations. Clearly the *BR-C* has a critical role in leg morphogenesis (see above). Characterization of genes identified in a recent large genetic screen for enhancers of *br*¹ leg malformation (WARD AND THUMMEL 2002) will likely shed light on the role of this important master regulator of metamorphosis in prepupal leg development.

The *Sb-sbd* protease has been strongly implicated in the regulation of the actin cytoskeleton during bristle development (see Introduction). However, three observations indicate that interactions between *Sb-sbd* and the actin cytoskeleton proceed via different mechanisms in bristles and leg imaginal discs. First, all *Sb-sbd* mutants behave as recessive alleles during leg

development. In contrast *Sb* alleles behave as dominant mutations during bristle development. Second, The genetic interactions between *Sb-sbd*, the *BR-C*, *zipper*, and *RhoA* described here and elsewhere (BEATON *et al.* 1988; GOTWALS AND FRISTROM 1991; HALSELL *et al.* 2000) are observed only in legs. Animals exhibiting SSNC for mutant alleles of these genes have wild-type bristles. These differences in *Sb-sbd* function during leg disc and bristle development are not surprising given that there is no cell biological evidence for any form of actin-myosin contractile apparatus in bristles. Our data also indicate that RhoA signaling plays no role in actin dynamics during bristle development. Third, the *Sb*^{63b} mutation interacts genetically with mutations in two other genes required for bristle morphogenesis, *singed* (*sn*) and *forked* (*f*). *singed* and *forked* encode actin bundling proteins related to echinoderm fascin and mammalian espin, respectively (BRYAN *et al.* 1993; CANT *et al.* 1994; PETERSON *et al.* 1994; TILNEY *et al.* 1995; BARTLES *et al.* 1996). Compared to *sn*, *f*, or *Sb-sbd* mutants, *sn*; *Sb-sbd* and *f*; *Sb-sbd* double mutants have extremely reduced bristles that appear as small nubs barely extending beyond the exoskeleton. However, the *sn*; *Sb-sbd* or *f*; *Sb-sbd* double mutant combinations do not exhibit any increase in the frequency of malformed legs above that found in *Sb-sbd* mutants (L. von Kalm, unpublished data). These data suggest that actin bundling proteins other than *sn* or *f* are expressed in developing legs.

Finally, our data suggest that type II transmembrane serine proteases (TTSPs) have the potential to activate intracellular signaling pathways during development. Vertebrate members of the TTSP family have been linked to developmental abnormalities and a variety of pathologies. The human TTSP Hepsin controls hepatocyte morphology and growth (TORRES-ROSADO *et al.* 1993). Over-expression of this protease is linked to ovarian, kidney, and prostate cancer (TANIMOTO *et al.* 1997; ZACHARSKI *et al.* 1998; LUO *et al.* 2001; MAGEE *et al.* 2001; DHANASEKARAN *et al.* 2001). MAGEE *et al.* (2001) reported that *hepsin* RNA over-

expression correlates with neoplastic transformation in the prostate, and that *hepsin* is expressed specifically in the transformed epithelial cells rather than the adjacent stroma. DHANASEKARAN *et al.* (2001) extended these findings to a study of the Hepsin protein and concluded that expression of Hepsin in prostate cancer correlates inversely with measures of patient prognosis. At least three other TTSPs, MT-SP1, TMPRSS2, and TMPRSS4 are associated with malignancy (TAKEUCHI *et al.* 1999; LIN *et al.* 1999; WALLRAPP *et al.* 2000). For example, TMPRSS4 is strongly over-expressed in pancreatic cancer when compared to normal pancreatic tissue (WALLRAPP *et al.* 2000). In this study the level of TMPRSS4 expression was shown to correlate with the metastatic potential of SUIT-2 pancreatic cancer cell lines. Human HAT, which is expressed in the lung, is potentially associated with chronic airway diseases (YAMAOKA *et al.* 1998), while the influenza virus surface protein neuraminidase is essential for viral infection (JONES *et al.* 1985). *Corin*, a candidate for the human *TAPVR* gene associated with congenital heart defects, is highly expressed in the region of the mouse embryonic heart where outflow tracts form and has been hypothesized to play a role in cellular differentiation in the early stages of human and mouse heart development (YAN *et al.*, 1999). Recent evidence suggests that Corin also plays a role in the regulation of blood pressure via activation of the cardiac hormone pro-atrial natriuretic peptide (YAN *et al.* 2000; WU *et al.* 2002).

In addition to Sb-sbd two other members of the TTSP family may be involved in “outside-in” signaling events, suggesting that these proteases are anchored in the membrane for this purpose rather than for cleavage of extracellular matrix. Enteropeptidase and MT-SP1 activities are potentially linked to intracellular signaling via activation of the proteolytically-activated G protein-coupled receptor PAR2 (KONG *et al.* 1997; TAKEUCHI *et al.* 2000; HOOPER *et al.* 2001). These observations raise the possibility that other members of the TTSP

family participate in signal transduction events and that aberrant intracellular signaling may underlie their association with pathology and developmental abnormalities. The enteropeptidase, MT-SP1, and Sb-sbd proteases all have extracellular domains in addition to the proteolytic domain that could potentially be involved in protein-protein interactions required to interact with cleavage targets (HOOPER *et al.* 2001). The Sb-sbd TTSP has an extracellular disulfide knotted domain (APPEL *et al.* 1993) and *in vitro* studies indicate that this domain is capable of mediating protein-protein interactions (KELLENBERGER *et al.* 1995). *In vivo* mutational analysis of the knotted domain in the *Drosophila* snake serine protease which is secreted into the perivitelline space of early embryos clearly demonstrates that it is essential for normal function of the snake protease (SMITH *et al.* 1992; 1994).

In future studies the Sb-sbd protease will provide an excellent model system in which to elaborate the molecular mechanisms underlying the developmental and pathological phenotypes associated with aberrant expression of type II transmembrane serine proteases.

ACKNOWLEDGMENTS

We thank Ann Hammonds, Jim Fristrom, Rob Ward, and Carl Thummel for communicating results prior to publication. We are grateful to Greg Winter and Liquin Luo for providing us with *drok* mutants prior to publication, Ann Hammonds for flies carrying *hs-Stubble*, and the Bloomington Stock Center for numerous fly stocks. We are indebted to David Kuhn and Jim Fristrom for critical reading of the manuscript. This work was supported by grants from the Department of the Army Prostate Cancer Research Program (DAMD17-98-1-8590) and the Florida Hospital Gala Endowed Program for Oncologic Research to LvK.

LITERATURE CITED

- Amano M., Ito M., Kimura K., Fukata Y., Chihara K., Nakano T., Matsuura Y., Kaibuchi K. (1996) Phosphorylation and activation of myosin by Rho-associated kinase (Rho-kinase). *J. Biol. Chem.* 271: 20246-20249.
- Andres A.J., Thummel, C.S. (1992) Hormones, puffs and flies: the molecular control of metamorphosis by ecdysone. *Trends Genet.* 8, 132-138.
- Andres A.J, Fletcher J.C, Karim F.D, Thummel C.S. (1993) Molecular analysis of the initiation of insect metamorphosis: a comparative study of *Drosophila* ecdysteroid-regulated transcription. *Dev Biol.* 160: 388-404.
- Appel L.F., Prout, M., Abu-Shumays, R., Hammonds, A., Garbe, J.C., Fristrom, D. and Fristrom, J. (1993) The *Drosophila* Stubble-stubblod gene encodes an apparent transmembrane serine protease required for epithelial morphogenesis. *Proc. Natl. Acad. Sci.* 90: 4937-4941.
- Barrett K, Leptin M, Settleman J. (1997) The Rho GTPase and a putative RhoGEF mediate a signaling pathway for the cell shape changes in *Drosophila* gastrulation. *Cell* 91, 905-915.
- Bartles J.R., Wierda, A., Zheng, L. (1996) Identification and characterization of espin, an actin-binding protein localized to the F-actin-rich junctional plaques of Sertoli cell ectoplasmic specializations. *J. Cell Sci.* 109: 1229-1239.
- Bayer C.A, Holley B., Fristrom J.W. (1996) A switch in broad-complex zinc-finger isoform expression is regulated posttranscriptionally during the metamorphosis of *Drosophila* imaginal discs. *Dev Biol.* 177: 1-14.
- Bayer C.A., von Kalm, L. and Fristrom, J.W. (1997) Relationships between protein isoforms and genetic functions demonstrate functional redundancy at the Broad-Complex during *Drosophila* metamorphosis. *Dev. Biol.* 187, 267-282.

- Beaton A.H., Kiss, I., Fristrom, D. and Fristrom, J.W. (1988) Interaction of the Stubble-stubblod Locus and the Broad-Complex of *Drosophila melanogaster*. *Genetics* 120, 453-464.
- Boedigheimer M., Laughon A. (1993) Expanded: a gene involved in the control of cell proliferation in imaginal discs. *Development*. 118, 1291-1301.
- Brock J., Midwinter K., Lewis J., Martin P. (1996) Healing of incisional wounds in the embryonic chick wing bud: characterization of the actin purse-string and demonstration of a requirement for Rho activation. *J. Cell Biol.* 135: 1097-1107.
- Bryan, J., Edwards, R., Matsudaira, P., Otto, J., Wulfschlegel, J. (1993) Fascin, an echinoid actin-bundling protein, is a homolog of the *Drosophila singed* gene product. *Proc. Natl. Acad. Sci. USA* 90: 9115-9119.
- Burridge K., Chrzanowska-Wodnicka M.. (1996) Focal adhesions, contractility, and signaling. *Ann. Rev. Cell Dev. Biol.* 12: 463-518.
- Burtis K.C, Thummel C.S, Jones C.W, Karim F.D, Hogness D.S. (1990) The *Drosophila* 74EF early puff contains E74, a complex ecdysone-inducible gene that encodes two ets-related proteins. *Cell*. 61: 85-99.
- Cant, K., Knowles, B. A., Mooseker, M.S., Cooley, L. (1994) *Drosophila* singed, a fascin homolog, is required for actin bundle formation during oogenesis and bristle extension. *J. Cell Biol.* 125: 369-380.
- Champagne M.B, Edwards K.A, Erickson H.P, Kiehart D.P. (2000) *Drosophila* stretchin-MLCK is a novel member of the Titin/Myosin light chain kinase family. *J. Mol. Biol.* 300:759-777.
- Clark H.F., Brentrup D., Schneitz K., Bieber A., Goodman C., Noll M. (1995) Dachsous encodes a member of the cadherin superfamily that controls imaginal disc morphogenesis in *Drosophila*. *Genes Dev.* 9:1530-1542.

Cohen S.M. (1993) Imaginal Disc Development. In "The Development of *Drosophila melanogaster*" (Ed. M. Bate and A. Martinez Arias), pp. 747-841. Cold Spring Harbor Laboratory Press, Plainview, NY.

Condic M.L., Fristrom, D. and Fristrom, J.W. (1991) Apical cell shape changes during *Drosophila* imaginal leg disc elongation: a novel morphogenetic mechanism. *Development* 111, 23-33.

D'Avino P.P. and Thummel C. S. (1998) crooked legs encodes a family of zinc finger proteins required for leg morphogenesis and ecdysone-regulated gene expression during *Drosophila* metamorphosis. *Development*. 125: 1733-1745.

Dhanasekaran S.M., Barrette T.R., Ghosh D., Shah R., Varambally S., Kurachi K., Pienta K.J., Rubin M.A., Chinnaiyan A.M. (2001) Delineation of prognostic biomarkers in prostate cancer. *Nature* 412:822-826.

DiBello P.R, Withers D.A, Bayer C.A, Fristrom J.W, Guild G.M. (1991) The *Drosophila* Broad-Complex encodes a family of related proteins containing zinc fingers. *Genetics* 129: 385-397.

Dobzhansky T. (1930) The manifold effects of the genes stubble and stubbloid in *Drosophila melanogaster*. *Z. indukt. Abstamm.- u. VererbLehre* 54: 427-457.

Edwards K.A., Kiehart D.P. (1996) *Drosophila* nonmuscle myosin II has multiple essential roles in imaginal disc and egg chamber morphogenesis. *Development*. 122: 1499-1511.

Emery I.F., Bedian V., Guild G.M. (1994) Differential expression of Broad-Complex transcription factors may forecast tissue-specific developmental fates during *Drosophila* metamorphosis. *Development*. 120:3275-3287.

Fehon R.G., Dawson I.A., Artavanis-Tsakonas S. (1994) A *Drosophila* homologue of membrane-skeleton protein 4.1 is associated with septate junctions and is encoded by the coracle gene. *Development*. 120, 545-557.

Fletcher J.C., Burtis K.C., Hogness D.S., Thummel C.S. (1995) The *Drosophila* E74 gene is required for metamorphosis and plays a role in the polytene chromosome puffing response to ecdysone. *Development*. 121: 1455-1465.

Fristrom D. (1988) The cellular basis of epithelial morphogenesis. A review. *Tissue Cell* 20: 645-690.

Fristrom D. and Fristrom, J.W. (1993) The Metamorphic Development of the Adult Epidermis. In "The Development of *Drosophila melanogaster*" (Ed. M. Bate and A. Martinez Arias), pp. 843-897. Cold Spring Harbor Laboratory Press, Plainview, NY.

Gates J., and Thummel C.S. (2000) An enhancer trap screen for ecdysone-inducible genes required for *Drosophila* adult leg morphogenesis. *Genetics*. 2000 Dec;156(4):1765-1776.

Gotwals P.J. and Fristrom, J.W. (1991) Three neighboring genes interact with the Broad-Complex and the Stubble-stubblويد locus to affect imaginal disc morphogenesis in *Drosophila*. *Genetics* 127, 747-759.

Hall A. (1998) Rho GTPases and the actin cytoskeleton. *Science* 279, 509-514.

Halsell SR, Kiehart DP. (1998) Second-site noncomplementation identifies genomic regions required for *Drosophila* nonmuscle myosin function during morphogenesis. *Genetics* 198 148, 1845-1863.

Halsell S.R., Benjamin I.C. and D.P. Kiehart (2000) Genetic analysis demonstrates a direct link between rho signaling and nonmuscle myosin function during *Drosophila* morphogenesis. *Genetics* 155: 1253-1265.

Hooper J.D., Clements J.A., Quigley J.P., Antalis T.M. (2001) Type II transmembrane serine proteases. Insights into an emerging class of cell surface proteolytic enzymes. *J. Biol. Chem.* 276:857-860.

Jones LV, Compans RW, Davis AR, Bos TJ, Nayak DP. (1985) Surface expression of influenza virus neuraminidase, an amino-terminally anchored viral membrane glycoprotein, in polarized epithelial cells. *Mol Cell Biol* 5, 2181-2189.

Karess R.E., Chang X.J., Edwards K.A., Kulkarni S., Aguilera I., Kiehart D.P. (1991) The regulatory light chain of nonmuscle myosin is encoded by spaghetti-squash, a gene required for cytokinesis in *Drosophila*. *Cell*. 65: 1177-1189.

Kellenberger C, Hietter H, Luu B. (1995) Regioselective formation of the three disulfide bonds of a 35-residue insect peptide. *Pept. Res.* 8, 321-327.

Kiss I., Beaton, A.H., Tardiff, J., Fristrom, D. and Fristrom, J.W. (1988) Interactions and developmental effects of mutations in the Broad-Complex of *Drosophila melanogaster*. *Genetics* 118, 247-259.

Kojima S., Mishima M., Mabuchi I., Hotta Y. (1996) A single *Drosophila melanogaster* myosin light chain kinase gene produces multiple isoforms whose activities are differently regulated. *Genes Cells*. 1: 855-871.

Kong W., McConalogue K., Khitin L.M., Hollenberg M.D., Payan D.G., Bohm S.K., Bunnett N.W. (1997)

Luminal trypsin may regulate enterocytes through proteinase-activated receptor 2.

Proc. Natl. Acad. Sci. U. S. A. 94: 8884-8889.

Konev A., Varentsova E.R, Khromykh IuM. (1994) Cytogenetic analysis of the chromosome region containing the *Drosophila* radiosensitivity gene. II. The vitally important loci of the 44F-45C region of chromosome 2. *Genetika*. 30:201-211.

- Kozma R., Sarner S., Ahmed S., Lim L. (1997) Rho family GTPases and neuronal growth cone remodelling: relationship between increased complexity induced by Cdc42Hs, Rac1, and acetylcholine and collapse induced by RhoA and lysophosphatidic acid. *Mol. Cell. Biol.* 17:1201-211.
- Kraut R., Campos-Ortega J.A. (1996) *inscuteable*, a neural precursor gene of *Drosophila*, encodes a candidate for a cytoskeleton adaptor protein. *Dev. Biol.* 174, 65-81.
- Lees A.D. and Picken, L.E.R. (1944) Shape in relation to fine structure in the bristles of *Drosophila melanogaster*. *Proc. Roy. Soc. Lond. Ser. B Biol. Sci.* 132, 396-423.
- Lin B., Ferguson C., White J.T., Wang S., Vessella R., True L.D., Hood L., Nelson P.S. (1999b) Prostate-localized and androgen-regulated expression of the membrane-bound serine protease TMPRSS2. *Cancer Res.* 59:4180-4184.
- Lindsley D.L. and Zimm, G.G., (1992) The genome of *Drosophila melanogaster*. Academic Press, San Diego.
- Lu Y., Settleman J. (1999) The *Drosophila* Pkn protein kinase is a Rho/Rac effector target required for dorsal closure during embryogenesis. *Genes Dev.* 13:1168-1180.
- Luo J., Duggan D.J., Chen Y., Sauvageot J., Ewing C.M., Bittner M.L., Trent J.M., Isacs W.B. (2001) Human prostate cancer and benign prostatic hyperplasia: Molecular dissection by gene expression profiling. *Cancer Res.* 61: 4683-4688.
- Magee J.A., Araki T., Patil S., Ehrig T., True L., Humphrey P.A., Catalona W.J., Watson M.A., Milbrandt J. (2001) Expression profiling reveals hepsin overexpression in prostate cancer. *Cancer Res.* 61:5692-5696.
- Morgan T.H. C., Bridges C., Sturtevant A.H. (1925) The Genetics of *Drosophila*. *Bibliogr. Genet.* 2: 145

- Nusrat A., Giry M., Turner J.R., Colgan S.P., Parkos C.A., Carnes D., Lemichez E., Boquet P., Madara J.L. (1995) Rho protein regulates tight junctions and perijunctional actin organization in polarized epithelia. *Proc. Natl. Acad. Sci. U S A.* 92:10629-10633.
- Odell GM, Oster G, Alberch P, Burnside B. (1981) The mechanical basis of morphogenesis. I. Epithelial folding and invagination. *Dev. Biol.* 85:446-462.
- Overton J. (1967) The fine structure of developing bristles in wild type and mutant *Drosophila melanogaster*. *J. Morphol.* 122, 367-380.
- Peterson N.S., Lankenau D.H., Mitchell, H.K., Young, P., Corces, V.G. (1994) forked proteins are components of fiber bundles present in developing bristles of *Drosophila melanogaster*. *Genetics* 136: 173-182.
- Riddiford L.M. (1993) Hormones and *Drosophila* Development. In "The Development of *Drosophila melanogaster*" (Ed. M. Bate and A. Martinez Arias), pp. 899-939. Cold Spring Harbor Laboratory Press, Plainview, NY.
- Ridley A.J. (1996) Rho: theme and variations. *Curr Biol.* 6: 1256-1264.
- Saxton, W.M., Hicks, J., Goldstein, L.S.B., Raff, E.C. (1991) Kinesin heavy chain is essential for viability and neuromuscular functions in *Drosophila*, but mutants show no defects in mitosis. *Cell* 64: 1093-1102
- Seabra M.C. (1998) Membrane association and targeting of prenylated Ras-like GTPases. *Cell Signal.* 10: 167-172.
- Smith C. and DeLotto, R. (1992) A common domain within the proenzyme regions of the *Drosophila* snake and easter proteins and *Tachypleus* proclotting enzyme defines a new subfamily of serine proteases. *Protein Science* 1, 1225-1226.

- Smith C., Giordano, H. and DeLotto, R. (1994) Mutational analysis of the *Drosophila* snake protease: an essential role for domains within the proenzyme polypeptide chain. *Genetics* 136, 1355-1365.
- Strutt D.I., Weber U., Mlodzik M.T. (1997) The role of RhoA in tissue polarity and Frizzled signalling. *Nature* 387:292-295.
- Takeuchi T., Harris J.L., Huang W., Yan K.W., Coughlin S.R., Craik C.S. (2000) Cellular localization of membrane-type serine protease 1 and identification of protease-activated receptor-2 and single-chain urokinase-type plasminogen activator as substrates. *J. Biol. Chem.* 275: 26333-26342.
- Tan J.L., Ravid S., Spudich J.A. (1992) Control of nonmuscle myosins by phosphorylation. *Ann. Rev. Biochem.* 61:721-759.
- Tanimoto H. Yan Y. Clarke J. Korourian S. Shigemasa K. Parmley TH. Parham GP. O'Brien TJ. (1997) Hepsin, a cell surface serine protease identified in hepatoma cells, is overexpressed in ovarian cancer. *Cancer Research.* 57:2884-2887.
- Tapon N. and Hall, A. (1997) Rho, Rac and Cdc42 GTPases regulate the organization of the actin cytoskeleton. *Curr. Op. Cell Biol.* 9, 86-92.
- Thummel C.S. and Pirrotta, V. (1992) New pCaSpeR P element vectors. *Dros. Inf. Serv.* 71, 150.
- Tilney L.G., Tilney M.S., Guild, G.M. (1995) F actin bundles in *Drosophila* bristles I. Two filament cross-links are involved in bundling. *J. Cell. Biol.* 130: 629-638.
- Tilney, L.G., Connelly, P., Smith, S. and Guild, G.M. (1996) F-actin bundles in *Drosophila* bristles are assembled from modules composed of short filaments. *J. Cell Biol.* 135, 1291-1308.
- Tohtong R., Rodriguez D., Maughan D., Simcox A. (1997) Analysis of cDNAs encoding *Drosophila melanogaster* myosin light chain kinase. *J. Muscle Res. Cell Motil.* 18:43-56.

- Torres-Rosado, A., O'Shea, K.S., Tsuji, A., Chou, S.H. and Kurachi, K. (1993) Hepsin, a putative cell-surface serine protease, is required for mammalian cell growth. *Proc. Natl. Acad. Sci.* 90, 7181-7185.
- Van Aelst L, D'Souza-Schorey C. (1997) Rho GTPases and signaling networks. *Genes Dev.* 11: 2295-2322.
- von Kalm, L., Fristrom, D. and Fristrom, J. (1995) The making of a fly leg: a model for epithelial morphogenesis. *BioEssays* 17, 693-702.
- Wallrapp C., Hahnel S., Muller-Pillasch F., Burghardt B., Iwamura T., Ruthenburger M., Lerch M.M., Adler G., Gress T.M. (2000) A novel transmembrane serine protease (TMPRSS3) overexpressed in pancreatic cancer. *Cancer Res.* 60:2602-2606.
- Ward R., Evans J.J., Thummel C.S. (2002) Genetic screens reveal a role for the Rho1 small GTPase in ecdysone-induced leg morphogenesis. (submitted)
- Winter C.G., Wang B., Ballew A., Royou A., Karess R., Axelrod J.D., Luo L. (2001) *Drosophila* Rho-associated kinase (Drok) links Frizzled-mediated planar cell polarity signaling to the actin cytoskeleton. *Cell.* 105: 81-91.
- Wu F., Yan W., Pan J., Morser J., Wu Q..J. (2002) Processing of pro-atrial natriuretic peptide by corin in cardiac myocytes. *J. Biol. Chem.* [epub ahead of print]
- Yamaoka K, Masuda K, Ogawa H, Takagi K, Umemoto N, Yasuoka S. (1998) Cloning and characterization of the cDNA for human airway trypsin-like protease. *J. Biol. Chem.* 273, 11895-11901.
- Yan W, Sheng N, Seto M, Morser J, Wu Q. (1999) Corin, a mosaic transmembrane serine protease encoded by a novel cDNA from human heart. *J Biol Chem* 1999 274, 14926-14935.
- Yan W., Wu F., Morser J., Wu Q. (2000) Corin, a transmembrane cardiac serine protease, acts as a pro-atrial natriuretic peptide-converting enzyme. *Proc. Natl. Acad. Sci. U S A.* 97: 8525-8529.

Young P.E, Richman A.M, Ketchum A.S, Kiehart D.P. (1993) Morphogenesis in *Drosophila* requires nonmuscle myosin heavy chain function. *Genes Dev.* 7: 29-41.

Zacharski LR. Ornstein DL. Memoli VA. Rousseau SM. Kisiel W. (1998) Expression of the factor VII activating protease, hepsin, in situ in renal cell carcinoma [letter]. *Thrombosis & Haemostasis.* 79:876-877.

Zhang F.L., Casey P.J. (1996) Protein prenylation: molecular mechanisms and functional consequences. *Annu. Rev. Biochem.* 65:241-269.

FIGURE LEGENDS

FIGURE 1. Defects in cell shape changes during leg imaginal disc morphogenesis result in malformed legs. (A) A *Sb*^{63b}/+ heterozygote leg showing the long, slender shape of a normal femur and tibia from the 3rd leg pair of an adult. Both *Sb* and *sbd* alleles behave as recessive mutations in the context of prepupal leg development. Note the dominant bristle phenotype in the trochanter (arrow). (B) A mildly malformed 3rd leg taken from an animal of the genotype *RhoA*^{J3.8}/+; *Sb*^{63b}/+. Note the abnormally short and thick tibia and dent in the femur. (C) A severely malformed leg taken from an animal of the genotype *RhoA*^{J3.8}/+; *Sb*^{63b}/+. Note the abnormally short and thick femur and tibia and associated twisting of the leg segments.

FIGURE 2. Model of *Sb*-*sbd* regulation of RhoA signaling and actin cytoskeletal dynamics during prepupal leg imaginal disc morphogenesis.

TABLE LEGENDS

TABLE 1. Genes that display the malformed leg phenotype in the mutant condition. ^a References indicate publications in which the malformed leg phenotype was first described. (1) BEATON *et al.* 1988; (2) KISS *et al.* 1988; (3) GOTWALS and FRISTROM 1991; (4) HALSELL *et al.* 2000; (5) EDWARDS and KEIHART 1996; (6) CLARK *et al.* 1995; (7) FLETCHER *et al.* 1995; (8) D'AVINO and THUMMEL 1998; (9) GATES and THUMMEL, 2000.

TABLE 2. Mutant alleles and genotypes of stocks used in this study. Where appropriate the Bloomington Stock number is indicated. Alleles are defined as gain-of-function (gof) or loss-of-function (lof) except in cases where genetic testing has determined that alleles are amorphic, or hypomorphic. (1) BEATON *et al.* 1988; (2) APPEL *et al.* 1993; (3) A. HAMMONDS and J. FRISTROM pers. comm; (4) DOBZHANSKY 1930; (5) HALSELL *et al.* 2000; (6) STRUTT *et al.* 1997; (7) SAXTON *et al.* 1991; (8) BARRETT *et al.* 1997; (9) Berkeley Drosophila Genome Project; (10) WINTER *et al.* 2001; (11) KARESS *et al.* 1991; (12) EDWARDS and KEIHART 1996; (13) KONEV *et al.* 1994; (14) GOTWALS and FRISTROM 1991; (15) YOUNG *et al.*, 1993; (16) MORGAN *et al.* 1925; (17) KISS *et al.* 1988.

TABLE 3. *RhoA* mutations enhance *Sb-sbd* leg malformation. Animals are either doubly heterozygous, *e.g.* *RhoA*^{J3.8/+}; *Sb*^{63b/+}, or transheterozygous for the *sbd*^{201/sbd}^l mutations, *e.g.* *RhoA*^{J3.8/+}; *sbd*^{201/sbd}^l. The numbers shown indicate the percentage of animals with malformed legs, with the total number of animals scored indicated in parenthesis. In this and all following tables, the highest percentage of malformation observed in other progeny classes (*e.g.* *RhoA*^{J3.8/+}; +/+ or +/+; *Sb*^{63b/+}) has been subtracted from the data. n.d. = not determined.

TABLE 4. Mutations in *DRhoGEF2*, *drok*, and *Df(2R)Jp1* enhance *Sb-sbd* leg malformation. Animals are either doubly heterozygous, *e.g.* *DRhoGEF2*^{1.1/+}; *Sb*^{63b/+}, or transheterozygous for the *sbd*^{201/sbd}^l mutations, *e.g.* *DRhoGEF2*^{1.1/+}; *sbd*^{201/sbd}^l. The numbers shown indicate the percentage of animals with malformed legs, with the total number of animals scored indicated in parenthesis. n.d. = not determined.

TABLE 5. Leg malformation associated with over-expression of *Sb-sbd* is suppressed by reducing *RhoA* gene dosage. All animals carry one copy of the third chromosome *hs-Stubble* transgene. The transgene was induced by heat-shocking 0hr or 3hr prepupae for 1 hour at 37°C. The numbers shown indicate the number of animals exhibiting at least one malformed second or third leg and the total number of animals scored. The percentage of animals with malformed legs is indicated in parenthesis. Data are averaged across two independent experiments. +/+ indicates that animals carry two wild-type *RhoA* alleles.

TABLE 6. *en(zip)* mutations enhance *zip^{Ebr}*, *Sb-sbd*, and *RhoA* leg malformation. Animals are either doubly heterozygous, *e.g.* *DRhoGEF¹¹⁻³/+*; *Sb^{63b}/+*, or transheterozygous for the *sbd²⁰¹/sbd^l* mutations, *e.g.* *DRhoGEF¹¹⁻³/+*; *sbd²⁰¹/sbd^l*. The numbers shown indicate the percentage of animals with malformed legs, with the total number of animals scored indicated in parenthesis. ^a = reduced viability relative to sibling classes.

TABLE 7. *en(zip)* mutations interact genetically with each other. All animals are doubly heterozygous for the alleles indicated., *e.g.* *DRhoGEF¹¹⁻³ + / + 12-5*. The numbers shown indicate the percentage of animals with malformed legs, with the total number of animals scored indicated in parenthesis. ^a = reduced viability relative to sibling classes.

TABLE 8. Interactions between *br^l* and *RhoA* mutants, mutations in *RhoA* pathway members, and *en(zip)* alleles in legs. 25°C and 18°C interaction data for males are shown. All animals are hemizygous for the X-linked *br^l* allele and heterozygous for the other allele tested. n.d. = not determined.

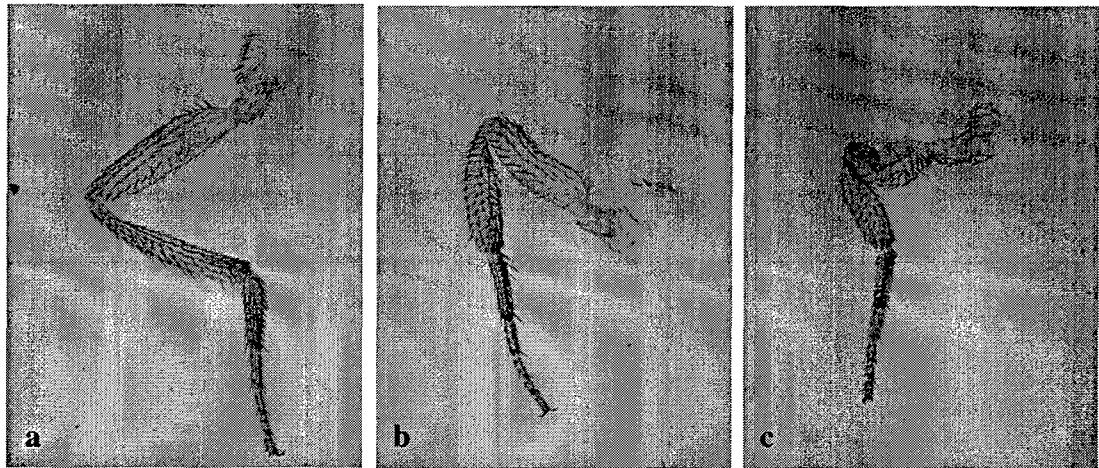


Fig.1. The presence of a *RhoA* mutation enhances the frequency of malformed legs in *Stubble* mutant animals. Most *Sb*^{63b}/+ animals exhibit normal, long, thin legs (a), 97% of *RhoA*^{J3.8}/+; *Sb*^{63b}/+ animals exhibit either weak (b) or severe (c) leg malformation. The femur and tibia are shorter and fatter than wild type, and in the more severe cases, are kinked or dented. The examples shown in these panel are from the third pair of legs. Often, if one leg is weakly malformed, the other leg of the pair is normal, but when severe malformation is seen, usually both legs of the pair are affected similarly.

Note in the text that only the proximal-most portion of the femur and coxa have the shortened bristles that are so obvious on the thorax and head of *Sb*^{63b}/+ animals.

Figure 2. Model for Sb-sbd signaling to RhoA in *Drosophila* leg imaginal discs.

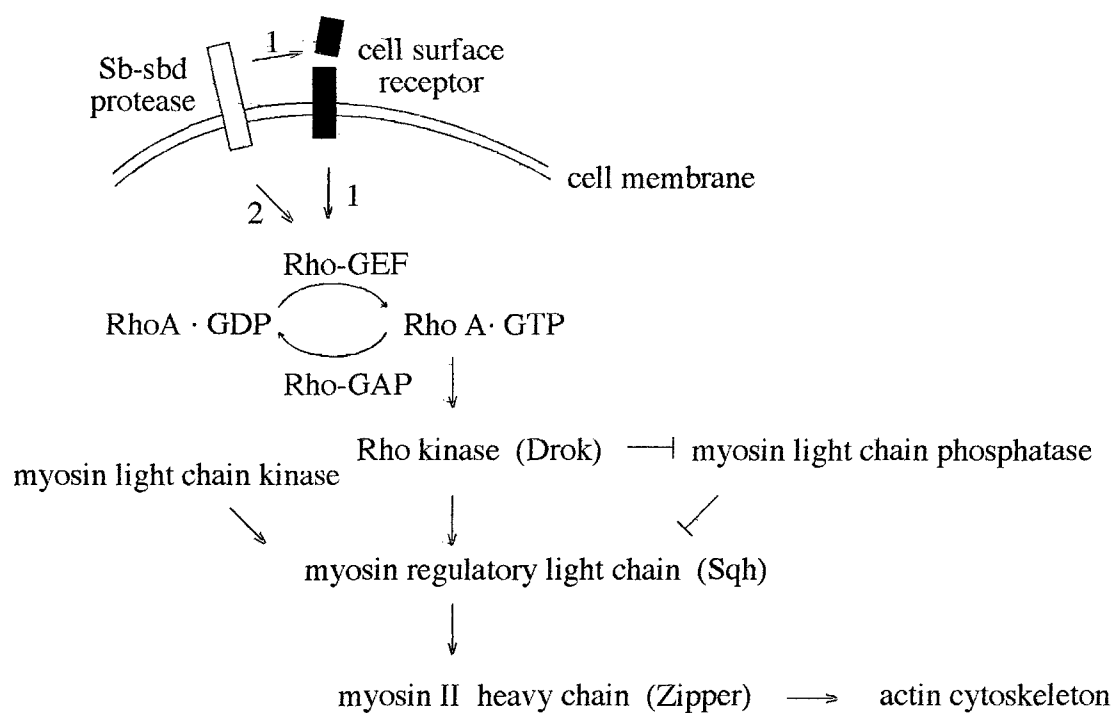


TABLE 1

Genes that display the malformed leg phenotype in the mutant condition.

Gene	Protein Product	Reference ^a
<i>Stubble-stubblويد</i>	Type II transmembrane serine protease	(1)
<i>Broad-Complex</i>	Zinc-finger transcription factors	(2)
<i>zipper</i>	Non-muscle myosin II heavy chain	(3)
<i>blistered</i>	<i>Drosophila</i> serum response factor	(3)
<i>RhoA</i>	Small GTPase	(4)
<i>DRhoGEF2</i>	RhoA-specific guanine nucleotide exchange factor	(4)
<i>spaghetti squash</i>	Myosin regulatory light chain	(5)
<i>dachsous</i>	Cadherin	(6)
<i>E74</i>	ETS transcription factors	(7)
<i>crooked legs</i>	Zinc-finger transcription factor	(8)
<i>vulcan</i>	SAPAP	(9)
<i>bancal</i>	hnRNPK	(9)

TABLE 2

Mutant alleles and genotypes of stocks used in this study

Mutant allele	Genotype of stock	Mutagen	Classification	Reference
<i>Sb¹</i>	<i>Sb¹/ry^{TM6B}, Tb Hu</i>	transpositional insertion	gof (bristles); lof (legs)	(1, 2)
<i>Sb⁶⁸</i>	<i>red Sb⁶⁸/e^{TM6B}, Tb Hu e ca</i>	transpositional insertion	gof (bristles); lof (legs)	(1, 2)
<i>Sb⁷⁰</i>	<i>Sb⁷⁰/TM6B, Tb Hu e</i>	transpositional insertion	gof (bristles); lof (legs)	(1, 3)
<i>Sb⁹⁴</i>	<i>Sb⁹⁴/TM6B, Tb Hu e</i>	X-ray	gof (bristles); lof (legs)	(1)
<i>sbd¹</i>	<i>sbd¹ ro e ca</i>	spontaneous	hypomorph	(4)
<i>sbd¹⁰⁵</i>	<i>w; sbd¹⁰⁵ e ca/TM6B, Tb Hu e</i>	X-ray	amorph (deletion)	(1)
<i>sbd²⁰¹</i>	<i>red sbd²⁰¹/e^{TM6B}, Tb Hu e</i>	EMS	hypomorph	(1)
<i>RhoA¹²⁸</i>	<i>RhoA¹²⁸/CyO</i>	EMS	lof	(5)
<i>RhoA^{13.10}</i>	<i>pr RhoA^{13.10}/CyO, ftz-lacZ</i>	EMS	lof	(5)
<i>RhoA¹²⁷</i>	<i>RhoA¹²⁷/CyO, ftz-lacZ</i>	P-element	likely amorph	(6)
<i>RhoA¹²⁰</i>	<i>RhoA¹²⁰/CyO, ftz-lacZ</i>	insertion/excision	likely amorph	(6)
<i>Df(2R)jps (BL3520)</i>	<i>w¹ N⁶⁴; Df(2R)jps w¹/CyO</i>	X-ray	deletion	(7)
<i>Df(2R)jp1 (BL3518)</i>	<i>w¹ N⁶⁴; Df(2R)jp1/CyO</i>	X-ray	deletion	(7)
<i>RhoGEF^{2.1}</i>	<i>w; RhoGEF^{2.1}/CyO, act-lacZ</i>	EMS	lof	(8)
<i>RhoGEF^{2.1}</i>	<i>w; RhoGEF^{2.1}/CyO, ftz-lacZ</i>	EMS	lof	(8)
<i>RhoGEF^{2.609} (BL11369)</i>	<i>cn¹ P1ry¹ RhoGEF^{2.609}/CyO, ry⁸⁶</i>	P-element insertion	lof	(9)
<i>drok¹</i>	<i>w drok¹/FM71</i>	EMS	lof	(10)
<i>drok²</i>	<i>yw drok² FRT19A/FM71</i>	EMS	likely amorph	(10)
<i>sgt¹</i>	<i>yw sgt¹ cl/FM6</i>	P-element insertion	strong hypomorph	(11, 12)
<i>sgt²</i>	<i>yw sgt² cl/FM7c</i>	P-element	likely amorph	(11, 12)
<i>Phr¹ (BL 5523)</i>	<i>Phr¹/CyO</i>	insertion/excision		
<i>Phr^{603x} (BL12322)</i>	<i>P1ry¹ Phr^{603x} cn¹/CyO; ry⁸⁶</i>	X-ray	lof	(13)
<i>zip²⁸</i>	<i>b pr cn sp zip²⁸/SMS</i>	P-element insertion	lof	(9)
<i>br¹</i>	<i>br¹</i>	EMS	weak dominant negative	(5, 14, 15)
		spontaneous	hypomorph	(16, 17)

TABLE 3

RhoA mutants enhance *Sb-sbd* leg malformation

	<i>RhoA</i> ^{J3.8} / +	<i>RhoA</i> ^{E3.10} / +	<i>RhoA</i> ^{72F} / +	<i>RhoA</i> ⁷²⁰ / +	<i>Df(2R)Jp8</i> / +
<i>Sb</i> ^{63b} / +	94% (344)	89% (272)	60% (186)	59% (246)	85% (198)
<i>Sb</i> ⁷⁰ / +	91% (383)	95% (253)	77% (242)	70% (206)	86% (180)
<i>Sb</i> ¹ / +	8% (350)	4% (343)	n.d.	n.d.	5% (252)
<i>Sb</i> ^{spi} / +	15% (455)	8% (277)	n.d.	n.d.	6% (154)
<i>sbd</i> ²⁰¹ / +	0% (395)	0% (260)	0% (182)	1% (125)	1% (230)
<i>sbd</i> ¹⁰⁵ / +	28% (230)	32% (391)	7% (131)	1% (109)	19% (206)
<i>sbd</i> ¹ / +	2% (344)	1% (193)	n.d.	n.d.	6% (257)
<i>sbd</i> ²⁰¹ / <i>sbd</i> ¹	86% (244)	89% (164)	n.d.	n.d.	89% (182)
<i>sbd</i> ²⁰¹ / <i>sbd</i> ²	18% (272)	40% (215)	n.d.	n.d.	6% (293)

TABLE 4

Mutations in *DRhoGEF2*, *drok*, and *Df(2R)Jp1* enhance *Sb-sbd* leg malformation

	<i>GEF2</i> ^{1,1} / +	<i>GEF2</i> ^{4,1} / +	<i>GEF2</i> ⁹⁴²⁹¹ / +	<i>GEF2</i> ^{11,3} / +	<i>drok</i> ¹ / +	<i>drok</i> ² / +	<i>Df(2R)Jp1</i> / +
<i>Sb</i> ^{63b} / +	11% (211)	2% (277)	11% (232)	45% (382)	11% (186)	28% (176)	43% (165)
<i>Sb</i> ⁷⁰ / +	12% (273)	3% (287)	9% (297)	41% (373)	65% (330)	57% (201)	28% (213)
<i>sbd</i> ²⁰¹ / +	1% (244)	0% (196)	0% (282)	1% (555)	2% (246)	0% (178)	n.d.
<i>sbd</i> ¹⁰⁵ / +	0% (186)	0% (187)	0% (228)	0% (139)	9% (140)	8% (136)	n.d.
<i>sbd</i> ²⁰¹ / <i>sbd</i> ¹	24% (206)	14% (192)	12% (222)	32% (163)	10% (243)	15% (259)	71% (149)

TABLE 5

Leg malformation associated with over-expression of Sb-sbd is suppressed by reducing *RhoA* gene dosage

	HS 0h AP		HS 3h AP	
	+/+	<i>RhoA</i> ⁷²⁰ /+	+/+	<i>RhoA</i> ⁷²⁰ /+
2 nd legs	17/97 (17%)	10/121 (8%)	75/108 (69%)	42/165 (25%)
3 rd legs	56/97 (58%)	35/121 (29%)	91/108 (84%)	91/165 (55%)

TABLE 6

en(zip) mutants enhance *zip*^{Ebr}, *Sb-sbd*, and *RhoA* leg malformation

	<i>zip</i> ^{Ebr} / +	<i>Sb</i> ^{63b} / +	<i>Sb</i> ⁷⁰ / +	<i>sbd</i> ²⁰¹ / <i>sbd</i> ¹	<i>RhoA</i> ^{J3.8} / +	<i>RhoA</i> ^{E3.10} / +	<i>Df(2R)Jp8</i> / +
<i>GEF2</i> ^{1/1-3} / +	81% (186)	45% (382)	41% (373)	32% (163)	100% (83) ^a	94% (177) ^a	94% (150) ^a
<i>12-5</i> / +	71% (186)	17% (229)	39% (257)	21% (185)	94% (148) ^a	93% (125) ^a	78% (209)
<i>RhoA</i> ¹²⁻⁶ / +	83% (165) ^a	61% (292)	74% (163)	52% (163)	lethal	lethal	lethal
<i>18-5</i> / +	41% (311)	34% (388)	37% (299)	26% (177)	81% (193)	75% (275)	72% (281)
<i>31-6</i> / +	22% (486)	16% (427)	26% (382)	41% (193)	56% (325)	83% (254)	51% (305)
<i>zip</i> ³³⁻¹ / +	97% (123) ^a	8% (274)	36% (264)	44% (163)	97% (214)	93% (200)	85% (237)

TABLE 7

en(zip) mutations interact genetically with each other

	<i>GEF2</i> ¹²⁻³	<i>I2-5</i>	<i>RhoA</i> ¹²⁻⁶	<i>I8-5</i>	<i>31-6</i>
<i>GEF2</i> ¹²⁻³	lethal				
<i>I2-5</i>	30% (311)	lethal			
<i>RhoA</i> ¹²⁻⁶	73% (229)	46% (267)	lethal		
<i>I8-5</i>	15% (453)	89% (85) ^a	27% (296)	lethal	
<i>31-6</i>	3% (452)	37% (259)	44% (102)	35% (249)	24% (224)

TABLE 8

Interactions between *br*¹ and *RhoA* mutants, mutations in RhoA pathway members, and *en(zip)*

mutants in legs

	<i>br</i> ¹ / Y 25°C	<i>br</i> ¹ / Y 18°C
<i>RhoA</i> ^{J3.8} / +	26% (99)	29% (40)
<i>RhoA</i> ^{E3.10} / +	45% (80)	63% (69)
<i>Df(2R)Jp8</i> / +	4% (295)	48% (93)
<i>GEF2</i> ^{1.1} / +	1% (195)	1% (163)
<i>GEF2</i> ^{4.1} / +	1% (175)	4% (241)
<i>GEF2</i> ⁰⁴²⁹¹ / +	4% (76)	1% (185)
<i>drok</i> ¹ / +	0% (224)	n.d.
<i>drok</i> ² / +	0% (195)	n.d.
<i>Df(2R)Jp1</i> / +	28% (169)	13% (70)
<i>GEF2</i> ¹¹⁻³ / +	5% (182)	9% (125)
<i>12-5</i> / +	0% (163)	2% (100)
<i>RhoA</i> ¹²⁻⁶ / +	4% (237)	4% (204)
<i>18-5</i> / +	0% (296)	0% (130)
<i>31-6</i> / +	0% (136)	0% (212)
<i>zip</i> ³³⁻¹ / +	0% (195)	n.d.



DEPARTMENT OF THE ARMY
US ARMY MEDICAL RESEARCH AND MATERIEL COMMAND
504 SCOTT STREET
FORT DETRICK, MARYLAND 21702-5012

REPLY TO
ATTENTION OF:

MCMR-RMI-S (70-1y)

28 July 03

MEMORANDUM FOR Administrator, Defense Technical Information
Center (DTIC-OCA), 8725 John J. Kingman Road, Fort Belvoir,
VA 22060-6218


SUBJECT: Request Change in Distribution Statement

1. The U.S. Army Medical Research and Materiel Command has reexamined the need for the limitation assigned to technical reports written for this Command. Request the limited distribution statement for the enclosed accession numbers be changed to "Approved for public release; distribution unlimited." These reports should be released to the National Technical Information Service.

2. Point of contact for this request is Ms. Kristin Morrow at DSN 343-7327 or by e-mail at Kristin.Morrow@det.amedd.army.mil.

FOR THE COMMANDER:

Encl


PHYLLIS M. RINEHART
Deputy Chief of Staff for
Information Management

ADB233865	ADB264750
ADB265530	ADB282776
ADB244706	ADB286264
ADB285843	ADB260563
ADB240902	ADB277918
ADB264038	ADB286365
ADB285885	ADB275327
ADB274458	ADB286736
ADB285735	ADB286137
ADB286597	ADB286146
ADB285707	ADB286100
ADB274521	ADB286266
ADB259955	ADB286308
ADB274793	ADB285832
ADB285914	
ADB260288	
ADB254419	
ADB282347	
ADB286860	
ADB262052	
ADB286348	
ADB264839	
ADB275123	
ADB286590	
ADB264002	
ADB281670	
ADB281622	
ADB263720	
ADB285876	
ADB262660	
ADB282191	
ADB283518	
ADB285797	
ADB269339	
ADB264584	
ADB282777	
ADB286185	
ADB262261	
ADB282896	
ADB286247	
ADB286127	
ADB274629	
ADB284370	
ADB264652	
ADB281790	
ADB286578	